

Development of cyclic peptide inhibitors of coagulation factor XII and matrix metalloproteinase 2

THÈSE N° 8467 (2018)

PRÉSENTÉE LE 13 AVRIL 2018

À LA FACULTÉ DES SCIENCES DE BASE

LABORATOIRE DE PROTÉINES ET PEPTIDES THÉRAPEUTIQUES

PROGRAMME DOCTORAL EN CHIMIE ET GÉNIE CHIMIQUE

ÉCOLE POLYTECHNIQUE FÉDÉRALE DE LAUSANNE

POUR L'OBTENTION DU GRADE DE DOCTEUR ÈS SCIENCES

PAR

Jonas Alfred Karl WILBS

acceptée sur proposition du jury:

Prof. U. Röthlisberger, présidente du jury

Prof. C. Heinis, directeur de thèse

Prof. C. A. Olsen, rapporteur

Dr E. Valeur, rapporteur

Prof. M. Dal Peraro, rapporteur



ÉCOLE POLYTECHNIQUE
FÉDÉRALE DE LAUSANNE

Suisse
2018

Acknowledgements

First of all, I would like to thank my PhD supervisor professor Christian Heinis. Thank you for giving me the possibility to work with something that I am truly passionate about, it has been a privilege. Also thank you for your scientific advice and general discussions, and for supporting my attendance to APS2017 and the Benzon symposium, two highlights of the last four years.

I would also like to express my thanks to all the jury members, Ursula Röthlisberger and Matteo Dal Peraro from EPFL, Christian A. Olsen from Copenhagen and Eric Valeur from Gothenburg, for devoting their time to my PhD thesis. I really appreciate your effort.

Next, I would like to thank all the lab members of LPPT whom I have worked with during the past four years. When I arrived, I immediately felt welcome, thanks to all the people there at the time: Sangram, Ranga, Raphael, Shiyu, Davide, Mike, Vanessa, Charlotte, Khan, Inma, Silvia, Lisa, Camille, Alessandro and Phillippe. Thank you for being so helpful and accommodating. A special thanks to the people in “Ranga’s kindergarten”, it was great to share the lab with you! I would also like to especially acknowledge Khan for mentoring me during the beginning of my PhD and for introducing me to the exciting MMP-2 project. Further, I would like to thank the people who have joined the lab during my time there: Kaycie, Joao, Patrick, Vanessa, Xudong, Christina, Ganesh, Simon, Lina, Milan, Manh, Yuteng, Sevan, Carl and Gontran. It has been great to work with all of you and I am convinced that the good spirit in the lab will remain. Additionally, I would like to give special thanks to my students, Luca and Gontran. It was a pleasure to work together and thank you so much for your valuable contributions.

I would like to address a particular thanks to all the people who have been involved in the FXII project, the main project of my PhD thesis. In my opinion this has been a true teamwork and the project would not have yielded such great results without the contribution of everyone involved. Thanks to Vanessa for initiating the project, and especially to Simon who let me join his project and whom I have worked with in close collaboration. It was really nice to work with you and I will always remember our fast-paced work when synthesizing the JS analogues and when we found the picomolar inhibitor. I also want to thank Christina, Luca and Gontran for their contributions. This project would not have been possible without external collaborations. I want to express my thanks to

professor Anne Angelillo-Scherrer and her whole lab, with a special mention of Raja, it has been a fantastic experience to work with such a competent and precise researcher as you in the FeCl₃ project. The moment when we found that JS33-R (as we called it then) inhibited thrombosis was priceless! Further I would like to acknowledge professor Robert Rieben and Mai for giving us the opportunity to test our inhibitor in an exciting animal model. I was deeply impressed by the precision and complexity of your work and I am very thankful for this experience. This project also benefited greatly from the contribution of professor Keith Cook, Alida and their team who tested our compound in rabbits. It has been really exciting to get the opportunity to be part of such an experiment.

In the BCH at EPFL there are many labs and persons who have contributed to my work and whom I would like to acknowledge, be it for scientific advice, borrowing of compounds or just pure entertainment. First I would like to thank all the members of the LCBIM, with special thanks to Ric, Anzhelika and Jens. You have contributed greatly in all the ways. I further thank all the members of LIP with special mentioning of Silvia, Helen, Fay, Nico and Yann. I also want to mention two persons from other labs; CK – vice president of the BCH peptide community and Nick – the man who taught me that simulations are more precise than experiments.

For making my life great also outside of the lab, I would like to thank the following persons: Ric – one of the most amazing guys ever and one of my best friends. Thank you for all the awesome experiences we have shared together in the Alps. I hope we will continue living the good life, let's start with Vättern! All my friends from Alingsås; with special mention of Johan, Marriz, Johanna, Lovisa, Malin, Jimmie, Fredric, it is always great to hang out with you, be it in Sweden or Switzerland. A special thanks to Johan, for all the scientific input from a MD perspective. All the people from Uppsala: Martin, Håkan, Jessica, Karro, Mimmi, Robert, Andreas, Adam, David, Torbjörn, Martin, Olle, Kickan and everyone else; I always enjoy very much to see you for skiing and other occasions. I hope we can keep the tradition of an annual trip to the Alps. My Australian community, including: Olof, Philip, Carl, Birger, Markus, Agnes, Jorien, Laura, Josh, Burak. Our get-togethers are always a welcome break from work.

A very special thanks goes to my family. Thank you for always believing in me and for helping and supporting me for whatever I am doing.

Finally, I want to thank you Camille for being such a great part of my life. Thank you for all the fun things we do together and for your support both private and scientifically. You are a great scientist and I am lucky to have you so close for immediate feedback. And thank you for bearing with me in all situations, such as when I just have to ski down here or hike up there. I hope you will continue to bear with me.

Abstract

Peptides represent a promising molecular class for drug development. They combine several strengths of small molecules (e.g. efficient tissue diffusion, low immunogenicity and access to chemical synthesis) and key properties of biologics such as monoclonal antibodies (e.g. high affinity and specificity). Around 60 peptides are currently used in the clinic. Most of the peptide drugs are natural products or derivatives thereof, as for example human peptide hormones or antibacterial peptides. In recent years, a range of methodologies were established to develop peptides binding to therapeutic targets *de novo*. Our laboratory is specialized on the *in vitro* evolution of bicyclic peptides by phage display. Bicyclic peptides have two macrocyclic rings that allow for binding protein targets with high affinity and selectivity. Members of our research group have developed bicyclic peptide ligands to a range of important disease targets, including the proteases coagulation factor XII (FXII) and matrix metalloproteinase 2 (MMP-2).

The aim of my thesis was to improve the potency and stability of phage-selected bicyclic peptide inhibitors of FXII and MMP-2, and to test their therapeutic potential in animal disease models. Specifically, I planned at improving the binding affinity, target selectivity and proteolytic stability of bicyclic peptides by substituting natural amino acids with unnatural ones. As described in the following, the substitutions to unnatural amino acids had led to substantial improvements in the bicyclic peptides, and this had enabled me the evaluation of the inhibitors in disease models.

In my first and second project, I aimed at improving the potency and stability of a bicyclic peptide FXII inhibitor that was previously developed in our lab by phage display, and to test the therapeutic potential of the resulting peptide *in vivo*. FXII has recently been identified as a promising target for safe anticoagulation therapy, based on the finding that mice deficient in the coagulation protease show reduced thrombosis but no abnormal bleeding. In the first project, I investigated if the insertion of a single carbon atom into the macrocyclic backbone of a phage-selected bicyclic peptide FXII inhibitor can improve its binding affinity. Molecules of this type are not present in the bicyclic peptide phage display libraries since each canonical amino acid contributes three atoms to the backbone. Positions within the macrocycle susceptible to atom insertion were first identified using a scanning methodology where glycine mutants were compared to β -alanine mutants. Upon insertion of atoms in the backbone using β -amino acids or homologated

cysteine analogues, two peptides showed 4.7- and 2.5-fold improved K_i values. The better one blocked FXII with a K_i of 1.5 ± 0.1 nM and was more potent than the lead peptide in inhibiting the activation of the intrinsic coagulation pathway. The strategy of ring size variation by one or several atoms should be generally applicable for the affinity maturation of in-vitro-evolved cyclic peptides.

In my second project, I aimed at improving further the potency of the bicyclic peptide FXII inhibitor described before, and to additionally improve its proteolytic stability. I achieved both these goals by replacing further natural amino acids to unnatural ones. Sub-nanomolar activity for human and mouse FXII (370 and 450 pM respectively) as well as a high stability ($t_{1/2} > 128 \pm 8$ h in plasma) permitted preclinical evaluation of the peptide. The inhibitor efficiently blocked intrinsic coagulation in blood plasma from human, mouse and rabbit. I further demonstrated that the peptide reduced experimental thrombosis induced by ferric chloride in mice and suppressed blood coagulation in artificial lungs in rabbits, all without increasing the risk of bleeding. This shows that FXII activity is controllable with a synthetic inhibitor in vivo, and that the optimized bicyclic peptide is a promising candidate for thromboprotection in various medical conditions.

In a third project, I aimed at improving the potency and stability of a bicyclic peptide MMP-2 inhibitor that was previously developed in our lab by phage display. MMP-2 is implicated in tumor growth and metastasis formation. Due to the strong structural similarities shared by MMP-2 with other MMPs, the development of selective inhibitors of MMP-2 has so far not been achieved. By substituting natural amino acids to unnatural ones, I succeeded at enhancing substantially both, the binding affinity and stability of the phage-selected bicyclic peptide. The resulting MMP-2 inhibitor has a high affinity (1.9 nM) and stability in plasma ($t_{1/2} = 4.4$ h) and thus provides a valuable research tool.

Key words: Peptide, medicinal chemistry, macrocycle, backbone, β -amino acid, coagulation factor XII, anticoagulants, sub-nanomolar, thrombosis, ferric chloride, artificial lung, ECMO, MMP, D-amino acid, hydroxamate

Résumé

Les peptides représentent un format moléculaire prometteur pour le développement de nouveaux principes actifs. Ils combinent à la fois les avantages des petites molécules (par exemple la diffusion efficace dans les tissus, une immunogénicité faible et la possibilité d'être synthétisés chimiquement) et ceux des protéines thérapeutiques telles que les anticorps (avec par exemple leur forte affinité et spécificité). Aujourd'hui, environ 60 peptides font l'objet d'essais cliniques. La plupart sont des composés naturels ou bien en sont des dérivés, comme par exemple les hormones peptidiques humaines ou les peptides antimicrobiens. Toutefois, ces dernières années, de nouvelles méthodologies sont apparues permettant le développement de peptides liant des cibles thérapeutiques « de novo ». Notre laboratoire s'est spécialisé dans l'une de ces méthodes qui consiste en l'évolution *in vitro* de peptides bicycliques via la technique du phage display. Ces peptides bicycliques possèdent deux chaînes macrocycliques qui leur permettent de se lier aux cibles d'intérêt avec une haute affinité et spécificité. Des membres de notre laboratoire ont généré des ligands bicycliques pour un grand nombre de cibles thérapeutiques comprenant des inhibiteurs du facteur de coagulation XII (FXII) et de la métalloprotéinase matricielle 2 (MMP-2).

L'objectif de ma thèse a été d'améliorer l'activité et la stabilité des peptides bicycliques sélectionnés par phage display pour FXII et MMP-2 ainsi que de tester leur potentiel thérapeutique avec des modèles animaux. Plus spécifiquement, j'ai voulu améliorer l'affinité de liaison, la sélectivité pour la cible et la stabilité protéolytique des peptides bicycliques en substituant certains acides aminés naturels par d'autres, non-naturels. Ainsi que décrit dans les paragraphes suivants, ces substitutions ont conduit à des améliorations conséquentes des peptides bicycliques ce qui a par la suite permis de tester ces inhibiteurs dans des modèles thérapeutiques *in vivo*.

Dans mes deux premiers projets, j'avais pour but d'améliorer l'activité et la stabilité d'un peptide bicyclique inhibiteur de FXII qui avait été au préalable développé dans notre laboratoire afin de par la suite tester son pouvoir thérapeutique *in vivo*. En effet, FXII a récemment été identifié comme une cible prometteuse pour le développement d'anticoagulants entraînant moins d'effets secondaires. En effet, certaines études ont montré que des souris déficientes pour FXII présentaient moins de thromboses tout en ne manifestant pas de saignements anormaux.

Au cours du premier projet, j'ai tenté de comprendre si l'insertion d'un atome de carbone dans le squelette macrocyclique d'un inhibiteur du FXII pourrait améliorer son affinité pour la cible. De telles structures ne sont pas présentes dans les bibliothèques de phage exposant des peptides bicycliques puisque ces derniers ne sont constitués que d'acides aminés naturels ayant une base moléculaire de trois atomes (2 atomes de carbone et 1 atome d'azote). Dans la chaîne peptidique du macrocycle, les positions susceptibles de tolérer l'insertion d'un atome ont été identifiées grâce à une méthode au cours de laquelle des mutants présentant une glycine à une position donnée étaient comparés à leurs homologues présentant une β -alanine. Par la suite, des substitutions avec un acide aminé β ou bien un homologue de cystéine ont permis l'identification de deux nouveaux peptides avec des constantes d'inhibition (K_i) 4,7 et 2,5 fois meilleures que celle du composé de départ. Le peptide le plus efficace bloque l'activité de FXII avec un K_i de $1,5 \pm 0,1$ nM et engendre une inhibition supérieure de l'activation de la cascade de coagulation intrinsèque. De plus, cette stratégie basée sur l'insertion d'un ou plusieurs atomes dans le squelette d'un macrocycle peptidique devrait pouvoir s'appliquer de façon générale pour la maturation d'affinité de peptides cycliques évolué in vitro.

Dans mon deuxième projet, j'ai voulu améliorer encore un peu plus l'activité de l'inhibiteur du FXII décrit dans le paragraphe précédent ainsi qu'augmenter sa stabilité protéolytique. J'ai pu atteindre ces deux objectifs en générant d'autres substitutions avec des acides aminés non naturels ce qui a eu pour résultat la mise à jour d'un peptide ayant une activité à des concentrations sub-nanomolaires contre les protéases FXII chez l'homme et la souris (respectivement 370 et 450 pM). D'autre part, le nouveau peptide a une très grande stabilité ($t_{1/2} > 128 \pm 8$ h dans du plasma) ce qui a permis son évaluation préclinique. Il a été prouvé que l'inhibiteur bloque efficacement la coagulation intrinsèque dans le plasma sanguin de l'homme, la souris et le lapin. J'ai également démontré que le peptide pouvait réduire les thromboses induites expérimentalement dans des souris en utilisant le chlorure ferrique et que la coagulation du sang était inhibée dans un modèle de poumon artificiel chez le lapin, le tout sans entraîner de risque de saignement. Ces données attestent que l'activité du FXII peut être modulée avec un inhibiteur synthétique et que la version optimisée de notre peptide bicyclique est prometteuse pour la protection contre les thromboses ainsi que d'autres complications médicales.

Dans le dernier projet, j'ai cherché à améliorer l'activité et la stabilité d'un peptide bicyclique inhibiteur de MMP-2. MMP-2 est impliquée dans le développement des tumeurs et des métastases. A cause de la grande similarité structurale entre MMP-2 et d'autres MMPs, le développement d'un inhibiteur sélectif n'a jusque maintenant pas été possible. En utilisant de nouveau des substitutions avec des acides aminés non naturels, j'ai pu à la fois augmenter l'affinité et la stabilité des peptides sélectionnés lors des campagnes de sélection de phage. Le meilleur peptide résultant de ce travail a un K_i de 1.9 nM et une stabilité de 4.4 h ce qui en fait un outil de recherche prometteur.

Key words: Peptide, chimie medicinale, macrocycle, acide aminé β , Facteur de coagulations XII, anticoagulants, thrombose, Chlorure ferrique, poumon artificiel, ECMO, MMP, acide aminé D, hydroxamate

Contents

Acknowledgements	i
Abstract	iii
Résumé.....	v
Contents	ix
List of abbreviations.....	xi
1. Introduction	1
1.1 Peptide therapeutics.....	3
1.1.1 Properties of peptide therapeutics	3
1.1.2 Examples of peptide therapeutics	4
1.1.3 Cyclic peptide therapeutics	9
1.2 Strategies for developing peptide therapeutics	13
1.2.1 Peptides from natural sources	13
1.2.2 Protein epitope mimetics	14
1.2.3 Strategies for de novo development of peptide therapeutics	19
1.3 Medicinal chemistry of peptides.....	23
1.3.1 Enhancing properties of peptides	23
1.3.2 Examples of modified peptides.....	26
1.4 Bicyclic peptides.....	33
1.4.1 Development of bicyclic peptides	33
1.4.2 Examples of bicyclic peptides	37
2. Aim of thesis.....	41
3. Improving the binding affinity of in-vitro-evolved cyclic peptides by inserting atoms into the macrocycle backbone	45
3.1 Abstract	47
3.2 Introduction	47
3.3 Results and discussion	49
3.4 Experimental section	54
3.5 Supporting information	57
4. A peptide macrocycle FXII inhibitor provides safe anticoagulation in a preclinical thrombosis model and in artificial lungs.....	59
4.1 Abstract	61

4.2	Introduction	61
4.3	Results	63
4.3.1	Engineered macrocycle inhibits human and mouse FXIIa with picomolar affinity	63
4.3.2	FXIIa inhibitor is stable in human plasma for several days	64
4.3.3	FXII900 efficiently inhibits the intrinsic coagulation pathway ex vivo	66
4.3.4	Pharmacokinetics in mice, rabbits, and pigs	67
4.3.5	FXII900 inhibits ferric chloride-induced arterial thrombosis in mice	69
4.3.6	FXII900 provides bleeding-free anticoagulation in artificial lungs	70
4.4	Discussion	73
4.5	Materials and Methods	75
4.6	Supporting information	85
5.	Selective inhibition off MMP achieved with peptide macrocycle	105
5.1	Abstract	107
5.2	Introduction	107
5.3	Results	109
5.3.1	Directed evolution of peptide macrocycle MMP-2 inhibitors	109
5.3.2	Substituting the zinc binding carboxylate with hydroxamate	110
5.3.3	Affinity maturation of MMP-2 inhibitor	112
5.3.4	Selectivity of MMP-2 inhibitors	112
5.3.5	Inhibition of MMP-2 autoactivation	113
5.3.6	Plasma stability of MMP-2 inhibitors	113
5.3.7	Stability improvement of MMP-2 inhibitor	115
5.3.8	Affinity improvement of MMP-2 inhibitor	116
5.3.9	MMP specificity profiling of M238 ^{hy}	117
5.3.10	MMP inhibition of single rings and linear M238 ^{hy}	120
5.3.11	Selectivity of M238 ^{hy}	120
5.1	Discussion	122
5.2	Materials and methods	124
5.3	Supporting information	130
6.	General conclusions and outlook	139
6.1	Backbone extension of a bicyclic peptide	141
6.2	Engineering and preclinical testing of a bicyclic peptide FXII inhibitor	143
6.3	Development of a bicyclic peptide MMP-2 inhibitor	146
7.	References	147

List of abbreviations

ACT	Activated clotting time
Aib	Amino isobutyric acid
AIP	Autoinducing peptides
AMP	Anti-microbial peptides
aPTT	Activated partial thromboplastin time
BSA	Bovine serum albumin
CDR	Complementarity-determining region
CPB	Cardiopulmonary bypass
Da	Dalton
DCM	Dichloromethane
DIPEA	N,N-Diisopropylethylamine
DMF	N,N-Dimethylformamide
DMSO	Dimethylsulfoxide
DPP-IV	Dipeptidyl peptidase IV
ECM	Extracellular matrix
ECMO	Extracorporeal membrane oxygenation
ESI-MS	Electrospray ionization mass spectrometry
Fc	Fragment crystallizable
FDA	Food and Drug Administration
Fmoc	Fluorenylmethyloxycarbonyl
FXIa/FXIIa	Activated coagulation factor XI/XII
GC-C	Guanylate cyclase C
GLP-1	Glucagon-like peptide 1
GPCR	G-protein coupled receptors

HAE	Hereditary angioedema
HBTU	2-(1H-benzotriazol-1-yl)-1,1,3,3-tetramethyluronium hexafluorophosphate
HDAC	Histone deacetylase
HOBt	Hydroxybenzotriazole
HPLC	High pressure liquid chromatography
IC_{50}	Half maximal inhibitory concentration
i.v.	Intravenous
K_i	Inhibition constant
K_m	Michaelis-Menten constant
LC-MS	Liquid chromatography mass spectrometry
MCoTI	Momordica cochinchinensis trypsin inhibitor
MeCN	Acetonitrile
MMP	Matrix metalloproteinase
MRSA	Methicillin-resistant <i>Staphylococcus aureus</i>
MW	Molecular weight
NCL	Native chemical ligation
NGS	Next generation sequencing
OBOC	One-bead-one-compound
pIII/pVIII	phage coat protein III/VIII
PCR	Polymerase chain reaction
PEM	Protein epitope mimicking
PK	Plasma kallikrein
PNA	Peptide nucleic acids
PPI	Protein-protein interactions
PT	Prothrombin time
(m or t)RNA	(messenger or transfer) ribonucleic acid
RT	Room temperature

SAR	Structure activity relationship
SPPS	Solid-phase peptide synthesis
$t_{1/2}$	Half-life
TATA	1,3,5-triacryloyl-1,3,5-triazinane
TBAB	N,N',N''-(benzene-1,3,5-triyl)-tris(2-bromoacetamide)
TBMB	1,3,5-tris(bromomethyl)benzene
TFA	Trifluoroacetic acid
TIMPS	Tissue inhibitors of metalloproteinases
uPa	Urokinase-type plasminogen activator

1. Introduction

1.1 Peptide therapeutics

1.1.1 Properties of peptide therapeutics

Peptides are defined as molecules consisting of two or more amino acid monomers linked together with peptide bonds. There is not a clear upper limit for the number of monomers, but in general peptides are considered to have less than 50 amino acid residues. As a molecular format for drug development, peptides represent a promising class as they possess many desirable inherent properties. Peptides can bind their targets with high affinity, due to the relatively large contact area made with the target, which also renders peptide binders highly target specific as well as enabling the targeting of protein-protein interactions (PPI) (1). Moreover, peptides are readily available through solid phase peptide synthesis (SPPS) which enables an efficient development. Furthermore, peptides as well as their metabolites, generally have low toxicity, minimizing the risk of negative side-effects in therapy.

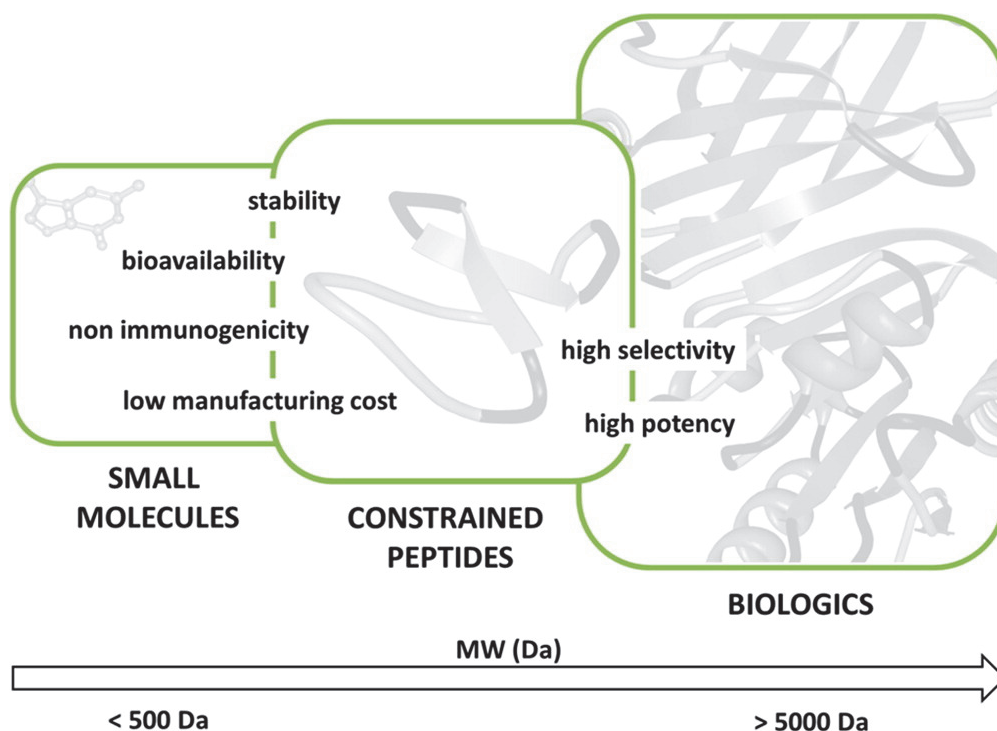


Figure 1. Peptides generally possess properties of both small molecule drugs and biologics. Reprinted with permission from (2), © 2014 American Chemical Society.

Peptides are often described as a drug-class filling the gap between traditional small molecules and the protein-based drugs (Figure 1) (2). In one aspect this is related to their molecular size, which ranges from 500 to 5000 Da, hence occupying the space in between Lipinski-“rule of five”-following (3) small molecules and proteins. On the other hand, this is also true for their inherent properties. Peptides are indeed combining advantages

of the two classes for example the strong and specific binding of protein-based drugs such as monoclonal antibodies with the synthetic availability of small molecules (4, 5). Unfortunately, also some limitations of the two classes are retained. Like small molecules, they have short biological half-lives. As for antibodies, peptides can in general not be used for intracellular targets and are, with few exceptions, requiring administration by injection.

1.1.2 Examples of peptide therapeutics

Many peptides drugs are natural products or derivatives thereof. Most of the approved peptide drugs can be broadly divided into two groups, peptides with human hormones as lead compounds or peptides acting on other targets for example the antimicrobial peptides (AMP). This chapter will mainly focus on hormone derived peptide drugs whereas other types will be described in chapters 1.1.3 and 1.2.1.

In humans, many peptides function as hormones, but can also play other roles such as neurotransmitters, growth factors and antimicrobial agents (4, 6). As such, peptides are ligands for many types of receptors such as G-protein coupled receptors (GPCR), growth factor receptors and ion channels. Peptides are often agonists of various signal transduction pathways. Hormones are produced and secreted in different organs such as the pituitary gland and the pancreas (7). Common peptide hormones include oxytocin, which plays a role in child birth, vasopressin, which controls the osmotic pressure of body fluids and somatostatin, a regulator of the endocrine system (8–10).

Given their important roles in human physiology, many naturally occurring peptide hormones have been used as lead compounds for therapeutic development (Table 1). Peptide drugs have been developed for many different therapeutic areas, including oncology, cardiovascular diseases, multiple sclerosis and diabetes. The most prominent peptide drug derived from a hormone is insulin, the blood glucose controlling hormone. Insulin is sometimes excluded from the category of peptide drugs due to its size of 51 amino acids, but is included here because of its importance. Over 400 million patients worldwide suffer from diabetes and are taking insulin daily (11). It was originally isolated from pig pancreas and introduced to the market as the first peptide therapeutic in the 1920s. In the 1980s, technological advancement had made it possible to recombinantly produce human insulin which then replaced the animal-derived insulins. Today a number of different insulin analogues are on the market. The native amino acid sequence has been altered in order to engineer fast-acting or basal insulin derivatives (Figure 2). The fast acting analogues are constructed with the purpose of forming less self-aggregates, and hence give a more rapid response after food intake. Examples of fast acting insulin analogues include lispro, aspart and glulisine (12). In contrast, basal insulin analogues are slow acting, mimicking steady secretion from a functioning pancreas.

Table 1. Approved peptide therapeutics which have used peptide hormones as lead compounds

Hormone lead	Peptide drug
Insulin	Insulin
	Lispro
	Aspart
	Glulisine
	Glargine
	Detemir
	Degludec
Vasopressin	Vasopressin
	Felypressin
	Ornipressin
	Desmopressin
	Terlipressin
Oxytocin	Oxytocin
	Atosiban
	Carbetocin
Somatostatin	Somatostatin
	Octreotide
	Lanreotide
	Pasireotide
Adrenocorticotrophic hormone	Corticotropin
	Tetracosactide
Calcitonin	Calcitonin
	Elcatonin
Gonadotropin-releasing hormone	Busreltin
	Leuprorelin
	Triptorelin
	Goserelin
	Gonadorelin
	Nafarelin
	Histrelin
	Deslorelin
	Cetrorelix
	Ganirelix
	Abarelix
	Degarelix
	Tesamorelin

Thyrotropin-releasing hormone	Taltirelin
Vasoactive intestinal peptide	Aviptadil
Brain natriuretic peptide	Nesiritide
Parathyroid hormone	Teriparatide
Amylin	Pramlintide
Bradykinin	Icatibant
Glucagon-like peptide-2	Teduglutide
α -melanocyte stimulating hormone	Afamelanotide
Glucagon-like peptide-1	Exenatide
	Liraglutide
	Lixisenatide
	Albiglutide
	Dulaglutide
Uroguanylin	Semaglutide
	Plecanatide

In this case the peptide sequence has been altered in order to reduce solubility and thereby prolong the release of the drug from the injection site into the blood stream. Insulin glargine is an example of this approach, a highly successful therapeutic among the top 10 selling drugs worldwide (2016 sales: 6.3 billion EUR = 7.5 billion USD) (13). Insulin detemir and degludec instead use fatty acid conjugation to prolong the plasma half-life. More recently, research has focused on developing a glucose responsive insulin (14).

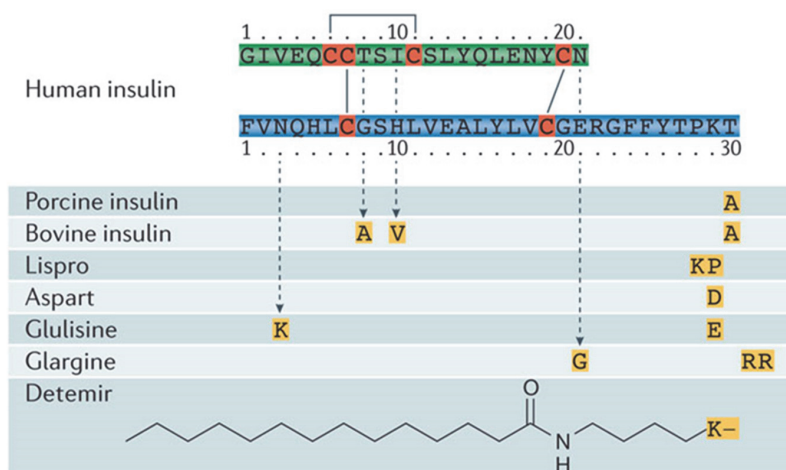


Figure 2. Sequences of human insulin and insulin analogues that have been approved and used for treatment of diabetes. Sequence differences between human insulin and the insulin analogues are highlighted in yellow. Residues involved in disulfide bridges are highlighted in red. Reprinted with permission from from (12), reprinting license nr. 4261840423681, © 2016 Macmillan Publishers Limited.

Besides insulin, the glucagon-like peptide 1 (GLP-1) analogues also account for a large portion of the peptide drug sales, with combined sales of 4 billion USD in 2014 (6). GLP-1 and analogues regulate blood glucose levels by stimulating insulin secretion (15). In contrast to insulin, this hormone cannot be administered in its native form due to rapid proteolytic degradation by dipeptidyl peptidase IV (DPP-IV). Instead peptides derived from the saliva of the Gila monster, a venomous lizard native to North America, which act as GLP-1 agonists and are resistant to degradation by DPP-IV, are used and marketed as exenatide and lixisenatide (Figure 3) (16). The best-selling GLP-1 analogue is liraglutide, with annual sale of around 2.5 billion USD. Liraglutide is the native sequence of GLP-1 with point mutations and fatty acid conjugation, which improve its pharmacokinetic properties (17). Albiglutide and dulaglutide are fusion proteins of native or point-mutated GLP-1 fused to human albumin and Fc fragment respectively. Formally the two are not classified as peptide drugs. All GLP-1 analogues were approved within the last 12 years. The latest addition to the GLP-1 analogues is semaglutide, which was approved by the FDA in December 2017 (18). This peptide includes non-natural building blocks and is conjugated with a fatty acid (19). The modifications increase biological half-life even further compared to liraglutide and would allow for once weekly administration.

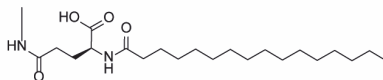
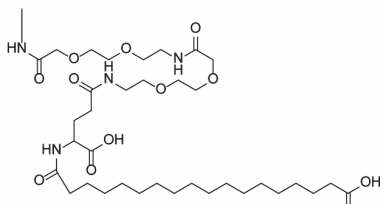
GLP-1	HAEGTFTSDVSSYLEGQAAKEFIAWLVKGR-NH ₂
Exenatide	HGEGTFTSDLKQMEEEAVRLFIEWLKDGGPSSGAPPPS-NH ₂
Lixisenatide	HGEGTFTSDLKQMEEEAVRLFIEWLKNGGPSSGAPPSKKKKKK-NH ₂
Liraglutide	HAEGTFTSDVSSYLEGQAAKEFIAWLVRGRG 
Semaglutide	HXEGTFTSDVSSYLEGQAAKEFIAWLVRGRG X = Aib 

Figure 3. Sequences of native GLP-1 and approved analogues for treatment of diabetes.

Another example of a hormone derived peptide drug is octreotide, an analogue of somatostatin approved in 1988 used to treat acromegaly and cancer. Octreotide is one of the best-selling peptide drugs with an annual sale of more than 1.6 billion USD in 2016

(20). Besides somatostatin, several other peptide hormones have served as lead compounds for therapeutic peptides including parathyroid hormone, vasopressin, gonadotropin-releasing hormone and oxytocin. Extensive medicinal chemistry approaches are often required in order to yield drug-like compounds. Interestingly, the top-selling non-insulin peptide drug is not derived from a hormone. Glatiramer, marketed by Teva as Copaxone was discovered serendipitously. It is a complex mixture of peptides of various length containing amino acid residues alanine, lysine, glutamic acid and tyrosine (21). Glatiramer is used to treat multiple sclerosis and it had annual sales in 2016 of 4.2 billion USD (22).

Many of the approved peptide therapeutics are analogues of natural hormones which have undergone medicinal chemistry approaches in order to tackle the intrinsic limitations of the molecular format. Much work is being performed within this field of peptide therapeutics and innovative approaches of chemically modifying peptide lead compounds is thought to be crucial for future development of peptides aiming at other targets than hormone receptors (23). Recent development of peptide drugs has shifted the focus from hormone derived analogues to peptides with novel molecular targets. These include cell surface receptors, antimicrobials, ion channels, structural proteins and enzymes (24).

As highlighted by the examples above, several peptide drugs are so called “blockbusters” with annual sales exceeding 1 billion USD. As of 2016 there are about 60 peptide drugs in the clinic, the exact number depending on the definition. Moreover around 170 are in clinical development and another 200 in preclinical development (6). These numbers suggest that there is substantial development in the field and that peptides as drug format is considered as promising, despite the fact that the “low-hanging fruit” in terms of hormone based peptide drugs have already been highly developed (25). The total sales of peptide based therapeutics, including insulin, is estimated to around 50 billion USD in 2015, which accounts for 5% of the total worldwide pharmaceutical market (6). The insulin derivatives are accounting for more than half of the total sales of peptide drugs. The two dominant therapeutic areas for which peptide drugs are used are metabolic disease and oncology (4). These areas are expected to grow further in the western world due to life-style and aging populations. The annual growth rate of peptide drug sales is estimated to 9-10%. The number of peptide molecules entering clinical development has been constantly increasing since 1990 (Figure 4) (24), with peak values of around 30 in 2010. However, in the last years these numbers are declining and will probably settle at a value of around 20 peptides entering clinical development each year. This trend reflects the saturation in the development of relatively straight-forward hormone-based analogues for validated targets but is counterbalanced by new innovative strategies of peptide drug development.

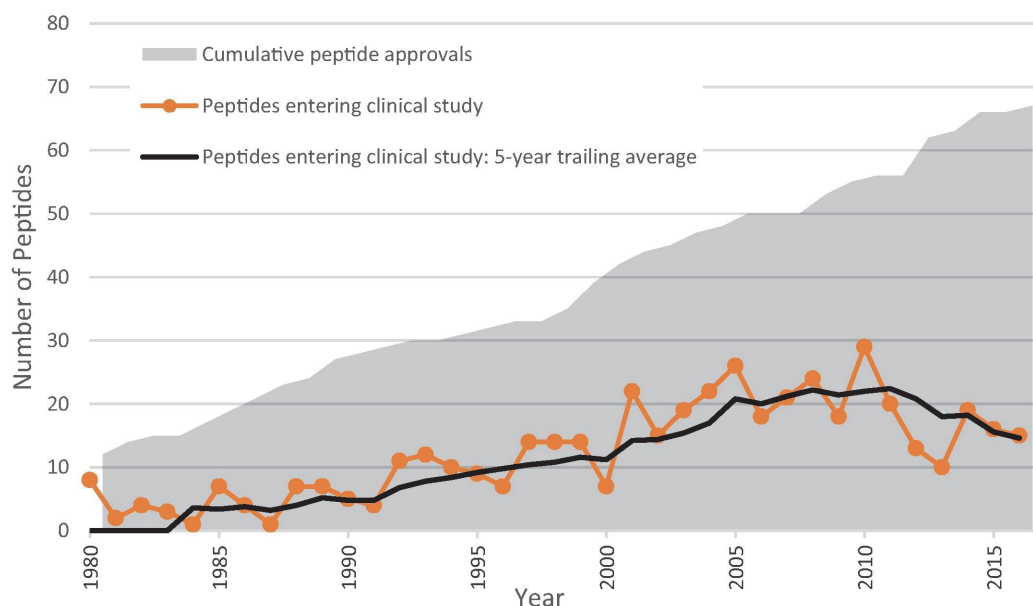


Figure 4. Cumulative number of peptides approved in major pharmaceutical markets and the number of peptides entering clinical development. Entry into clinical development is defined as the year of the first Phase 1 or pilot human study. Reprinted with permission from (24), © 2017 Elsevier Ltd.

1.1.3 Cyclic peptide therapeutics

Cyclic peptides have a number of advantages over linear peptides. First, cyclic peptides can generally bind to their targets with higher affinity. The cyclization constrains the backbone, which reduces conformational flexibility. The peptide can then be pre-organized toward its biologically active conformation and thereby improving binding affinity by reducing the entropic penalty upon target binding. Second, cyclic peptides are often less prone to proteolytic degradation as compared to linear peptides (1). The cyclic structure makes the peptide less accessible to proteases. Third, cyclic peptides bind more specific to their targets. This is also related to their reduced conformational flexibility. Cyclization is also used as a tool in the pursuit of making peptides beyond the rule of five having oral availability and cell permeability (26). While often native cyclic peptides are used as lead compounds also the conversion of linear peptides to cyclic analogues has been demonstrated (27).

New cyclization techniques as well as various novel screening platforms, the latter covered in the next chapter, propel the discovery of new cyclic peptide therapeutics (28). Generally, cyclic peptides can be constructed in four different formats namely: head-to-tail, head-to-side chain, side chain-to-tail or side chain-to-side chain (Figure 5) (29). Head-to-tail cyclization can mostly be readily achieved via peptide bond formation, but also other reaction types can be used such as native chemical ligation (NCL) or Staudinger ligation. For side chain cyclization a wide range of chemistries have been

utilized including disulfide bridge formation, ring-closing metathesis and azide-alkyne cycloadditions (30). An interesting approach in order to render more stable disulfide cyclized peptides by introducing a thioacetal was recently reported (31). This modification is prolonging the biological half-life of model peptides without compromising target binding.

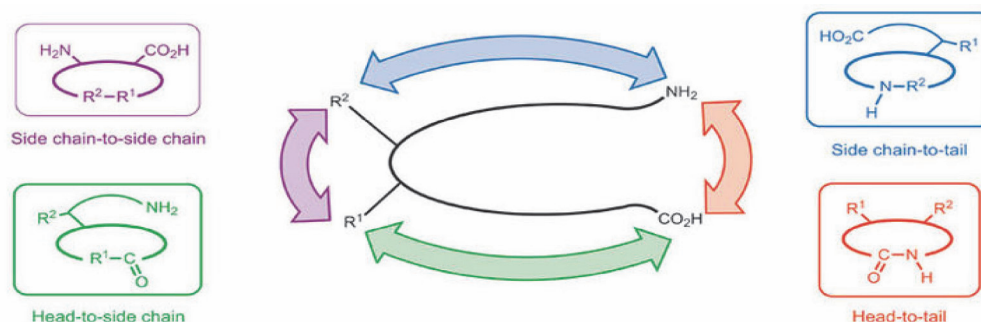


Figure 5. Four different approaches can be used in order to construct macrocyclic peptides. The different strategies can be used in combination for constructing multicyclic peptides. Reprinted with permission from (29), reprinting license nr. 4262470475054, © 2011 Macmillan Publishers Limited.

Oxytocin is an example of a cyclic peptide drug, which has been used in the clinic for a long time (Figure 6). It was the first peptide hormone to have its sequence determined and to be synthesized (32, 33), efforts for which Vincent du Vigneaud was awarded the Nobel prize in 1955 (34). The main biological function of oxytocin, which has been used in therapeutic purposes, is the induction of contraction of smooth muscles in the uterus during labor. This function has been exploited for promoting contractions during late stage of labor and for the prevention of postpartum hemorrhage (35). Oxytocin is however also active as a neuropeptide, influencing behavior. It has therefore recently been evaluated as a potential treatment for psychiatric disorders, including autism (36, 37).

An important class of peptide drugs are the AMPs. A majority of these peptides have a cyclic structure. The most well-known examples include the nonribosomally synthesized peptides vancomycin and cyclosporine A. The former was first isolated in 1957 from the bacteria *Streptomyces orientalis* and is used today to treat infections caused by methicillin-resistant *Staphylococcus aureus* (MRSA) (38). Several nonribosomally synthesized AMPs have been isolated, mainly from bacteria, including approved drugs such as polymyxin B and gramicidin C (39). More recently also ribosomally synthesized AMPs from different sources such as human, pig, frog and plants have been used as lead compounds and are in clinical trials for different applications (40, 41). New development of AMPs use various types of optimization of the naturally derived lead compounds (42). Cyclosporin A (Figure 6) was isolated 1970 from the fungus *Tolypocladium*

inflatum. It was first evaluated for its antifungal properties but is now widely used as an immunosuppressant following organ transplantation, for which it was approved by the FDA in 1983 (43).

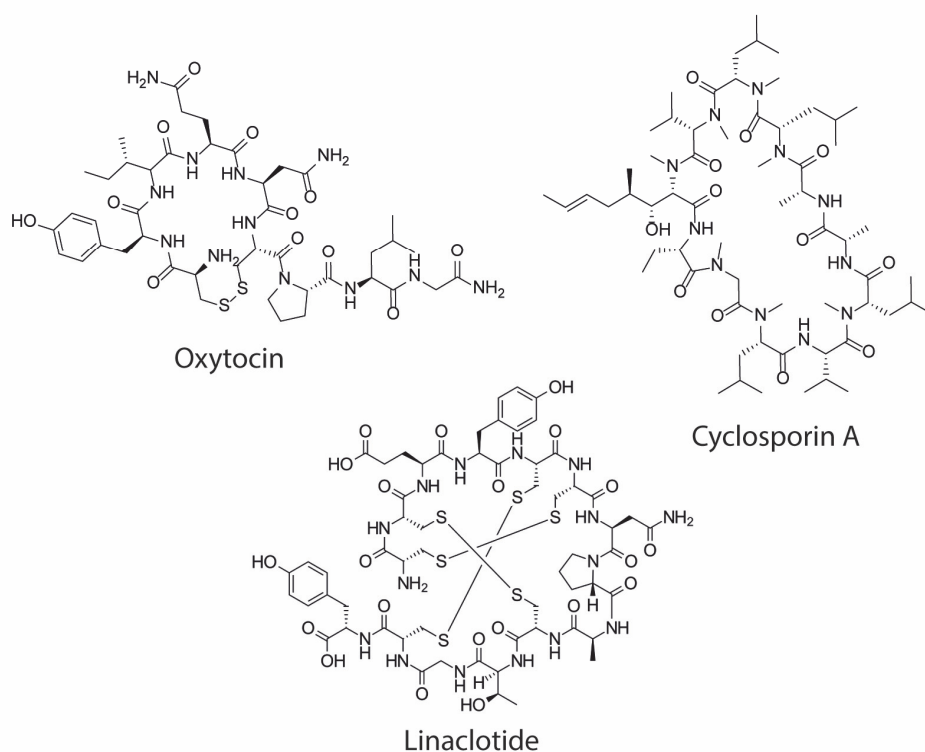


Figure 6. Chemical structures of three approved cyclic peptide therapeutics derived from different sources. Oxytocin is the native peptide hormone, cyclized through a disulfide bridge. It was the first peptide hormone to have its structure determined and to be chemically synthesized. Oxytocin was first approved in 1962. Cyclosporin A is a natural product found in fungus. It is head-to-tail cyclized and heavily N-methylated, which renders it orally available, a very rare property of a peptide therapeutic. Linaclotide is a derivative of a bacterial toxin, cyclized through three different disulfide bridges.

Several cyclic peptides have been approved as drugs in the last decade (44). This includes the three antibacterial peptides telavancin, dalbavancin and oritavancin, all belonging to the same class of molecules as vancomycin. Pasireotide, approved 2012, is a somatostatin analogue similar to lanreotide and octreotide, but with tailored receptor specificity for the sst1 and sst5 receptors, rendering it suitable for treatment of different tumor types and Cushing's disease (10, 45). Interestingly, during the medicinal chemistry approach the disulfide bond was removed and instead head-to-tail cyclization is employed. This is likely contributing to the largely increased half-life of 12 h. Another interesting example is linaclotide, which was approved in 2012 for the treatment of constipation-domi-

nant irritable bowel syndrome (Figure 6) (46–48). Linaclotide is a derivative of the bacterial enterotoxin ST of *E.coli* which causes diarrhea. ST is an agonist of guanylate cyclase C (GC-C), a membrane-spanning enzyme expressed on the luminal surface of epithelial cells in the intestine. Activation of this enzyme leads to chloride secretion and increased colonic transit. ST and linaclotide contain three disulfide bridges constraining conformation and providing proteolytic stability. Linaclotide is a truncated version of ST also containing amino acids substitutions rendering it even more proteolytically stable. The intestinal location of GC-C facilitates oral administration of linaclotide although the peptide is not orally available. GC-C is also activated by two endogenous receptor agonist peptide hormones guanylin and uroguanylin. In contrast to ST and linaclotide they contain only two disulfide bonds. Uroguanylin was used as a lead peptide in order to develop plecanatide (approved in 2017), differing only one amino acid from the native sequence (49, 50). Plecanatide is thought to be superior to linaclotide in the sense that it is actually a less potent agonist, therefore resulting in less side-effects such as diarrhea. A wide range of cyclic peptide are in clinical development and it can be expected that many more will be approved.

1.2 Strategies for developing peptide therapeutics

1.2.1 Peptides from natural sources

Historically, the most common strategy for developing peptide drugs has been to select a peptide with known biological effect as lead compound. This strategy has been described by several examples in chapters 1.1.2 and 1.1.3 of this thesis and medicinal chemistry approaches will be discussed in chapter 1.3. In this chapter examples of peptides from natural sources other than hormones and antimicrobial peptides are discussed.

A traditional source of bioactive peptides is venomous organisms. The conotoxins are one of the most prominent examples within this class. They are highly constrained peptides, containing several disulfide bridges and post-translational modifications, derived from cone snails (51, 52). Conotoxins generally target receptors and ion channels in nervous and muscle tissue. Ziconotide is a conotoxin approved by the FDA in 2004 for the treatment of chronic pain. Orally available conotoxins have been constructed by head-to-tail cyclization and the format is considered promising for therapeutic applications (53, 54).

Other well-known peptides isolated from natural sources include chlorotoxin, a 36 amino acid cysteine knot peptides found in scorpion venom (55, 56). The peptide has found application due to its tumor targeting abilities. Bivalirudin is a 20 amino acid direct thrombin inhibitor which was developed using the hirudin peptide found in the saliva of medical leeches as a lead compound (57, 58). Linaclotide and exenatide/lixisenatide as described above were derived from a bacterial toxin and saliva from the Gila monster respectively.

An interesting source which has been exploited is the cyclotides. These are a family of plant derived head-to-tail cyclized peptides of around 30-40 amino acids (59, 60). The peptides contain six cysteine residues which are oxidized to form three disulfide bonds which form a cyclic cysteine-knot topology (Figure 7) (61). This motif yields a very rigid structure, which is stable to thermal and chemical degradation as well as to proteolytic cleavage. Notably the highly stable structure also has the potential of rendering the cyclotides orally available (62). Cyclotides hence possess several intrinsic properties which overcome some severe limitations of peptide drugs. This makes them very interesting as lead compounds. The biological function of cyclotides is not yet fully understood but the primary intrinsic function is hypothesized to be host defense (63). For example, the first identified cyclotide, kalata B1, isolated from *Oldenlandia affinis* of the Rubiaceae family, has been shown to cause mortality in budworms. Kalata B1 has been used as indigenous medicine in Africa, where women drank tea made from *Oldenlandia affinis* to accelerate childbirth. This highlights the thermal stability and oral availability of the cyclotides.

While some cyclotides can be used for pharmaceutical applications as their native sequence, most recent applications focus on grafting biologically active peptide sequences identified by other techniques onto the cyclotide scaffold. The mostly utilized cyclotides for grafting are kalata B1 and momordica cochinchinensis trypsin inhibitor (MCoTI). Some recent and interesting examples include the development of a coagulation factor XII (FXII) inhibitor by substrate screening and grafting onto a MCoTI scaffold (64), an orally active bradykinin receptor antagonist developed by grafting a known antagonist peptide sequence onto kalata B1 (65) and a MCoTI graft which acts on intracellular targets, inhibiting p53 degradation (66).

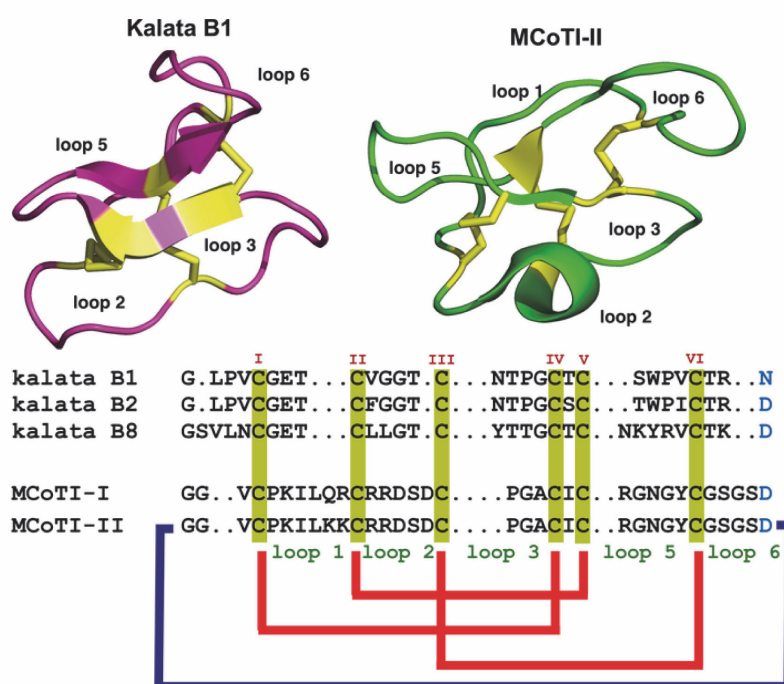


Figure 7. Primary and tertiary structures of cyclotides Kalata B1 (PDB ID:1NB1) and MCoTI-II (PDB ID:1IB9) belonging to the Möbius and trypsin inhibitor subfamilies respectively. The sequence of kalata B8, a hybrid cyclotide isolated from the plant *O. affinis*, is also shown. Conserved Cys and Asp/Asn (required for cyclization) residues are marked in yellow and light blue, respectively. Disulfide connectivities and backbone cyclization are shown in red and by a dark blue line, respectively. Adapted with permission from (61), reprinting license nr. 4262540872131, © 2017 Wiley-VCH Verlag GmbH&Co

1.2.2 Protein epitope mimetics

Inhibitors of PPI can be designed rationally based on peptide sequences at the interface of interacting proteins (67). At the interaction sites, proteins frequently have well defined secondary structures. The mimicking of these interacting epitopes is often useful in the development of drugs aiming at challenging targets such as PPI. The term “peptidomimetics” is sometimes used to describe such compounds. There is no clear

rule to define peptidomimetics, however recently, a classification system was proposed, in order to group the different types together (68). In this chapter I will describe peptidomimetics having a peptide-based scaffold, which are mimicking the binding epitopes of proteins, mainly with a focus on secondary structure. Small-molecule peptidomimetics will be excluded. The chapter will include medicinal chemistry approaches which aim at introducing or locking secondary structures. Some of this work is related to backbone modifications, which is a broader field also serving other purposes, but will be included in this chapter.

A common binding motif which is often found as a key mediator in PPI is the α -helix (69). Therefore peptide sequences having an α -helical conformation, derived from a protein, are attractive as ligands of therapeutic targets (70). Shorter peptides are however not stable in their α -helical conformation in solution (71) and many strategies have been developed in order to lock them in the correct conformation for binding. One of the most well-known approaches for locking peptides in a α -helical conformation is peptide stapling. The principle works by selecting two residues that have side-chains pointing towards the same face of the helix and connecting them covalently. The residues which are normally stapled together are i and $i+3$, $i+4$, $i+7$ or $i+11$. Different chemistries have been utilized in order to achieve the covalent linkage, with the most common being an all-hydrocarbon cross link achieved through the incorporation of unnatural amino acids undergoing olefin ring closing metathesis, first established by Verdine and co-workers (Figure 8A) (72). The length of the side-chain in the staple can be varied depending on the distance of the connected residues. The properties of the stapled peptide are further tuned by varying parameters such as staple position, stereochemistry and number of staples. Lately computational tools have been used in the design of stapled peptides (73). Hydrocarbon-stapled peptides can be generated readily on automatic peptide synthesizers and have been developed for a range of targets, both intracellular and extracellular (74, 75). In addition, the stability of peptides is often improved upon hydrocarbon stapling. Other peptide stapling strategies involving only the side chains of the peptide building blocks include amide bond formation, azide-alkyne cyclo-addition, disulfide bridge or thioether bond (Figure 8) (76).

A slightly different approach in which the N-terminal intramolecular hydrogen bond is replaced by a staple, termed 'hydrogen-bond-surrogate' has recently been established and shown to stabilize helicity (77). Some stapling techniques involve building blocks external to the side chains such as photoswitchable linkers or double azide-alkyne cyclo-additions (76, 78). One interesting approach was recently reported in which thiol reactive linkers were used to generate peptides stapled through two cysteine residues in fixed positions in a phage display library (79). Using this strategy α -helical binders to β -catenin were developed. Stapled peptides have also been shown compatible with and optimized using one-bead-one-compound (OBOC) libraries (80). Recently the tight

binding of the α -helix in a PPI was exploited by Huhn and co-workers to develop covalent inhibitors to block the anti-apoptotic interaction of BH3 and BFL-1 (81). The group of Fairlie have also utilized peptide stapling for α -helix enhancement in their development of more potent analogues of GLP-1 and covalent inhibitors of Bcl2 (82, 83).

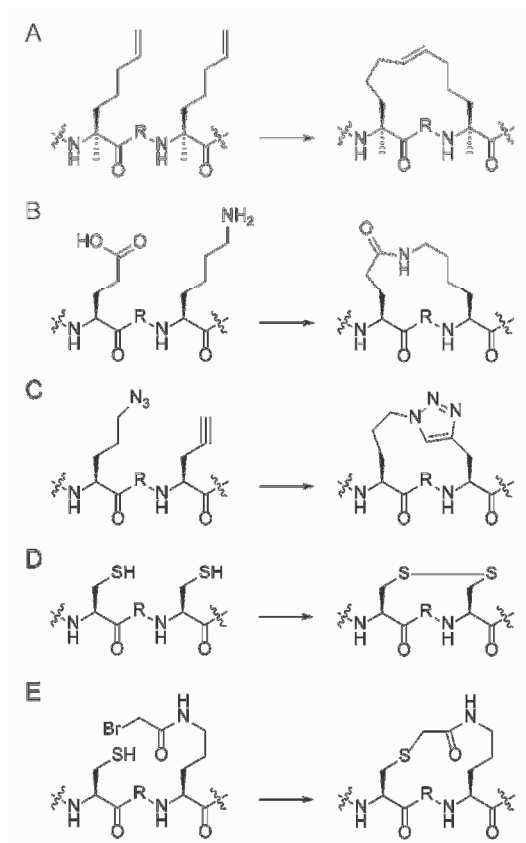


Figure 8. Overview of different chemistries utilizing only amino acid building blocks for peptide stapling. (A) Olefin ring closing metathesis (B) Peptide coupling (C) azide-alkyne cyclo-addition (click chemistry) (D) Disulfide bridge formation (E) Thioether formation

Another well-known class of peptidomimetics is the foldamers, which possess inherent propensities for forming secondary structures and are often used to mimic helices. In this case mainly backbone modifications lead to a stabilization of the helix. The concept was introduced in the 1990s, where it was found that peptides composed solely of β -amino acids folded into helical structures (84). Based on their substitution pattern on the carbon atoms 2 and 3 the beta amino acids can be divided into the types β^2 , β^3 and $\beta^{2,3}$ (Figure 9). The introduction of β -amino acids also renders the peptides highly stable towards proteolysis. However, the β -peptides do not form α -helices and as a consequence their side chains do not resemble the same patterns as of α -helical peptides. With the purpose of developing peptides adopting the native α -helical formation yet stable to proteolysis, Gellman and co-workers designed hybrid peptides composed of β - and α -amino acids (85). If the distribution and proportion between the two building

blocks is properly chosen, the resulting peptide very closely resembles an α -helix. Patterns such as $\alpha\alpha\beta$, $\alpha\alpha\alpha\beta$, and $\alpha\alpha\beta\alpha\alpha\beta$ have been found by crystallography to form α -helical secondary structures. The hybrid formats of α/β , α/γ , β/γ peptides as well as the different types of β -amino acids together with the introduction of the helix inducing unnatural building block amino isobutyric acid (Aib, Figure 9) provides a high level of diversity for foldamers (86). Peptide based foldamers have been generated against a wide range of therapeutic targets and provide a promising format for further development (87).

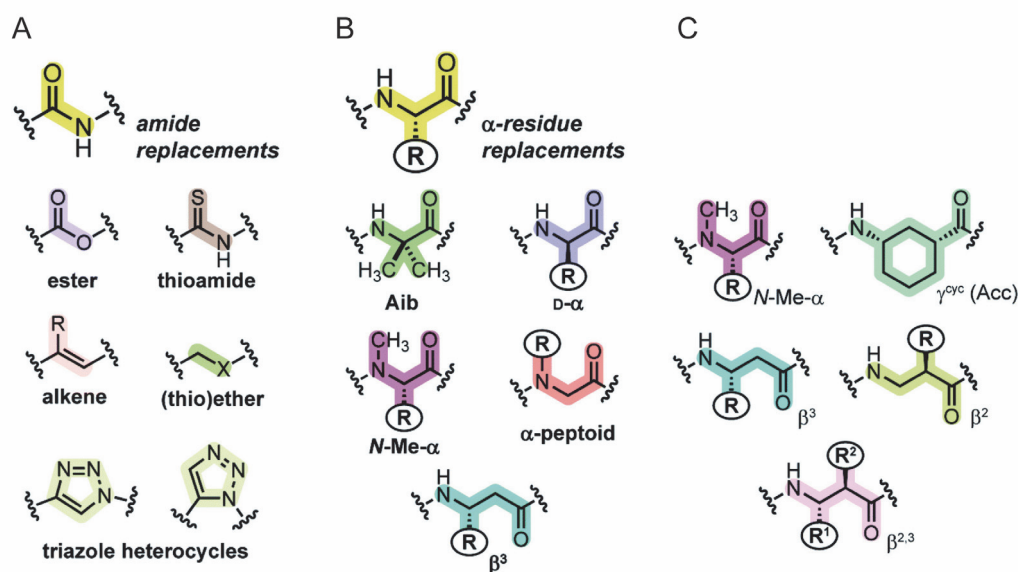


Figure 9. (A) Backbone replacements of the amide bond utilized in foldamers. (B) Modifications of the side chains on building blocks in foldamers. (C) Constrained building blocks and β -amino acids for secondary structure stabilization Reprinted with permission from (88) reprinting license number 4270191028188, © 2014 The Royal Society of Chemistry.

In the generation of foldamers, not only β -amino acids have been used for backbone modifications. The replacement of amide bonds in the peptide backbone with ester, thioester, thioamide, alkene or triazole heterocycles influence the hydrogen bonding patterns of the structure and can be used to design foldamers with enhanced properties (Figure 9) (88). Conformationally constrained cycloalkane β or γ amino acid building blocks have also been used in the backbone to stabilize either helical or sheet secondary structures (87, 88). In one recent example, Grison and co-workers design a mimic of the p53 helical structure using an alternating sequence of trans-2-aminocyclobutanecarboxylic acid and γ -amino acids (89). The peptides were designed so that interaction forming residues would remain in the same position as in the native p53. The constructed peptides efficiently mimicked the α -helical structure, were resistant against proteolysis and displayed strong target affinity. In a similar approach 5-

membered thiazole-based γ -amino acids were used by Mathieu et al. in an alternating fashion to induce helical conformations (90).

While one focus of backbone modification has been secondary structure mimicking, the strategy can at the same time be used for improving proteolytic stability of peptide, as highlighted by Gellman and others (85). In a systematic study of 4 commonly used backbone modifications (N-methylation, C- α -methylation, β -amino acid incorporation and D-amino acid incorporation) Werner et al. found significant differences between the modifications in the ability to protect a peptide sequence against degradation (91). The most efficient modification was the introduction of D-amino acids. Also the position of the backbone modification influenced the level of protection. Interestingly, the C- α -methylated Aib also provided a high level of protection, hence there might be a demand of α -methylated amino acids bearing natural (or unnatural) side chains for target interactions. However, the study used an artificial peptide sequence and only chymotrypsin as proteolytic pressure, therefore the results are not fully representing degradation of biologically active peptides in blood plasma, but could be considered as an indication of how to effectively improve proteolytic stability. A simple yet very efficient backbone modification is the replacement of a peptide bond with a thioamide bond near or at the proteolytic cleavage site. This approach was recently utilized to improve the stability of therapeutically relevant peptides GLP-1 and gastric inhibitory polypeptide (GIP) (92). A single backbone modification improved the stability of these peptides 750-fold as compared to the native sequences, without compromising the biological activity.

The group of Cai have used extensive backbone modification for generating a new class of peptidomimetics; γ -AA-peptides (Figure 10) (93, 94). The construct was inspired by the structure of peptide nucleic acids (PNA) in which the bases are attached to the nitrogen atom in a N-(2-aminoethyl) glycine backbone. The γ -AA-peptides consist of such building blocks with functionalities introduced via side-chains at the nitrogen atom and at the γ -carbon. The peptides are built up using SPPS and macrocyclic structures can be achieved through various approaches such as head-to-tail cyclization or thioether linkage (95). This molecular format is highly stable and has been shown to mimic various properties of biologically active peptides, such as cell penetration and helical structures. Moreover, combinatorial libraries of γ -AA-peptides have been constructed using the OBOC approach and peptidomimetics against several targets have been isolated.

Other notable backbone modifications of peptides include the replacement of the α -carbon by nitrogen which renders azapeptides. The peptides can be constructed having a side-chain attached to the nitrogen in α -position or without side-chain. Introduction of azapeptide bonds induces β -turn motifs and proper incorporation can be identified by "azascan" (96). A number of other strategies for backbone extension incorporating

heteroatoms have also been demonstrated such as α -aminoxypeptides, α -hydrazionpeptides and β -aminoxypeptides.

β -sheet mimetics are less common in the literature as compared to α -helix mimetics but strategies to induce and stabilize this secondary structure in peptidomimetics exist. Three general approaches are common namely the use of turn mimetics, macrocyclization and β -strand enforcing amino acids (68). Turn inducing amino acids that have been used include L-Pro, D-Pro and Gly. Also conformationally restricted bicyclic dipeptide building blocks have been used for this purpose (97).

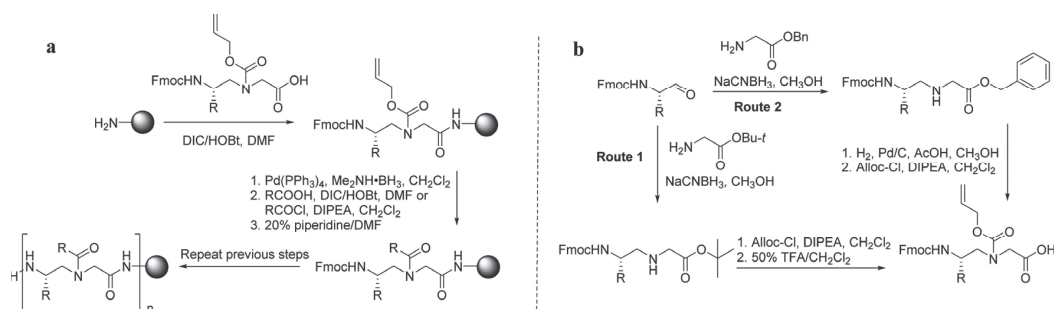


Figure 10. (A) The synthesis of the γ -AA-peptides is performed using metal catalysis and standard peptide solid phase chemistry. The diversity of the library is introduced via the side chain of the building block as well as through the reaction with a wide range of commercially available carboxylic acids or acetyl chlorides. (B) The N-protected building blocks are available through two synthetic routes. Reprinted with permission from (93), © 2016 American Chemical Society

1.2.3 Strategies for de novo development of peptide therapeutics

Peptide therapeutics can be developed de novo by screening large libraries of peptides with random sequences. A number of display systems have evolved in order to facilitate the screening of large peptide libraries. In general an in vitro display system consists of three steps: the generation of a combinatorial library where phenotype is linked to genotype, multiple rounds of biopanning and identification of the selected compounds (98). The system most used is phage display. In phage display the DNA of bacteriophages is modified so that a combinatorial peptide or protein sequence is fused to one of the coat proteins on the surface of the phage (Figure 11). A random library can be constructed using NNK codons, the size and structure of the library can be selected according to the type of the desired molecular format. In this way phenotype (displayed peptide) is linked to genotype (DNA of phage). The diversity of a phage display library is typically around 10^9 - 10^{11} , and libraries are required to be designed accordingly in terms of size. Two different coat proteins are normally used; pVIII which can display multiple copies of the combinatorial peptides or pIII which displays 1-5 copies. The phage library is typically screened against an immobilized protein target and several rounds of biopanning

ensure the enrichment of binding clones. These are subsequently DNA sequenced, lately by next generation sequencing (NGS) which allows for thorough sequencing and analysis of the output phage pool. Phage display has been used extensively for the identification of binders to therapeutic targets and has yielded over 40 biological drug candidates which have entered clinical trials, out of which most are monoclonal antibodies (99). A number of the phage display identified biologicals have been approved as drugs, including Adalimumab, the world's best-selling drug with annual revenue of 16.1 billion USD in 2016 (100). Phage display of peptide libraries have also yielded drugs which are used in the clinic, for example romiplostim, trebananib and peginesatide, the latter however withdrawn (44, 99, 101).

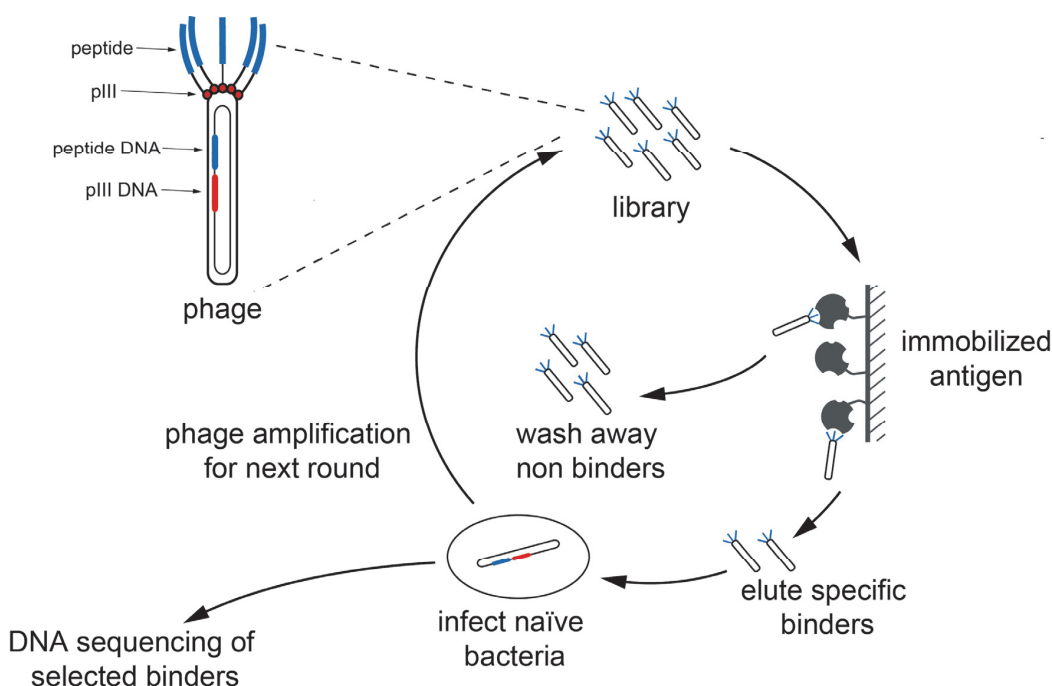


Figure 11. In phage display a combinatorial library of peptides is displayed on the coat protein of a filamentous phage. The peptides are encoded by DNA encapsulated in the phage. Generally, libraries are subjected to several rounds of selection against an immobilized target. After each round, binders are amplified by infection of bacteria. Hit sequences are identified by DNA sequencing.

With the purpose of overcoming the intrinsic limitations of peptide drugs and to enhance binding, a number of strategies have been introduced into phage display. Chemical modifications and various cyclization techniques have been utilized (102). Some notable innovative approaches of using phage display include the modification of peptides with carbohydrates (103) and encoding of peptide modifications using silent barcodes (104). Mirror image phage display is another technique which has been used to develop D-antagonists to HIV and cancer related targets (105, 106). A bicyclic peptide format has been used together with phage display for developing ligands for a wide range of targets

and will be reviewed in detail in chapter 1.3. Other in vitro display methods which utilize a cell based system are bacteria and yeast display, in which peptide libraries are displayed on the cell surface.

In vitro displays systems which omit the use of a cell based platform are also available. In mRNA display the combinatorial peptides are fused to their encoding mRNA directly (Figure 12A). In contrast to phage display, these approaches do not require a transformation step, which is the main limitation for diversity (98). mRNA display libraries can readily reach a diversity of 10^{13} . These systems also have another major advantage over phage display, which is the potential of incorporating unnatural building blocks directly in the combinatorial library. This potential has been widely exploited by Suga and co-workers by the development of the FIT and RaPID systems which allow for the in vitro selection of peptides incorporating virtually any natural or unnatural amino acid (107, 108). The core of the FIT system are artificial ribozymes, 'flexizymes', which allow transesterification of the 3'-hydroxy group of tRNA with an activated amino acid of choice. When combined with an mRNA display system it is called RaPID. This approach has been used to identify peptides to different therapeutic targets, macrocyclic peptides using various cyclization chemistries and peptides likely to be cell-permeable (109–111). A different in vitro screening technology termed 'split-intein circular ligation of peptides and proteins' (SICLOPPS), utilizes the split-intein mechanism to generate libraries of cyclic peptides expressed intracellularly (112). This approach is particularly powerful when used in a reverse-two-hybrid system, for example in *E. coli*.

One approach which in contrast to the above mentioned in vitro screening platforms does not use any biological system is the OBOC library (Figure 12B) (113, 114). Here combinatorial peptide libraries are synthesized on solid support using the split and pool technique. This allows for a high diversity and for the incorporation of unnatural building blocks. Similar to the in vitro techniques the libraries are screened and binders identified. This can typically be done either by Edman sequencing, mass spectrometry or lately by DNA encoding (115). For example the OBOC technique has been used to discover tumor targeting peptides (116).

Several de novo developed cyclic peptides are present. Polyphor has used a protein epitope mimicking (PEM) discovery platform to develop cyclic peptides for various targets (117, 118). This was done by grafting pharmacophores of naturally occurring host-defense peptides onto PEM scaffolds followed by iterative synthesis and optimization. Murepavadin and balixafortide are antimicrobial and anti-cancer compounds developed using this technology. Other de novo developed cyclic peptides include APL-2, ALRN-6924 and RA101495 (44). The peptides were developed by phage display and mRNA display technologies.

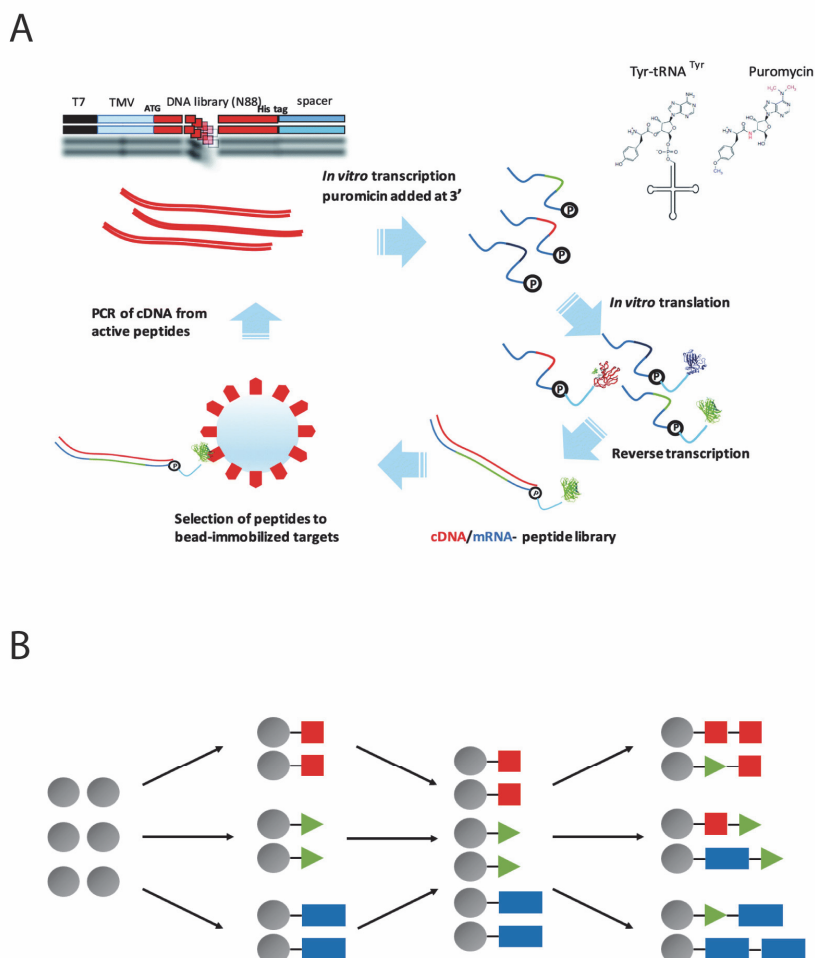


Figure 12. (A) Overview of the mRNA-display in vitro selection process. After transcription of the library, the mRNA is modified with puromycin at the 3' end. Upon translation of the mRNA, the peptide is covalently bound to the mRNA that encoded it. The mRNA is then reverse transcribed to cDNA and selection is performed against an immobilized target. The mRNA portion of this display construct is then reverse transcribed. The bound peptides are eluted and their encoding DNA is then amplified by PCR, thus completing the first round of selection and amplification. (B) OBOC libraries can be readily constructed using traditional combinatorial chemistry employing split-and-pool synthesis. The modular nature of amino acids makes it ideal for peptide libraries, but the technique can be used for any type of modular chemistry. The solid support, consisting of beads, is split into equal parts which is each reacted with a different reagent. The beads are then pooled together and subsequently split again and reacted with another building block. These steps are repeated until the desired size of the library is reached. The library is then screened against a target and binding compounds are identified, for example using a DNA tag or by MS. A reprinted with permission from (98), reprinting license number 4264261154793 © 2016 The Royal Society of Chemistry.

1.3 Medicinal chemistry of peptides

1.3.1 Enhancing properties of peptides

While peptides have many properties that make them suitable for drug development, they also possess several limitations which need to be overcome. Peptide lead compounds often have to be improved by chemical means in order to combat these shortcomings. One of the most pronounced drawbacks of the peptide format is the often high susceptibility to proteolytic cleavage, which renders peptide drugs metabolically unstable. In addition, they are generally rapidly cleared from the circulation due to excretion. Another limitation of peptide-based drugs is their poor membrane permeability. This limits the use of peptides for intracellular targets and for administration orally. As with small molecule drugs, modifications can also be required to influence the affinity of the peptide. Medicinal chemistry approaches are sometimes necessary in the development of hormone-based peptide drugs to tailor the affinity for certain receptor subtypes in order to achieve the desired pharmacological effect. In a similar manner, the specificity of peptide drugs can be adjusted with the purpose of minimizing off-target binding which can result in side-effects. For de novo developed peptide lead compounds, it is often required to improve the affinity and/or specificity of the initial hit compounds.

A number of different strategies exist for the improvement of the pharmacodynamic and pharmacokinetic properties of peptides. The perhaps most widely used approach to address the susceptibility to proteolytic cleavage of peptide drugs is the introduction of D-amino acids. If D-amino acid insertion is tolerated in terms of affinity, specificity etc. it can be a useful strategy to render peptides less susceptible to proteolytic cleavage. The D-amino acid can be used to replace an amino acid at a known or identified proteolytic cleavage site. As the D-amino acid is not recognized by the protease, the peptide remains intact. A different approach to protect peptides from exopeptidase cleavage is to protect the end of the peptides. The principle is again to make the ends less recognizable by the proteases. This can be achieved by acetylation of the N-terminal and/or amidation of C-terminal. Also other alkylation chemistries can be used. Another strategy with the same goal is to introduce or modify cyclization of the peptide backbone. Cyclic peptides are generally more stable than linear peptides. Therefore, again if allowed in terms of target binding, cyclization of a linear peptide lead can be useful for improving stability. Also replacement of an existing cyclic backbone with a different cyclization chemistry can be used. In chapter 1.2.2 backbone modifications of protein epitope mimetics were discussed. Many backbone modifications have been used to improve the stability of peptide lead compounds. This includes the introduction of β -amino acids. Similarly to the D-amino acids they are not recognized by proteases. Additionally, peptide bond surrogates are used with the same purpose (Figure 9).

The pharmacokinetics of peptides can also be addressed using chemical modifications. These can be based on conjugations. This includes the conjugations to larger proteins which remain longer in the circulation such as albumin or Fc fragments, but also the conjugation to poly ethylene glycol (PEG) of various chain length, which can largely improve the plasma half-life of peptides. Instead of a covalent conjugation, a moiety which binds albumin, for example a fatty acid, can be introduced in the peptide for prolonging the half-life. As shown by the basal insulin analogues, modifications which affect self-aggregation can also be used to tailor pharmacokinetics.

Different types of methylation patterns have been applied in peptide medicinal chemistry in order to improve the properties, mainly membrane permeability, of peptide lead compounds. One of the most common methylation sites within peptides is the amide bond nitrogen atom in the backbone of the peptide. N-methylation functionalities are present in nature, the most common being histone N-methylation, which plays an important role in epigenetics (119). In this case the methylation occurs on a lysine or arginine side chain. No N-methylated peptide bonds have been observed in mammals, however non-ribosomally synthesized peptides from different natural sources contain N-methylated peptide bonds. These peptides have been found to have a variety of biological functions. Most of the naturally occurring N-methylated peptides are found in sources such as fungi, bacteria or plants. Examples include ennatiins, hemiasterlins, echinomycin and bouvardin. A well-known example of a N-methylated peptide is cyclosporine A, which has been mentioned earlier in the chapter about cyclic peptide therapeutics. Cyclosporine A has a head-to-tail cyclized scaffold and 7 out of 11 peptide bonds are N-methylated. The peptide is orally available and diffuses passively over membranes targeting intracellular PPI. N-methylation of amide bonds provide a number of properties for peptides which are attractive in drug development. Upon N-methylation the peptides are less susceptible to proteolysis and more importantly it can increase oral availability and cell permeability (120). However, the modification influences conformation of the peptide bond as well as the directions of the side-chains surrounding the N-methylated peptide bond. In addition, hydrogen bonding capability is demolished, influencing the secondary structure of the peptide. Besides N-methylation, peptides are sometimes also methylated at the α -carbon. However, this approach is not as common, likely due to its synthetic complexity and lack of commercially available building blocks (121). One α -methylated amino acid which is widely used is Aib (alpha methylated Ala). As mentioned above, it is often used to induce helices but has also been used for proteolytic stability improvement.

A different form of N-alkylated peptide backbone is the peptoid format. A peptoid residue is a N-substituted glycine with a side chain attached to the backbone nitrogen instead of the α -carbon as in normal peptides (122). Peptoids are highly resistant to proteolytic cleavage due to the lack of backbone amide bonds. They have also been shown to

have superior membrane permeability as compared to peptides, with up to 26-fold increase observed (123, 124).

While many of the medicinal chemistry strategies mentioned above are used for improving stability, half-life or permeability, they can also be used for improving or tailoring target affinity and specificity of peptide drugs. When working with these properties it can also be of great importance to vary the side-chains of the peptide. By introducing unnatural amino acids, the interactions of the peptide with its target can be strongly influenced. A wide-range of protected unnatural amino acid building blocks are commercially available, allowing for facile synthesis and rapid screening of peptide libraries.

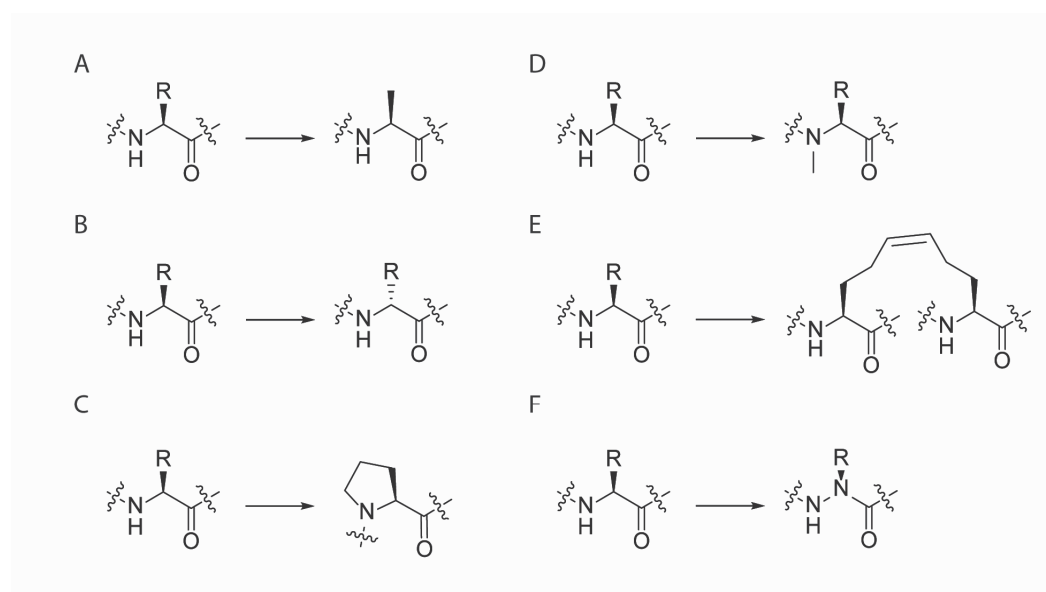


Figure 13. A number of different scanning strategies are utilized in order to identify positions in the peptide sequence susceptible for optimization, for example in terms of affinity and/or stability. (A) Alanine scan (B) D-amino acid scan (C) Proline scan (D) N-methylation scan (E) Stapling scan (F) Aza peptide scan

It is sometimes necessary to identify positions within the peptide which can be targeted by medicinal chemistry approaches. For example, proteolytic cleavage sites or pharmacophores can be identified. A number of scanning strategies have emerged where peptide leads are varied systematically in order to identify important residues for binding but also position where variations to the natural peptide structure are allowed in order to increase stability (Figure 13) (125). The simplest method is alanine scanning, in which single residues are mutated to alanine in order to identify the side chains responsible for binding. Other scanning strategies include D-amino acid scan, proline scan, N-methylated scan, lactam scan, peptide-staple scan and aza-amino acid scan. Many of these scanning techniques strive to allow for the incorporation of unnatural building blocks and/or change to the backbone structure of the peptide. The type of scan utilized is constantly evolving and depends on factors such as lead peptide, target, and time constraints.

1.3.2 Examples of modified peptides

An early example that nicely illustrates the power of medicinal chemistry applied to peptides is desmopressin, an analogue of vasopressin, the plasma osmolality regulating hormone. Vasopressin is rapidly degraded in vivo, with a half-life of only 4-20 minutes (9). Desmopressin was developed in the 1960s and substituting the Arg-8 residue in vasopressin to D-Arg was done in order to reduce proteolytic cleavage by trypsin. In addition, desmopressin also has a deaminated N-terminal, which protects from exopeptidase cleavage. These modifications resulted in a highly stable vasopressin analogue, with an elimination half-life of more than 3 h (126). The high stability also provided a foundation for alternative formulations such as oral or nasal (127). It is worth mentioning that the modifications also resulted in a receptor selectivity, (desmopressin is selective for V2, whereas vasopressin is an agonist of V1 and V2) which renders desmopressin antidiuretic but with less vasoconstrictor activity (128). Other vasopressin analogues have been developed in parallel with desmopressin, such as terlipressin, which retains the vasoconstrictor activity but has increased stability through natural amino acid substitution and additions, namely Arg8→Lys and Gly-Gly-Gly at N-term (9, 129). Extensive medicinal chemistry approaches have been undertaken in order to tailor the receptor selectivity of vasopressin analogues, including the use of unnatural amino acids (130).

Another prominent example where peptide engineering, including the use of D-amino acids, was applied to improve proteolytic stability is the development of octreotide, an analogue of somatostatin (Figure 14). In this case, the pharmacophore of the peptide was identified as residues 7-10 in the cyclic 14-mer (131). The cyclic structure was kept, with two cysteine residues flanking the pharmacophore sequence (131, 132). In the sequence Trp was replaced by D-Trp. However, this peptide was initially less active than natural somatostatin. The activity was regained by introducing D-Phe at the N-terminus and a threonol building block at the C-terminus in order to mimic the residues of native somatostatin. The half-life of somatostatin is normally 2-3 minutes whereas octreotide has a half-life of 90-120 min (133). It should be mentioned though that similarly to desmopressin, octreotide has an altered receptor affinity profile as compared to the natural lead peptide. Other somatostatin analogues have also been developed, in which synthetic building blocks are included, namely lanreotide and pasireotide. Lanreotide has similar pharmacodynamics as octreotide, whereas pasireotide was engineered to have a more universal binding profile similar to native somatostatin (10, 134, 135). In addition to the above mentioned pharmacophore, the developers of pasireotide identified Lys4, Phe6 and Phe11 as important for receptor activity. For improved stability it was decided to use a hexameric peptide scaffold rather than an octamer as used in octreotide and lanreotide. The Lys4 is incorporated as hydroxyproline aminoethylurethane residue, which is also used for replacement of the disulfide bridge with a backbone cyclization. Phe6 is not represented, perhaps the proline ring resembles its functionality. Phe7 is represented

by an optimized unnatural phenylglycine, Trp8 is replaced by D-Trp, Lys9 and Phe11 are kept native. Interestingly, Thr10 is not identified as essential for universal receptor binding. This residue is however replaced by O-benzyl-tyrosine. More recently, work has been undertaken to replace the Phe-residues in the native somatostatin sequence by unnatural analogues with decreased or increased electron density in the aromatic rings (136, 137). By doing so, the authors managed to tune the receptor type affinity as well as to improve the stability of the peptide. A further study on somatostatin analogues could adjust the receptor specificity and antagonism/agonism by the incorporation of N-imidazolebenzyl-histidine or naphthylalanine in the Trp8 position (138). In another study, the authors incorporate alpha-dialkylated residues with the purpose of constraining the backbone of the macrocycle (139).

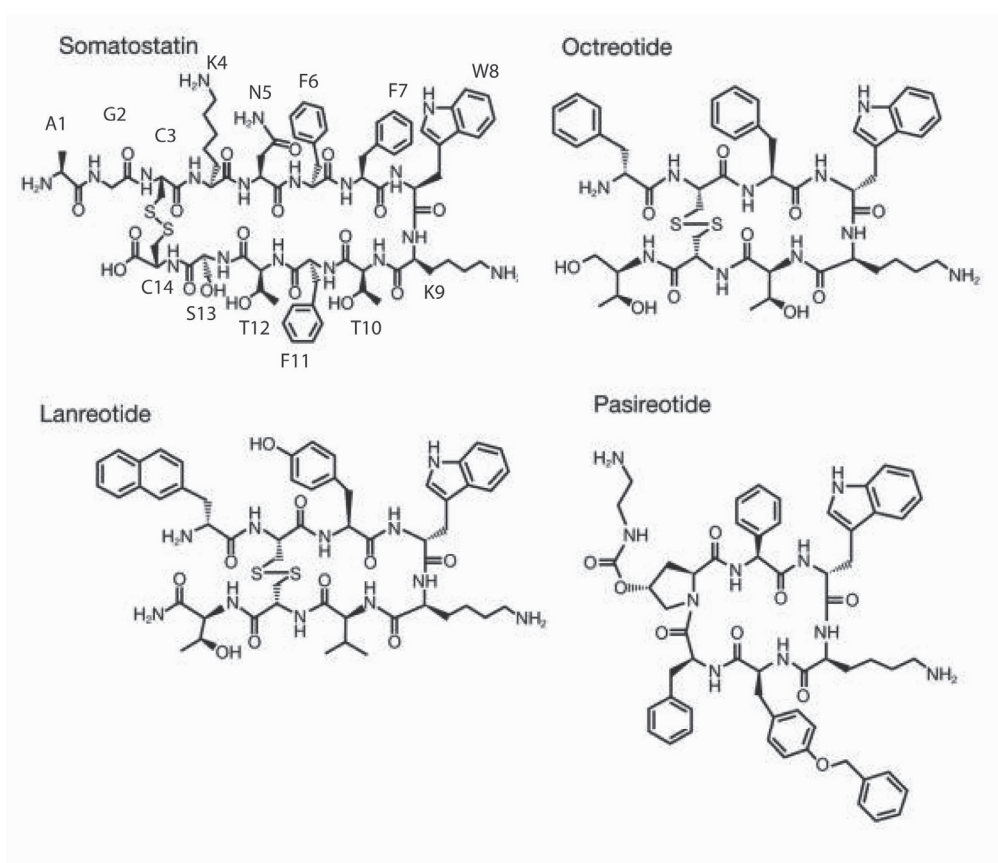


Figure 14. Several analogues have been developed using the peptide hormone somatostatin as lead sequence (upper left). The pharmacophore is generally identified as amino acids F7, W8, K9 and T10. Reprinted with permission from (135) reprinting license number 4264280910391, © 2012 Golor et al.

There are further examples where unnatural amino acids have been used to improve pharmacokinetics. Carbetocin used oxytocin as a lead peptide and it was found that by deaminating the N-terminus and substituting the disulfide bridge with a thioether the duration of action was increased (140). Further, the hydroxyl group of a tyrosine was

changed to a methyloxyl. Together these changes improved the half-life more than 10-fold to 42 minutes (141). There are however some indications of changed pharmacodynamics of carbetocin as compared to native oxytocin (141, 142). Several analogues of the nine amino acid inflammatory mediator bradykinin have been developed through extensive medicinal chemistry campaigns for both agonistic and antagonistic functions as well as receptor subtype specificity (143). Of these, the only approved drug is icatibant, which was approved in 2008 for the treatment of hereditary angioedema (144). The peptide is composed out of five natural residues and five unnatural, including three proline derivatives (145). The modifications render it proteolytically stable with a half-life of 1–2 hours (146). The development of somatostatin and oxytocin analogues highlight the rising importance of unnatural amino acids and much work is being undertaken in the development of their synthesis and incorporation in drugs (147–149).

Systematic scanning approaches have been used to improve properties of peptides and a few examples are discussed below. Miranda and co-workers were able to substantially improve the stability of calcitonin gene-related peptide receptor antagonists by systematically replacing labile residues by citrulline, homoarginine and other unnatural building blocks (150). Frey et al studied the SAR of Bak derived peptides and were able to improve the potency by introducing non-canonical amino acids (151). Murray and co-workers used an enhanced form of the alanine scan termed multi attribute positional scan, substituting residues of the lead peptide not only by alanine but also by representative basic, acidic and hydrophobic residues (152). The authors were thereby able to improve properties of peptide toxin lead compounds targeting ion channels.

In an interesting approach Biron and co-workers applied a N-methyl scan using the somatostatin analogue Veber-Hirschmann cyclic hexapeptide as a lead compound (Figure 15) (153).

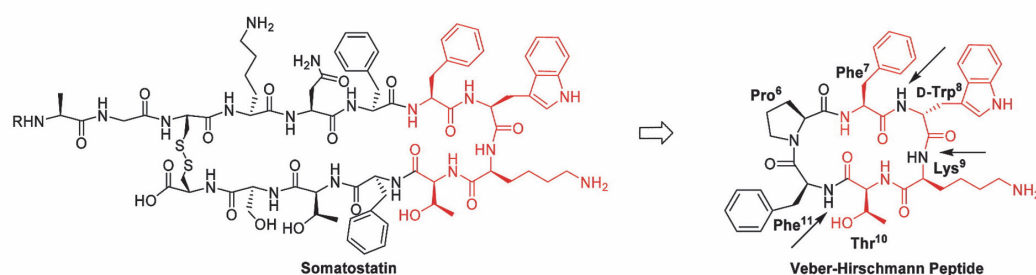


Figure 15. The Veber-Hirschmann peptide (right) is a somatostatin analogue selective towards receptor subtypes sst2 and sst5, administered by injection. The pharmacophore of somatostatin is indicated in red. A library scan of N-methylated lead compounds showed that N-methylation in the indicated positions resulted in compounds with retained affinity and oral availability. Adapted with permission from (154), © 2008 American Chemical Society

The objective was to make an orally available compound with retained biological activity, which could potentially be used as a substitute of octreotide. By incorporating 3 N-methylations a cyclic peptidomimetic was obtained having 10% oral availability. The lead peptide without N-methylations showed no oral availability. In addition, it was demonstrated that the N-methylations increased elimination half-life fivefold to 74 minutes. The same group, led by prof Kessler, have performed groundbreaking work related to optimization of the synthesis of N-methylated peptides and amino acids as well as in the investigation of the conformational influence of multiple N-methylation in cyclic peptides (154).

The group of Lokey are performing extensive research in the field of membrane permeability and diffusion of cyclic peptides. They have used a library based approach synthesizing 1200 derivatives of natural membrane permeable peptides in order to identify new scaffolds for cell permeability (155). In the study it was found that as expected N-methylation strongly increases permeability, but only when applied on solvent exposed amide bonds. Also the importance of side-chains is highlighted, permeability can be achieved by introducing lipophilicity via the side-chains. Similar conclusions were made about analogues of the orally available Sanguinamide A, where it was found that N-methylation of a solvent exposed peptide bond increased permeability and, surprisingly, solubility (156). It should be noted that the increase in membrane permeability is highly dependent on the position of the N-methylation. Interestingly, permeability was also influenced by the structure of a side-chain adjacent to the N-methylation site. Removal of a β -branch in the side chain strongly increased permeability, likely due to conformational flexibility.

The traditional model of a naturally originating peptide being cell permeable and orally available is cyclosporine A. However, many other naturally occurring cyclic peptides of different scaffolds have also recently been identified as membrane permeable by passive diffusion, having in common with cyclosporine the heavy N-methylation pattern (157). The ability of the formation of intramolecular hydrogen bonds which are not solvent exposed in nonpolar solvents is crucial for membrane permeability. The most permeable compounds had every amide bond involved in either intramolecular hydrogen bonds or N-methylated. The investigations by Lokey and co-workers highlight the potential of N-methylations for increasing membrane permeability, however the position is highly important and other parameters such as the lipophilicity and conformation of side-chains also have a strong influence. The side-chains can be used to shield polar regions of the peptide and flexibility can balance hydrophobicity with solubility (158). These modifications together with macrocyclization has the potential of generating orally available peptides beyond the rule of 5.

Naturally, modifications such as N-methylation can also alter binding properties of peptides. Scanlon and co-workers used a systematic N-methylation scan to improve the pharmacokinetic properties of a phage display derived linear peptide binding to malaria related target AMA-1 (159, 160). Multiple N-methylations indeed improved the proteolytic stability 30-fold, but also increased the potency of the inhibitor. As described earlier, various medicinal chemistry approaches have resulted in the alternation of receptor specificity of somatostatin analogues. To this end N-methylation has also been used to increase the activity for the sst5 receptor (161). In another study, Skogh et al. performed a N-methyl scan using substance P 1-7, a pain relieving neuroactive peptide, as a lead compound (162). While N-methylation, especially when present at several sites, strongly increased the stability of the compound, its potency was diminished. These studies show that N-methylation is a useful strategy for improving permeability and stability of peptide lead compounds, but care has to be taken since target binding can be compromised or altered.

There have been cases reported where systematic carbon- α methylation scan has been used, but with limited success (163). A number of α -carbon methylated amino acids with side-chains longer than alanine have been used in peptides to stabilize helical structures (164). The type of helix is affected by the side-chain of the amino acid. In several studies cyclic quaternary amino acids were used to induce helical conformations (165–167).

By systematically substituting peptide residues with peptoid residues in a cyclic hexapeptide the cell permeability was enhanced (Figure 16) (168). However, as with N-methylation, the position is highly important. The intrinsic properties render peptoids highly flexible in their structure, which can impair target selectivity and/or binding. The inherent structural flexibility is related to the lack of side-chains in α -position and lack of hydrogen bonding through the backbone nitrogen. Peptoids have been studied for various therapeutic applications. A number of examples exists where peptoids are indeed mimicking secondary structures such as helices, loops and turns (169). In some cases, the flexibility of the peptoids is even beneficial for target binding. Despite the structural flexibility, peptoids were designed as α -helical mimetics incorporating natural and unnatural side-chains (170). Known antimicrobial peptides were used as lead compounds. The peptoids demonstrated helicity and antimicrobial activity. As highlighted in the example above, replacing a peptide backbone with a peptoid can have beneficial effects on membrane permeability, but also stability can be improved. Park et al. have reported an elegant way of identifying peptoid replaceable residues within a lead peptide by applying a sarcosine scan combined with alanine and proline scans (171). The resulting peptide-peptoid-hybrid showed only slight loss in activity. Likely this approach could also be used on other peptide lead molecules in order to identify positions where peptoid side-chains can increase binding affinity. Moreover new side chains could easily be intro-

duced in such a position. In another study a macrocyclic peptide-peptoid hybrid is developed through extensive medicinal chemistry approaches, allowed through the high diversity of peptoid building blocks (172). By replacing amino acids, peptoid side chains and N-methylation, the potency of a CXCR7 inhibitor was improved by more than 230-fold. In addition, passive permeability and oral availability of 18% was achieved.

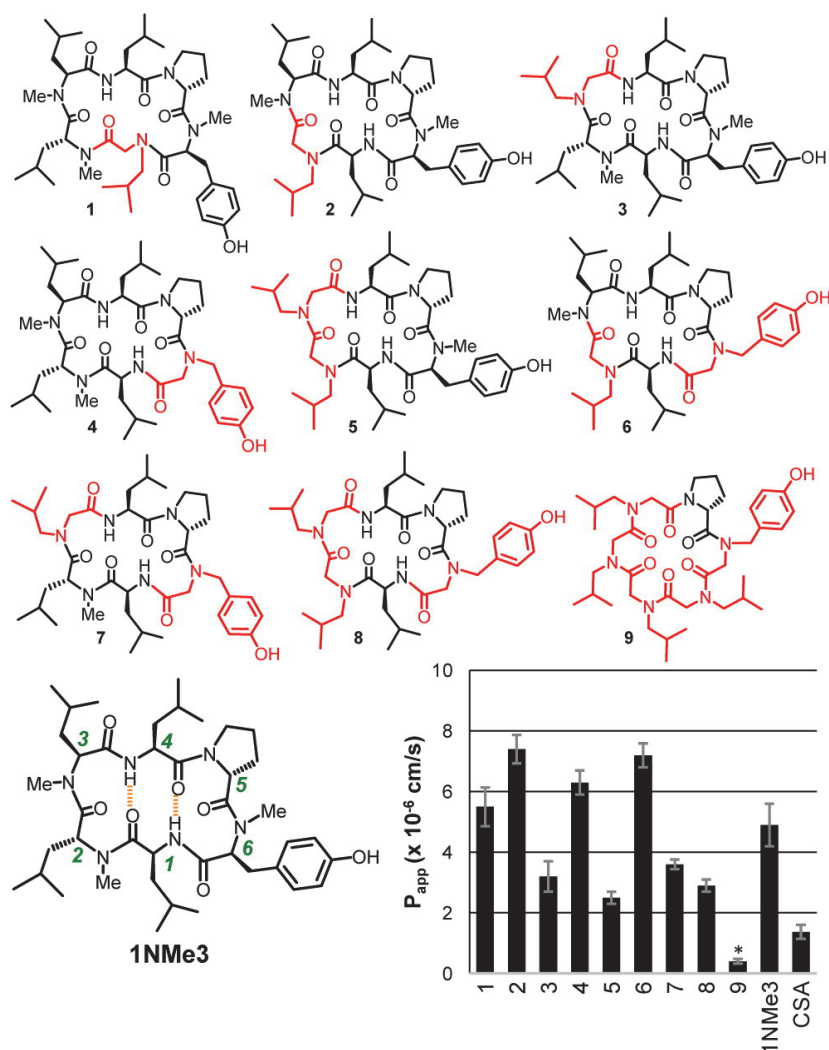


Figure 16. Substitution of N-methylated peptide residues into peptoid residues increased membrane permeability of a hexapeptide. As indicated in the lower right panel, the position is important. Reprinted with permission from (168), © 2015 American Chemical Society

The relatively facile synthesis of peptoids has also been utilized in the generation and screening of large synthetic libraries. Much work has been undertaken by the group of Kodadek. Traditionally they have used OBOC peptoid libraries encoded by MS. Lately they have been utilizing different approaches in order to facilitate screening of these libraries. By screening several libraries with derivatives from primary hits and by obtaining SAR in various ways including using an equivalent of alanine scanning (peptoid →

N-methyl scan) they were able to develop sub-micromolar binders to MMP-14 (173). One limitation of such libraries is the encoding step by MS, which sometimes is not able to identify the structure of hit compounds due to poor or complicated fragmentation. This can limit the number and type of building blocks used in the library. To overcome this drawback DNA encoded libraries of peptoids were recently developed (115, 174). Together with NGS and Fluorescence-activated cell sorting (FACS) this allows for fast and deep analysis of hit structures and for incorporation of a range of building blocks which were previously found to be difficult to encode, such as heterocycle containing haloacids and chloropentenoic acids.

As highlighted by the studies above, peptoids can be used in libraries to achieve an enormous diversity far exceeding the diversity of a peptide library. This is due to the high availability of primary amines. Peptoids can also be used in a similar fashion as N-methylation, in order to improve stability and permeability of lead compounds. Peptide-peptoid hybrids is a promising format which can overcome intrinsic limitation of both classes of molecules.

1.4 Bicyclic peptides

1.4.1 Development of bicyclic peptides

As described in previous sections of this thesis there are many different strategies of developing therapeutic peptides and a number of different formats exist. One successful approach has been cyclization, which provides many advantages over linear peptides. Within this peptide format there is a special branch; bicyclic peptides, on which we are focusing in our laboratory.

As cyclic peptides in general, bicyclic peptides are also present in nature, and have been found to be bioactive in various functions (175). The format is attractive as a new modality in drug discovery due to its increased stability and rigidity as compared to linear and monocyclic peptides. The bicyclic structure allows for a larger interaction surface, without inducing too much flexibility in the scaffold and without compromising the proteolytic stability. Several formats and cyclization strategies have been reported for the generation of bicyclic peptides, such as the combination of head-to-tail-amide/thioether, NCL-amide/disulfide, ring-closing metathesis/ring-closing metathesis and others. Bicyclic peptide lead compounds have been developed using a number of approaches including rational design, phage display, mRNA display, SICLOPPS and one-bead-two-compounds libraries.

The bicyclic peptide format used in our laboratory was pioneered by Timmerman et al. who used thiol reactive scaffolds to achieve mono-, bi-, or tricyclic peptides via cyclization through cysteine residues (176). The cyclization chemistry was highly efficient and could be performed in aqueous conditions. Heinis et al. developed a strategy for displaying a library of random peptides containing three cysteine residues on phage (described in section 1.1.3) and cyclizing them using such a trifunctional thiol reactive linker molecule, generating bicyclic peptides (177). The reaction takes place at room temperature and was found to not impair phage infectivity, hence allowing for the screening of large libraries of bicyclic peptides against immobilized targets. Having constructed the phage library such that the cysteine residues are placed in the middle and one residue away from each end, with 6 random amino acids between, the resulting peptide is composed of two macrocyclic rings connected through the organic linker (Figure 17). The bicyclic peptides are thought to be more rigid than monocyclic peptides, having two bonds constraining each ring (102). Moreover, both rings can potentially interact with the target simultaneously, allowing tight binding and in a way mimicking the complementarity-determining regions (CDR) of an antibody (178). The recently reported development of a potent cyclic peptide as an influenza hemagglutinin inhibitor, derived from a CDR, further supports the theory that cyclic peptides can functionally mimic CDRs

(179). Bicyclic peptides of this format were indeed shown to have large interaction surfaces with their target proteins, which is also likely causing their generally high target specificity (180). They were also demonstrated to be more stable than linear or monocyclic peptides (181).

When screening compound libraries with the purpose of identifying target binders, a high diversity is crucial. The generation of random peptide libraries can indeed provide an almost unlimited diversity, however the phage display format limits the number of compounds to around 10^{10} due to inherent limitations of the technology (a limited number of bacteria can be transformed with DNA plasmid). To further increase the diversity of bicyclic peptide libraries, with this limitation in mind, our laboratory has undertaken two strategies: the usage of different linker molecules and the alternation of library format.

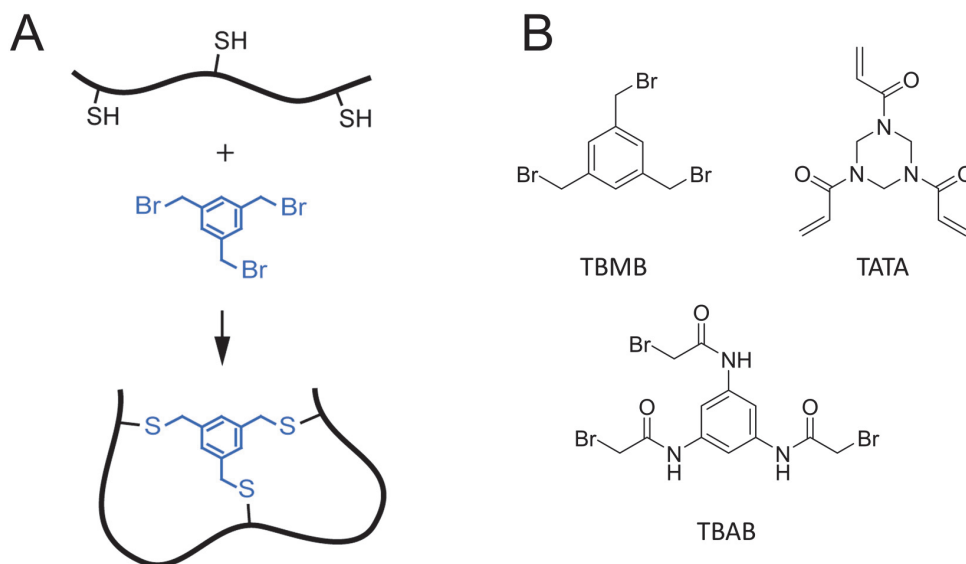


Figure 17. (A) Bicyclic peptides are formed by reacting a peptide containing three cysteine residues with a trifunctional linker molecule (blue). (B) Three different linker molecules are used in the bicyclic peptide libraries.

The initial linker used in the proof-of-concept study was tris-(bromomethyl)benzene (TBMB), which was selected due to its threefold rotational symmetry ensuring the formation of a unique structural isomer. It was thought that by introducing hydrogen binding moieties in the linker molecule, additional target interactions could be formed and the backbone conformation of the bicyclic peptide could be influenced (182). Two new linker molecules were designed, having the same symmetry as TBMB: 1,3,5-triacryloyl-1,3,5-triazinane (TATA) and N,N',N''-(benzene-1,3,5-triyl)tris(2-bromoacetamide) (TBAB). Indeed, the binding affinity of a bicyclic peptide was strongly compromised

when cyclized with a different linker molecule, indicating a structural role of the linker. In a further study it was shown that when phage selections were performed against the same target but using different linker molecules, specific consensus sequences were found for each linker (183). A majority of consensus sequences were found exclusively in selections with one of the three linkers. The replacement of the linker with another yielded peptides several order of magnitudes less potent, confirming the results of the previous study. Crystal structures of the bicyclic peptides binding to their target revealed non covalent interactions between the linker molecule and the peptide sidechains, inducing a specific conformation of the backbone. The linker is therefore thought to act as a structural scaffold of the bicyclic peptide and hence introducing diversity to the library.

Another approach of generating diversity of bicyclic peptide libraries, which is related to the cyclization strategy, is the selection of disulfide linked peptides (184). In the 6x6 library mentioned above there is a probability of a fourth cysteine to occur in any of the random positions. Therefore, the formation of two disulfide bridges in such a library generates a high topological diversity. These peptides are constructed in the same way as above during a phage selection but by oxidation rather than cyclization by a reaction using a linker. In addition to the topological diversity introduced by the position of the fourth cysteine, a single peptide sequence could lead to three different regioisomers which further expands the variety of possible conformations (Figure 18).

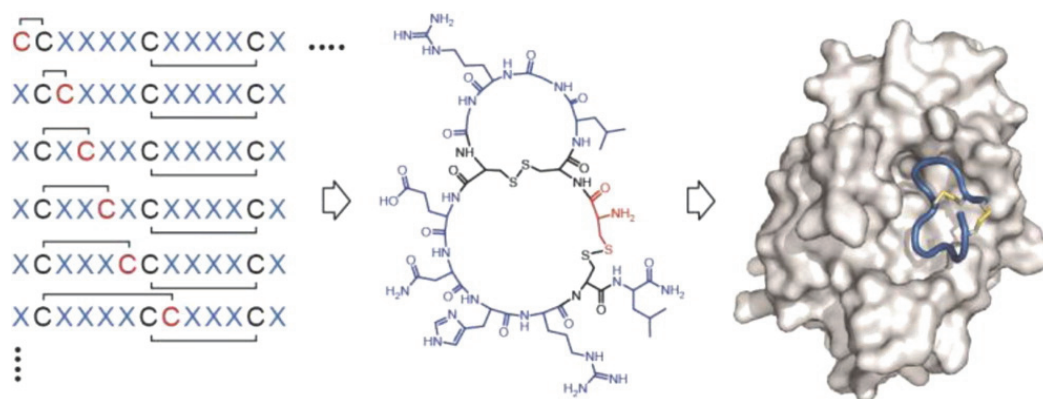


Figure 18. In the bicyclic peptide libraries with three fixed cysteines, a fourth cysteine can occur in any of the random positions (left). In such a peptide, a bicyclic structure can be obtained by disulfide formation between the cysteine residues (middle). Three different regioisomers can be formed, further increasing the diversity of the library. Reprinted with permission from (184), © 2013 American Chemical Society.

The second strategy to increase diversity in bicyclic peptide phage display libraries is to change the format of the peptides. In this case the length of the random regions between the cysteine residues (the two macrocyclic rings) was varied (Figure 19) (185). Loop length diversity had already been applied in the tailoring of molecular recognition surfaces in protein scaffolds, and was shown to be readily applicable to bicyclic peptides.

Bicyclic peptide phage libraries were generated with combinations of differently sized macrocyclic rings of the format Cys-(Xaa)_m-Cys-(Xaa)_n-Cys, wherein the number 'm' and 'n' of random amino acids between the cysteine residues was 3, 4, 5 or 6. When screened against the same target as the 6x6 library, the diverse formats yielded novel consensus sequences, presumably binding differently to the active site of the enzyme. One advantage of isolating differently binding peptides is the increased success rate of affinity maturation libraries constructed based on the initial hit(s). These libraries are created in a semi-randomized manner to ensure that high diversity is reached for all residues. Interaction forming residues of the initial hit peptide are identified using alanine scanning as described in a previous chapter. Subsequently, a new library is generated in which these residues are kept constant and less important amino acids are randomized. This library is then panned against the target in one or two rounds of affinity selection with increased stringency, often achieved by reducing the amount of immobilized target. In order to facilitate the identification of consensus sequences and the following construction of affinity maturation libraries Rebollo et al. established a method utilizing NGS for the identification of bicyclic peptide hit compounds (186). Using this technique enabled the identification of rare target-binding peptide motifs, as well as the definition of more precisely consensus sequences and sub-groups of consensus sequences. This approach is now established and routinely used in our laboratory.

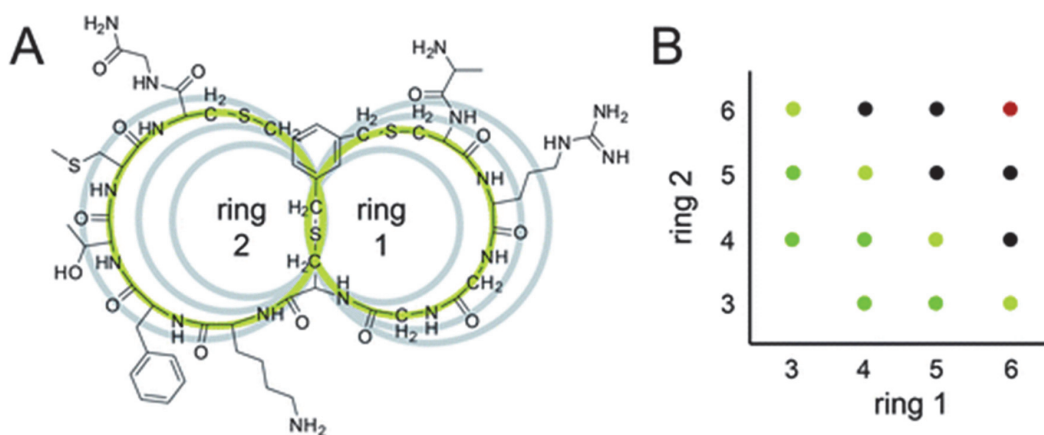


Figure 19. Bicyclic peptide libraries with different loop lengths were constructed in order to increase diversity. By varying the loop length, the size of the binding interface of the peptide-target interaction is adjusted. (A) A representative peptide of size 4x5 is indicated in green. (B) The scheme shows the loop combinations in the different libraries (dark green, light green and black) and of the former 6x6 library (red). Reprinted with permission from (185) reprinting license number 4265410782621, © 2013 The Royal Society of Chemistry

1.4.2 Examples of bicyclic peptides

Using the strategies detailed above, our laboratory has generated bicyclic peptide inhibitors and ligands to several important therapeutic targets. In general, initial binders isolated from phage display demonstrate target affinities in the nanomolar to micromolar range. These hit compounds can then be optimized using various strategies as highlighted in the previous chapter and as exemplified below.

In the first proof-of-principle study, bicyclic peptide inhibitors of the 6x6 format cyclized with TBMB were generated against the proteases cathepsin G and plasma kallikrein (PK) (177). The latter is a serine protease involved in contact activation and the kallikrein-kininogen system (187). Over-activation of PK can lead to increased inflammation and vascular leakage ultimately resulting in the swelling disorder hereditary angioedema (HAE), which occurs in patients lacking functional C1 inhibitor, the endogenous inhibitor of the protease. Companies such as CSL Behring and Shire have approached PK as a therapeutic target with approved inhibitors as well as a number of new molecules in late stage development. The bicyclic peptide inhibitor PK15 inhibits PK with a K_i of 2 nM and was developed by phage selection and subsequent affinity maturation (177). PK15 was shown to be highly specific and did not inhibit the homologous proteins factor XIa (FXIa) and thrombin. However, the high specificity also resulted in PK15 not efficiently inhibiting orthologous proteases, such as mouse PK or rat PK, preventing the evaluation of the compound in small laboratory animals. The specificity of the PK inhibitor could be tailored by reducing the interaction surface of the bicyclic peptide (Figure 20) (188). Using a 3x3 library, bicyclic peptides inhibiting human and rat PK, but also human FXIa were isolated. This result indicated that the smaller bicyclic peptides bind to regions that are identical in hPK, rPK and hfXIa.

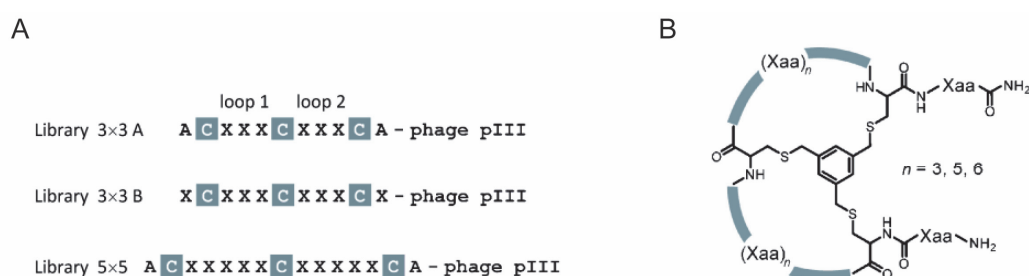


Figure 20. (A) The strategy of Baeriswyl et al. to make a PK binder with cross-species affinity was to reduce the binding interface of the peptide. This was done by using libraries with smaller loop size in the phage selection. Instead of 6x6 libraries used previously, 3x3 and 5x5 libraries were used. Random amino acids are indicated as X, Alanine as A and the fixed cysteins as C. (B) Structure of the bicyclic peptides having loops of 3, 5 or 6 amino acids. Reprinted with permission from (188) reprinting license number 4270220768830, © 2012 Wiley-VCH Verlag GmbH&Co

Next, peptide libraries with loops of five amino acids were generated in order to have slightly larger binding interface and therefore not inhibit FXIa. This strategy resulted in several peptides inhibiting PK at sub-nanomolar concentrations while also inhibiting rat and monkey PK. The 5x5 peptides were more specific than the 3x3 peptides and inhibited FXIa only in the micromolar range.

Another example of a bicyclic peptide serine protease inhibitor is the urokinase-type plasminogen activator (uPA) inhibitor UK18 (180). uPA is involved in cancer metastasis and extracellular matrix degradation and is therefore a relevant therapeutic target (189). As with the selections against PK, the 6x6 library cyclized with TBMB was used for the phage selection. The initial peptide hit isolated after two rounds of selection, UK18, potently inhibits uPA with a K_i of 53 nM, which represents around 200-fold stronger binding than the best monocyclic peptide. As with PK15, UK18 was highly specific to human uPA and did not bind any related proteases (Figure 21A).

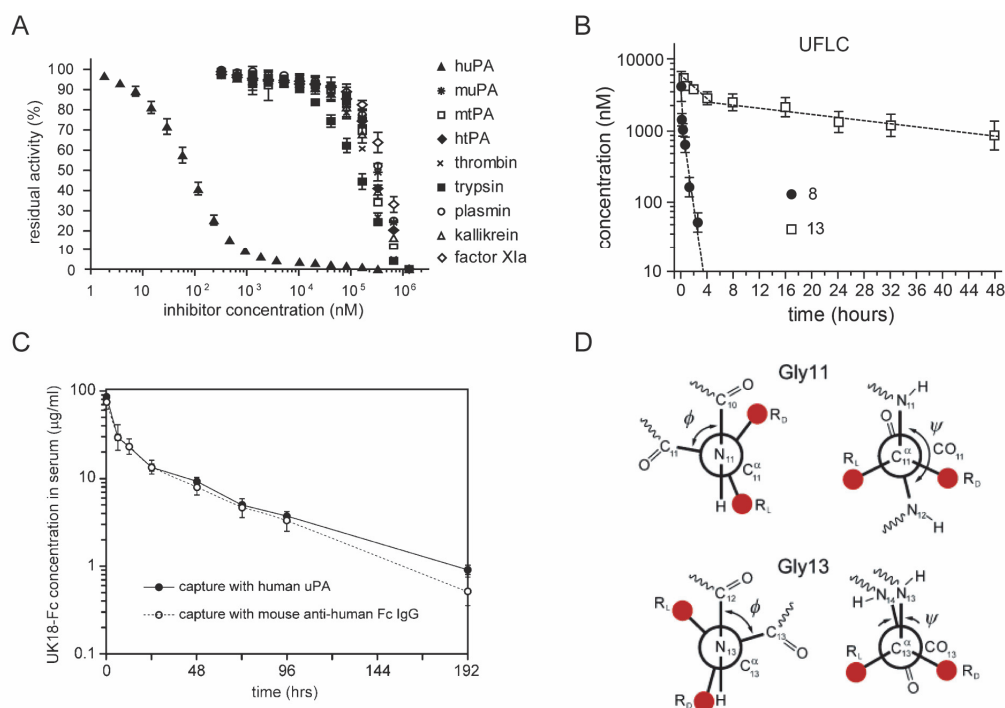


Figure 21. (A) The specificity of UK18 was determined in enzymatic inhibition assays. (B) Pharmacokinetics of fluorescein conjugated UK18 (8) and UK18-SA21 (13) after i.v. injection in mice. Peptide concentration was determined by liquid chromatography. (C) Pharmacokinetics of a bicyclic peptide UK18-H12-Fc-streptag/Fc-his6tag in female BALB/c mice. Serum concentrations of the heterodimer were measured with two different ELISA assays at the indicated time points. (D) Newman projections of Gly11 and Gly13 in UK18 with the ϕ and ψ torsion angles found in the crystal structure. D-amino acid substitutions in Gly11 would create a clash between the side chain of the amino acid and the carbonyl group of Arg10; D-amino acid substitutions of Gly13 were not expected to create steric conflicts. Reprinted with permission from (180, 181, 190, 191), reprinting license 4270240211893, © 2012 American Chemical Society, © 2013 Wiley-VCH Verlag GmbH & Co.

The pharmacokinetics of UK18 were subsequently examined. It was found that the bicyclic peptide was cleared rapidly in mice having a half-life of 30 min (181). Two strategies were evaluated for improving the half-life, namely conjugation with an albumin binding peptide SA21 and Fc fusion (181, 190). The peptide conjugates showed retained activity and their half-lives were successfully prolonged to 24 h and 36 h respectively (Figure 21B and C). In an additional mouse study, it was shown that the SA21 conjugate could efficiently diffuse into solid tumors (192). More recently, UK18 was used as a model peptide fused to a different albumin binding tag for half-life improvement (193). The UK18 peptide has also been subjected to medicinal chemistry approaches with the purpose of improving binding affinity. In the crystal structure of UK18 bound to uPA a glycine residue was observed that has a positive ϕ dihedral angle when bound to the target. Replacement by a D-amino acid, which favors positive ϕ dihedral angles, increased both binding affinity and proteolytic stability of UK18 (Figure 21D) (191).

Other medicinal chemistry approaches have also been used in bicyclic peptide lead compounds. One example is the inclusion of a synthetic di-thiol amino acid into a phage selected hit (194). In the selections mentioned above, of four cysteine containing peptides cyclized through a disulfide bridge, a majority of the identified binders contained a pair of adjacent cysteine residues. By substituting two adjacent cysteines in such a peptide binding affinity could be increased 40-fold, somewhat unexpectedly largely by enthalpic rather than entropic effects.

In a final example, bicyclic peptides were selected against the therapeutic target β -catenin (195). This protein plays a key role in the Wnt growth factor signaling pathway and its upregulation is associated with several types of human cancer (196). Again, the bicyclic peptide 6x6 library was used for selection, cyclized with the three different linkers TBMB, TATA and TBAB. This study also highlights the structural diversity introduced by the different linker molecules as specific consensus sequences were found for each. Fluorescence polarization experiments showed that the isolated peptides bound to multiple sites of β -catenin. Several peptides were found to interfere with the native ligand ICAT and thus bound to β -catenin at a prime target site for therapeutic intervention to which no synthetic ligand was previously identified.

In addition to the three examples above, bicyclic peptides have been selected against several other targets such as the cancer related receptors HER2 and Notch1 (197, 198). Bicyclic peptides inhibiting *S. aureus* Sortase A were also identified and could potentially be developed further into antimicrobial agents (199).

2. Aim of thesis

Peptide drugs are used for the treatment of a wide range of diseases. They are typically developed based on bioactive peptides found in nature or peptide ligands generated *de novo* by *in vitro* evolution. Often, peptides from these two sources do not readily have the required properties as such as sufficiently good binding affinity, selectivity or stability, and they need to be engineered. This applies also to many of the bicyclic peptides developed in our laboratory by phage display. The aim of my PhD project was to develop new strategies and apply existing ones to improve the potency, selectivity and proteolytic stability of phage-selected bicyclic peptides. A further objective was to characterize the developed peptides *in vitro* and *in vivo* in relevant preclinical animal models. The ultimate goal of my thesis was to develop a peptide drug candidate that has the potential to be translated into a therapeutic.

Former members of our laboratory had applied phage display to develop bicyclic peptide inhibitors of the proteases coagulation factor XII (FXII) and matrix metalloproteinase 2 (MMP-2). The bicyclic peptides showed inhibitory constants in the nanomolar range. The bicyclic peptides did not have the required affinity, selectivity and stability to be evaluated in animal disease models. In my thesis, I aimed at substituting natural amino acids in the bicyclic peptides to unnatural ones, in order to improve said properties. This thesis is split into three different parts, where the first two are related to the engineering of the FXII inhibitor and the latter to the MMP-2 inhibitor. The specific aims of the projects are as follows:

- i) In the first project, my aim was to test if insertion of one or two carbon atoms at different positions into the macrocycle backbone of the phage-selected bicyclic peptide FXII inhibitor can improve its binding affinity. This project had a dual aim, namely the testing of a new affinity maturation strategy and the improvement of the potency of the inhibitor towards its potential development into a drug lead.
- ii) The second project constitutes the largest part of my PhD thesis and several intermediate goals were defined, with the final aim of testing an optimized bicyclic peptide FXII inhibitor in different animal disease models. A first intermediate goal was to further improve the affinity of the inhibitor by inserting additional unnatural amino acids that enhance the binding affinity. A second objective was to improve the affinity for mouse FXII, since the lead peptide had low affinity for the murine homologue and was thus limiting possible *in vivo* studies in this species. A third objective was to improve the proteolytic stability of the inhibitor. After the optimization of the inhibitor, the next goal was to characterize it, first *ex vivo*, to identify suitable species for *in vivo* experimentation and later in several therapeutically relevant preclinical *in vivo* models.

- iii) The aim of my third project was to improve the binding affinity, target selectivity and proteolytic stability of the above mentioned phage-selected bicyclic peptide MMP-2 inhibitor. The development of selective MMP inhibitors has been a long-standing challenge. For MMP-2, no synthetic inhibitors are available that efficiently block the activity of this protease but not that of other MMPs. It was our hypothesis that the bicyclic peptide structure would form a large enough contact area with the protease in order to achieve high target specificity. My next aim in this project was to fully characterize the specificity of the bicyclic peptide MMP-2 inhibitor. A further goal was to optimize the specificity in order to achieve less inhibition of closely related proteases. A near-term goal of this work was to establish a powerful tool that allows selective inhibition of the protease *in vivo*, allowing study of the protease *in vivo*.

3. Improving the binding affinity of in-vitro-evolved cyclic peptides by inserting atoms into the macrocycle backbone

This chapter is based on the following research article:

J. Wilbs, S. J. Middendorp, C. Heinis, Improving the Binding Affinity of in-Vitro-Evolved Cyclic Peptides by Inserting Atoms into the Macrocyclic Backbone, *Chembiochem* **17**, 2299–2303 (2016). Reprinting license number: 4274090904498 © 2017 Wiley-VCH Verlag GmbH&Co.

Author contributions: J.W. and C.H. conceived the strategy. J.W. synthesized and characterized the peptides. J.W., S.J.M. and C.H. designed and performed the blood coagulation experiments. J.W., S.J.M. and C.H. wrote the manuscript.

3.1 Abstract

Cyclic peptides binding to targets of interest can be generated efficiently with powerful in vitro display techniques, such as phage display or mRNA display. The cyclic peptide libraries screened with these methods are generated by altering in a combinatorial fashion the amino acid sequence of the peptides, the number of amino acids in the macrocycle rings, and the cyclization chemistry. A structural element that cannot easily be varied in the cyclic peptides is the backbone, which is built from amino acids, each of which contributes three atoms to the macrocyclic ring structure. Here, we proposed to improve the affinity of a phage-selected bicyclic peptide inhibitor of coagulation factor XII (FXII) by screening variants with one or two carbon atoms inserted into different positions of the backbone, and thus tapping into a structural space that was not sampled by phage display. Two mutants showed 4.7- and 2.5-fold improved K_i values. The better one blocked FXII with a K_i of 1.5 ± 0.1 nM and inhibited activation of the intrinsic coagulation pathway (EC_{50} 1.7 μ M). The strategy of ring size variation by one or several atoms should be generally applicable for the affinity maturation of in-vitro-evolved cyclic peptides.

3.2 Introduction

Peptide macrocycles have a number of favorable properties that make them attractive for the development of therapeutics. They can bind with high affinity and selectivity to protein targets, their degradation products are nontoxic, they offer different administration options, and they can be chemically synthesized. Another advantage is their fast development: they can be isolated from large combinatorial libraries generated by either chemical (200) or ribosomal synthesis (102, 107, 201). In vitro display techniques such as phage display or mRNA display allow the generation and screening of billions of peptide macrocycles in a short time and for a moderate cost. Chemical and structural diversity of peptide macrocycle libraries is obtained by varying the amino acid sequence, the number of amino acids, (185, 202) and the cyclization chemistry (102, 182).

For some protein targets, it has been difficult to generate high-affinity peptide macrocycles by in vitro display techniques, despite the enormous size and diversity of the screened library. For therapeutic application, peptide macrocycles typically require a dissociation constant in the low nanomolar or picomolar range. A frequently chosen strategy to further improve in vitro-evolved cyclic peptide ligands is to modify the side chains that make interactions with the target. The modular architecture of peptides, the commercial availability of many unnatural amino acids, and automated synthesis and purification methods allow efficient preparation of medium-sized libraries of such peptides. We recently applied such an approach to improve the binding affinity of the bicyclic peptide FXII618 (1, Figure 22A), (203) a nanomolar inhibitor of coagulation factor XII

(FXII) isolated by phage display. Synthesis and testing of around 50 bicyclic peptides with altered amino acid side chains led to the identification of one variant with substantially improved inhibitory activity (204).

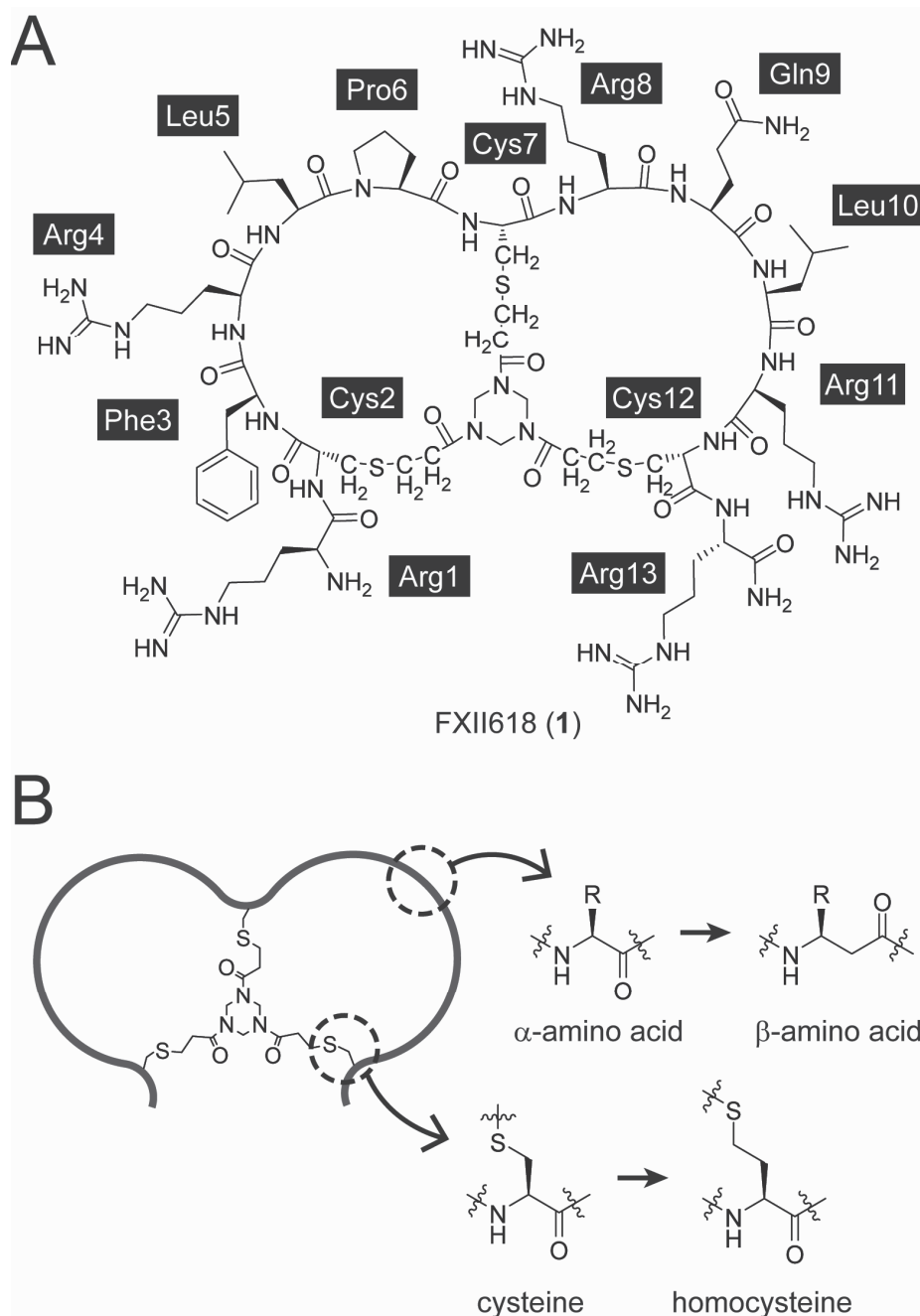


Figure 22. (A) Chemical structure of FXII618 (1). (B) Affinity maturation strategy. Carbon atoms are inserted into the backbone by replacing α -amino acids with β -amino acids, or by replacing cysteines connected to the cyclization linker by cysteine homologues with longer side chains.

In this work, we aimed to identify additional modifications that improve the inhibitory activity of **1** by an approach that is based on the modification of the peptide backbone instead of the side chains. Specifically, we inserted one or two carbon atoms at different positions of the macrocyclic rings. Peptides screened by phage display are composed of canonical amino acids, each of which contributes three atoms to the macrocyclic ring. More precisely, they contain $3 \times n + m$ backbone atoms, where "n" is the number of amino acids and "m" the number of atoms contributed by the cyclization linker. In the phage display screen in which **1** was isolated, cyclic peptides with $3 \times n + m + 1$ or $3 \times n + m + 2$ backbone atoms were thus not sampled. We speculated that inserting carbon atoms in some sites of the backbone could lead to small changes in conformation, and that this in turn could strengthen existing molecular interactions or allow the formation of new noncovalent contacts of **1** with FXII.

The strategy of inserting atoms into the backbone has been applied to several nature-derived cyclic peptides for studying structure-activity relationships or enhancing biological activity. For example Ghadiri and co-workers inserted single atoms into histone deacetylase (HDAC) inhibitors, measured their cytotoxic activity towards tumor cells, and determined their structures (205). The Muir group varied the macrocycle size of autoinducing peptides (AIPs) secreted by *Staphylococcus aureus*, in order to study their structure-activity relationships (206). Hansen and co-workers extended the ring size of amphipathic cyclic peptides by different numbers of atoms to investigate the effects on antimicrobial and hemolytic activity (207). Inserting or deleting single carbon atoms at different positions in macrocyclic rings of peptide ligands has not been used as a systematic approach for improving the binding affinity of in-vitro-evolved cyclic peptides.

A synthetically efficient way of generating cyclic peptides with additional carbon atoms in the ring is replacing α -amino acids with β -amino acids that contain an additional carbon atom between the amino and carboxyl groups (Figure 22B). Substituting β - for α -amino acid has been applied extensively to α -helical peptides, as β -amino acids can substantially improve stability (208–211). In some α -helical peptides, β -amino acids have also improved binding affinity, as for example in an analogue of parathyroid hormone receptor-1 agonist (212) or an engineered VEGF signaling inhibitor based on the Z-domain (213). The strategy of α -to- β -amino acid substitution has also been applied to a handful of nature-derived cyclic peptides, including the above mentioned HDAC inhibitors and AIPs (205, 206). In this work, we chose to apply β -amino acids to access variants of **1** with a single carbon atom inserted in different positions of the backbone.

3.3 Results and discussion

In order to identify amino acid positions where insertion of a carbon atom could potentially improve the binding affinity of **1**, we synthesized two series of peptide variants:

one with individual amino acids replaced by β -alanine, and the other with glycine (Table 2). Comparison of the resulting peptides allowed an understanding of whether an additional carbon atom at a specific position enhances binding to FXII, independent of the amino acid side chain. Unmodified **1** inhibited FXII with a K_i of 7 ± 0.4 nM. Substitution of Phe3, Arg4, or Leu5 to β -alanine (**2**, **4**, **6**) or glycine (**3**, **5**, **7**) reduced the inhibitory activity significantly (> 300 -fold). For all three positions, substitution to β -alanine gave a larger drop in activity than substitution to glycine, thus indicating that an additional carbon atom in these three positions of the main chain negatively affected binding. Substitution of Pro6 to β -alanine (**8**) or glycine (**9**) reduced affinity (\sim three and 15-fold, respectively). The smaller loss in affinity for the β -alanine variant suggests that insertion of one carbon atom in this position enhances binding to FXII. Amino acid substitution at Arg8 had the opposite effect: a larger affinity drop for β -alanine (19- versus twofold; **10**, **11**). At Gln9 and Leu10, substitution to β -alanine and glycine reduced the inhibitory activity more than 100-fold (**12**, **13**, **14**, **15**). Finally, at Arg11, replacement with both β -alanine and glycine reduced binding by a small factor (threefold; **16** and **17**).

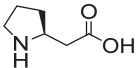
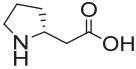
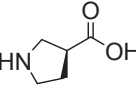
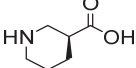
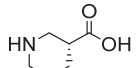
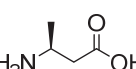
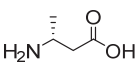
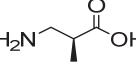
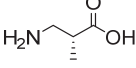
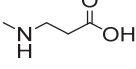
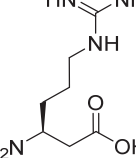
Table 2. β -alanine and glycine screen. Standard deviations were determined for peptides with $K_i < 1$ μ M and are indicated. For peptides with $K_i > 10$ μ M, the remaining protease activity at a concentration of 10 μ M is indicated in brackets.

position	β -alanine		Glycine	
	<chem>NCC(=O)O</chem>		<chem>NCC(=O)O</chem>	
	peptide	K_i (nM)	peptide	K_i (nM)
Phe3	2	> 10000 (65%)	3	2289
Arg4	4	> 10000 (83%)	5	6513
Leu5	6	> 10000 (75%)	7	> 10000 (51%)
Pro6	8	25 ± 1	9	109 ± 21
Arg8	10	132 ± 65	11	14 ± 0.6
Gln9	12	963 ± 36	13	2000
Leu10	14	1673	15	1119
Arg11	16	22 ± 0.7	17	23 ± 4

Based on these results, we considered Pro6 and Arg11 as the most promising sites for α -to- β -amino acid substitutions. β -Amino acids can have side chains at either the α (C2) or β (C3) carbon (β 2- and β 3-residues, respectively). Given that these carbon atoms can have R or S configuration, four diastereoisomeric β -amino acids exist for each side chain. We first substituted Pro6 with a range of cyclic β -amino acids (**18-22**; Table 3). All these substitutions reduced inhibitory activity 80-fold or more. It is likely that the cyclic β -amino acids imposed conformational constraints, thus hindering efficient binding to FXII. We subsequently synthesized peptides in which Pro6 was substituted with acyclic β -amino

acids: methyl groups linked to either C3, C2, or the amino group (**23-27**; Table 3). We reasoned that the methyl groups could potentially replace interactions formed by the proline ring. Three of these (**23, 26, 27**) showed double-digit K_i values, but all had weaker values than the peptide with β -alanine in this position.

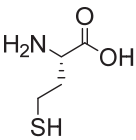
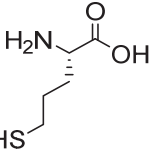
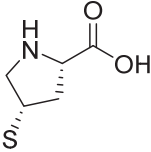
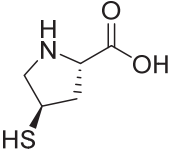
Table 3. Substitution of Pro6 and Arg11 by β -amino acids. Standard deviations were determined for peptides with $K_i < 1 \mu\text{M}$. For peptides with $K_i > 10 \mu\text{M}$, the remaining protease activity at a concentration of $10 \mu\text{M}$ is indicated in brackets.

position	peptide	β -amino acid		K_i (nM)
		Name	structure	
Pro6	18	(S)- β^3 -homoproline		1810
Pro6	19	(R)- β^3 -homoproline		> 10000 (89%)
Pro6	20	(S)- β^2 -proline		6783
Pro6	21	(S)- β^2 -homoproline		> 10000 (68%)
Pro6	22	(R)- β^2 -homoproline		578 \pm 132
Pro6	23	(S)- β^3 -homoalanine		82 \pm 10
Pro6	24	(R)- β^3 -homoalanine		4628
Pro6	25	(S)- β^2 -homoalanine		232 \pm 7
Pro6	26	(R)- β^2 -homoalanine		35 \pm 1
Pro6	27	N-Me- β -alanine		74 \pm 8
Arg11	28	(S)- β^3 -homoarginine		1.5 \pm 0.1

Another position that tolerated the β -alanine substitution reasonably well was Arg11. We replaced this with the β 3-amino acid structurally best resembling L-Arg (S configuration in C3; (S)- β 3-homoarginine; **28**). This substitution yielded a peptide with a 4.7-fold improved K_i (1.5 ± 0.1 nM; we named this FXII700). Given that **16** and **17** (β -alanine and glycine at Arg11) had comparable affinity, it is likely that the affinity improvement achieved with the (S)- β 3-homoarginine substitution resulted from interactions of the arginine side chain with FXII; these are apparently better for the β 3-amino acid than for L-Arg.

Another efficient strategy for inserting carbon atoms into the macrocyclic rings of **1** is substitution of cysteines with homocysteine or 5-mercaptonorvaline (one or two additional carbons in the side chains, respectively; Figure 22B). The thiol groups of homocysteine and 5-mercaptonorvaline have slightly higher pK_a values than for cysteine, (214) and were thus expected to react optimally with the acrylamide functional groups of the cyclization reagent 1,3,5-triacryloyl-1,3,5-triazinane (TATA) at a slightly higher pH than for cysteine. We found that peptides containing two cysteines and either homocysteine or 5-mercaptonorvaline reacted efficiently with TATA, even when the pH was not increased. Most likely, TATA reacts first with a cysteine (intermolecularly) and only then with homocysteine or 5-mercaptonorvaline (intramolecularly). The first, intermolecular event is likely the rate-limiting step, and the slower reaction of homocysteine or 5-mercaptonorvaline compared to cysteine therefore does not slow the formation of the bicyclic peptide. We synthesized six variants of **1** (each of the three cysteines replaced by either of the two cysteine analogues; Table 4).

Table 4. Substitution of cysteines with homocysteine, 5-mercapto-norvaline and 4-mercapto-proline. Standard deviations were determined for peptides with $K_i < 1$ μ M. For peptides with $K_i > 10$ μ M, the remaining protease activity at a concentration of 10 μ M is indicated in brackets.

position	homocysteine		5-mercapto-norvaline		(2S,4S) 4-mercapto-proline		(2S,4R) 4-mercapto-proline	
								
	peptide	K_i (nM)	peptide	K_i (nM)	peptide	K_i (nM)	peptide	K_i (nM)
Cys2	29	6 ± 0.6	32	12 ± 0.3	35	> 10000 (68%)	38	> 10000 (62%)
Cys7	30	7 ± 1	33	33 ± 5	36	1228	39	5.8 ± 1
Cys12	31	2.8 ± 0.5	34	5.8 ± 1.2	37	2.5 ± 0.4	40	4 ± 1.1

Replacement of Cys12 with homocysteine and 5-mercaptonorvaline improved binding by 2.5- and 1.2-fold, respectively ($K_i = 2.8 \pm 0.5$ nM (**31**) and 6 ± 1 nM (**34**)). Replacement

of the other two cysteines retained binding affinity in the case of homocysteine (**29** and **30**) and slightly reduced binding for 5-mercaptonorvaline (**32** and **33**). We named bicyclic peptide **31** (with the highest affinity) FXII701. Having found that cysteine analogues with longer side chains can improve affinity, we also tried the conformationally constrained cyclic amino acid 4-mercaptoproline (2S,4S or 2S,4R configuration; Table 4). In these two amino acids, the sulfur and carbon α atoms are separated by two carbon atoms, as in homocysteine. Replacement of Cys12 with 4-mercaptoproline (2S,4S or 2S,4R) improved binding 2.8- and 1.7-fold, respectively ($K_i = 2.5 \pm 0.4$ nM (**37**) and 4 ± 1 nM (**40**)). Replacement of Cys7 with 4-mercaptoproline improved the binding for one of the diastereomers (2S,4R, **39**; $K_i = 6 \pm 1$ nM) but not for the other (2S,4S, **36**; $K_i = 1230$ nM). Replacement of Cys2 with both 4-mercaptoproline diastereomers reduced binding more than 1000-fold (**35**, **38**)

We combined the two substitutions that improved the inhibitory activity of **1** by large factors: Arg11 to (S)- β 3-homoarginine and Cys12 to homocysteine. The resulting peptide (**41**) showed $K_i = 2.7 \pm 0.3$ nM, thus demonstrating that the affinity enhancement of the two modifications is not additive. This is not surprising given the close proximity of Arg11 and Cys12. Insertion of a carbon atom at one of the two positions presumably allows a small conformational change in this region of the macrocycle, thereby resulting in stronger molecular interactions of an amino acid side chain, such as for Arg11 with FXIIa.

Finally, we tested whether the modified bicyclic peptides **28** and **31** block the intrinsic coagulation pathway more efficiently than the lead peptide **1**. All three peptides dose-dependently prolonged the intrinsic coagulation time (aPTT) of human plasma, with **28** and **31** superior to **1** (Figure 23A). The inhibitor with the highest affinity, **28**, showed the best prolongation ($EC_{2x}=1.7\mu M$, compared to $3.1\mu M$ for **1**, where EC_{2x} is the inhibitor concentration at which the coagulation time is doubled). Extrinsic coagulation (PT) was similar for the three compounds, thus showing that the high target selectivity was retained (Figure 23).

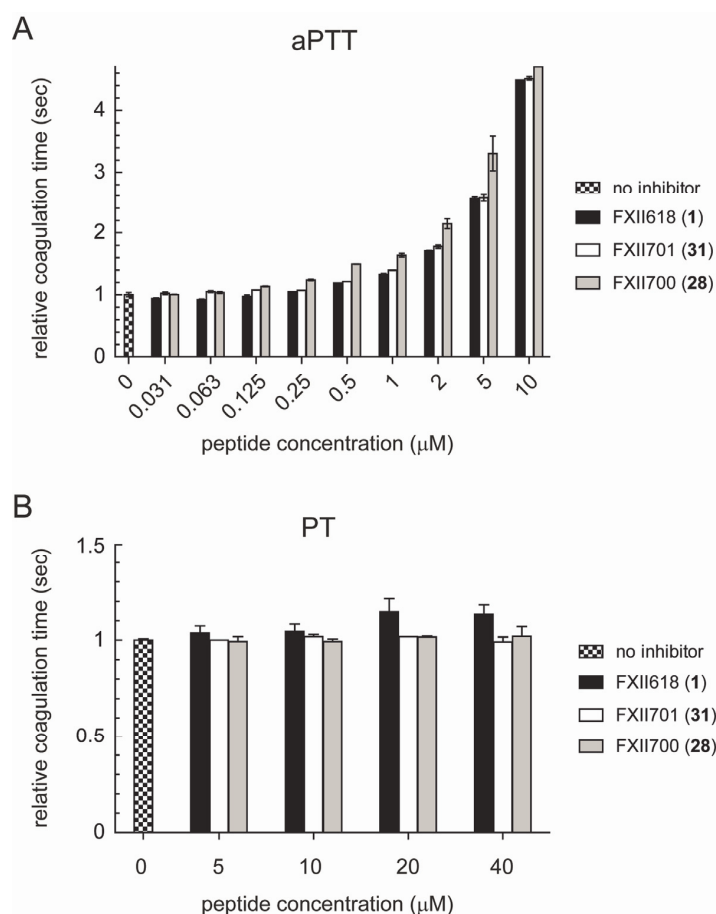


Figure 23. (A) aPTT and (B) PT coagulation data aPTT for bicyclic peptides **1** (FXII618), **28** (FXII700) and **31** (FXII701).

In summary, we have improved the binding affinity of in-vitro-evolved cyclic peptide ligands by varying the size of the macrocyclic rings by one or two carbon atoms. This chemical space is not sampled by screening genetically encoded cyclic peptide libraries, and potentially offers a rich source for slightly improved ligands. Indeed, synthesis and screening of a small library of backbone-modified bicyclic peptide variants of FXII inhibitor **1** yielded several inhibitors with substantially improved K_i values.

3.4 Experimental section

Materials: Fmoc-L- α -amino acids, O-(benzotriazol-1-yl)-N,N,N',N'-tetramethyluronium hexafluorophosphate (HBTU), 1-hydroxybenzotriazole hydrate (HOBt), and Rink Amide AM resin were purchased from GL Biochem (Shanghai, China). Fmoc- β -amino acids were purchased from Chem-Impex (Wood Dale, IL), PolyPeptide (Malmo, Sweden), and TCI (Tokyo, Japan). Fmoc cysteine derivatives were purchased from PolyPeptide.

Peptide synthesis: Solid-phase peptide synthesis was performed on an Advanced ChemTech 348 Ω peptide synthesizer (AAPPTec, Louisville, KY) by standard Fmoc procedures. Rink Amide AM resin was the solid support (0.03 mmol scale), and DMF was the solvent. Each amino acid was coupled twice (4 equiv, 0.2 M in DMF) by using HBTU/HOBt (4 equiv, 0.45 M in DMF) and DIPEA (6 equiv, 0.5 M in DMF; RT, 30 min, 400 rpm). The resin was washed four times with DMF after the coupling reaction. The N-terminal Fmoc protecting group was removed with piperidine (20% v/v) in DMF (RT, 2 \times 5 min, 400 rpm). The resin was washed five times with DMF after deprotection.

Peptide cleavage from the resin: The side chains were deprotected, and the peptide was cleaved from the Rink Amide AM resin by incubation with cleavage solution (5 mL; TFA (90% v/v), 1,2-ethanedithiol (2.5% v/v), phenol (2.5% w/v), thioanisole (2.5% v/v), H₂O (2.5% v/v)) for 2 h with shaking. The resin was removed by vacuum filtration, and the peptides were precipitated with ice-cold diethyl ether (50 mL), incubated for 30 min at -20 °C, and pelleted by centrifugation (2700 g, 5 min). The diethyl ether was discarded, and the precipitate was then washed twice with diethyl ether. The remaining solvent was evaporated at RT.

Peptide cyclization with TATA: The crude peptide (typically ~50 mg) was dissolved (~3.5 mM) in MeCN/H₂O (33:67, 6 mL). TATA (10 mM, 1.2 equiv) in MeCN was added. The reaction was started by the addition of degassed aqueous NH₄HCO₃ buffer (60 mM, pH 8.0) for a final peptide concentration of 1 mM and incubated at 30°C for 1 h in a water bath. The peptide was lyophilized.

Peptide purification by reversed-phase HPLC: Modified peptide powder was dissolved in DMSO (1 mL) with MeCN (2 mL containing TFA (0.1%)) and H₂O (7 mL containing TFA (0.1%)), and purified on a preparative Vydac TP1022 250 C18 column (22 mm, 10 mm) with a linear gradient of solvent B (MeCN with TFA (0.1%)) over solvent A (H₂O with TFA (0.1%)): 13 min, 15-28% solvent B, 20 mLmin⁻¹. Fractions containing the desired peptide product were identified by ESI-MS analysis and lyophilized. The purity of peptides was assessed by RP-HPLC, and the identity was confirmed by mass spectrometry (Figure S3.1 and Table S3.1 in the Supporting Information).

Protease inhibition assays: The inhibitory activity of the synthesized bicyclic peptides was determined by incubation with protease and quantification of the residual activity at various peptide concentrations using a fluorogenic substrate. Peptides were prepared as 2 mM stock solutions in H₂O. Residual enzymatic activity was measured in Tris-HCl (150 μ L, 10 mM, pH 7.4) containing NaCl (150 mM), MgCl₂ (10 mM), CaCl₂ (1 mM), Triton X-100 (0.01% v/v), and BSA (0.1% w/v). The final concentration of human β -FXIIa (#HFXIIAB; Molecular Innovations, Novi, MI) was 0.5 or 1 nM, with peptide at 10 μ M to 0.1 nM. The final concentration of the fluorogenic substrate Boc-QGR-AMC (Bachem,

Bubendorf, Switzerland) was 50 μ M. Fluorescence was recorded in an Infinite M200 Pro plate reader (λ_{ex} =368 nm, λ_{em} =467 nm; Tecan, Männedorf, Switzerland) every minute for 60 min at 25°C. Sigmoidal curves were fitted to the data by using the following dose-response equation.

$$y = A_1 + \frac{A_2 - A_1}{1 + 10^{(\text{LOG}_{10} x - x)p}}$$

where x = peptide concentration, y = % activity of reaction without peptide, A1 = 100%, A2 = 0%, p = 1. IC_{50} values were derived from the fitted curve in GraphPad Prism 5 software.

The inhibitory constant K_i was calculated according to Cheng and Prusoff; $K_i = IC_{50} / (1 + ([S]_0/K_m)$, wherein IC_{50} is the functional strength of the inhibitor, $[S]_0$ is the total substrate concentration, and K_m is the Michaelis-Menten constant. The K_m for Boc-QGR-AMC was determined to be 256 ± 42 μ M (mean \pm SD, n=4).

Coagulation assays: Coagulation times (aPTT and PT) were determined in human plasma by using a STart4 coagulation analyzer (Diagnostica Stago, Asnieres sur Seine, France). Human single donor plasma was used (Innovative Research, Novi, MI). For extrinsic coagulation, plasma (50 μ L) was placed in the incubating chamber of the instrument for 2 min at 37°C. Innovin (100 μ L; recombinant human tissue factor, synthetic phospholipids, and calcium in stabilized HEPES buffer system; Dade Behring/Siemens B4212-50) was added by using the pipette connected to the instrument. Upon addition of this reagent the electromagnetically induced movement of a steel ball in the plasma is monitored. The time until the ball stops moving is recorded as coagulation time. For the intrinsic coagulation, plasma (100 μ L) was incubated with 100 μ L of Pathromtin* SL (silicon dioxide particles, plant phospholipids in HEPES buffer system, Siemens OQGS29) for 2 min at 37°C. Coagulation was triggered by addition of $CaCl_2$ (100 μ L, 25 mM; Siemens).

3.5 Supporting information

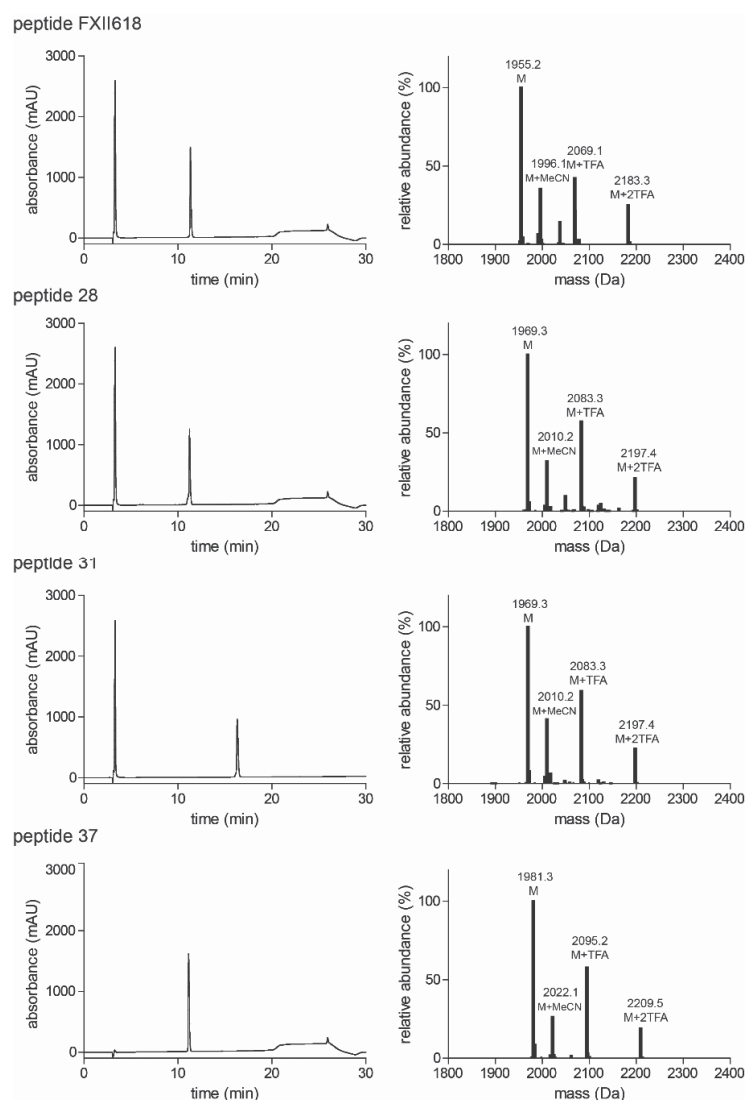


Figure S3.1. Analysis of important bicyclic peptide FXII inhibitors by reversed phase chromatography and mass spectrometry.

Table S3.1. Identity and purity of important bicyclic peptide FXII inhibitors analysed by reversed phase chromatography and mass spectrometry.

Peptide	Observed [M+3H] ³⁺	Observed [M+4H] ⁴⁺	Calculated MW	Theoretical MW	Purity (%)
FXII618	652.8	489.8	1955.2	1955.4	99
28	657.5	493.4	1969.3	1969.4	94
31	657.5	493.4	1969.3	1969.4	96
37	661.4	496.4	1981.3	1981.4	99

4. A peptide macrocycle FXII inhibitor provides safe anti-coagulation in a preclinical thrombosis model and in artificial lungs

This chapter is based on a manuscript for submission by the following authors:

Jonas Wilbs, Simon J. Middendorp, Alida Cooke, Caitlin T. Demarest, Raja Prince, Mai M. Abdelhafez, Christina Lamers, Kaycie Deyle, Robert Rieben, Anne Angelillo-Scherer, Keith E. Cook, and Christian Heinis

Author contributions: J.W., S.J.M, C.L., and C.H. developed and characterized the FXIIa inhibitor. J.W., S.J.M., and C.H. designed and performed the pharmacokinetic experiments in rabbits. M.M.A., J.W., R.R., and C.H. designed and performed the pharmacokinetic experiments in pigs. R.P., J.W., A.A.S., and C.H. designed and performed the pharmacokinetic and thrombosis experiments in mice. A.C., C.T.D., K.E.C., and J.W. designed and performed the artificial lung experiments in rabbits. J.W. and C.H. wrote the manuscript. All authors contributed to editing and critical proof-reading of the manuscript.

4.1 Abstract

Inhibiting thrombosis without inherently generating bleeding risks is a major challenge in medicine. The discovery that mice deficient in coagulation factor XII (FXII) show reduced thrombosis without abnormal bleeding suggested that targeting FXII could offer a solution to this longstanding problem. Several strategies to control FXII activity, including monoclonal antibodies, were developed and successfully evaluated in preclinical models. In contrast, the development of small molecule inhibitors proved more challenging. Herein, we have engineered a peptide macrocycle inhibitor of activated FXII (FXIIa) with sub-nanomolar activity ($K_i = 370 \pm 40$ pM) and a high stability ($t_{1/2} > 128 \pm 8$ h in plasma), allowing for the preclinical evaluation of a first synthetic FXIIa inhibitor. The 1899 Da inhibitor, termed FXII900, efficiently blocked FXIIa in mice, rabbits, and pigs. We show that it reduced experimental thrombosis induced by ferric chloride in mice and suppressed blood coagulation in an extracorporeal membrane oxygenation (ECMO) setting in rabbits, all without increasing the risk of bleeding. This shows that FXIIa activity is controllable with a synthetic inhibitor *in vivo*, and that the inhibitor FXII900 presented herein is a promising candidate for safe thromboprotection in various medical conditions.

4.2 Introduction

Coagulation is required to stop the bleeding at sites of vessel wall injuries, but excess coagulation can also lead to thrombosis. Blood vessel blockages, can occur in the arterial and venous circulation to cause myocardial infarctions, ischemic strokes, and pulmonary embolisms, which collectively are the leading causes of disability and death in the industrialized world (215). In all of the anticoagulants widely used for the acute and prophylactic treatment of thrombosis (216, 217), bleeding is a common side effect, and the initiation of any therapy to treat coagulation deficiencies must always weigh these risks and benefits, considering the severity of the potential side effects. Thus, there is a growing need for the development of effective anticoagulants that ideally would not impair hemostatic ability (218).

A promising novel perspective for developing safe anticoagulants with reduced or no bleeding risks is the inhibition of coagulation factors XII (FXII) and XI (FXI), both being proteases of the intrinsic coagulation pathway (219). FXII is the initiating protease of the procoagulant and proinflammatory contact system, and it drives both the intrinsic pathway of coagulation and the kallikrein-kinin system (220). Mice lacking FXII have a highly reduced risk of injury-induced arterial and venous thrombosis (221, 222) and are protected from pathological thrombosis in cerebral ischemia (223). At the same time, humans naturally lacking FXII and FXII-knockout mice have a normal hemostatic capacity

and do not bleed abnormally (221, 224), which indicated that drugs targeting the protease could potentially produce antithrombotic effects without significantly compromising hemostasis. Concordantly, the reduction of FXII expression in mice by antisense oligonucleotides suppressed thrombosis (225, 226). The inhibition of FXII by protein-based inhibitors such as antibodies (227, 228) or insect- and plant-derived proteins (229–231) also reduced thrombosis in animal models and showed potential avenues for therapeutic anticoagulation.

FXII-driven blood coagulation is a major challenge in cardiopulmonary bypass (CPB) surgeries in which a heart-lung machine temporarily supports the circulation. Contact between FXII and artificial surfaces, such as the oxygenator membrane or tubing, induces a conformational change that leads to the proteolytic activation of the FXII zymogen that turns on the contact system. Activation of the procoagulant intrinsic coagulation pathway and the proinflammatory kallikrein-kinin system leads to blood clotting and inflammation (187). The risk of contact activation is particularly high in extracorporeal membrane oxygenation (ECMO), a form of CPB in which an artificial lung system is used for longer periods of time as a life support for patients with severe cardiac and/or pulmonary failure (232). The standard strategy for suppressing contact system activation in extracorporeal circuits relies on high doses of heparin, which inhibits also proteases of the extrinsic and common coagulation pathway and thus bears an inherent risk of bleeding (233). Several strategies for suppressing contact activation were established in experimental models, but heparin remains the anticoagulation strategy of choice (234). In a recent study, Renne and co-workers showed that a human FXIIa-inhibiting antibody, 3F7, prevented clotting and thrombosis in a cardiopulmonary bypass system in rabbits without increased therapy-associated bleeding (227), indicating the usefulness of targeting FXII.

FXII is implicated in several other medical conditions (235), including hereditary angioedema (HAE) (236), reperfusion injury (237), Alzheimer's disease (238, 239), and multiple sclerosis (240), meaning that potential FXII inhibitors could be used in a variety of treatments not limited to thrombosis prevention. In Type III HAE, for example, a mutation in FXII increases its activity, leading to excessive bradykinin release that causes edema (241). A derivative of the above-mentioned FXIIa inhibitory antibody 3F7 has entered a phase I clinical evaluation for the treatment of HAE (242).

While high-affinity protein-based FXIIa inhibitors were successfully generated over the last years (243), the development of synthetic, small molecule inhibitors has been more challenging. Small molecules have a number of strengths that make them attractive for drug development, including a uniform composition, efficient tissue penetration, high stability, low immunoreactivity, and ease of production by chemical synthesis. The best small molecule FXIIa inhibitors reported to date are the coumarin derivative 44 (IC_{50} =

4.4 μM) (244) and H-D-Pro-Phe-Arg-chloromethylketone (PCK; $IC_{50} = 0.18 \mu\text{M}$) (223). While they have proven to be useful as research compounds in FXIIa inhibition studies, their covalent inhibition mechanism and their moderate potency and selectivity limit their drug development potential.

We have recently identified high-affinity FXIIa inhibitors based on peptide macrocycles using phage display, including the bicyclic peptide FXII618 ($K_i = 8.1 \text{ nM}$) (203). In previous work, the substitution of individual amino acids in FXII618 to unnatural ones further improved the affinity (245, 246), though due to their limited binding to animal FXIIa homologs and low proteolytic stability in plasma, these particular peptide macrocycle inhibitors could not be evaluated in vivo. For this reason, we have now further improved the inhibitor to achieve picomolar potency towards human and mouse FXIIa, and we enhanced the stability in plasma to several days (half-life in human plasma ex vivo). These properties allowed for the pre-clinical evaluation of the inhibitor in various animal models. We show herein that synthetic FXIIa inhibitors can be developed to efficiently prevent thrombosis in mice and suppress coagulation in artificial lungs in rabbits without increasing the risk of bleeding.

4.3 Results

4.3.1 Engineered macrocycle inhibits human and mouse FXIIa with picomolar affinity

The N-terminal arginine in FXII618 (Arg1) is rapidly cleaved by plasma proteases ($t_{1/2}$ around 4 h in human plasma) and its loss reduces the K_i of the inhibitor 40-fold (204). In a previous study substituting Arg1 with diverse unnatural amino acids, the stability could be improved at the price of a weaker inhibition, wherein amino acids with positively charged side chains showed the smallest affinity losses (204). In a new attempt, we replaced Arg1 with a panel of di-peptides that could potentially reach a larger surface area on FXIIa to form productive interactions (Figure 24A, Table S4.1). Both amino acids in the di-peptides were D-amino acids to prevent proteolysis, and one of the two was D-Arg to maintain a positive charge. We developed a synthesis and screening approach based on coumarin-labeled peptides that allowed the comparison of the activities of crude peptides to avoid the need for purifying large numbers of peptides in the initial screening tests (supplementary data). Several di-peptides improved the K_i values around two-fold over FXII618 (Figure 24A). A stability assay showed that the di-peptides based on D-amino acids were resistant to proteolysis, prolonging the plasma half-life around five-fold to 20 hours (Figure S4.1). The best inhibitor, Arg1 \rightarrow D-Arg-D-Ser (FXII850) was synthesized without the coumarin label and showed a K_i of $5 \pm 2 \text{ nM}$, which was a 1.6-fold improvement compared to FXII618 ($K_i = 8.1 \pm 0.7 \text{ nM}$; Figure 24B and C, Figure S4.2). We also tested a panel of diverse amino acid substitutions for Arg8, a position in FXII618

that had not been systematically optimized, using the same screening strategy based on coumarin-labeled peptides (Figure 24A, Table S4.1). The substitution Arg8→His showed improved inhibition, particularly of mouse FXIIa, which allowed for the consideration of pre-clinical studies in mice. The peptide without the coumarin label (FXII851) inhibited human and mouse FXIIa with K_i values of 6.5 ± 0.3 nM and 36 ± 3 nM, respectively, which corresponded to 1.2- and 2.4-fold improvements over FXII618 (Figure 24B and C, Figure. S4.2).

We next combined the beneficial amino acid substitutions identified in this work, the Arg1→D-Arg-D-Ser (FXII850) and Arg8→His (FXII851) with the two previously identified substitutions, Arg11→(S)-β3-homoarginine (βhArg; FXII700; $K_i = 1.5 \pm 0.1$ nM) (246) and Phe3→4-fluorophenylalanine (Phe4F; FXII800; $K_i = 0.84 \pm 0.03$ nM) (204) (Figure 24B and C, Table S4.2). In addition, we deleted the C-terminal Arg13 that we had previously found to not contribute to the binding affinity (unpublished result). The resulting inhibitor, FXII900, blocked human and mouse FXIIa with K_i values of 0.37 ± 0.04 nM and 0.45 ± 0.11 nM, respectively, and was thus substantially more potent than any of its precursors (Figure 24C). A specificity profile against a panel of homologous plasma proteases showed that FXII900 is highly selective (Figure 24D, Table S4.3). All physiologically relevant proteases displayed 100,000-fold or higher selectivity (K_i values > 40 μM), with only trypsin being inhibited at low micromolar concentrations ($K_i = 1.46 \pm 0.12$ μM). FXII900 could be efficiently synthesized in gram-scale, by solid-phase peptide synthesis of the linear precursor and subsequent macrocyclization of the crude peptide with the 1,3,5-triacryloyl-1,3,5-triazinane linker (TATA). Only a single HPLC purification step was required to obtain $> 95\%$ pure product with an isolated yield greater than 50% (Figure S4.3).

4.3.2 FXIIa inhibitor is stable in human plasma for several days

Incubating FXII900 in human plasma at 37°C for extended time periods and then quantifying the remaining FXIIa inhibitory activity was used to measure the stability of the inhibitor in plasma (Figure 24E). Mass spectrometric analysis of the various plasma samples showed only FXII900 and no degradation products, wherein the quantity of the intact inhibitor was reduced over time (Figure 24F, right panel). This data suggested that after an initial cleavage event occurred, the inhibitor was rapidly degraded and, therefore, not detectable. The half-life of FXII900 was 128 ± 8 h, around 25-fold longer than that of FXII618. It was also much longer than that of FXII850 carrying only the Arg1→D-Arg-D-Ser modification ($t_{1/2} = 18.5 \pm 1.3$ h; Figure 24E), indicating that more than one of the introduced mutations contributed to the improved stability. In order to identify which modification(s) were important for stability, we synthesized FXII900 variants in which the amino acid substitutions were individually reverted (Figure S4.4, Table S4.4).

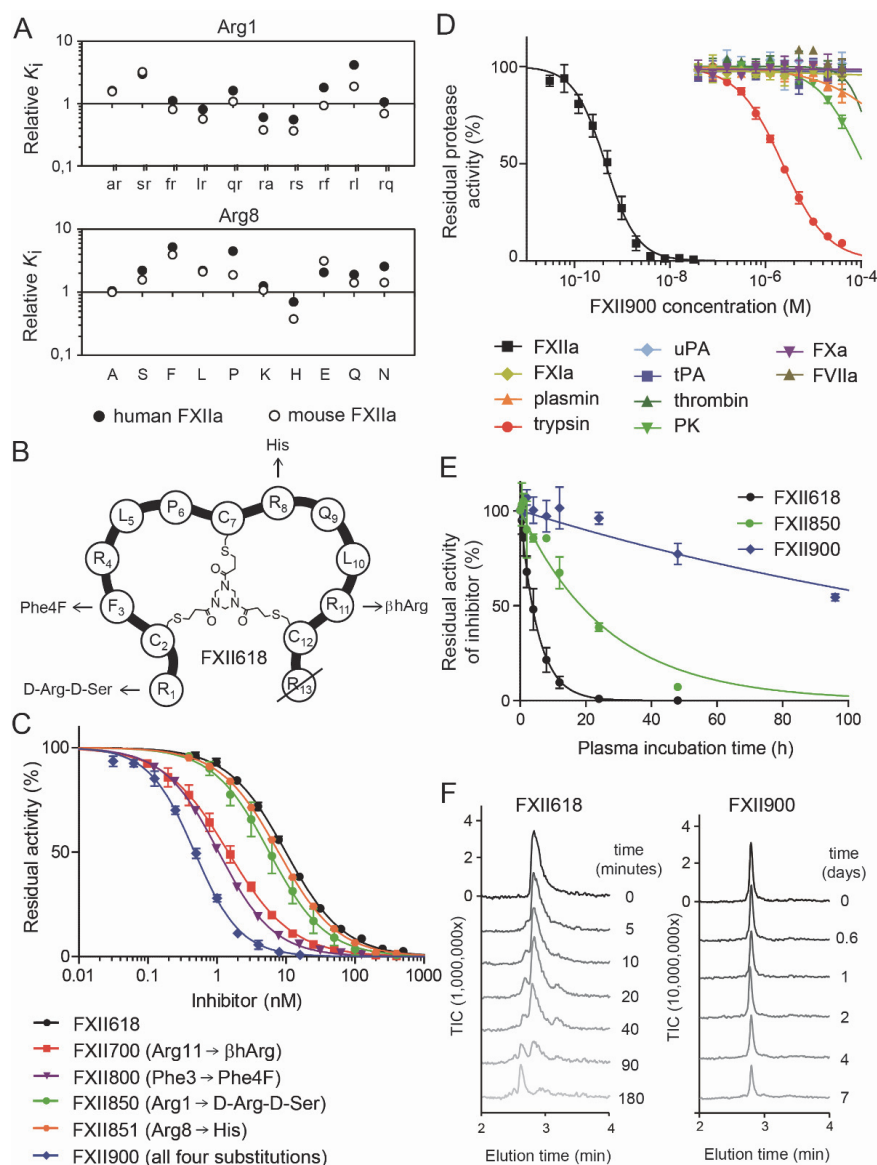


Figure 24. Improving affinity and stability of bicyclic peptide FXIIa inhibitor. (A) Amino acids Arg1 and Arg8 of FXII618 were individually substituted to two D-amino acids or natural amino acids, respectively. The relative K_i values for human and mouse FXIIa are indicated as compared to the lead peptide FXII618. Average values of three measurements are shown. (B) Schematic representation of the lead peptide FXII618. Amino acid substitutions that improve the activity and/or stability are indicated. (C) Inhibition of human FXIIa by FXII618, variants of FXII618 containing a single amino acid substitution, and FXII900 in which four beneficial modifications were combined and Arg13 was deleted. Residual FXIIa activity was measured at least three times. Means \pm SD are indicated. (D) Specificity profiling of FXII900. Residual activities of human FXIIa and 11 homologous human proteases were measured three times. Means \pm SD are indicated. (E) Proteolytic stability of FXII900 and two precursors. Bicyclic peptide was incubated in human plasma at 37°C for the indicated time periods, and the remaining inhibitor activity was quantified in a FXIIa activity assay using fluorogenic substrate. Means \pm SD are indicated. (F) Proteolytic stability of FXII618 and FXII900. Bicyclic peptide was incubated in plasma at 37°C for the indicated time periods and analyzed by LC-MS.

Mass spectrometric analysis of the variants incubated in human plasma revealed that the Arg11→βhArg contributed the most to the stability improvement (Figure S4.5).

4.3.3 FXII900 efficiently inhibits the intrinsic coagulation pathway *ex vivo*

To assess the ability of FXII900 to block FXII-driven blood plasma coagulation and to evaluate further its selectivity, we performed coagulation tests to measure activated partial thromboplastin time (aPTT) and prothrombin time (PT). aPTT and PT measure the time until coagulation upon initiation of the intrinsic and extrinsic pathways, respectively, meaning that selective FXIIa inhibition would prolong aPTT but not PT. FXII900 prolonged aPTT in human plasma with an $EC_{1.5x}$ of $0.79 \pm 0.08 \mu\text{M}$, thus 4.3-fold better than its precursor FXII618 ($EC_{1.5x}$ of $3.4 \pm 0.3 \mu\text{M}$; Figure 25A). FXII900 did not affect PT, even at the highest concentration tested (120 μM), confirming the selectivity for the FXII target (Figure 25B).

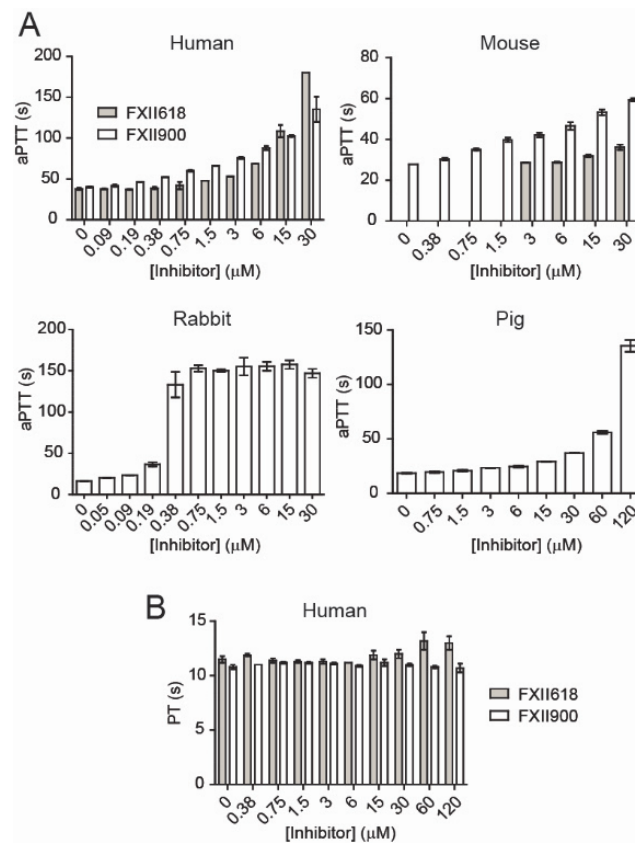


Figure 25. Inhibition of the intrinsic coagulation pathway in human, mouse, rabbit, and pig plasma *ex vivo*. (A) Prolongation of the aPTT in the presence of different concentrations of FXII900. For human and mouse plasma, the aPTT of FXII618 was measured for comparison. (B) PT in the presence of different concentrations of FXII900 and FXII618. All coagulation times were measured in triplicate and means \pm SD are indicated.

This contrasts with FXII618 that showed a slight prolongation of PT at the highest concentration tested (1.2-fold at 120 μ M), indicating an improved selectivity of FXII900 over FXII618. The inhibitor also efficiently prolonged the aPTT in plasma of all other species tested, namely mouse ($EC_{1.5x} = 2.9 \pm 0.5 \mu$ M), rabbit ($EC_{1.5x} = 0.102 \pm 0.001 \mu$ M) and pig ($EC_{1.5x} = 12.2 \pm 0.7 \mu$ M; Figure 25A). In mouse plasma, the aPTT improvement was more than 10-fold compared to FXII618 ($EC_{1.5x} > 30 \mu$ M).

4.3.4 Pharmacokinetics in mice, rabbits, and pigs

We assessed the pharmacokinetic properties in three species, mice, rabbits, and pigs, as suitable models for thrombotic diseases are available for these animals. In mice, we determined the pharmacokinetics following subcutaneous administration (5 mg/kg, $n = 2$ per time point). FXII900 reached a plasma concentration of around 1 μ M after three minutes and remained above this concentration for 30 minutes as determined by LC-MS (Figure 26A, upper panel). The aPTT was prolonged as expected based on the plasma concentrations, namely it was extended by two-fold at 15 minutes and remained prolonged by over 1.5-fold until 30 minutes (Figure 26A, lower panel).

In rabbits, we determined the pharmacokinetic properties for intravenous and subcutaneous administration. Upon intravenous administration ($n = 3$, 3.7 mg/kg), FXII900 showed an elimination half-life of 12 ± 2 min (Figure 26B, upper panel; pharmacokinetic parameters are provided in Table S4.5). The aPTT was initially more than eight-fold prolonged and remained more than three-fold prolonged for the entire time monitored (40 min; Figure 26B, lower panel). When applying the same dose subcutaneously ($n = 4$, 3.7 mg/kg), the peptide remained in a narrower concentration range, staying above 100 nM and below 300 nM for between 10 and 80 minutes after administration (Figure 26C, upper panel). The aPTT with the subcutaneous administration was prolonged by more than two-fold for 40 minutes (Figure 26C, lower panel).

We further determined the pharmacokinetics of FXII900 in pigs, as this species offers models for indications in which FXII plays a role, such as ischemic reperfusion injury (237, 247). For this study, we applied conditions that are used in the disease model for reperfusion injury, which included heparin anticoagulation to prevent induction of thrombosis through the catheters that is used to induce ischemia or to measure blood pressure (2500 IU when ACT fall below 180 seconds). After intravenous administration ($n = 3$, 4 mg/kg) the inhibitor reached a maximal concentration of around 7 μ M and was cleared with a $t_{1/2}$ of 36 ± 5 min (Figure 26D, upper panel). The clearance rate and volume of distribution were 11.8 ± 1.8 ml/kg/min and 610 ± 140 ml/kg (Table S4.6). Despite the application of heparin that bore the risk of shielding the effect of FXII900, a two-fold prolongation of the aPTT was seen in plasma samples taken a short time after the administration of the inhibitor (Figure 26E). The same effect was not seen for the negative

control peptide, FXII901, a variant of FXII900 with three modifications (Phe4F3→Phe, Arg4→Ala, βhArg11→Arg, using the amino acid numbering of FXII618; Figure S4.6) that reduce its inhibitory constant 100,000-fold for FXIIa ($K_i = 39 \pm 14 \mu\text{M}$), though also lower its plasma half-life due to proteolytic degradation (Figure 26D, lower panel). The small and short effect of FXII900 on aPTT can be explained with the comparatively high inhibitor concentrations required to prolong the aPTT in pig plasma ($\text{EC}_{1.5x} = 12.2 \pm 0.7 \mu\text{M}$).

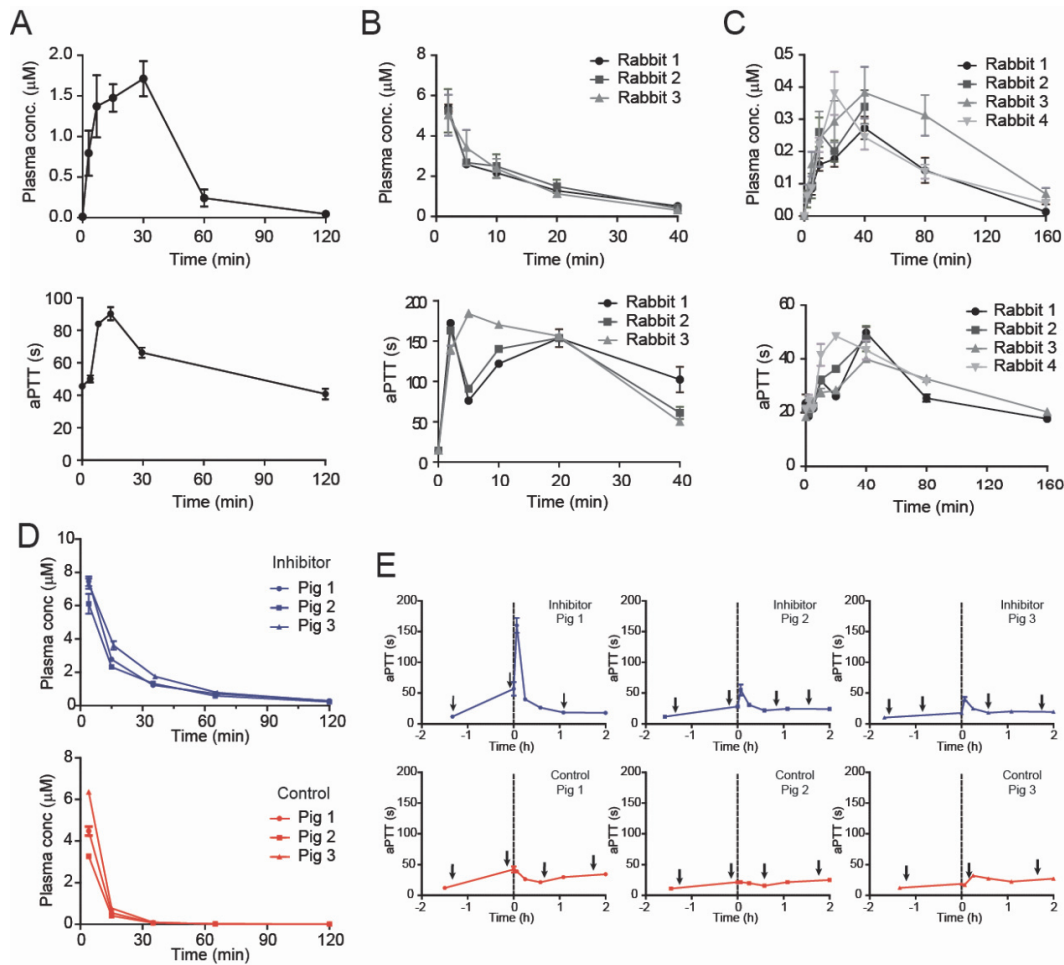


Figure 26. Pharmacokinetics of FXII900 in mouse, rabbit, and pigs and inhibition of FXII-driven coagulation. (A) Pharmacokinetics in mouse after subcutaneous administration (5 mg/kg). Concentration of FXII900 in plasma (upper panel) and aPTT (lower panel) are indicated. Two mice were used for each time point, and the samples were analyzed in triplicate. Means \pm SD were combined. (B) Pharmacokinetics in rabbit after intravenous administration (3.7 mg/kg, n = 3). Concentration of FXII900 in plasma (upper panel) and aPTT (lower panel) are indicated. Plasma samples were analyzed in triplicate. Means \pm SD are indicated for each rabbit. (C) Pharmacokinetics in rabbit after subcutaneous administration (3.7 mg/kg, n = 4). Concentration of FXII900 in plasma (upper panel) and aPTT (lower panel) was measured. Plasma samples were analyzed in triplicate. Means \pm SD are indicated for each rabbit. (D) Pharmacokinetics in pig after intravenous administration (4 mg/kg, n = 3). Concentrations of FXII900 and inactive peptide FXII901 in plasma were

determined in triplicate, and means \pm SD are indicated. (E) Prolongation of aPTT in pig. Pigs anticoagulated with heparin (injections of 2500 IU when ACT was below 180 s; injections are indicated by arrows) were treated with FXII900 or the negative control FXII901 at time 0 (indicated by dashed line; $n = 3$ in each group, 4 mg/kg), and the aPTT was measured in plasma samples taken over time. aPTT was measured in triplicate. Means \pm SD are indicated

4.3.5 FXII900 inhibits ferric chloride-induced arterial thrombosis in mice

We next evaluated the thromboprotective properties of FXII900 in a ferric chloride (FeCl_3)-induced arterial thrombosis mouse model. When applied directly onto the blood vessels, FeCl_3 induces thrombosis through aggregation of the red blood cells, which in turn activates platelets at the application site (248, 249). FXII900, or an inactive control peptide FXII901, were administered subcutaneously ($n = 10$ for both groups, 5 mg/kg), with 7.5% FeCl_3 applied to the mesenteric arterioles while the blood flow was monitored by intravital microscopy. Mice that were injured by FeCl_3 could be clearly identified due to a speckled pattern that supposedly represented an accumulation of platelets (Figure 27A) (250). Seventeen out of the 20 mice showed this pattern (nine treated, eight control) and were taken for further analysis (Figure S4.7 and S4.8). The arterioles of the mice receiving the inactive control peptide FXII901 rapidly formed clots, and in a majority of the animals, the vessels were completely occluded after around 10 minutes, as exemplified in the lower micrographs in Figure 27A and shown for all mice in Figure S4.7. In contrast, mice that were treated with the inhibitor FXII900 showed only the characteristic speckled pattern with the occasional formation of a blood clot (Figure 27A, upper micrographs; Figure S4.8). In this group, no complete occlusion was observed. We quantified the anticoagulant effect of FXII900 by comparing the rates for both clot formation (a clearly visible blood clot; Figure 27B, left panel) and blood vessel occlusion (a blood clot with a diameter of the blood vessel; Figure 27B, right panel). Of the eight mice receiving the control peptide, seven showed blood clotting and four showed full-vessel occlusion. In contrast, in the FXII900-treated mice, only three showed blood clotting, and in no mice were the vessels fully occluded ($p = 0.02$ and 0.005 , respectively). In addition, the few mice in the treated group that showed signs of coagulation developed these blood clots in average around 10 minutes later than the control group ($p = 0.006$; Table S4.7).

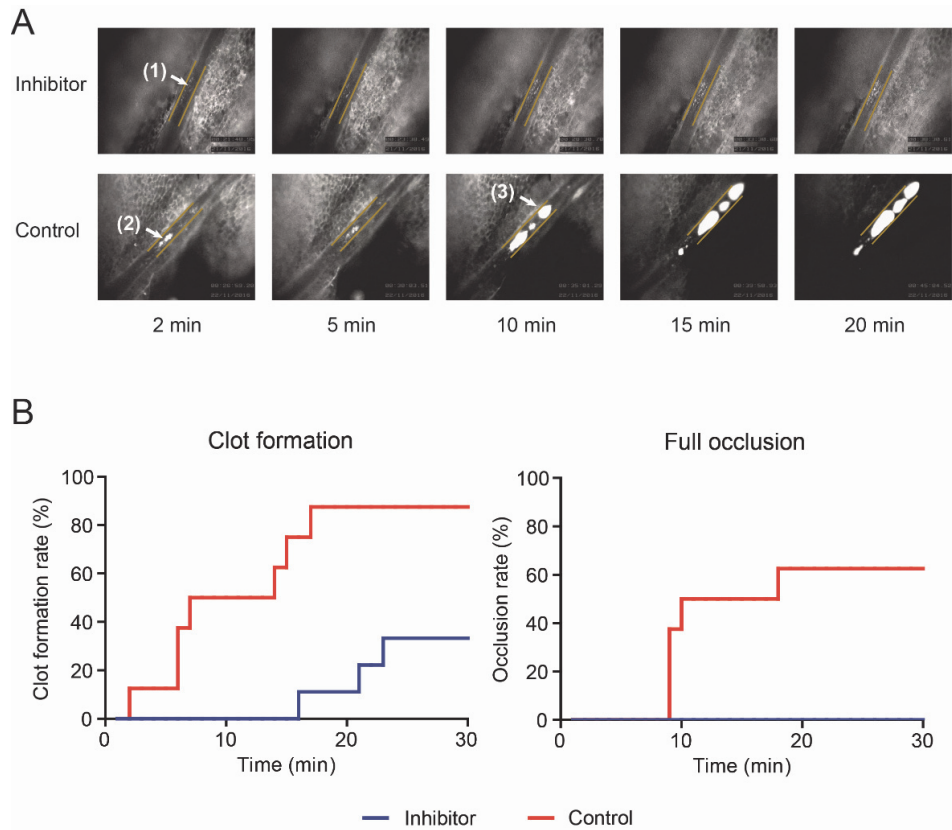


Figure 27. Thromboprotection of FXII900 in a ferric chloride-induced thrombosis mouse model. (A) Intravital fluorescence microscopy images showing mesenteric arterioles in which thrombosis was induced by topical application of FeCl_3 (7.5%, 1 min). Platelets were fluorescently labeled with Rhodamine 6G for visualization. Representative images are shown for two mice, one treated with FXII900 (upper panels) and one with inactive control peptide FXII901 (lower panels) 15 min before application of ferric chloride (5 mg/kg, subcutaneous injection). Vessel walls at the FeCl_3 application site are indicated with yellow markers. Three distinct morphological changes, a characteristic speckled pattern (1), clot formation (2), and vessel occlusion (3), are indicated. (B) The percentage of mice showing either clot formation or full occlusion at different time points after ferric chloride application is indicated over time. Clot formation was defined as the appearance of an aggregate with a diameter of around $10\ \mu\text{m}$. Full occlusion of the blood vessel was defined as a blood clot having the same diameter as the blood vessel.

4.3.6 FXII900 provides bleeding-free anticoagulation in artificial lungs

To test the clinical potential of FXII900 for inhibiting FXII-driven coagulation in ECMO, we tested the inhibitor in an artificial lung rabbit model. New Zealand White rabbits were anesthetized, either treated intravenously with FXII900 ($n = 4$, 2 mg/kg bolus and 0.075 mg/kg/min infusion for four hours) or left untreated (control group, $n = 3$), and were mounted for a four-hour period to a venous/venous ECMO configuration using a polymethylpentene (PMP) fiber artificial lung system (251). Coagulation parameters and the resistance of the lung device, a measure for occlusive thrombus formation, were

measured over the entire duration of the experiment, and clot formation in the lung device was analyzed after the four hours were completed (Figure 28; data for the individual rabbits is shown in Figure S4.9).

Treatment with FXII900 prolonged the coagulation parameters aPTT and activated clotting time (ACT) around 10-fold during the entire course of the experiment (Figure 28A and B). For most aPTT measurements, no coagulation was observed at 240 seconds, being the maximal aPTT value measurement with the device used (Figure S4.9A). In untreated rabbits, the coagulation times remained at baseline values of around 20 seconds (aPTT) and 170 seconds (ACT) throughout the experiment. Increased blood pressure at the inlet of the artificial lung indicates clogging of the device that can be caused by blood coagulation. We therefore measured the resistance at the artificial lung, indicated by the difference in pressure at the inlet and outlet of the lung divided by the flow. In all rabbits treated with FXII900, the resistance remained at the baseline of 50 mmHg/L/min during the entire experiment, except for one rabbit in which the resistance started to increase strongly after two hours at baseline (Figure 28C and Figure S4.9C). This was in stark contrast to the untreated animals in which the resistance doubled from 50 mmHg/L/min to 100 mmHg/L/min or higher.

With excessive bleeding as the main concern when applying standard anticoagulation in ECMO systems, we analyzed if FXII900 affected the hematological parameters of bleeding time and platelet count. Rabbits treated with the inhibitor showed completely normal bleeding times throughout the experiment (4–5 min; Figure 28D and Figure S4.9D). The platelet count was essentially the same in the two groups, decreasing around two-fold from an initial level of 2×10^8 cells/ml (before connecting the lung) and remaining constant over the entire course of the experiment (Figure 28E and Figure S4.9E).

At the end of the experiment, we determined the extent of blood clot formation inside of the artificial lungs by measuring the total volume of the blood clot in each lung. A visual inspection of the membranes showed a substantially reduced amount of clotted blood in the inhibitor-treated rabbits. This finding was confirmed by quantifying volume of the clot in relation to the device volume, which was $10 \pm 6\%$ for the FXII900-treated and $37 \pm 10\%$ for the untreated rabbits ($p = 0.03$; Figure 28F and Figure S4.9F).

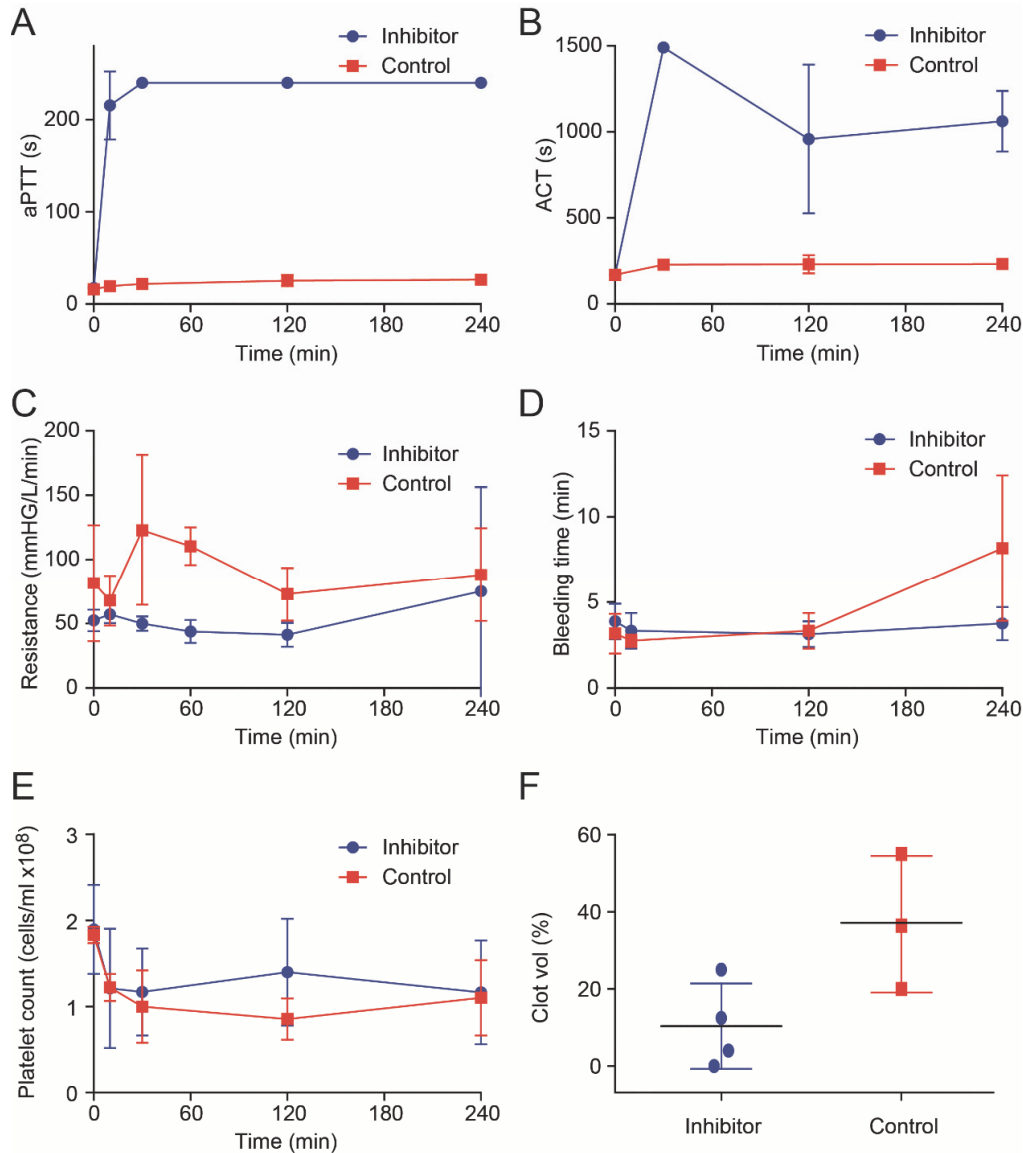


Figure 28. Bleeding-free anticoagulation in an artificial lung model in rabbits. Rabbits were connected veno-venous to an artificial lung system for four hours. FXII900 was injected as a bolus (2 mg/kg) before the start of the extracorporeal circulation and as a constant infusion (0.075 mg/kg/min) over the full time course of the experiment (n = 4; data shown in blue). Rabbits in the control group were untreated (n = 3, data shown in red). Values indicated for the time point 0 refer to measurements made before connection of the artificial lung. Mean \pm SD is indicated for the rabbits in each group unless indicated. Data of individual rabbits is shown in Figure S4.9. (A) aPTT. Coagulation times of 240 s indicate that plasma did not coagulate at this time. (B) ACT. Clotting times of 1500 s indicate that blood did not coagulate at this time. (C) Resistance calculated based on pressure at the inlet and outlet of the device and the flow rate. (D) Bleeding time measured by incision-provoked injuries at the ears. (E) Platelet count. (F) Volume of blood clots indicated in % of volume of the artificial lungs. For the control group, mean \pm SD is indicated only for three out of the four rabbits, as for one animal the volume was not determined.

4.4 Discussion

The role of FXII in thrombosis observed in experimental animal models, but not in hemostasis offers an exciting potential strategy for safe anticoagulation based on interference with the plasma protease. Various protein-based inhibitors have been developed and showed that suppression of FXII activity provides efficient anticoagulation without increasing bleeding risks. The development of high-affinity small molecule FXIIa inhibitors has been lagging behind. Given the attraction of small, synthetic molecules as drug modality, we have improved in this work the binding affinity and stability of FXII618, a peptide macrocycle FXIIa inhibitor that was previously developed by phage display. The generated inhibitor, FXII900, blocks FXIIa with a K_i of 370 pM, shows 100,000-fold selectivity over other plasma proteases, and is stable in blood.

The improvement of the binding affinity of FXII618 by 21-fold and proteolytic stability by 25-fold was achieved by combining random screening and rational design strategies. Two amino acid substitutions that enhance the affinity and/or stability of the inhibitor were identified by screening a panel of singly mutated peptides, and were combined with two previously identified beneficial mutations. Individual reversion of the four amino acid substitutions in FXII900 showed that each single one contributes to improving the binding affinity and that mainly the modification of Arg11 to β hArg improves the stability. The higher binding affinity translates into a prolongation of the aPTT in all species. In human plasma, the $EC_{1.5x}$ was reduced 4.3-fold, and in mouse plasma even 10-fold. The much enhanced potency in mouse plasma was of interest in view of the planned pharmacologic study in mice. FXII900 did not prolong PT at 120 μ M at all, which was in contrast to FXII618 that prolonged PT slightly at this highest concentration tested, indicating that modification of the four amino acids had also improved the selectivity of the inhibitor. The enhancement of affinity, selectivity and stability achieved in this work is owed mostly to unnatural amino acids that could be incorporated due to the synthetic nature of the inhibitor, which is an advantage over protein-based inhibitors that need to be produced by recombinant expression and do not easily allow the incorporation of unnatural building blocks.

FXII900 is composed of nine natural amino acids, four non-natural ones, and a central core structure that connects the side chains of the three cysteines. The inhibitor can be conveniently synthesized by automated solid-phase peptide synthesis in large quantities. All applied non-natural amino acids are inexpensive, allowing for production of inhibitor for a moderate cost. Crude linear peptide was cyclized efficiently by the chemical linker TATA and only a single HPLC purification step was required to obtain > 95% pure product with an isolated yields greater than 70%. We provide a supplementary figure that describes the exact peptide sequence and the conditions recommended for

peptide cyclization, that may be used for ordering the peptide from companies offering custom peptide synthesis (Figure S4.3).

FXII900 is rapidly cleared by renal filtration, as could be expected based on the small size and the polar structure. The elimination half-life ranges from 12 minutes in rabbits to 36 minutes in pigs. Based on allometric scaling, this half-life in human can be expected in the range of one hour. No degradation products were detected in plasma samples of all species, suggesting that the inhibitor fully resists proteases in the blood circulation and that it is filtered out as an intact molecule, which is in line with the high stability and long half-life in plasma found *ex vivo*. Despite the fast clearance, single-dose injection of FXII900 prolonged aPTT in all three species tested. In pig, the effects were small and seen only for a few minutes after injection. The small effect was expected given the relatively high $EC_{1.5x}$ for aPTT in pig plasma, caused most likely from a weaker inhibition of the porcine FXIIa. The relatively short circulation time allows flexible adjustment of the duration for which the body is exposed to the inhibitor in therapeutic applications. Indeed, continuous infusion in the rabbit ECMO study allowed for maintaining the aPTT above 200 sec over the four hours of the experiment, despite the relatively fast clearance of 16.1 ml/kg/min. The pharmacokinetic profile of FXII900 makes it attractive for acute disease treatment such as CPB, including ECMO, or anticoagulation for short time periods after ischemic stroke or after surgery.

We have evaluated the pharmacologic activity of FXII900 in a ferric chloride-induced thrombosis mouse model. FXII-deficient mice show strong reduction of coagulation in this model, indicating that FXII plays a central role in this process. We found that a bolus injection of FXII900 efficiently protected mice from thrombosis. At the single dose of 5 mg/kg tested, none of the nine treated mice showed thrombotic vessel occlusion whereas five of the eight in the untreated group formed a thrombus. It has to be stated that thrombosis in myocardial infarction, ischemic stroke, or pulmonary embolism is more complex than in the applied mouse thrombosis model, as thrombosis is also caused by triggers that are not dependent on FXII activation. Independent of this, the results obtained show that a synthetic FXIIa inhibitor can efficiently suppress coagulation in cases where coagulation is mediated via FXII activation.

We have further tested if FXII900 is suited to suppress coagulation activated by the membrane of artificial lungs, using a rabbit model. Heart-lung machines are used for heart surgery because of the difficulty of operating on the beating heart. Approximately half a million of the cardiac operations performed per year in the US use CPB. Heart-lung machines are additionally used to support patients with cardiorespiratory dysfunction. More than 7000 patients are treated annually with extracorporeal life support and the heart-lung machine is rescuing many lives by supporting oxygenation and systemic blood circulation (252). Contact of blood with nonphysiological surfaces induces FXII

contact activation and thus coagulation, that is currently suppressed by high dose of heparin, which bears bleeding risks. Analysis of nearly 80,000 ECMO patients showed that hemorrhage is the major adverse event, with bleeding from surgical sites happening in 6.3% to 29.3% patients, depending on the patient group (252). We found that FXII900 substantially reduced coagulation in an artificial lung, as measured by the resistance of the device which remained low and indicated reduced clogging by coagulation, and the volume of the blood clots in the device which was more than three-fold smaller in the treated rabbits. Importantly, all rabbits treated with FXII900 showed normal bleeding times. These findings indicate that a small molecule FXIIa inhibitor is suitable to reduce blood coagulation in CPB. While heparin may still be required to suppress coagulation triggered through other routes than FXII, application of a small molecule FXIIa inhibitor may allow reduction of the high heparin dose, reducing bleeding risks. In addition to its role in thrombosis in ECMO and CPB in general, FXIIa initiates the inflammatory kallikrein-kinin system (187). Bradykinin plasma concentrations are largely elevated in patients on CPB and particularly the longer lasting ECMO. Targeting FXIIa may provide an additional anti-inflammatory benefit to these patients, to reduce or prevent adverse effects such as damage of organs.

In summary, we show that a synthetic FXIIa inhibitor with sub-nanomolar affinity, high selectivity and good stability can be developed. We show that control of FXIIa with such a synthetic inhibitor allows for efficient anticoagulation in relevant animal disease models without increasing risks of bleeding. The synthetic nature and the small size promise a minimal risk of immunogenicity and allow efficient production. With its excellent binding properties and stability, the inhibitor may be readily applicable in its current form for application in acute procedures or conditions associated with increased risk of thrombosis such as CPB during heart surgery or extracorporeal membrane oxygenation, without compromising hemostasis at wound site.

4.5 Materials and Methods

Study design: The objectives of this study were to improve the pharmacologically relevant properties of a peptide macrocycle inhibitor of FXIIa, to assess the pharmacokinetic properties of the resulting inhibitor in three species, and to evaluate the inhibitor in clinically relevant animal models. The inhibitor was engineered by synthesizing variants of the lead peptide and testing their inhibitory activity, specificity and stability in various assays *in vitro*. Inhibitors showing improved activities were prepared with greater than 95% purity and their activities were tested at least in triplicate. The affinity of the final peptide FXII900 was determined in quadruplicate from three different synthetic batches. The pharmacokinetic properties in mice, rabbits, and pigs were assessed by quantifying the inhibitor in plasma samples using liquid chromatography and mass spectrometry, and by measuring aPTT in plasma samples in triplicate. The pharmacologic effects of the

inhibitor were tested in a FeCl₃-induced thrombosis model in mice and in an artificial lung model in rabbits. In all animal experiments, subjects were randomly assigned to groups.

Peptide Synthesis: Solid-phase peptide synthesis was performed on an Advanced ChemTech 348 Ω peptide synthesizer (AAPPTec) using standard Fmoc procedures. Rink Amide AM resin was used as solid support and dimethylformamide (DMF) as solvent. Peptide variants were synthesized at a 0.03 mmol scale to obtain around 10–20 mg of pure peptide. Peptide couplings were performed twice for each natural amino acid by reacting amino acid (4 eq., 600 μ l of 0.2 M in DMF), HBTU/HOBt (4 eq. each, 267 μ l of 0.45 M in DMF), and DIPEA (6 eq., 360 μ l of 0.5 M in DMF) at RT for 30 minutes at 400 rpm. The coupling of unnatural amino acids (2 eq., 600 μ l of 0.1 M in DMF) was performed once using HATU (2 eq., 650 μ l of 0.1 M in DMF) and DIPEA (4 eq., 250 μ l of 0.5 M in DMF). The resin was washed four times with DMF after the coupling reaction. The N-terminal Fmoc protecting group was removed with piperidine (20% v/v) in DMF (RT, 2 \times 5 min, 400 rpm). The resin was washed five times with DMF after Fmoc removal. The peptides were synthesized from the C-terminal end to the N-terminus by first coupling a glycine to the resin followed by the coumarin-containing amino acid Fmoc- β -(7-methoxy-coumarin-4-yl)-Ala-OH (Bachem). These two coupling steps as well as HATU couplings were followed by an acetylation capping step using acetic anhydride (1 ml of 10% [v/v] in DMF) and DIPEA (1 ml of 15% [v/v] in DMF) at RT for 30 minutes at 400 rpm. Fmoc-L- α -amino acids, HBTU, HOBt, and Rink Amide AM resin were purchased from GL Biochem. Non-canonical Fmoc-amino acids were purchased from Bachem, Chem-Impex, PolyPeptide, and TCI. Peptides were cleaved from the solid support and protecting groups were removed by incubation in 5 ml cleavage cocktail (90% TFA, 2.5% ethane-1,2-dithiol, 2.5% phenol, 2.5% thioanisole, 2.5% H₂O) for two hours with shaking. The resin was removed by vacuum filtration, and the peptides were precipitated with ice-cold diethyl ether (50 ml), incubated for 30 minutes at -20°C, and pelleted by centrifugation (2700 g, 5 minutes). The diethyl ether was discarded, the precipitate washed twice with diethyl ether, and the remaining solvent evaporated at RT. The linear peptide of FXII900 was synthesized at a one gram-scale by GL Biochem.

Peptides cyclization and purification: Crude peptide at a concentration of 1 mM was reacted with 1.2 mM of TATA in 70% NH₄HCO₃ buffer (60 mM, pH 8.0) and 30% MeCN for one hour at 30°C. The peptide and TATA were prepared and mixed using the solvents, concentrations, and volumes exemplified for the cyclization of ~ 50 mg crude peptide. To 6 ml of 3.5 mM peptide in MeCN/H₂O (1:2), 2.7 ml of 10 mM TATA in MeCN and 2 ml of MeCN were added and the reaction started by the addition of 12 ml NH₄HCO₃ buffer (60 mM, pH 8.0). The cyclized peptides synthesized on a 50 mg scale were purified by reversed-phase HPLC (Waters Prep LC 4000 system) using a preparative C18 RP column (Vydac C18 TP1022 column, 250 \times 22 mm, 10 μ m, 300 Å) and a linear

gradient of 15–28% solvent B (MeCN, 0.1% [v/v] TFA) in solvent A (H₂O, 0.1% [v/v] TFA) in 19 minutes at a flow of 20 ml/min. Absorbance was detected at 220 nm. The cyclized peptides were injected directly as the reaction mixture or after lyophilization of the reaction by dissolving the peptide in 10 ml of H₂O containing 10% (v/v) MeCN and 0.1% (v/v) TFA. Fractions containing the desired peptide were lyophilized.

HPLC and mass spectrometric analysis: The molecular mass of the purified peptides was determined on a single quadrupole mass spectrometer in positive ion mode using electrospray ionization (LCMS-2020, Shimadzu). The purity of the peptides was determined by analytical RP-HPLC (Agilent 1260 HPLC system) using an analytical C18 column (Agilent Zorbax 300SB-C18, 4.6 mm × 250 mm, 5 μm) and a linear gradient of 0–50% solvent B (MeCN, 0.1% [v/v] TFA) in solvent A (H₂O, 5% [v/v] MeCN, 0.1% [v/v] TFA) in 15 minutes at a flow of 1 ml/min. Absorbance was detected at 220 nm.

Peptide concentration determination: Lyophilized peptide was weighed and dissolved in water to obtain peptide stocks of 1 mM. The concentrations of crude peptides containing the coumarin amino acid were determined by measuring the absorption at 325 nm ($\epsilon = 12000 \text{ M}^{-1} \text{ cm}^{-1}$). The peptides were typically diluted several fold with water to measure the concentration in an absorption range of 0.1–1.

Screening method based on coumarin-labeled peptides: In order to test the inhibitory activity of peptides without prior purification, we developed the following method. Variants of the lead FXII618 peptide were synthesized with the C-terminal amino acid Fmoc- β -(7-methoxy-coumarin-4-yl)-Ala-OH. The fluorophore 7-methoxy-coumarin allowed precise quantification of the crude peptide. After solid-phase peptide synthesis, cleavage, and ether precipitation, the peptides were chemically cyclized and their K_i values were determined in a FXIIa activity assay using a fluorogenic substrate. Peptides synthesized and characterized with this strategy displayed an around 2.5-fold higher apparent K_i than analogous HPLC-purified peptides without the tag. For example, the reference peptide FXII618 carrying the coumarin amino acid had an around 2.5-fold weaker K_i ($20 \pm 3 \text{ nM}$) compared to the purified FXII618 without the tag (8.1 ± 0.7). Despite the difference, this method allowed for a comparison between peptides and the identification of the most active variants of FXII618. The best peptides from the screen were synthesized without the coumarin label, purified, and characterized.

Protease inhibition assays: The inhibitory activity of bicyclic peptides was determined by measuring the residual protease activity with a fluorogenic substrate. The assay was performed in buffer containing 10 mM Tris-Cl, pH 7.4, 150 mM NaCl, 10 mM MgCl₂, 1 mM CaCl₂, 0.1% w/v BSA, 0.01% v/v Triton-X100, and 1% v/v DMSO in a volume of 150 μl. FXIIa activity was measured with the fluorogenic substrate Boc-Gln-Gly-Arg-AMC (Bachem) at a final concentration of 50 μM. Mouse α -FXIIa (Molecular Innovations cat #

MFIIA) and human β -FXIIa (Molecular Innovations cat # HFXIIAB) were used at final concentrations of 0.4 nM. The reaction was pipetted as follows: 50 μ l of bicyclic peptide in assay buffer were added to 50 μ l of FXIIa in assay buffer and incubated for 10 minutes at 25°C before 50 μ l of 150 μ M fluorogenic substrate in assay buffer were added to measure the residual protease activity with an Infinite M200Pro fluorescence plate reader (excitation at 368 nm, emission at 467 nm; Tecan) for a period of 30 minutes with a read every minute at 25°C. Stock solutions of 1 mM bicyclic peptide were prepared by either dissolving the unpurified cyclization reaction with water or by dissolving purified and lyophilized peptide in water. The bicyclic peptides were serially diluted two-fold using assay buffer. Sigmoidal curves were fitted to the data using the following dose response equation, wherein x = peptide concentration, y = % protease activity, and p = Hill slope. IC_{50} values were derived from the fitted curve:

$$y = \frac{100}{1 + 10^{(\log IC_{50} - x)p}}$$

The inhibition constants (K_i) were calculated according to the equation of Cheng and Prusoff, $K_i = IC_{50}/(1 + ([S]_0/K_m)$, wherein IC_{50} is the functional strength of the inhibitor, $[S]_0$ is the total substrate concentration, and K_m is the Michaelis-Menten constant. A K_m of 260 μ M was used for the substrate Boc-Gln-Gly-Arg-AMC.

For testing the specificity of the bicyclic peptides, the following final concentrations of human serine proteases were used: tPA (Molecular Innovations) 7.5 nM, uPA (Molecular Innovations) 1.5 nM, factor XIa (Innovative Research) 6 nM, plasma kallikrein (Innovative Research) 0.25 nM, thrombin (Molecular Innovations) 1 nM, plasmin (Molecular Innovations) 2.5 nM, trypsin (Molecular Innovations) 0.05 nM, factor VIIa (Haematologic Technologies) 50 nM, and factor Xa (Haematologic Technologies) 6 nM. Two-fold dilutions of the peptide were prepared that ranged from 0.04 to 40 μ M. The following fluorogenic substrates were used at a final concentration of 50 μ M: Z-Phe-Arg-AMC (Bachem) for plasma kallikrein; Boc-Phe-Ser-Arg-AMC (Bachem) for factor Xa; Z-Gly-Gly-Arg-AMC (Bachem) for tPA, uPA, thrombin, and trypsin; H-D-Val-Leu-Lys-AMC (Bachem) for plasmin; and D-Phe-Pro-Arg-ANSNH-C4H9 (Haematologic Technologies) for FVIIa and FXa.

Plasma stability assays: Peptide (2 μ l of 2 mM in H₂O) was added to 398 μ l of citrated human plasma (Innovative Research) to obtain a final peptide concentration of 10 μ M. The mixture was incubated in a water bath at 37°C. At different time points (0, 0.5, 1, 2, 4, 8, 12, 24, 48, and 96 hours), samples of 30 μ l were removed, diluted to 200 μ l with aqueous buffer (10 mM Tris-HCl, pH 7.4, 150 mM NaCl, 10 mM MgCl₂, 1 mM CaCl₂), and incubated for 20 minutes at 65°C to inactivate plasma proteases. The peptide/plasma samples were stored at -20°C until the residual inhibitory activity of the peptides was measured in a FXIIa inhibition assay. For the activity assay, the peptide/plasma samples

were centrifuged for five minutes at 16,000 g, serial two-fold dilutions of the supernatant were prepared (peptide concentration ranges from 0.5 nM to 0.5 μ M), and the residual activity of 0.5 nM human α -FXIIa was measured using 50 μ M Boc-Gln-Gly-Arg-AMC substrate. IC_{50} values were derived from the fitted curve using the equation indicated above. Residual inhibition in % was calculated using the equation $IC_{50,0h}/IC_{50,xh} \times 100$, wherein $IC_{50,0h}$ is the functional strength of the inhibitor at time point 0 and $IC_{50,xh}$ the functional strength of the inhibitor after one of the different plasma incubation periods mentioned above.

Plasma degradation assays: Plasma stability and peptide cleavage sites were assessed by incubating the bicyclic peptides in mouse plasma and analyzing the products with an LC-MS system (LCMS-2020, Shimadzu). Peptide (2 μ l of 2 mM in H₂O) was added to 48 μ l of citrated mouse plasma (Innovative Research) to obtain a final peptide concentration of 80 μ M. The mixture was incubated in a water bath at 37°C. At different time points (0, 15, 24, 72, 96, 120, and 144 hours), samples of 5 μ l were removed, mixed with 5 μ l of 6 M guanidinium hydrochloride, and incubated for 30 minutes at RT. Plasma proteins were precipitated by incubation with 200 μ l of ice cold EtOH and 0.1 % (v/v) formic acid for 30 minutes and centrifuged at 9000 g for 20 minutes at 4°C. The supernatant was evaporated in a Speedvac at 50°C and reduced pressure, then the residue was dissolved in 40 μ l of deionized water containing 0.1% (v/v) CHOOH and analyzed by LC-MS. The samples were analyzed using an analytical C18 column (Phenomenex C18 Kinetex column, 50 \times 2.1 mm, 2.6 μ m, 100 Å) and a linear gradient of 5–35% solvent B (MeCN, 0.05% [v/v] CHOOH) in solvent A (H₂O, 0.05% [v/v] CHOOH) in 5.5 minutes at a flow of 1 ml/min. The masses of the intact peptide and degradation products were measured on a single quadrupole mass spectrometer in positive ion mode using electrospray ionization. Peptides were quantified based on the absolute intensities of the detected mass peaks (M^{3+} and M^{4+}).

Coagulation assays: The coagulation parameters aPTT and PT were determined in blood plasma using a STAGO STart4 Coagulation analyzer (Diagnostica). Citrated plasma from human (single donor), mouse (CD1, Innovative grade), rabbit (NZW, Innovative grade), and pig (Innovative grade) were supplied by Innovative Research. Coagulation was monitored by an electromagnetically induced movement of a steel ball in the plasma. The time until the ball stopped moving was recorded as the coagulation time. Frozen plasma samples were thawed for around 30 minutes at RT before use. For aPPT measurements in human plasma, 100 μ l of plasma was placed into the cuvette, 100 μ l of Pathromtin* SL (silicon dioxide particles, plant phospholipids in HEPES buffer system; Siemens) was added and incubated for two minutes at 37°C in the device before the coagulation was triggered by the addition of 100 μ l of pre-warmed (37°C) CaCl₂ solution (25 mM, Siemens). For aPTT measurements in mouse, rabbit, and pig plasma, 100 μ l of plasma was placed into the cuvette, 100 μ l of Dade Actin (Cephalin, Ellagic acid in

HEPES buffer system; Siemens) was added and incubated for three minutes at 37°C in the device before coagulation was triggered by addition of 100 µl of pre-warmed (37°C) CaCl₂ solution. For PT measurements in human plasma, 50 µl of plasma was placed into the cuvette and incubated for one minute at 37°C before coagulation was triggered by the addition of 100 µl of pre-warmed (37°C) Innovin (recombinant human tissue factor, synthetic phospholipids, and calcium in stabilized HEPES buffer system; Dade Behring/Siemens).

Animal studies: All experiments in mice and pigs were conducted in accordance with the terms of the Swiss animal protection law and were approved by the animal experimentation committee of the cantonal veterinary service (Canton of Berne, Switzerland). The pharmacokinetic studies in rabbits were performed at Washington Biotech Inc. following ethical standards for animal studies of the Office for Laboratory Animal Welfare (OLAW), a division of the US Public Health Service as administered by the National Institutes for Health. The extracorporeal circulation studies in rabbits were performed in compliance with the Allegheny Health Network Institutional Animal Care and Use Committee.

Pharmacokinetics study in mice: C57BL/6J wild-type mice (male, 25–30 g, Charles River) were injected subcutaneously over the shoulders with 5 mg/kg of FXII900 (0.5 mg/ml in PBS, pH 7.4). The mice were anaesthetized three minutes before the scheduled blood collection time point (40 mg/kg pentobarbital). An abdominal midline incision was performed and 450 µl of whole blood was drawn from the inferior vena cava into a syringe containing sodium citrate (50 µl 3.2% [w/v] sodium citrate). The mice were euthanized by cervical dislocation. The blood was immediately processed to plasma by centrifugation for 10 minutes at 2000 g at 4°C, and stored at -80°C. The concentration of FXII900 in the plasma samples was determined by LC-MS as described below. Two mice were used for each time point.

Pharmacokinetic study in rabbits: The pharmacokinetic properties of FXII900 applied intravenously were determined as described previously (193). Female New Zealand White rabbits were injected with 3.7 mg/kg FXII900 dissolved in 1 ml PBS, pH 7.4 via the ear vein. Blood samples (2.7 ml) were collected at different time points into sodium citrate tubes (BD Vacutainer ref # 363083) and immediately processed to plasma by centrifugation at 1400 g for 15 minutes. The concentration of FXII900 in the plasma samples was determined by LC-MS as described below. The pharmacokinetic properties of FXII900 applied subcutaneously were determined as follows. Female New Zealand White rabbits (2.5–2.9 kg) were injected subcutaneously over the shoulders with 3.7 mg/kg of FXII900 dissolved in 1 ml PBS pH 7.4. Blood samples (1.8 ml) were collected at different time points into sodium citrate tubes (BD Vacutainer ref # 363080) and immediately processed to plasma by centrifugation at 1800 g for 10 minutes. The plasma was

stored at -80°C . The concentration of FXII900 in the plasma samples was determined by LC-MS as described below.

Pharmacokinetic study in pigs: Pigs (30 ± 5 kg) were anesthetized and prepared following procedures used to study an ischemia/reperfusion injury (253). In this procedure, the ACT is monitored and 2500 IU of heparin are injected when ACT values fall below 180 s. Pigs were injected intravenously with 4 mg/kg of FXII900 dissolved in 1 ml PBS, pH 7.4. Blood samples (2.7 ml) were collected at different time points into sodium citrate tubes (BD Vacutainer ref # 363083) and immediately processed to plasma by centrifugation at 1400 g for 15 minutes at RT. The aPTT was measured as described above. The concentration of FXII900 in the plasma samples was determined by LC-MS as described below.

Quantification of inhibitor in plasma samples: The concentration of FXII900 in the plasma samples was quantified based on peak intensities of total ion current (TIC) chromatograms acquired by LC-MS (LCMS-2020, Shimadzu). To 15 μl of plasma sample, 1 μM of internal standard peptide and 5 μl of 6 M guanidinium hydrochloride solution were added and mixed. Plasma proteins were precipitated by the addition of 400 μl of ice cold ethanol (99.9% v/v EtOH, 0.1% v/v TFA) and incubated on ice for one hour. Precipitate was removed by centrifugation (9000 g, 20 minutes, 4°C) and the supernatant dried by centrifugal evaporation under vacuum. Dried samples were dissolved by sequentially adding 2 μl of DMSO and 18 μl of H_2O containing 0.1% (v/v) CHOOH and analyzed by LC-MS. The samples were analyzed using an analytical C18 column (Phenomenex C18 Kinetex column, 50×2.1 mm, $2.6 \mu\text{m}$, 100 \AA) and a linear gradient of 5–30% solvent B (MeCN, 0.05% [v/v] CHOOH) in solvent A (H_2O , 0.05% [v/v] CHOOH) in 4.5 minutes at a flow of 1 ml/min. The mass was measured on a single quadrupole mass spectrometer in positive ion mode using electrospray ionization. Peptides were quantified based on the absolute intensities of the detected mass peaks (M^{3+} and M^{4+}).

Ferric chloride-induced thrombosis in mice: 57BL/6J wild-type mice (male, 25–30 g, Charles River) were injected intravenously with Rhodamine 6G (100 μl , 1 mM, ACROS Organics product 41902) to fluorescently label the platelets and leucocytes. The mice were injected subcutaneously over the shoulders with FXII900 or the negative control FXII901 (0.5 mg/ml in PBS, pH = 7.4) and subsequently anesthetized with ketamine (80 mg/kg) and xylazine (16 mg/kg) via intraperitoneal injection. An abdominal midline incision was made to expose the mesenteric arterioles which were imaged by intravital microscopy using a Mikron IVM500 microscope (Mikron Instruments) coupled with a 50 W mercury lamp (HBO 50 microscope illuminator, Zeiss) attached to combined blue (exciter 455DF70, dichroic 515DRLP, and emitter 515ALP) and green (exciter 525DF45, dichroic 560DRLP, and emitter 565ALP) filter blocks. Thrombus formation was induced by the application of a 1×2 mm filter paper saturated with FeCl_3 solution (7.5% w/v,

Roth, art no 5192.1) onto the blood vessel for one minute. The blood flow, clot formation and vessel occlusion were monitored for 30 minutes wherein images were recorded every minute using a digital video cassette recorder (DSR-11, Sony) and analyzed using ImageJ software. Mice were euthanized by final bleeding and cervical dislocation. Time to clot formation and full occlusion of the blood vessel were determined as follows. Clot formation was defined as the formation of a clear aggregation with a diameter of around 10 μm or larger. Occlusion was defined as a clot covering the full diameter of the vessel. Mice showing no speckled pattern at the site of FeCl_3 application were assumed to be not injured at the blood vessel and were excluded from the analysis.

Artificial lungs: Mini-lungs were created that allowed for blood exposure to the fibers in the artificial lung, but for construction simplicity, do not transfer gas (254). Polymethylpentene (PMP) fiber (3M) with 50% porosity, a 380 μm outer diameter, and two layers at 30° cross angles were cut into 1.78 \times 1.78 cm squares. Five of these layers were put together, making sure the fibers all ran in the same direction, and they were sealed together into a fiber bundle using a hot plate on each side of the square sheets. These fiber bundles were melted such that they had a 1.57 \times 1.57 cm square frontal area perpendicular to the flow. Eight of these 10-layer “chiclets” were placed together to make up the fiber bundle of one mini lung device, giving a final surface area of 526 cm^2 . These fiber bundles were placed in a square plastic housing of 3.05 cm in length, making sure the fiber bundles were in the device tightly so that no shunting could occur around the fiber bundle. This housing was attached to plastic end caps that were placed on each end with a 1/8"-barbed tube fitting for 3/16"-ID tubing to allow the device to be connected to tubing in the circuit. These end connectors were coated with Teflon tape before connecting them to the plastic end caps to prevent leakage. The device was held together with two screws going from end cap to end cap. The entire device was secured with silicone to eliminate leakage. The silicone was left to dry for 24 hours, and the device leak tested as follows. Filtered deionized water was run through the device to check for leaks within the device. If no leaks were found, the device was left to dry with filtered air running through the device for 24 hours.

Extracorporeal circulation in rabbits: New Zealand white rabbits of 3.2 – 4.2 kg (Charles River) were anesthetized via intramuscular injections of ketamine (30 mg/kg) and xylazine (5 mg/kg). One of the ear veins was catheterized via a 24G winged catheter, and the rabbits were intubated with a 3.0 ET tube. The animals were kept anesthetized throughout the four-hour experiment via inhaled isoflurane (2%) and were ventilated with a peak inspiratory pressure (PIP) of < 20 cmH_2O , positive end expiratory pressure of 5 mmHg, tidal volume of 4–6 ml/kg, and a respiratory rate of 22–60 breaths/min. Tidal volume and respiratory rate were adjusted to maintain normal arterial blood gases and the listed PIP. Phenylephrine was applied intravenously at a rate of 0.5–5 $\mu\text{g/kg min}$ to maintain blood pressure. For monitoring blood pressure and collecting blood samples,

the rabbits' right or left carotid arteries were cannulated using a 16-gauge angiocatheter (Becton Dickinson) and were secured with silk ties. The device and circuit were first primed with filtered CO₂ and then with saline (NaCl, 0.9% [w/v]) containing solumedrol (30 mg/kg). At this point, rabbits of the inhibitor-treated group were injected with 2 mg/kg of FXII900 as a 2 mM solution in PBS (pH 7.4) via the ear vein and the circuit was connected to the rabbits via a venovenous ECMO configuration using a 14-gauge angiocatheter (Becton Dickinson) and a 6" pressure tubing that was cut to length from a 24" pressure tubing (Edwards Lifesciences) in the right and left internal jugular veins, respectively. The circuit was placed in a roller pump (Cobe), and the blood flow was set to 45 ml/min. After connecting the extracorporeal circuit, rabbits of the inhibitor-treated group were infused with 0.075 mg/kg/min FXII900 via the ear vein for the entire duration of the study. After four hours, the animals were euthanized by pentobarbital injection (Fatal-Plus, Vortech, 1 ml/10 lbs). At the end of the experiment, 5 ml of heparin was run through the artificial lung while it was still connected to the rabbits. Then the circuit was removed, and the device was washed with saline carefully so no clot shedding would occur. Saline was run through the device until the saline was clear. Clot volume was measured by measuring the volume of the device prior to the experiment and again at the end of the experiment after washing. This was done by completely filling the device with saline and recording this amount of saline as the device volume. The difference between the beginning and ending volume was determined to be the clot volume. From the clot volume, the percent of clot within the device was calculated.

Data acquisition during extracorporeal circulation: Platelet and white blood cell counts, hematocrit, arterial blood gases (ABG), ACT, aPTT, fibrinopeptide A (FPA), device resistance, and bleeding time were measured prior to circuit attachment and at 10, 30, 120, and 240 minutes following the initiation of ECMO. For the platelet counts, a syringe with 0.05 ml of 3.2% sodium citrate (w/v) was used to draw 0.45 ml of blood for a total volume of 0.5 ml. This was then centrifuged at 60 g for 10 minutes, and 20 µl of the plasma was placed in 20 ml of ISOTON® diluent and counted using a Coulter Counter (Beckman Coulter, Inc. Brea, CA) with a 50 µl aperture tube. For counting, cells were considered platelets if their diameters were 1.8–5.6 µm. For white blood cell counts, 40 µl of whole blood was placed in 20 ml of the ISOTON® diluent. Six drops of ZAP-OGLOBIN lysing solution were added to the mixture and mixed gently. This was allowed to sit for two minutes. The white blood cells were also counted using the Coulter Counter (Beckman Coulter) with a 50 µl aperture tube where any particle above 3.6 µm in diameter was considered a white blood cell. Arterial blood gases were measured by drawing 0.4 ml of blood into a heparinized syringe and run using an arterial blood gas analyzer (ABL800 FLEX, Radiometer). The ACT and hematocrit were measured by collecting 0.5 ml of blood. The ACT was measured using a Hemochron analyzer with tubes containing glass beads as the activator. The hematocrit was measured via capillary centrifugation. For

aPTT measurements, blood samples (1.8 ml) were collected at different time points into tubes containing sodium citrate (0.2 ml, 3.2% [w/v] sodium citrate) and immediately processed to plasma by centrifugation at 2000 g for 15 minutes at 4°C. The samples were then analyzed as described above. All platelet counts, WBC counts, FPA, and FXIIa levels were corrected for hemodilution by adjusting the raw values based on the hematocrit. The inlet and outlet pressure and blood flow rate were measured using a Biopac system (Aero Camino Goleta, CA) and pressure transducers at the inlet and outlet of the device (Edwards Lifesciences), and the resistance was calculated with the standard $R = (P_i - P_o)/Q$ where P_i is the inlet pressure in mmHg, P_o is the outlet pressure in mmHg, and Q is the flow in L/min. The bleeding time was measured by cutting small incisions of 4–5 mm at different sites of the right or left ear in each animal. Blood from the incision was removed with gauze every 30 seconds, and the time until the bleeding stopped was measured.

Statistical analysis: For all experiments, the mean \pm standard deviation is indicated unless stated otherwise. This includes all values and data points in graphs. All statistical analyses were performed using GraphPad Prism 5 or Microsoft Excel software. A chi-squared test was used to determine whether mice were protected against clot formation and full occlusion in the FeCl₃ thrombosis model. A one-tailed student's t-test was applied to determine the significance of the difference in the time until clot formation occurred between the two groups. A one-tailed test is appropriate since the effect is only expected in one direction. The same test was used for clot formation in the artificial lung devices. For all tests, $p < 0.05$ was considered significant.

4.6 Supporting information

Table S4.1. *K_i* values of coumarin-labeled FXII618 modified at Arg1 or Arg8.

Table S4.2. Overview of FXII618 variants and their *K_i* values.

Table S4.3. Specificity of FXII900.

Table S4.4. Characterization of FII900 with individually reversed beneficial mutations.

Table S4.5. Pharmacokinetic parameters in rabbits.

Table S4.6. Pharmacokinetic parameters in pigs.

Table S4.7. Time to clot and full occlusion in ferric chloride-induced thrombosis mouse model.

Figure S4.1. Stability of FXI618 variants carrying two D-amino acids at the N-terminus.

Figure S4.2. FXIIa inhibitors FXII850 and FXII851.

Figure S4.3. Synthesis of FXII900.

Figure S4.4. Reversion of beneficial amino acid substitutions in FXII900.

Figure S4.5. Plasma stability of FXII900 containing C-term Arg and variants with reverted beneficial mutations.

Figure S4.6. Negative control peptide FXII901.

Figure S4.7. Ferric chloride-induced thrombosis in mice treated with negative control peptide FXII901.

Figure S4.8. Ferric chloride-induced thrombosis in mice treated with FXIIa inhibitor FXII900.

Figure S4.9. Inhibition of FXIIa-driven coagulation in artificial lung rabbit model: data for individual rabbits.

Figure S4.10. Analytical data of important peptides

Supplementary Tables

Table S4.1. K_i values of coumarin-labeled FXII618 modified at Arg1 or Arg8. All peptides were synthesized with the additional amino acid β -(7-methoxy-coumarin-4-yl)-Ala-OH at the C-terminus for accurate concentration determination. This approach enabled the determination of K_i values for the crude bicyclic peptide. For comparison, the crude bicyclic peptide FXII618 modified with the coumarin amino acid inhibited human and mouse FXIIa with K_i values of 20 ± 3 nM and 230 ± 30 nM, respectively. The K_i values of the crude peptides carrying the coumarin amino acid are around two-fold higher than those of purified peptides without coumarin. Standard deviations are indicated for K_i s smaller than 300 nM. All K_i s were measured in triplicate. Mean \pm SD are indicated.

Modification in Arg1			Modification in Arg8		
Altered amino acid	K_i human FXIIa (nM)	K_i mouse FXIIa (nM)	Altered amino acid	K_i human FXIIa (nM)	K_i mouse FXIIa (nM)
R1ar	32 ± 5	350	R8A	20.5 ± 0.4	230 ± 30
R1sr	59 ± 4	750	R8S	44.0 ± 1.6	360
R1fr	22 ± 5	190 ± 20	R8F	103 ± 3	900
R1lr	16 ± 5	131 ± 17	R8L	44.3 ± 0.9	490
R1qr	32 ± 4	250 ± 8	R8P	88.8 ± 1.5	440
R1ra	12.4 ± 0.3	88 ± 4	R8K	24.9 ± 0.9	250 ± 40
R1rs	10.9 ± 1.6	85 ± 14	R8H	13.6 ± 0.4	88 ± 13
R1rf	36.3 ± 1.1	220 ± 60	R8E	41.3 ± 0.5	730
R1rl	83 ± 5	440	R8Q	38.3 ± 1.2	330
R1rq	21 ± 3	160 ± 30	R8N	51 ± 3	330

Table S4.2. Overview of FXII618 variants and their K_i values. K_i values were measured at least three times. Mean \pm SD are indicated.

Inhibitor name	Modification to FXII618	K_i human FXII (nM)	K_i mouse FXII (nM)	Reference
FXII618	-	8.1 ± 0.7	86 ± 9	Baeriswyl, V., <i>et al.</i> , ACS Chem. Biol., 2015
FXII700	Arg11 \rightarrow β hArg	1.5 ± 0.1	N.D.	Wilbs, J., <i>et al.</i> , ChemBioChem, 2016
FXII800	Phe3 \rightarrow Phe4F	0.84 ± 0.03	N.D.	Middendorp, S., <i>et al.</i> , J. Med. Chem., 2017
FXII850	Arg1 \rightarrow D-Arg-D-Ser	5 ± 2	35 ± 9	-
FXII851	Arg8 \rightarrow His	6.5 ± 0.3	36 ± 3	-
FXII900	Arg11 \rightarrow β hArg, Phe3 \rightarrow Phe4F, Arg1 \rightarrow D-Arg-D-Ser, Arg8 \rightarrow His, deletion of Arg13	0.37 ± 0.04	0.45 ± 0.11	-

Table S4.3. Specificity of FXII900. The indicated values are averages of at least three measurements. Mean \pm SD are indicated.

Protease	K_i (nM)	% residual activity at 40 μM inhibitor
FXIa	> 40,000	95.1 \pm 0.6
Plasmin	> 40,000	86 \pm 5
Trypsin	1460 \pm 120	9.2 \pm 1.1
uPA	> 40,000	98.7 \pm 1.8
tPA	> 40,000	97 \pm 4
Thrombin	> 40,000	95 \pm 6
Plasma Kallikrein	> 40,000	72 \pm 3
FXa	> 40,000	97.1 \pm 1.3
FVIIa	> 40,000	97.1 \pm 1.3

Table S4.4. Reversion of beneficial mutations. The indicated values are averages of at least three measurements. Mean \pm SD are indicated.

Peptide	K_i human FXII (nM)	K_i mouse FXII (nM)
FXII618	8.1 ± 0.7	86 ± 9
FXII900	0.37 ± 0.04	0.45 ± 0.11
FXII900 (with C-term Arg)	0.34 ± 0.03	0.50 ± 0.15
Phe3→Phe4F reverted	0.70 ± 0.06	1.9 ± 0.5
Arg8→His reverted	0.31 ± 0.02	0.91 ± 0.04
Arg11→βhArg reverted	0.51 ± 0.10	0.9 ± 0.4

Table S4.5. Pharmacokinetic parameters in rabbits. FXII900 was administrated intravenously (n = 3, 3.7 mg/kg) and the concentration was quantified by LC-MS.

Parameter	Value
$t_{1/2\beta}$ (min)	12 ± 2
CL (ml/kg*min)	16.1 ± 1.0
V_D (ml/kg)	280 ± 50

Table S4.6. Pharmacokinetic parameters in pigs. FXII900 was administrated intravenously (n = 3, 4 mg/kg) and the concentration was quantified by LC-MS.

Parameter	Value
$t_{1/2\beta}$ (min)	36 ± 5
CL (ml/kg*min)	11.8 ± 1.8
V_D (ml/kg)	610 ± 140

Table S4.7. Time to clot formation and full occlusion in ferric chloride-induced thrombosis mouse model.

Time points at which clot formation and blood vessel occlusion were observed.

Control	Time to clot (min)	Time to full occlusion (min)	Inhibitor	Time to clot (min)	Time to full occlusion (min)
1	14	18	1	-	-
2	17	-	2	-	-
3	6	9	3	23	-
4	-	-	4	-	-
5	6	9	5	-	-
6	7	9	6	21	-
7	2	10	7	16	-
8	15	-	8	-	-
			9	-	-

Supplementary Figures

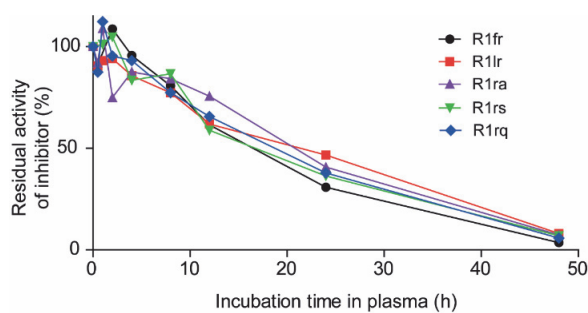


Figure S4.1. Stability of FXI618 variants carrying two D-amino acids at the N-terminus. The peptides were incubated in human plasma as indicated. Residual inhibitory activity was tested in a FXIIa activity assay using a fluorogenic substrate. Residual inhibition in % was calculated as $(IC_{50,0h}/IC_{50,xh}) \times 100$, wherein $IC_{50,0h}$ is the functional strength of the inhibitor at time point 0 and $IC_{50,xh}$ is the functional strength of inhibitor after one of the different plasma incubation periods.

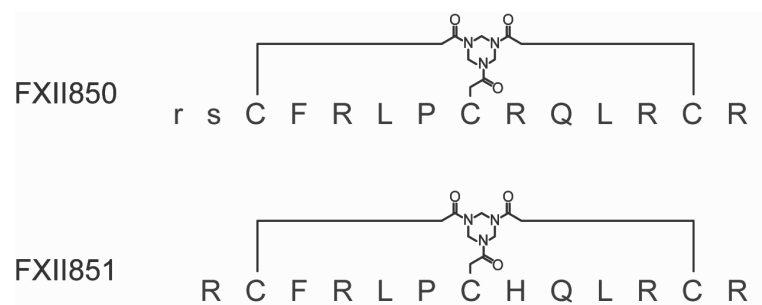


Figure S4.2. FXIIa inhibitors FXII850 and FXII851.

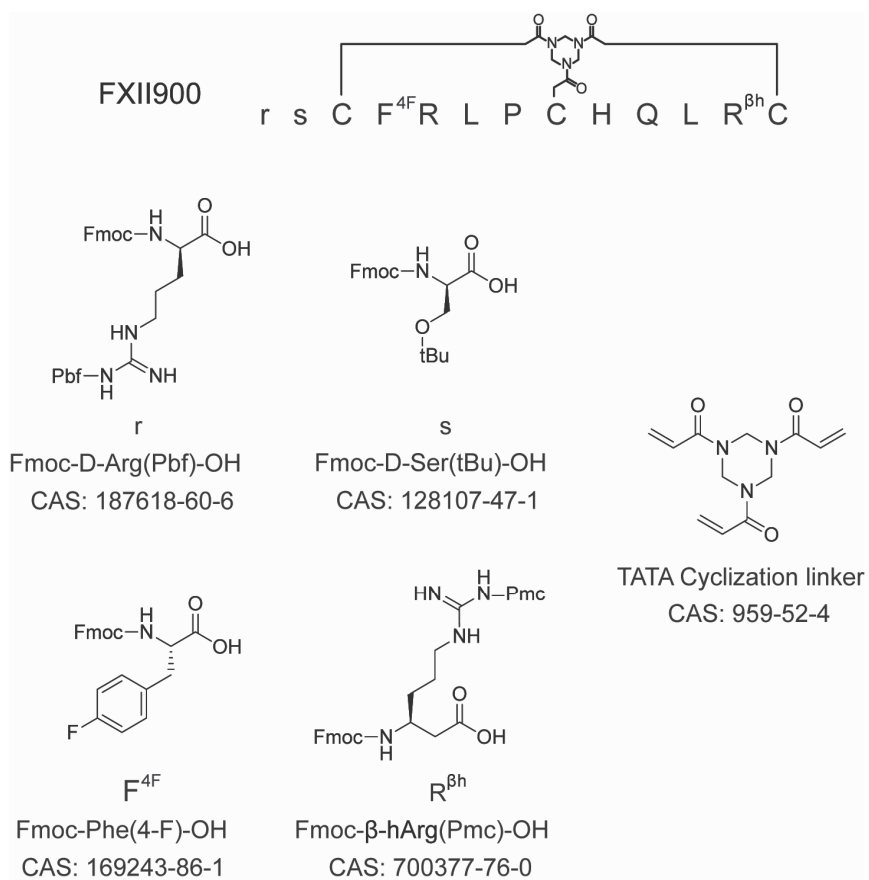


Figure S4.3. Synthesis of FXII900. The structure of FXII900 is represented and the chemical structures of the unnatural amino acids and the chemical linker are shown below.

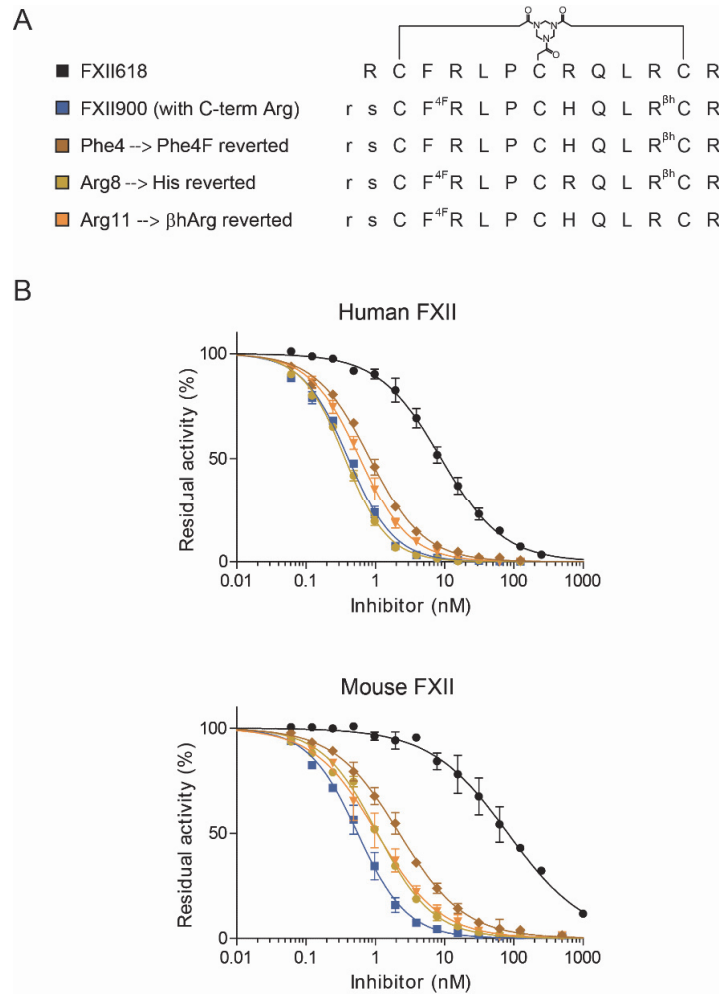


Figure S4.4. Reversion of beneficial amino acid substitutions in FXII900. The three amino acids Phe4F3, His8, and βhArg11 were individually reverted in FXII900 (containing a C-terminal Arg) to the original residues Phe3, Arg8, and Arg11, in order to assess the contribution of these modifications to the stability of the inhibitor as well as to the inhibition of human and mouse FXIIa. **(A)** The amino acid sequences of the bicyclic peptides are indicated. All peptides contain a C-terminal Arg. **(B)** The residual activity of human and mouse FXIIa at different peptide concentrations was measured in triplicate. Means ± SD are indicated

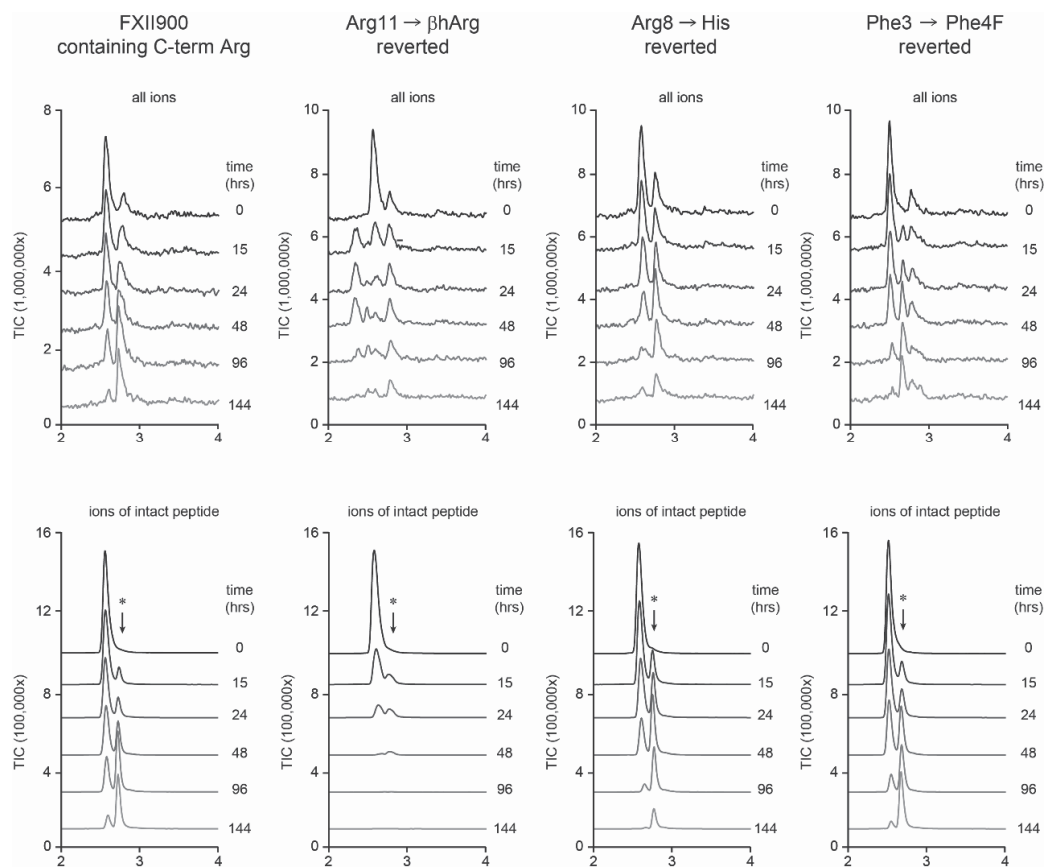


Figure S4.5. Plasma stability of FXII900 containing C-term Arg and variants with reverted beneficial mutations. The three amino acids Phe4F3, His8, and β hArg11 were individually reverted in FXII900 containing a C-terminal Arg to the original residues Phe3, Arg8, and Arg11, respectively, and the stability in plasma was assessed. Peptides were incubated at a concentration of 80 μ M in plasma at 37°C. After precipitation and removal of plasma proteins, the peptides and their degradation products were analyzed LC-MS. Total ion counts (TIC) are indicated in the top panels. The lower panels show the ion count of the intact peptides. For all peptides, a species was found with an additional mass of one dalton. It is assumed that this mass results from the hydrolysis of the C-terminal amide group.

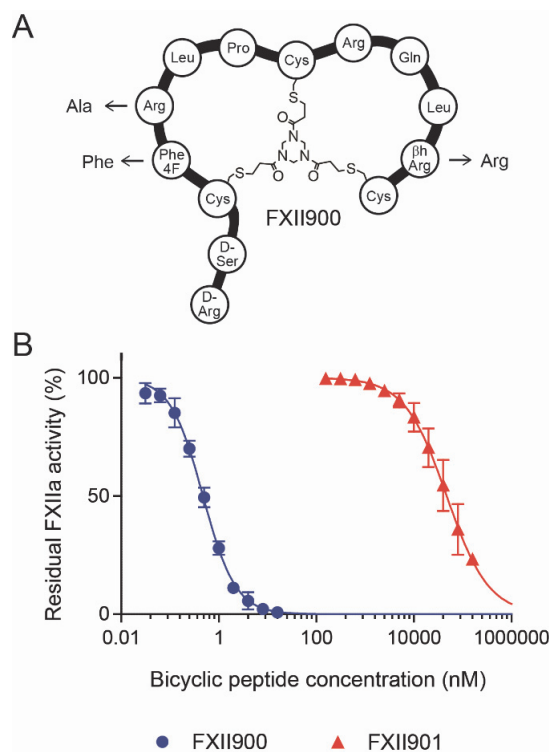


Figure S4.6. Negative control peptide FXII901. (A) The amino acid substitutions made in FXII900 to render it inactive at low micromolar concentrations. (B) Inhibition of FXIIa by FXII900 and FXII901. Means \pm SD of three measurements are shown.

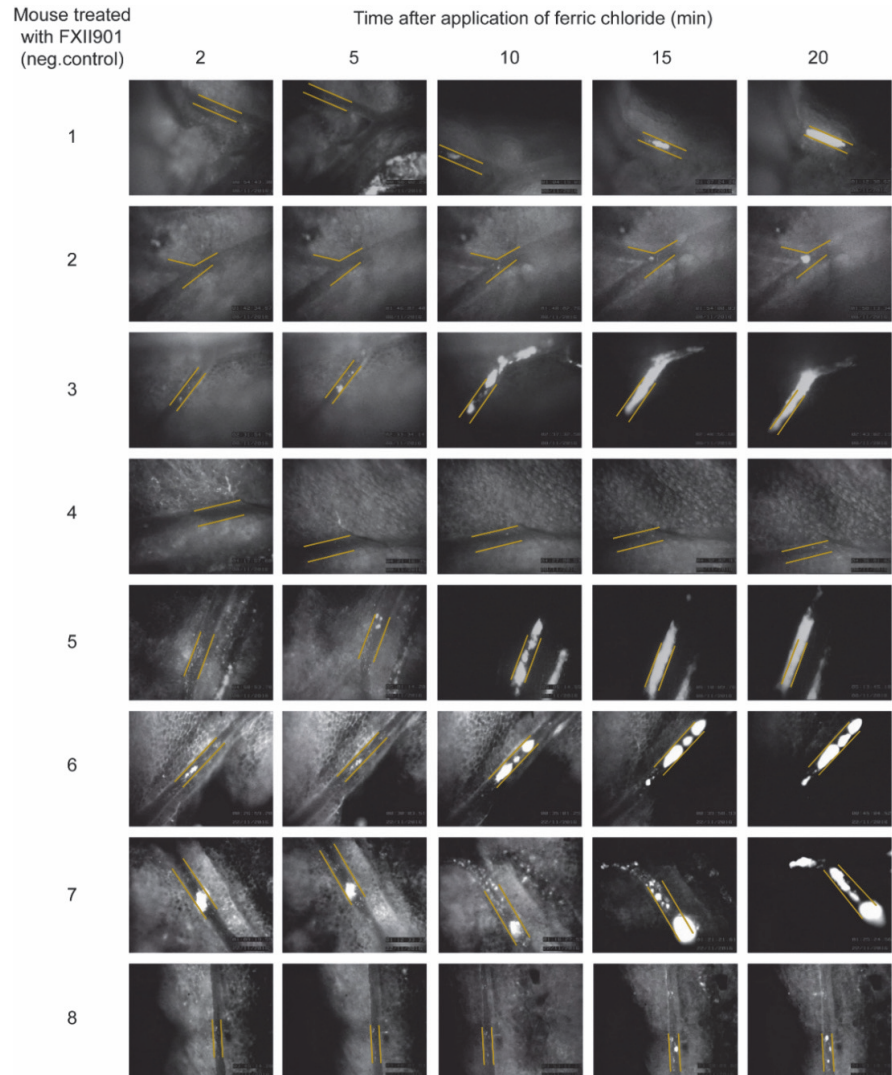


Figure S4.7. Ferric chloride-induced thrombosis in mice treated with negative control peptide FXII901. Intravital fluorescence microscopy images of mesenteric arterioles in which thrombosis was induced by topical application of FeCl_3 (7.5%, 1 min). Platelets were fluorescently labeled with Rhodamine 6G for visualization. Vessel walls at FeCl_3 application site are indicated with yellow markers.

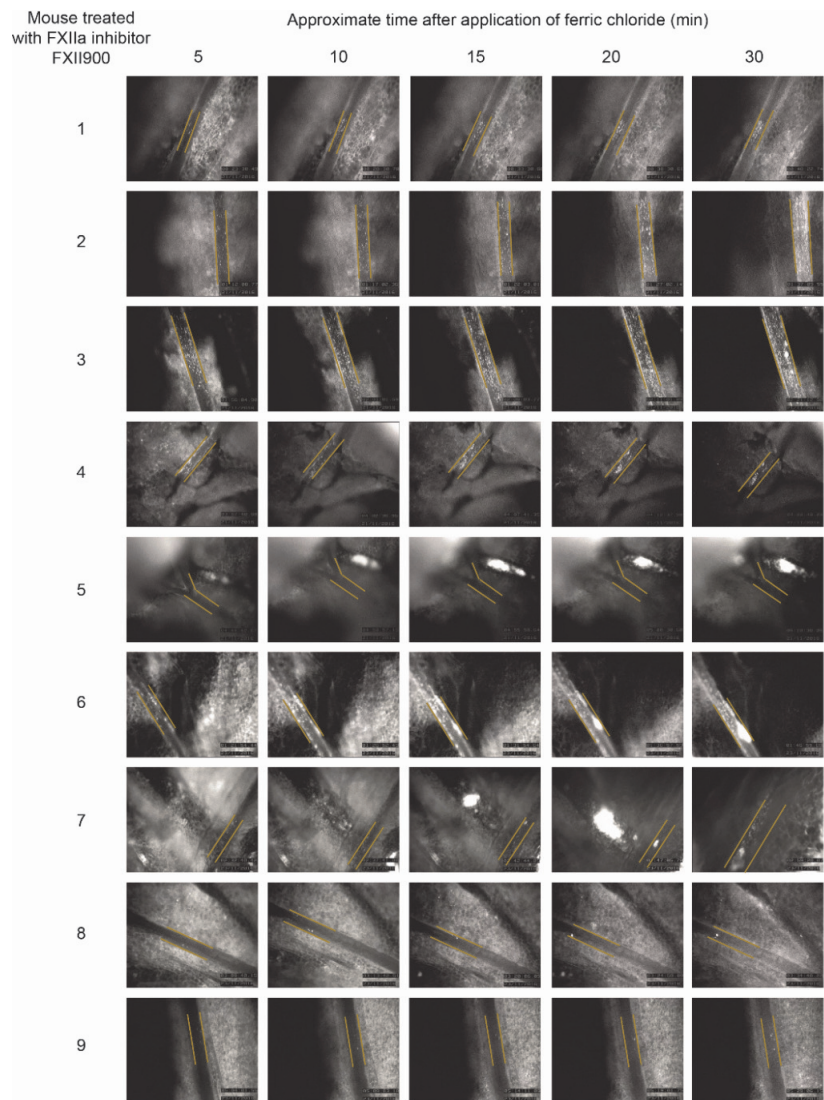


Figure S4.8. Ferric chloride-induced thrombosis in mice treated with FXIIa inhibitor FXII900. Intravital fluorescence microscopy images of mesenteric arterioles in which thrombosis was induced by topical application of FeCl_3 (7.5%, 1 min). Platelets were fluorescently labeled with Rhodamine 6G for visualization. Vessel walls at FeCl_3 application site are indicated with yellow markers.

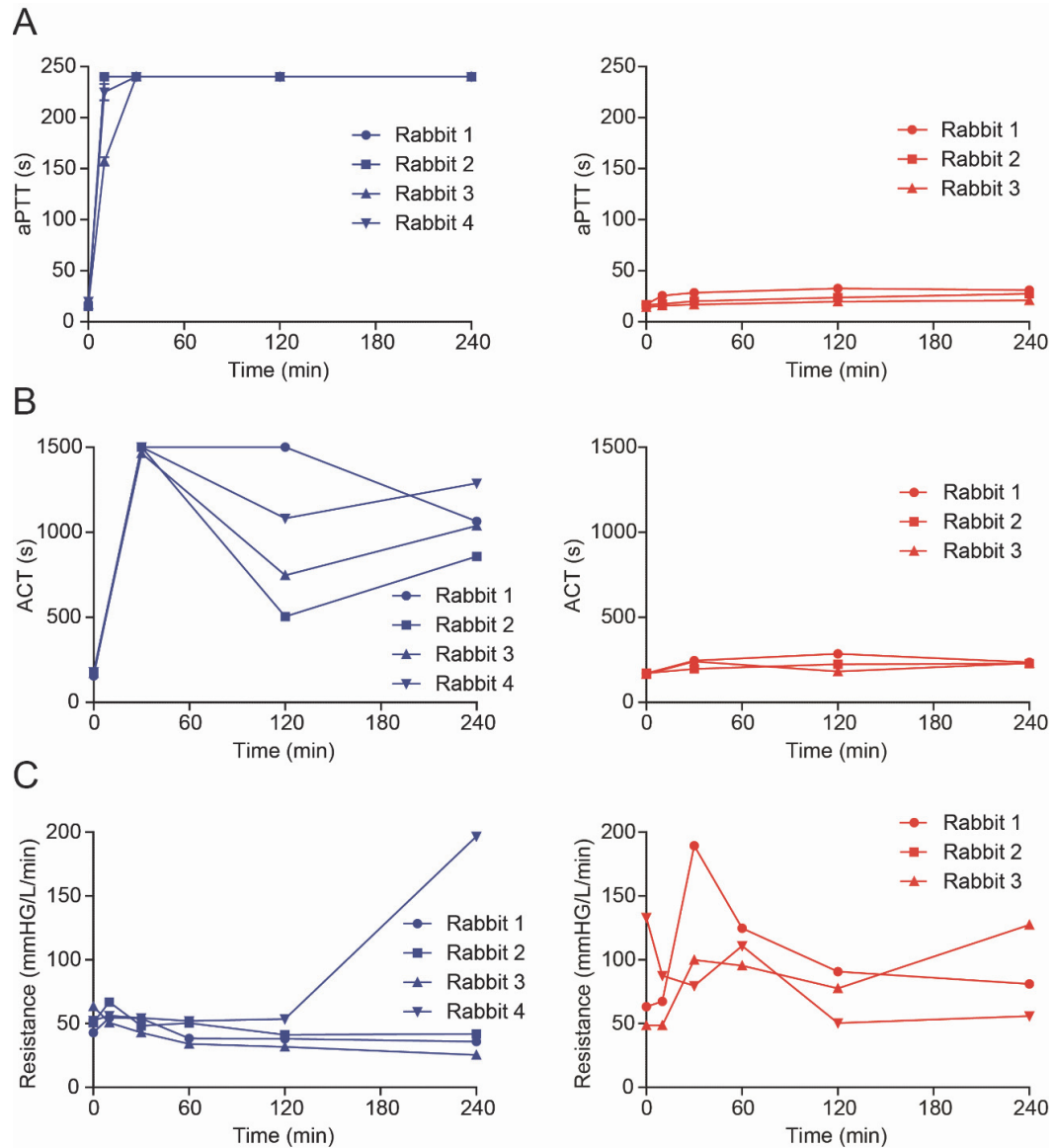


Figure S4.9. Inhibition of FXIIa-driven coagulation in artificial lung rabbit model: data for individual rabbits. Rabbits connected veno-venous to an artificial lung system for four hours were injected with FXII900 as a bolus (2 mg/kg) before start of the extracorporeal circulation and as a constant infusion (0.075 mg/kg/min) over the full time course of the experiment (n = 4; data shown in blue), or were not treated (n = 3). Data for individual rabbits is shown in this figure. Mean values \pm SD for the two groups are shown in Figure 28. Values indicated for the time point 0 refer to measurements made before connection of the artificial lung. Results of FXII900 are shown in blue and those of the untreated in red. (A) aPTT. Coagulation times of 230 s indicate that plasma did not coagulate at this time. (B) ACT. Clotting times of 1500 s indicate that blood did not coagulate at this time. (C) Resistance calculated based on pressure at the inlet and outlet of the device and the flow rate. (D) Bleeding time measured by incision-provoked injuries at the ears. (E) Platelet count. (F) Volume of blood clots indicated in % of volume of the artificial lungs. For rabbit 2, the volume is not available.

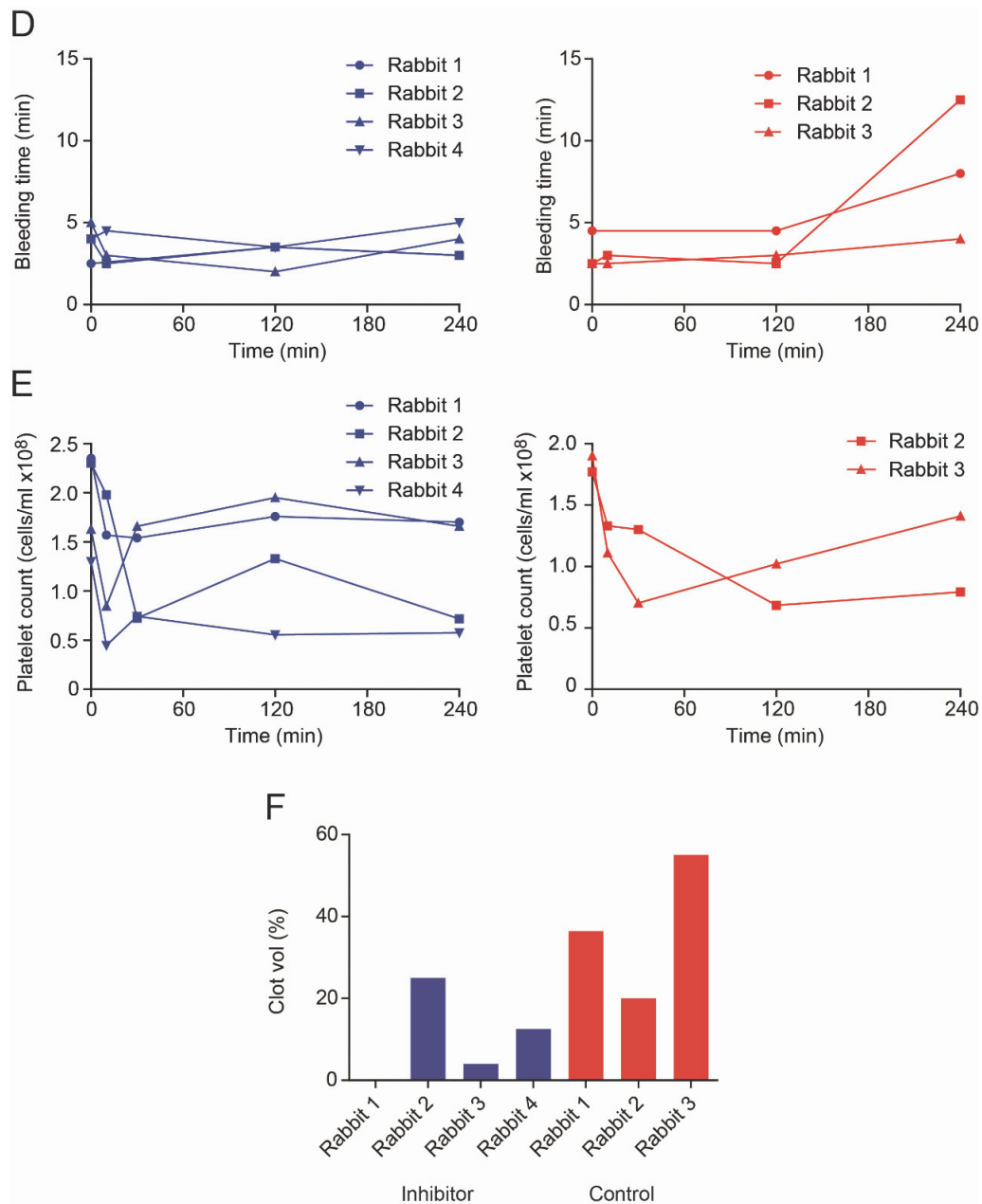


Figure S4.9. Continued

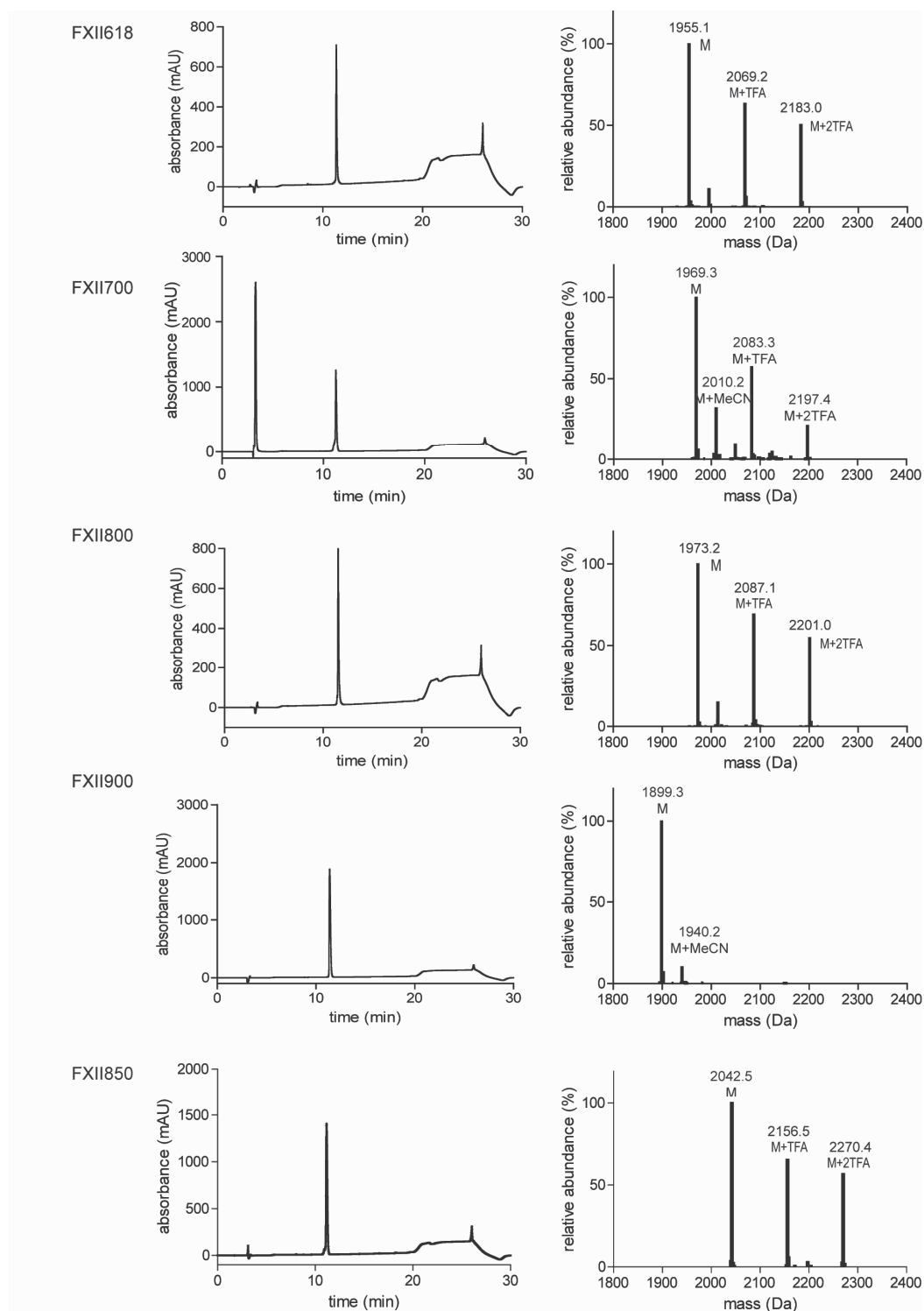


Figure S4.10. Analytical HPLC and mass spectrometric data for key peptides

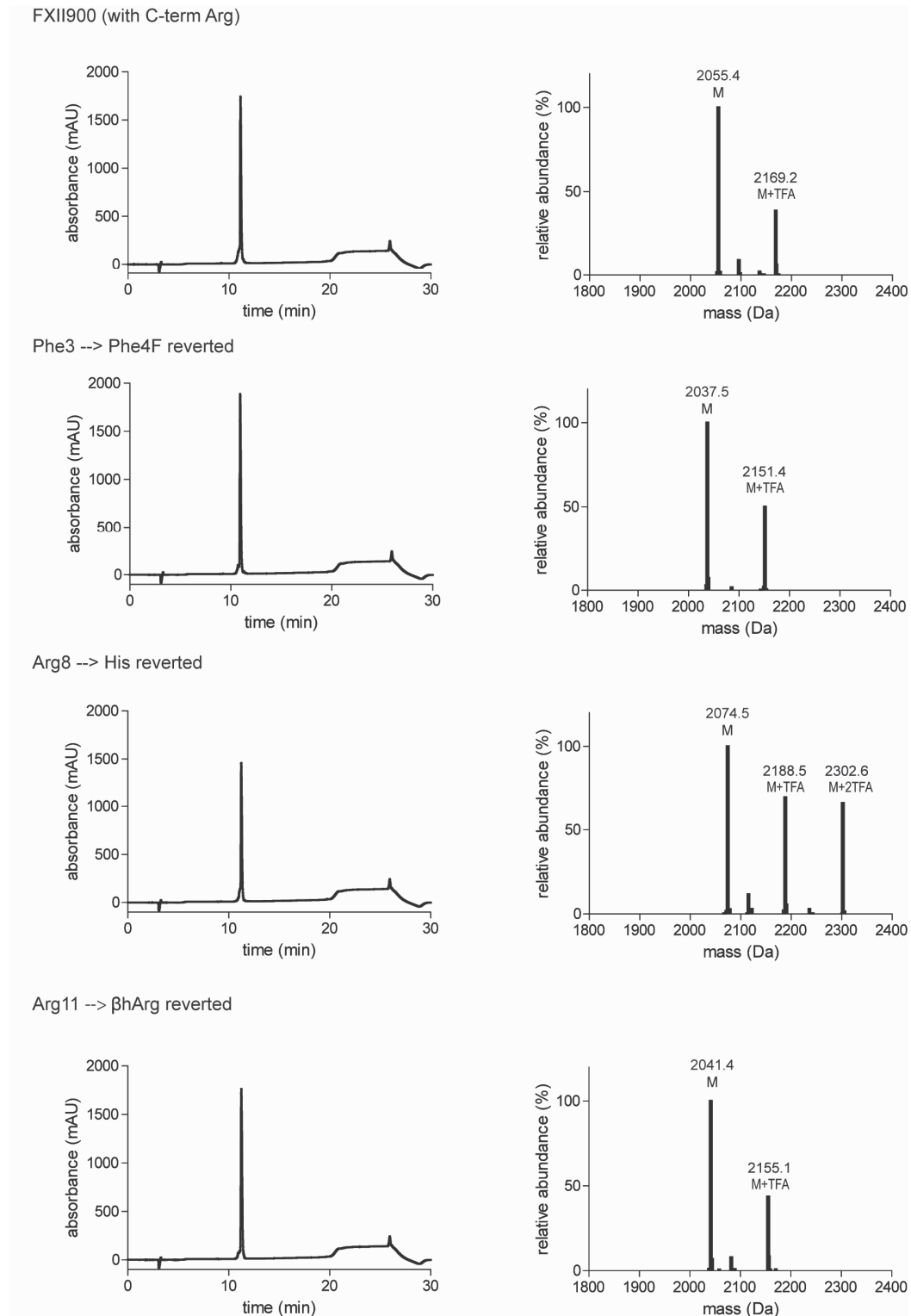


Figure S4.10. Continued

5. Selective inhibition of MMP achieved with peptide macrocycle

This chapter is based on a manuscript for submission by the following authors:

Maola Khan, Jonas Wilbs, Jeremy Touati and Christian Heinis

Author contributions: M.K and J.W contributed equally. M.K. and J.T. expressed MMP-2 and performed phage selections. M.K. introduced the hydroxamic acid modification. J.W. performed systematic affinity and stability improvements and selectivity analysis. J.W. and C.H. wrote the manuscript. All authors contributed to editing and critical proof-reading of the manuscript.

5.1 Abstract

Matrix metalloproteinases (MMPs) are important therapeutic targets but the development of selective small molecule inhibitors has, despite impressive efforts, not been achieved to most members of this class. In this work, we have addressed this long-standing challenge with a combinatorial approach to screen billions of macrocycles composed of natural amino acids and a synthetic chemical core. By optimization of the zinc-binding group and substituting natural amino acids to unnatural ones, we succeeded at enhancing substantially the binding affinity and stability of the phage-selected bicyclic peptide. The resulting MMP-2 inhibitor has a high affinity (1.9 nM) and stability (4.4 h) and thus provides a valuable research tool. The applied combined strategies promise to deliver selective synthetic inhibitors also to other important MMP targets.

5.2 Introduction

The matrix metalloproteinases (MMPs) are a family of endopeptidases comprised of 23 members in humans (255). The enzymes utilize a zinc ion in the active site for substrate cleavage and are expressed as zymogens, in which the zinc ion is chelated by a cysteine residue in the pro-domain in addition to three histidine residues in the catalytic domain. Upon proteolytic cleavage of the pro-domain, usually by another MMP, the enzyme becomes active. The main physiological function of the MMPs is degradation of the extracellular matrix (ECM) to facilitate tissue remodeling and angiogenesis (255–257). This is achieved by the degradation of collagen and other ECM supporting components but also by the release of growth factors and cytokines (258, 259). Even though each MMP has a large variety of substrates, often overlapping with other MMPs, the enzymes were traditionally classified based on their substrate preference. The MMPs have been generally divided into the following groups: collagenases (MMP-1, 8, 13, 18), gelatinases (MMP-2, 9), stromelysins (MMP-3, 10, 11, 12), matrilysins (MMP-7, 26) and membrane type (MMP-14, 15, 16, 17, 24, 25) (260). MMP activity is regulated *in vivo* by transcription, zymogen activation and tissue inhibitors of metalloproteinases (TIMPS) (256, 261, 262). Upregulation and/or increased expression of MMPs has been observed in various diseases, predominantly cancer, where MMPs contribute to tumor metastasis and neovascularization (263–267). MMP activity and overexpression have been correlated to poor prognosis and tumor aggressiveness (268). As a consequence, large efforts have been made, both in industry and academia, in order to develop MMP inhibitors as therapeutics. Several compounds were evaluated in clinical trials as cancer therapeutics, however no MMP inhibitor was successfully approved as a therapeutic (269). The early MMP inhibitors were small molecule peptidomimetics, often utilizing a hydroxamic acid moiety for tight binding to the active site zinc ion. The most prominent examples include bati-

mastat, marimastat, CGS 27023A, prinomastat and tanomastat (270–274). Several explanations for the clinical failures of the MMP inhibitors have been proposed. One is poor design of the clinical trials, in which mostly patients with already progressed cancers were enrolled even though in preclinical studies MMP inhibitors were found to be most efficient in the early stages of the disease (275). A second reason is the lack of specificity of the hydroxamate based inhibitors. With several MMPs being antitargets in cancer and extensive off target binding, the lack of specificity caused poor efficacy and severe side effects, ultimately leading to the termination of the MMP inhibitor programs (276). Despite the lack of success in the clinic, MMP inhibitors remain promising as potential therapeutics or as research tools (275–277). Presently, the focus lies on developing inhibitors highly selective for a specific MMP and to this end several approaches have been undertaken (278–282). Instead of targeting the catalytic domain, new MMP inhibitors can target exosites including the hemopexin domain, collagen binding site and pro domain (283). Several selective small molecule inhibitors have been reported, with or without zinc binding moieties. Other approaches include in silico screening and natural product derived inhibitors. In addition, a number of highly selective antibodies have been generated. However, developing specific MMP inhibitors has been challenging and despite the recent efforts selective inhibitors have only been found for a handful of MMPs.

MMP-2 is a target which has been strongly associated to aggressive cancer (284, 285) and several knock-out models confirm its involvement in tumor growth, neovascularization and metastasis (286–290). However, the development of a specific MMP-2 inhibitor has been particularly challenging given its high similarity to MMP-9. To date numerous molecular formats have been utilized in order to identify potent and selective MMP-2 inhibitors, including small molecules, peptides, natural products and antibodies. Rosello and coworkers synthesized small molecules with the purpose of inhibiting MMP-2 and 14 selectively. The most selective compound inhibits MMP-2 with an IC_{50} of 0.09 nM, but also inhibits MMP-8, 9 and 14 in the single digit nanomolar range (291, 292). Derivatives of gelatinase inhibitor SB-3CT have been reported to inhibit MMP-2 selectively in the low nanomolar range, but suffer from limitations in solubility and metabolism (293, 294). Recently other selective small molecule MMP-2 inhibitors were described with affinities in the nanomolar range, however the compounds were not fully selective or were only evaluated against MMP-9 (295–297). Several peptide based inhibitors and transition state analogues were reported, but with lacking selectivity over MMP-9 (298, 299). Chlorotoxin, a natural product, inhibits MMP-2 with a selectivity over other MMPs, but is also targeting other biomolecules (300, 301). In addition, antibodies were developed but with lack of- or not fully characterized selectivity (302, 303). Up to now, the most promising MMP-2 inhibitor in terms of potency and selectivity is a peptide based inhibitor, APP-IP which binds the active site of MMP-2 with an IC_{50} of 30 nM and has affinity in the micromolar range for MMPs 3, 7, 9 and 14 (304–306). When used as a 23 kDa fusion protein

with TIMP-2, thereby utilizing hemopexin domain binding, the molecule inhibits MMP-2 with a K_{iapp} of 0.7 pM whereas activities of MMPs 1, 3, 7, 8, 9 and 14 remain above 70% at 420 nM (307).

Even though APP-IP is potent and selective, it has a poor proteolytic stability which limits its use as research tool and as therapeutic. Recently our laboratory has generated bicyclic peptide inhibitors to a number of proteases which bind to their targets with high affinity and selectivity and are less prone to proteolysis (180, 188, 203). The peptides are generally developed by phage display and subsequent lead optimization (204, 246). In this work we aimed at utilizing this approach to make a potent, selective and proteolytically stable MMP-2 inhibitor which is readily available through chemical synthesis.

5.3 Results

5.3.1 Directed evolution of peptide macrocycle MMP-2 inhibitors

Peptides of a phage library of the form ACX₆CX₆CG-pIII (diversity > 4 billion peptides; Figure 29A) were cyclized by reacting the three cysteine residues with TBMB and subjected to three rounds of affinity selection with activated MMP-2. A strong enrichment of phage in round 2 and 3 of the selection and five strong consensus sequences among isolated peptides indicated isolation of binders (Figure 29A). One peptide isolated 20 times, M21 inhibited the protease efficiently with a K_i of 4 μ M while all other peptides showed no inhibition or only at high micromolar concentrations. In an alanine scan, the critical amino acids were unambiguously found to be the first four in the second ring of the macrocycle (DAIW) (Figure 29B). The same phage peptide library was also oxidized instead of reacted with TBMB to form bicyclic peptides based on two disulfide bridges, a strategy that we have recently reported (184). In this selection, four peptides containing only two cysteines were strongly enriched (Figure 29C). One of the monocyclic peptides inhibited MMP-2 more efficiently than the best bicyclic peptide inhibitors described above (K_i = 0.05 μ M). Peptides with only two cysteines are very rare in the applied library and indicate, along with the good inhibitory activity, a strong competitive advantage of this peptide format for the inhibition of the metalloproteinase. Comparison of these sequences with human proteins revealed a striking similarity to the 10-amino acid linear peptide APP-IP that was found by Higashi and co-workers to inhibit MMP-2 (306) (Figure 30A). The linear part of the isolated monocyclic peptides is likely forming similar interaction as the C-terminal amino acids of the linear APP-IP. These latter amino acid segment Asp-Ala-Leu-Met binds in a linear and stretched conformation to the active site of MMP-2, possibly explaining the strong enrichment of peptides with a linear moiety.

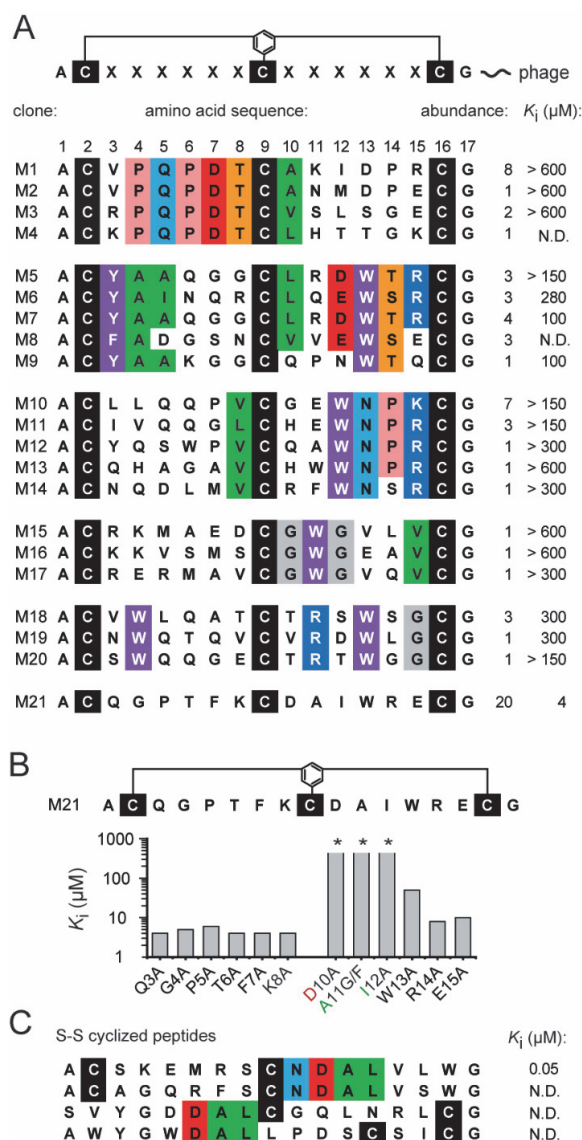


Figure 29. (A) Five consensus sequences were isolated after three rounds of selection as illustrated. The most abundant clone, M21, inhibited MMP-2 with highest affinity. (B) An alanine scan of M21 showed that residues D10, A11 and I12 were the most important for binding. The K_i values of systematically substituted peptides are indicated. (C) Four peptides containing only two cysteines were enriched in the selection. One of them bound the target with higher affinity than the best bicyclic peptide. All monocyclic peptides shared the same binding motif as identified in M21.

5.3.2 Substituting the zinc binding carboxylate with hydroxamate

The X-ray structure of APP-IP showed that the two oxygen atoms of the carboxylate of aspartate coordinate in a bidentate manner to the active site zinc ion of MMP-2 (PDB ID 3AYU) (Figure 30A) (306). Based on sequence comparison we hypothesized that the aspartate residues in M21 and the monocyclic peptide form the same interaction as in APP-

IP. Hydroxamate is known to chelate zinc with a higher affinity than carboxylate, mainly due to its tendency to form bidentate rather than monodentate interactions with the ion (308). It has also been found to form additional hydrogen bonding interactions with the enzyme (309, 310). Therefore, we reasoned that substitution of aspartate with L-alanyl-hydroxialanine in these peptides could significantly increase the binding strength. Although the monocyclic lasso-type peptide was a better inhibitor than bicyclic M21, we chose to modify the latter one as the bicyclic peptide was found to be metabolically more stable. To prepare bicyclic peptide M21^{hy}, a Fmoc-based synthetic strategy was developed in which the linear peptide M21 was synthesized with a 2-phenylisopropyl ester side chain protected aspartate. This protection group was orthogonally removed using 2% (v/v) TFA in DCM and the hydroxamic acid moiety was introduced via a peptide coupling of the aspartic acid residue with hydroxylamine. All remaining protecting groups were removed under acidic conditions and the peptide was cyclized with TBMB. M21^{hy} inhibited MMP-2 with a 35-fold improved K_i of 116 ± 8 nM (Figure 30A).

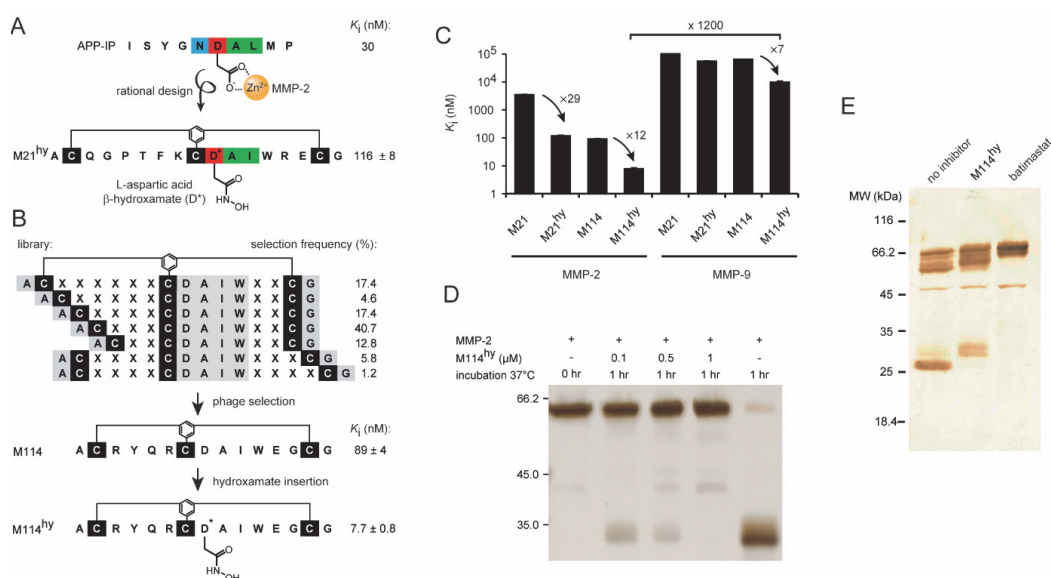


Figure 30. (A) The previously identified linear peptide MMP-2 inhibitor APP-IP binds by chelation of the active site Zn-ion. The binding of M21 could be improved by introducing a Zn chelator which is stronger than the carboxylate. (B) In the affinity maturation strategy of M21 libraries of different sizes were used. The best peptide was identified in the 4x6 library. (C) Hydroxamate modification had a strong effect on MMP-2 binding, but did not influence MMP-9 binding to the same extent. K_i values of the different peptide for the two enzymes are indicated. (D) SDS-PAGE showing that M114^{hy} inhibits the autodegradation of MMP-2. The band at 32 kDa is a known degradation product formed upon autodegradation of MMP-2 (E) M114^{hy} inhibits autodegradation of MMP-2 when applied to a cell culture of HT1080 fibrosarcoma cells. MMP-2 species were detected in the cell media by western blot.

5.3.3 Affinity maturation of MMP-2 inhibitor

In an attempt to further improve the binding affinity of the peptide and at the same time to optimize the ring sizes, we performed an additional round of phage display using affinity maturation libraries. Seven different library formats were constructed in which the size of the two rings was varied. The binding motif DAIW in the second ring was kept constant. Obviously, the peptides on phage did not contain the hydroxamate group. After sequencing of the clones, it seemed that the ACX₃CX₆CG library was the preferred format (Figure 30B). We therefore used this format when optimizing residues in the second ring. The motif QAR was chosen to be kept constant in the first ring as it was the most common motif in the first ring of the 3x6 library and moreover it was the only motif found in the same position in multiple libraries. The arginine residue before the middle cysteine was the most conserved residue of the first ring in the 3x6 and 4x6 libraries, the two most common formats. We then synthesized peptides having the five most abundant residues in position 5 of the second ring and glycine in position 6. The results show that Glu is the preferred residue in position 5 of the second ring (Figure S5.1). For the first ring optimization we choose 10 different motifs present in the isolated peptides from the 2x6, 3x6 and 4x6 formats. The motifs were chosen based on amino acid abundance. Predominantly motifs having an arginine in the position before the middle cysteine were selected and compared to the QAR motif. We synthesized peptides without hydroxamate groups as this was technically easier. Several of the selected motifs had similar affinities. We found that RYQR was the preferred motif of the first ring (Figure S5.1). The affinity matured peptide M114 of the format ACX₄CX₆CG, inhibited MMP-2 with a K_i value of 89 ± 4 nM.

5.3.4 Selectivity of MMP-2 inhibitors

The strong chelation of the active site zinc ion has largely contributed to the off target binding of previously developed MMP inhibitors. Here we wanted to determine the specificity of bicyclic peptide MMP-2 inhibitors containing a hydroxamic acid moiety for zinc chelation and affinity enhancement. When incorporated in the original lead peptide M21 identified from phage display using the ACX₆CX₆CG library, the hydroxamate modification increased binding affinity 29-fold to MMP-2 (Figure 30C). The K_i value for MMP-9 was of more than 2 orders of magnitude larger. For the affinity matured peptide M114, which had a 45-fold higher affinity for MMP-2 than M21, the hydroxamic acid increased the MMP-2 binding affinity by a factor 12. In the case of MMP-9 the binding was increased 7-fold for M114^{hy} as compared to the peptide without hydroxamic acid. The selectivity of M114^{hy} for MMP-2 over MMP-9 was 1200-fold. These results indicate that both the affinity maturation as well as hydroxamate modification increase the affinity of the peptide for both enzymes. However, the effect was more pronounced for MMP-2, therefore ultimately resulting in a higher selectivity.

5.3.5 Inhibition of MMP-2 autoactivation

We next evaluated the ability of M114^{hy} to inhibit MMP-2 in a situation more physiologically relevant than an enzymatic assay using an artificial substrate. Previous studies have shown that MMP-2 is autoactivated and autocatalytically cleaved at several sites (311, 312). These processes are likely of importance in vivo. Here we incubated the active 62 kDa active enzyme together with different concentrations of the inhibitor. The results show that M114^{hy} dose-dependently inhibits the autoproteolysis of MMP-2 (Figure 30D). For all inhibitor concentrations, a majority of the active 62 kDa enzyme remains. Without inhibitor the enzyme is degraded to the 32 kDa fragment observed by Howard et al. (311). This band is also detected for the lower inhibitor concentrations whereas for the highest concentration the only degradation product found is the 42 kDa fragment, which is a precursor of the 32 kDa species.

We then compared the degradation of MMP-2 in HT1080 human fibrosarcoma cell culture media following selective MMP-2 inhibition by M114^{hy}, broad spectrum MMP inhibition by batimastat or no inhibition. Without inhibitor or with only M114^{hy} a broad band was detected around 66 kDa (Figure 30E). This band is likely consisting of two species, 72 kDa pro-enzyme and 62 kDa active enzyme, a similar result was detected by Bergmann et al. (312) With broad spectrum inhibition only the upper part of this band is observed, hence no active MMP-2 is formed. This would mean that enzymes other than MMP-2 contribute in the activation of the enzyme. It has been previously reported that MMP-2 is activated by MMP-14, which is inhibited by batimastat, hence the absence of active 62 kDa MMP-2 in this setting is expected. No degradation products are present for the broad spectrum inhibition, suggesting the blockage of all MMP-2 degrading enzymes. A difference in degradation products is observed when MMP-2 is inhibited as compared to no inhibition. This implies that other MMPs degrade MMP-2 but a certain degradation product (~26kDa) can only be formed by MMP-2 autoproteolysis. An unidentified band at ~46 kDa is likely a degradation product formed by a species not inhibited by batimastat.

5.3.6 Plasma stability of MMP-2 inhibitors

As described in the introduction, a potent and selective linear peptide MMP-2 inhibitor, APP-IP, has been previously reported. However, its use as a therapeutic or research tool might be limited due to poor proteolytic stability, which is often the case for linear peptides. In contrast, bicyclic peptides typically show superior proteolytic stability as compared to their linear counterparts. We compared the proteolytic stability of the bicyclic peptide M114^{hy} to APP-IP. The proteolytic stability was assessed by incubating the peptides in mouse plasma at 37°C and quantifying the remaining peptide by analytical

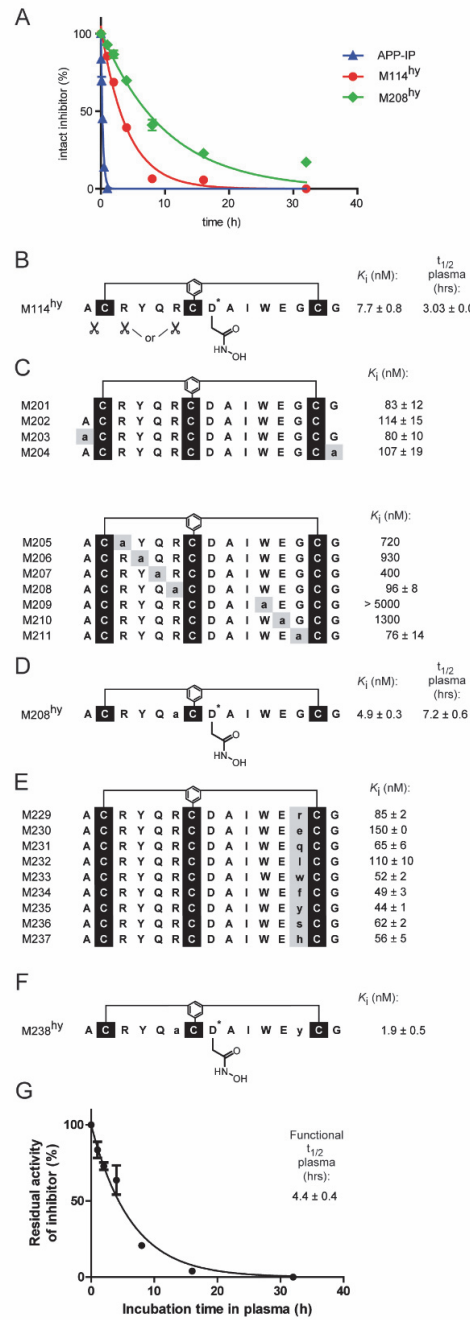


Figure 31. (A) The peptides were incubated in mouse plasma and remaining peptide quantified at the indicated timepoints. The stability analysis showed that the bicyclic M114^{hy} was more stable than the linear APP-IP. (B) Mass spectral analysis showed that M114 was cleaved at the N-terminal alanine and at one of the arginines. (C) A series of peptides was synthesized in which residues non-crucial for binding were substituted with D-alanine. The binding affinities are indicated. (D) Replacing the Arg6 of the first loop increased the stability without compromising affinity. (E) A series of D-amino acid substituted peptides in position Gly13 were synthesized since it was found that D-Ala improved the binding affinity of M114 when in this

position. (F) Peptide M238^{hy} combines Arg6→D-Ala and Gly13→D-Tyr modifications and had a four-fold improved affinity over M114^{hy}. (G) The stability of M238^{hy} was assessed by incubating the peptide in plasma and quantifying the remaining functional strength of the inhibitor at the indicated time points. The improved inhibitor was found to have a functional half-life of 4.4 h. In contrast, no remaining functionality was detected for M114^{hy} after 1 h.

HPLC area under curve. The experiment showed that APP-IP indeed is rapidly degraded in plasma, having a half-life of around 15 min (Figure 31A). The bicyclic peptide M114^{hy} had a substantially longer half-life of 3.00 ± 0.04 h. This results demonstrate that the bicyclic structure of M114^{hy} improves its stability by making it less accessible to proteases present in plasma.

5.3.7 Stability improvement of MMP-2 inhibitor

Even though M114^{hy} had a relatively long proteolytic half-life of 3 h, an increased stability would be desirable for its potential use as a research tool or therapeutic. In this work we therefore aimed to improve the proteolytic stability of M114^{hy} further. We choose an approach in which we identified the proteolytic cleavage sites in the peptide sequence and replaced key amino acids by D-alanines. We hypothesized that the incorporation of D-amino acids would make the peptide less recognizable by proteases. By mass spectral analysis of the early degradation products, molecular masses corresponding to the peptide without N-terminal alanine as well as peptide with one ring opened and missing one arginine residue had been observed. It was however not clear which arginine had been cleaved (Figure 31B).

We next wanted to see how modifying these potential cleavage sites would affect the target affinity of the peptide. A requirement of the stability improving peptide modifications was that they should have only minimal or no impact on target affinity. Peptides containing only single mutations were compared to the lead peptide M114. In these series, all peptides were synthesized without hydroxamate modifications, to allow a rapid screening approach. It was assumed that the properties of these peptides would later translate into hydroxamate modified peptides. In a first series, the C-terminal and N-terminal residues were either removed or replaced by D-Ala (Figure 31C). These modifications had no substantial effect on the affinity of the peptides, and would hence be allowed for potential stability improvement. However, replacement or removal of the C-terminal Gly residue slightly decreased the affinity.

In the next series we screened peptides where all amino acids inside the two rings, except those of the important Asp-Ala-Ile binding motif, were replaced by D-Ala. The affinity was substantially decreased for all peptides with the exception of M208, where Arg6 in the first ring was replaced and M211 where Gly13 in the second ring was replaced (Figure 31C). Both positions would therefore allow D-amino acid incorporation. In order to identify the previously observed arginine cleavage site, we incubated in mouse plasma

peptides M205 and M208 where the Arg3 and Arg6 respectively were individually replaced by D-Ala, and analysed the degradation products by MS. Endopeptidic cleavage was found only for M205 but not for M208, indicating that only Arg6 was prone to proteolysis (Figure S5.2). When further analysing the degradation products of M114 and M114^{hy}, these results were confirmed by the detection of molecular species which could only be formed by cleavage of the Arg6 (Figure S5.3 and S5.4). We then synthesized the peptide M208^{hy}, containing the Arg6→D-Ala modification as well as the hydroxamic acid moiety and tested its proteolytic stability. The replacement of Arg6 by D-Ala in the first loop increased the proteolytic stability of the peptide 2.4-fold to 7.2 ± 0.6 h (Figure 31A and D). No degradation products except loss of hydroxamate and/or N-terminal arginine were observed (Figure S5.5).

Finally, we synthesized a set of peptides with Arg3 and Arg6 replaced by Ala and D-Ala respectively and with and without C- and N-terminal residues. By removing the N-terminal cleavage site as well as replacing both arginines, which are known to be cleaved by trypsin, with amino acids allowed in terms of affinity we hoped to further improve the stability. However, when comparing these peptides to each other and to M208 and M208^{hy} the stability was found to decrease when ends were removed or Arg3 replaced by alanine (Figure S5.6). Moreover we found that the hydroxamic acid moiety decreases the half-life of the peptides. Based on these results we chose to incorporate only the Arg6→D-Ala modification for stability improvement.

5.3.8 Affinity improvement of MMP-2 inhibitor

After affinity maturation and hydroxamic acid introduction, the affinity of the bicyclic peptide MMP-2 inhibitor increased to reach a K_i value below 10 nM. However, in order to be used as a research tool or therapeutic and to fully block MMP-2, even stronger target binding is desirable. In parallel with the stability improvement we therefore set out to further improve the affinity. To identify which amino acids of the affinity matured peptide were important for target binding we performed an additional alanine scan, but excluding the previously identified important motif of the second ring (DAI). The results show that Trp11 but also Tyr4 are important for target binding (Figure S5.7A). With the hypothesis that the interactions formed by these residues could be improved, we substituted the Trp11 with several unnatural analogues (data not shown) and the Tyr4 with a panel of natural amino acids (Figure S5.7B). Unfortunately none of the substitutions increased the target affinity. Tyr4 could however be substituted with Phe without losing affinity.

In the D-alanine scan described above it was observed that substituting Gly13 in the second ring with D-Ala slightly enhanced the binding affinity of M114 (Figure 31C). This result is in line with an observation in a previous study where Chen et al. describe that glycine residues in bicyclic peptide ligands can sometimes be replaced by D-amino acids

for improved target affinity (191). If the ϕ dihedral angle of the glycine residue is positive, incorporation of a D-amino acid residue can be favourable at that position since D-amino acids adopt positive ϕ dihedral angles. Including a D-amino acid could possibly increase affinity by forming new interactions between the side chain and the target. Furthermore, the conformational flexibility of the unbound peptide could potentially be decreased, resulting in a lower entropic penalty upon binding. Since Gly13 benefited from the introduction of a D-Ala, it is likely that this residue adopts a positive ϕ dihedral angle. We therefore decided to screen a panel of D-amino acids in the Gly13 position. Several of the D-amino acids improved the affinity, with the best ones being D-Tyr and D-Phe, which improved the affinity 2-fold (Figure 31E). Subsequently we investigated several combinations of the above identified modifications in a series of 4 peptides (including M208^{hy}). The modifications included Tyr4→Phe, Arg6→D-Ala, and Gly13→D-Tyr/D-Phe. All peptides in this set contained the hydroxamic acid moiety. By analysing this group of peptides we found that Tyr was the preferred residue in position 4 and D-Phe was slightly preferred in position 13. The best peptide, M238^{hy} was binding MMP-2 with a K_i of 1.9 ± 0.5 nM (Figure 31F).

Finally we set out to validate the stability of the peptide M238^{hy}, having all three modifications in place (Arg6→D-Ala, Gly13→D-Phe and hydroxamic acid). In order to get more relevant values, we determined the functional half-life of the inhibitors using a new method recently developed in our laboratory. The method is based on enzymatic activity assays following the plasma incubation rather than quantification by analytical HPLC. By measuring the remaining functional strength of the inhibitor both the activity of intact inhibitor as well as of potentially active metabolites is determined. When analysed in this assay M238^{hy} shows a functional half-life of 4.4 ± 0.4 h (Figure 31G). For the lead peptide M114^{hy} no remaining functionality could be detected at the earliest sample time point (1 h).

5.3.9 MMP specificity profiling of M238^{hy}

Next we set out to do a selectivity screen against all other MMPs which would likely be inhibited by M238^{hy}. The goal was to compare important residues of the enzymes in close proximity to the binding site (Figure 32A). To identify the enzymes which could likely be inhibited by a MMP-2 inhibitor, we first performed a BLAST screen of the catalytic domain of MMP-2 (Table S5.1). For the similarity search the amino acid sequence of the two parts of the MMP-2 catalytic domain as a single sequence, with fibronectin domains removed, was used as reported by Hashimoto (306). The BLOSUM62 scoring matrix was used. For the specificity profiling a kit of 10 MMPs was analysed. The kit contained most of the MMPs having the highest similarity to the MMP-2 catalytic domain. A majority of the MMPs screened, were not inhibited by M238^{hy} and had K_i values exceeding 50 μ M (Figure 32B). With the exception of MMP-2, only two proteases were inhibited with K_i

values below 1 μ M (MMP-3 and 12, K_i values of 4.1 ± 1.1 and 600 ± 100 nM respectively). The strong affinity for MMP-3 was surprising given that most previously reported MMP-2 inhibitors only lacked selectivity over MMP-9. This data implicates that M238^{hy} is forming different interaction with the target as compared to most other MMP inhibitors. Hence potentially also other MMPs could be inhibited.

To gain further insight in the target interaction mechanisms we identified key residues within the enzymes important for the binding and subsequently aligned the catalytic domains of the MMPs and compared these residues. The interaction forming residues were thought to lie within close proximity to the binding motif DAIW of the inhibitor. Given the fact that M238^{hy} and APP-IP share this consensus motif and are both chelating to the zinc ion through the Asp residue they likely bind to MMP-2 in a very similar way. We therefore used the published crystal structure (PDB ID 3AYU) to identify key residues of the MMP-2 catalytic domain. Residues within 4-6 Å of the DALM motif in APP-IP were selected (Fig 32A and B, yellow and blue respectively). By comparing these residues of all MMPs in the sequence alignments and cross-analysing the affinities of M238^{hy} for the MMPs in the kit important key residues for selectivity could be identified. The most important residue was identified as Ala87 (Hashimoto numbering) in the non-prime side of the substrate binding cleft. Only enzymes containing an alanine or glycine in this position were inhibited by M238^{hy} (MMP-2, 3, 7 and 12, Figure 32B). If the enzyme contained any larger residue in this position it fully abolished binding. These results are well in line with a previously published study in which the selectivity of APP-IP for MMP-2 over MMP-9 was studied (305). Consequently, we tested the affinity of M238^{hy} for MMP-20, which is the only other MMP, besides the ones already tested, having an alanine or glycine in this position. Indeed, MMP-20 was also inhibited with a K_i value of 410 ± 50 nM.

While Ala87 is likely the most important residue for selectivity, also other residues have an impact, which is seen by the different affinities of M238^{hy} for MMPs 2, 3, 7, 12 and 20. Several studies indicate differences in the S1' pocket as substrate selectivity determinants for MMPs (313, 314). We hypothesize that M238^{hy} forms interactions in this pocket via the Tyr4 residue of the first ring. It is known that the S1' pocket favours hydrophobic interactions (315), as utilized by several small molecule inhibitors. Indeed also the Tyr3 residue of APP-IP is forming interactions in this pocket (306). Moreover our alanine scan confirmed that Tyr4 of M238^{hy} is involved in target binding. Mainly two important residues have been identified in the S1' site region, Leu116 and Ile141 (316, 317). Both MMP-20 and MMP-12 differed in this region as compared to MMP-2. MMP-20 has a Thr residue in both positions whereas MMP-12 has a Thr residue in 141. It is likely that these differences contribute to the two orders of magnitude loss in affinity for these enzymes. However, also other differences seem to have an influence, such as Leu81→Thr in MMP-20 as well as Phe4→Met and Ala87→Gly in MMP-12, which lie close to each other on the

non-prime side. M238^{hy} has even more than 10-fold lower affinity for MMP-7, which is likely also due to differences in the S1' pocket. MMP-7 has a Tyr in position 116 and has been reported to have a particularly shallow S1' pocket (316).

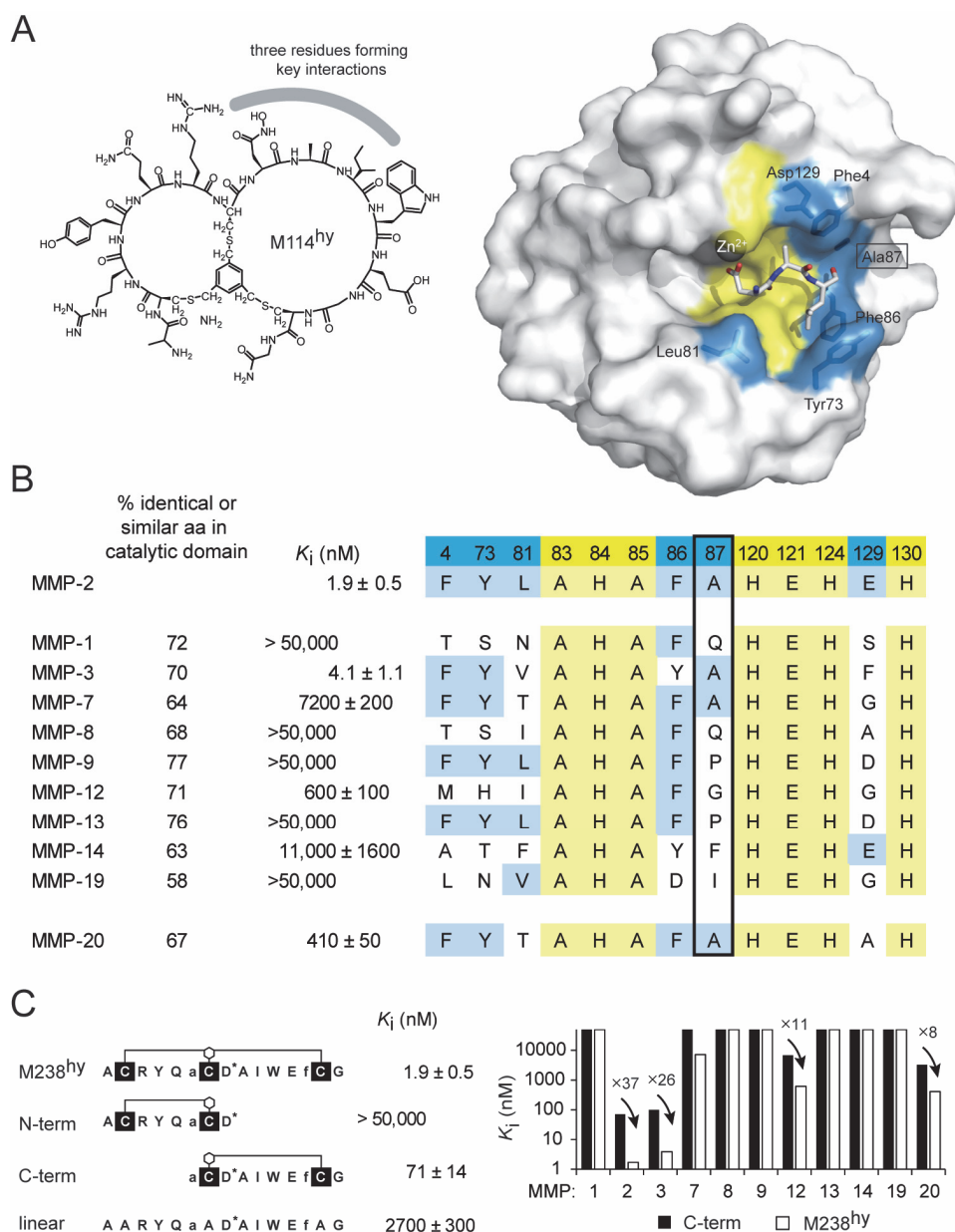


Figure 32. (A) The residues D10, A11 and I12 are most important for binding to MMP-2 (left). Residues of MMP-2 within 4–6 Å of DALM in APP-IP were selected and are indicated in yellow and blue respectively (right). (B) Inhibition constants of M238^{hy} are indicated for a panel of MMPs (left). The key interaction residues of these enzymes with the peptide are shown (right). (C) the single rings of M238^{hy} and the linear peptide were tested for MMP-2 inhibition. The C-terminal ring was found to inhibit MMP-2 around 37-fold less than the bicyclic peptide (left). The C-terminal ring of M238^{hy} was tested for inhibition of a panel of MMPs.

This hypothesis is further supported by Higashi et al. who observed that differences in the S1' pocket were the main cause of APP-IP selectivity for MMP-2 over MMP-7 (305). Higashi and co-workers further claim that the Gln in position 93 of MMP-9 (Gly93 in MMP-2) contributes to selectivity. This observation could explain why APP-IP does not inhibit MMP-3 whereas M238^{hy} does, since MMP-3 has an Asn in this position. From the crystal structure (PDB ID 3AYU) it is evident that Pro10 of APP-IP would clash with any residue pointing towards the solvent in position 93 of the enzymes, which indeed is the case for MMP-3 and 9 (PDB ID 2D1O and 4H3X) (314, 318). We speculate that M238^{hy} and APP-IP adopt somewhat different conformations in the far part of the non-prime side of the substrate binding cleft.

5.3.10 MMP inhibition of single rings and linear M238^{hy}

To understand which parts of M238^{hy} are interacting with the MMPs, we synthesized the peptide's first and second ring separately, cyclized with a bivalent linker via the cysteine residues. In addition, a linear variant of the peptide was made, having replaced the cysteines by alanines. The hydroxamic acid moiety was included in all constructs. As expected, the N-terminal ring did not inhibit any of the enzymes (Figure 32C). This emphasizes the fact that the interactions in the non-prime side of the substrate binding cleft are crucial for inhibitor activity, despite the presence of the hydroxamate and S1' binding residues.

The C-terminal ring shows inhibitory activity against MMPs 2, 3, 7 (K_i around 35 μ M), 12 and 20. This is expected since these proteases have an alanine or glycine residue in position 87. If compared to the bicyclic peptide, the affinity is always improved by introducing the first ring, but to various degrees. This suggests that the first ring is indeed making interactions with the enzymes, probably in or around the S1' site. The best interactions are made with MMP-2 and 3 where introduction of the first ring improves affinity 47- and 26-fold respectively. The effect is less pronounced for MMP-12 and 20 (11-fold and 8-fold respectively) and even less for MMP-7 (5-fold). This is consistent with our previous hypothesis that S1' interactions are decreasing for these enzymes and thereby selectivity is achieved.

The linear peptide was inhibiting MMP-2 with a K_i of 2700 ± 300 nM, but no other MMP was inhibited. The strong loss in activity indicates the importance of the bicyclic conformation for target binding. It is likely that the peptide is locked in its binding conformation by the cyclization scaffold.

5.3.11 Selectivity of M238^{hy}

With the purpose of making a more specific inhibitor and to gain further insight into which residues of M238^{hy} are important for specificity, we set out to screen a selection of the previously reported peptides for specificity over MMP-3. Peptides of high diversity

but with minimal loss of affinity for MMP-2 were chosen for the screen, all without hydroxamate. Initially, all peptides were analyzed for MMP-3 inhibition using the previously used enzyme, here termed MMP-3-a (MMP-3 catalytic domain, Enzo life sciences, kit cat # BML-AK308-0001). From the initial screen, which was done only once and with only three data points for each peptide, a subset of peptides was selected, having higher selectivity than lead peptide M114 (Figure 33A, indicated by arrows). The largest increase in selectivity was observed for peptide M222, where S1' binding Tyr4 residue was modified into Glu. In addition, the introduction of D-Ala either at the N-terminus or in position 6 increased selectivity. Several of the D-amino acids in position 13 increased selectivity. The selected peptides were then analysed in duplicate, but using a different enzyme construct, here termed MMP-3-b (MMP-3 catalytic domain, Enzo life sciences, cat # ALX-201-042-C005). With this enzyme, the affinity of the peptides was generally lower, hence selectivity increased. This difference in binding affinity is hard to explain, since according to the supplier the only differences of the enzymes are that MMP-3-a contains residues Phe100-Thr272 with a C-terminal His-tag for purification whereas MMP-3-b instead contains residues Gly98-Pro273. Surprisingly M222 showed a lower selectivity than M114 in this assay. Instead M221, (Tyr4→Arg) showed high selectivity. The other selectivity improving modifications were the same as for the first set.

Since M238^{hy} contains the selectivity enhancing modifications Arg6→D-Ala (M212 vs M214) and Gly13→D-amino acid, we were surprised that it was not more selective. We hypothesized that either the hydroxamate or the Gly13→D-Phe modifications decreased selectivity. Peptides M234 and M114^{hy} were tested against MMP-3-b and it was observed that while the specificity was increased by Gly13→D-Phe indeed the hydroxamate decreased specificity (Figure 33B). Despite the decrease of specificity by the hydroxamate, M114^{hy} is more selective than M238^{hy} (MMP-3-b assay) even though the latter contains Gly13→D-Phe. We then tested also M208^{hy} which is M238^{hy} without Gly13→D-Phe. Unexpectedly, this peptide is less selective than M114^{hy} indicating that when in combination with hydroxamate, the Arg6→D-Ala modification decreases selectivity. Finally, we synthesized four different derivatives of M238^{hy}, each containing one of the identified selectivity increasing modifications (Figure 33C). These peptides were again tested with MMP-3-a. Only one of these peptides showed an improved selectivity as compared to M238^{hy} namely M240^{hy} in which Tyr4 was replaced by Arg. This modification improved the selectivity 3-fold, but also decreased the affinity for MMP-2, which however stayed well below 10 nM.

A		K_i (nM):			Selectivity	
		MMP-2	MMP-3-a	MMP-3-b	MMP-2 / MMP-3-a	MMP-2 / MMP-3-b
M114	A C R Y Q R C D A I W E G C G	89 ± 4	169 ± 14	570 ± 120	1.90	6.40
M214	A C A Y Q R C D A I W E G C G	94 ± 2	102		1.09	
M216	A C R Y A R C D A I W E G C G	140 ± 20	313	1007 ± 2	2.24 ←	7.19
M211	A C R Y Q R C D A I W E a C G	76 ± 14	143		1.88	
M201	A C R Y Q R C D A I W E G C G	83 ± 12	137		1.66	
M202	A C R Y Q R C D A I W E G C G	114 ± 15	330	650 ± 80	2.89 ←	5.70
M203	a C R Y Q R C D A I W E G C G	80 ± 10	379	630 ± 9	4.74 ←	7.88
M204	A C R Y Q R C D A I W E G c a	107 ± 19	158		1.48	
M212	A C A Y Q a C D A I W E G C G	100 ± 13	356	1040 ± 30	3.56 ←	10.4
M221	A C R R Q R C D A I W E G C G	160 ± 20	510	1630 ± 30	3.19 ←	10.2
M222	A C R E Q R C D A I W E G C G	330	2200	1050 ± 130	6.62 ←	3.18
M226	A C R F Q R C D A I W E G C G	87 ± 12	174	580 ± 80	2.00 ←	6.67
M229	A C R Y Q R C D A I W E r C G	85 ± 2	118		1.39	
M231	A C R Y Q R C D A I W E q C G	65 ± 6	134	520 ± 40	2.06 ←	8.00
M233	A C R Y Q R C D A I W E w C G	52 ± 2	155	600 ± 50	2.99 ←	11.5
M236	A C R Y Q R C D A I W E s C G	62 ± 2	110		1.77	
M237	A C R Y Q R C D A I W E h C G	56 ± 5	155	440 ± 80	2.78 ←	7.86
B						
M234	A C R Y Q R C D A I W E f C G	49 ± 3		440 ± 60		9.00
M114 ^{hy}	A C R Y Q R C D A I W E G C G	7.7 ± 0.8		40 ± 2		5.19
M208 ^{hy}	A C R Y Q a C D A I W E G C G	4.9 ± 0.3		13.5 ± 0.9		2.76
M238 ^{hy}	A C R Y Q C D A I W E f C G	1.9 ± 0.5	4.1 ± 1.1	6.9 ± 1.6	2.16	3.63
C						
M239 ^{hy}	a C R Y Q a C D A I W E f C G	3.6 ± 0.3	5.3 ± 1.3		1.47	
M240 ^{hy}	A C R R Q a C D A I W E f C G	5.3 ± 0.2	33 ± 6		6.23	
M241 ^{hy}	A C R Y A a C D A I W E f C G	3.1 ± 0.2	4.8 ± 0.9		1.55	
M242 ^{hy}	A C R Y Q a C D A I W E w C G	2.0 ± 0.3	4.4 ± 0.9		2.20	

Figure 33. (A) A set of previously screened peptides were selected for specificity screen against MMP-3-a. Peptides without hydroxamate modifications were compared to lead peptide M114. The difference from M114 is indicated in grey. From the initial screen, peptides having a higher selectivity than M114 were selected as indicated by arrows. These peptides were then screened in duplicate against a different enzyme (MMP-3-b). The K_i values of the peptide for enzymes MMP-2, MMP-3-a and MMP-3-b are indicated. (B) Hydroxamate modification decreases specificity, especially when in combination with Arg6→D-Ala. Modification Gly13→D-Phe increases specificity. (C) Four peptides were synthesized containing the identified modifications beneficial for selectivity. The peptides additionally had modifications Arg6→D-Ala and hydroxamate for direct comparison with M238^{hy}.

5.1 Discussion

Despite the failure of MMP inhibitors in clinical trials, the enzyme class remains important as drug targets. This is highlighted by the recent development of new inhibitors of different formats than the classic small molecule hydroxamate-based compounds. The lack of selectivity has been stated as one of the main reasons for the failure of the early MMP inhibitors. However, for the same reason, the biological roles and involvement in pathologies of the individual MMPs is not yet fully understood. To gain this insight, highly specific MMP inhibiting tool compounds could be applied, for example in cell

based assays or disease models. This knowledge could then facilitate drug development in terms of target validation and/or anti-target identification within the class of MMPs.

Herein we utilized phage display of bicyclic peptides, which have been demonstrated to bind with high affinity and specificity to their targets, to develop a selective MMP-2 (/3) inhibitor. By using affinity maturation, SAR studies and medicinal chemistry, we could improve the affinity of the lead peptide isolated in the initial phage display by more than three orders of magnitude (M21: $K_i = 4 \mu\text{M}$, M238^{hy} $K_i = 1.9 \text{ nM}$). This demonstrates the power of the bicyclic peptide format when developed by phage display together with the introduction of unnatural building blocks.

For selective MMP-2 inhibitors, the main challenge has been to prove selective over the other gelatinase MMP-9. The two enzymes are unique in their structure, having three fibronectin II type collagen binding domains which are required for their ability to cleave gelatine. The presence of these domains separates the gelatinases from other MMPs. In addition, the two enzymes share a 64% sequence identity in the catalytic domain. Achieving selectivity for MMP inhibitors containing a hydroxamic acid moiety has been particularly challenging. Our initial lead peptide M114^{hy} as well as M238^{hy} show strong selectivity for MMP-2 over MMP-9. This indicates that the peptides contain selectivity enhancing groups, not found for most other MMP-2 inhibitors. However, several other MMPs have high similarity to MMP-2, therefore it is important to screen also those. In this screen we found that MMP-3 was also inhibited by M238^{hy}. In addition we identified regions and specific residues of the MMPs, crucial for selectivity of the inhibitor. In contrast to many other studies we have herein analyzed the sequences of all human MMPs. In particular selectivity seems to be determined by the S1' pocket of the enzyme as well as of residues on the non-prime side such as Ala87. We believe that our findings could be of value when designing inhibitors specific for certain MMPs. However, crystal structures would be a great complement to our activity assay based results in order to gain in-depth knowledge about which interactions control MMP selective inhibition.

Furthermore, we have demonstrated that by introducing unnatural amino acids we could improve the proteolytic stability and affinity. The stability was improved by identifying proteolytic cleavage sites and subsequently replacing labile residues by D-amino acids. By introducing D-amino acids in a glycine position new target interactions could be formed and thereby increasing binding affinity. These approaches are general and can be readily applied to peptide binders of any format.

Finally, we made an effort in order to improve the selectivity of the inhibitor for MMP-2 over MMP-3 by SAR studies. It was somewhat unclear how selectivity was affected, but as expected the hydroxamate decreased selectivity. The selectivity could be increased by substitutions in the Tyr4 position as well as in the Gly13 position. We believe

that it is likely that further modifications in these two positions could influence affinity and specificity of the inhibitor by interactions at the S1' site and non-prime side of the substrate binding pocket. In summary, M238^{hy} provides a useful research tool for the investigation of the physiological and pathological roles of MMP-2 and 3. In contrast to other selective inhibitors, the proteolytic stability of M238^{hy} allows for application in cell based assays or in vivo. The inhibitor is readily available through ordinary peptide synthesis followed by hydroxamate modification and cyclization, simple reactions which have been optimized in our lab. Following the potential target validation, the bicyclic peptide could possibly even be developed into a therapeutic.

5.2 Materials and methods

Expression and purification of pro-MMP-2: Human pro-MMP-2 was expressed in transiently transfected human embryonic kidney cells as follows. Suspension-adapted HEK-293 cells were grown in 1 L serum-free ExCell 293 medium (SAFC Biosciences) in the presence of 4 mM glutamine and 3.75 mM histone deacetylase inhibitor valproic acid in an orbitally shaken five-liter glass bottle at 180 rpm at 37°C in the presence of 5% CO₂. Cells at a density of 20x10⁶ cells/ml were transfected with the vector pcDNA3-MMP2 (a kind gift from Prof. Dr. Eric Howard, University of Oklahoma, USA) using linear polyethylenimine. After 7 days, cells were harvested by centrifugation at 2,500 rpm for 15 min at 4°C. Cell debris was removed from the medium by filtration through 0.45 µm PES membranes. The recombinant protein was purified from the conditioned medium by size exclusion chromatography on a HiPrep 26/60 Sephacryl S-200 high resolution column (GE Healthcare) using PBS pH 7.4 as buffer. The purity of the proMMP-2 was greater than 95% judging by SDS-PAGE.

Biotinylation of human proMMP-2: The recombinant proMMP-2 (4.5 µM) in PBS (pH 7.4) was incubated with 5-fold excess of EZ-link Sulfo-NHS-LC-Biotin (22.5 µM, Pierce) for 1 h at 25°C. The excess of biotin was subsequently reduced by repetitive concentration and dilution steps with TNC buffer (50 mM Tris-HCl (pH 7.5), 150 mM NaCl, 10 mM CaCl₂, 0.02% (w/v) NaN₃ and 0.05% (w/v) Brij-35) in a Vivaspinn-20 filter (MWCO of 10'000, Sartorius-Stedim Biotech GmbH). The ability of the biotinylated MMP-2 to bind to either streptavidin or neutravidin was verified by incubating the protein with magnetic streptavidin and neutravidin beads respectively and analysing the bound and unbound protein fractions by SDS-PAGE.

Activation of human pro-MMP-2: Purified pro-MMP-2 (1 to 5 µM) in TNC buffer was incubated 1 h at 37°C with freshly prepared 4-aminophenylmercuric acetate (APMA, stock solution: 50 mM dissolved in 200 mM NaOH) at a final concentration of 2 mM. Activated MMP-2 was purified by size exclusion chromatography on a Superdex 75 10/300 GL high resolution column (GE Healthcare) using TNC buffer.

Phage selection of bicyclic peptides: Bacterial cells of the library glycerol stock were inoculated in 500 mL of 2YT/chloramphenicol (30 µg/ml) medium to obtain an OD₆₀₀ of 0.1. The culture was shaken (200 rpm) for 16 h at 30°C. After 30 min of centrifugation at 8500 rpm and 4°C, the phage were purified by precipitation with 0.2 volumes of 20% (w/v) polyethylene glycol 6000 (PEG6000), 2.5 M NaCl on ice and centrifugation at 4000 rpm for 30 min. PEG purified phage, typically 1011-1012 t.u. (transducing units), were reduced in 20 ml of 20 mM NH₄HCO₃, 5 mM EDTA, pH 8.0 with 1 mM TCEP at 42°C for 1 h. The concentration of TCEP was subsequently reduced by repetitive concentration and dilution steps with reaction buffer (20 mM NH₄HCO₃, 5 mM EDTA, pH 8.0, de-gassed) in a Vivaspin-20 filter (MWCO of 10'000, Sartorius-Stedim Biotech GmbH) as described previously. The volume of the phage solution was adjusted to 32 ml with reaction buffer and 8 ml of 50 µM tris-(bromomethyl)benzene (TBMB) in MeCN were added to obtain a final TBMB concentration of 10 µM. The reaction was incubated at 30°C for 1 h before non-reacted TBMB was removed by precipitation of the phage with 0.2 volumes of 20% (w/v) PEG6000, 2.5 M NaCl on ice and centrifugation at 4000 rpm for 30 minutes. The phage pellet was then dissolved in 3 ml washing buffer (10 mM Tris-Cl, pH 7.4, 150 mM NaCl, 10 mM MgCl₂, 1 mM CaCl₂). Biotinylated active MMP-2 (180 µg) was added to 50 µl magnetic streptavidin beads (Dynabeads M-280 from Invitrogen Dynal Biotech AS) in washing buffer and incubated on a rotating wheel for 10 min at room RT. The magnetic beads were then washed with 0.5 ml washing buffer and incubated for 30 min at RT with 0.5 ml washing buffer containing 1% (w/v) BSA and 0.1% (v/v) Tween 20. At the same time the chemically modified phage (typically 1010-1011 t.u. dissolved in 3 ml washing buffer) were blocked by addition of 1.5 ml of washing buffer containing 3% (w/v) BSA and 0.3% (v/v) Tween 20 for 30 minutes. The blocked beads/antigen mixture (0.5 ml) and phage (4.5 ml) were mixed together and incubated for 30 minutes on a rotating wheel at room temperature. The beads (and antigen/phage bound to them) were washed eight times with washing buffer containing 0.1% (v/v) Tween 20 and twice with washing buffer. The phage were eluted either by incubation with 100 µl of 50 mM glycine, pH 2.2 for 5 minutes (pH-dependent elution), and then transferred to 50 µl of 1 M Tris-Cl, pH 8.0 for neutralisation or by incubation with 100 µl of 250 µM of the competitive hydroxamate inhibitor GM6001 (Enzo Life Sciences, Inc.) in washing buffer (pH 7.4) for 30 minutes (competitive elution). The eluted phage were incubated with 30 ml TG1 cells at OD₆₀₀ of 0.4 for 90 minutes at 37°C and the cells were plated on large 2YT/chloramphenicol (30 µg/ml chloramphenicol) plates. Second and third round of panning were performed following the same procedure but using in the second round neutravidin-coated magnetic beads instead of streptavidin in order to prevent the enrichment of streptavidin-specific peptide binders. Neutravidin beads were prepared by reacting 0.8 mg neutravidin (Pierce) with 0.5 ml tosyl-activated magnetic beads (2 x 10⁹ beads/ml; Dynabeads M-280, Invitrogen Dynal Biotech AS) according to the supplier's instructions.

Peptide Synthesis: Solid-phase peptide synthesis was performed on an Advanced ChemTech 348 Ω peptide synthesizer (AAPPTec) using standard Fmoc procedures. Rink Amide AM resin was used as solid support and DMF as solvent. Peptide variants were synthesized at a 0.03 mmol scale to obtain around 10-20 mg of pure peptide. Peptide couplings were performed twice for each natural amino acid by reacting amino acid (4 equiv, 600 μ l of 0.2 M in DMF), HBTU/HOBt (4 equiv each, 267 μ l 0.45 M in DMF) and DIPEA (6 equiv, 360 μ l 0.5 M in DMF) at RT for 30 min at 400 rpm. The coupling of unnatural amino acids (2 equiv, 600 μ l 0.1 M in DMF) was performed once using HATU (2 equiv, 650 μ l 0.1 M in DMF) and DIPEA (4 equiv, 250 μ l 0.5 M in DMF). The resin was washed four times with DMF after the coupling reaction. The N-terminal Fmoc protecting group was removed with piperidine (20% v/v) in DMF (RT, 2 \times 5 min, 400 rpm). The resin was washed five times with DMF after Fmoc removal. Fmoc-L- α -amino acids, HBTU, HOBt and Rink Amide AM resin were purchased from GL Biochem. Non canonical Fmoc-amino acids were purchased from Bachem, Chem-Impex, PolyPeptide and TCI. Peptides were cleaved from the solid support and protecting groups removed by incubation in 5 ml cleavage cocktail (90% TFA, 2.5% ethane-1,2-dithiol, 2.5% phenol, 2.5% thioanisole, 2.5% H₂O) for 2 h with shaking. The resin was removed by vacuum filtration, and the peptides were precipitated with ice-cold diethyl ether (50 ml), incubated for 30 min at -20°C, and pelleted by centrifugation (2700 g, 5 min). The diethyl ether was discarded, the precipitate washed twice with diethyl ether and the remaining solvent evaporated at RT.

Hydroxamate modification: All peptides which were hydroxamate modified were synthesized with using Fmoc-Asp (2-phenylisopropyl ester)-OH (Bachem, cat # B-2475). The procedure reported above for peptide synthesis was followed until the cleavage from the solid support. The 2-phenylisopropyl ester protecting group was selectively removed by the addition of 5 ml TFA (2% (v/v)) in dichloromethane and left shaking for 2 min. The mixture was removed by filtration and the procedure repeated five times. The solid support was then washed five times with DMF. For introducing the hydroxamic acid moiety a peptide coupling was performed by adding NH₂OH•HCl (2 equiv, 1 ml, 0.06 M in DMF added to equimolar amount of KOH), pyBOP (1.2 equiv, 1 ml, 0.036 M in DMF) and DIPEA (6 equiv, 1 ml, 0.18 M in DMF). The reaction was performed twice and was run at RT, shaking at 400 rpm for 5 min. After the coupling reaction the resin was washed four times with DMF and peptides were subsequently cleaved from the solid support as reported above.

Peptide cyclization and purification: Crude peptide at a concentration of 1 mM was reacted with 1.4 mM 1,3,5-Tris(bromomethyl)benzene (TBMB) in 70% NH₄HCO₃ buffer (60 mM, pH 8.0) and 30% MeCN for 1 h at 30°C. The peptide and TBMB were prepared and mixed using the solvents, concentrations and volumes exemplified for the cyclization of ~ 50 mg crude peptide. To 6 ml 4.2 mM peptide in MeCN/H₂O (1:2), 3.5 ml 10 mM

TBMB in MeCN and 2 ml MeCN were added and the reaction started by addition of 14 ml NH_4HCO_3 buffer (60 mM, pH 8.0). The cyclized peptides synthesized on a 50 mg scale were purified by reversed-phase HPLC (Waters Prep LC 4000 system) using a preparative C18 RP column (Vydac C18 TP1022 column, 250 × 22 mm, 10 μm , 300 Å) and a linear gradient of 20–45% solvent B (MeCN, 0.1% (v/v) TFA) in solvent A (H_2O , 0.1% (v/v) TFA) in 25 min at a flow of 20 ml/min. Absorbance was detected at 220 nm. The cyclized peptides were injected after lyophilization of the reaction and dissolving the peptide in 10 ml H_2O containing 10% (v/v) DMSO, 10% (v/v) MeCN and 0.1% (v/v) TFA. Fractions containing the desired peptide were lyophilized.

HPLC and mass spectrometric analysis: The molecular mass of purified peptides was determined on a single quadrupole mass spectrometer in positive ion mode using electrospray ionization (LCMS-2020, Shimadzu). The purity of the peptides was determined by analytical RP-HPLC (Agilent 1260 HPLC system) using an analytical C18 column (Agilent Zorbax 300SB-C18, 4.6 mm × 250 mm, 5 μm) and a linear gradient of 0–50% solvent B (MeCN, 0.1% (v/v) TFA) in solvent A (H_2O , 5% (v/v) MeCN, 0.1% (v/v) TFA) in 15 min at a flow of 1 ml/min. Absorbance was detected at 220 nm.

Peptide concentration determination: Lyophilized peptide was weighed and dissolved in DMSO (3% (v/v)) in water by sequential addition to obtain peptide stocks of 2 mM by weight. The concentrations of the peptides were determined by measuring the absorption at 280 nm. The stock solution was then diluted based on the absorbance to a final concentration of 1 mM.

MMP inhibition assays: The inhibitory activity of bicyclic peptides was determined by measuring residual protease activity with a fluorogenic substrate. The assay was performed in buffer containing 50 mM Tris-Cl, pH 7.5, 150 mM NaCl, 10 mM CaCl_2 and 0.1% w/v BSA, in a volume of 150 μl . For all MMPs, with the exception of MMP-19, activity was measured with the FRET substrate Mca-Lys-Pro-Leu-Gly-Leu-Dap(DnP)-Ala-Arg-NH₂ (FS-6, GL Biochem) at final concentrations of 5–20 μM . For MMP-19 the substrate OMNIMMP® RED: TQ3-GABA-Pro-Cha-Abu-Smc-His-Ala-Dab(6'-TAMRA)-Ala-Lys-NH₂ (Enzo life sciences) was used at a final concentration of 0.75 μM . The following enzymes and concentrations were used: MMP-1 (Enzo life sciences kit, cat # BML-AK308-0001) 10 mU/ μl , substrate 20 μM , MMP-2 (expressed in house) 0.5 nM, substrate 10 μM , MMP-3-a (Enzo life sciences kit) 7.5 mU/ μl , substrate 20 μM , MMP-3-b (Enzo life sciences, cat # ALX-201-042-C005) 3 nM, substrate 20 μM , MMP-7 (Enzo life sciences kit) 0.25 mU/ μl , substrate 20 μM , MMP-8 (Enzo life sciences kit) 3 mU/ μl , substrate 20 μM , MMP-9 (Enzo life sciences kit) 4 mU/ μl , substrate 10 μM , MMP-12 (Enzo life sciences kit) 2.5 mU/ μl , substrate 10 μM , MMP-13 (Enzo life sciences kit) 0.1875 mU/ μl , substrate 5 μM , MMP-14 (Enzo life sciences kit) 2.5 mU/ μl , substrate 10 μM ,

MMP-19 (Enzo life sciences kit) 0.75 mU/μl, substrate 0.75 μM, MMP-20 (Enzo life sciences, cat # BML-SE540-0010) 7.5 mU/μl, substrate 5 μM. The reaction was pipetted as follows: 50 μl bicyclic peptide in assay buffer was added to 50 μl of enzyme in assay buffer and incubated for 15 minutes at 37°C before 50 μl of 15-60 μM fluorogenic substrate in assay buffer was added to measure the residual protease activity with an Infinite M200Pro fluorescence plate reader (FS-6: excitation at 325 nm, emission at 400 nm; OMNIMMP® RED: excitation at 545 nm, emission at 576 nm, Tecan) for a period of 30 min with a read every minute at 37°C. The bicyclic peptides were serially diluted from the 1 mM stock solutions 2-fold using assay buffer. Sigmoidal curves were fitted to the data using the following dose response equation wherein x = peptide concentration, y = % protease activity, p = Hill slope. IC_{50} values were derived from the fitted curve.

$$y = \frac{100}{1 + 10^{(\log IC_{50} - x)p}}$$

The inhibition constants (K_i) were calculated according to the equation of Cheng and Prusoff $K_i = IC_{50}/(1 + ([S]_0/K_m))$ wherein IC_{50} is the functional strength of the inhibitor, $[S]_0$ is the total substrate concentration, and K_m is the Michaelis-Menten constant. K_m values were determined for the enzymes which were inhibited with IC_{50} values below 50 μM and were as follows: MMP-2: 30 ± 2 μM, MMP-3: 90 ± 7 μM, MMP-7: 42 ± 5 μM, MMP-12: 58 ± 1 μM, MMP-14: 10.1 ± 0.1 μM, MMP-20: 37 ± 4 μM. These values are in accordance of what has been previously reported for this substrate (319).

Inhibition of MMP-2 autoproteolysis: 100 nM MMP-2 in TNC buffer was incubated with and without 0.1, 0.5 and 1 μM M114^{hy} for 1 h at 37°C. 20 μl of the reaction was analyzed by SDS-PAGE using a 10% acrylamide gel (CBS Scientific cat # FK01012-10) and Tris-Tricine ClearPAGE SDS running buffer, and silver staining (Pierce Silver Stain Kit, Thermo Fisher Scientific).

Inhibition of MMP-2 in cell culture: HT1080 cells were cultured in 10 ml DMEM media supplemented with 10% fetal bovine serum (FBS) and non-essential amino acids (NEAA, final conc. 0.1 mM or 100 μL of 100X stock (Thermo Fisher Scientific) in 75 cm² flasks. Cells at 80-90% confluency were washed with serum free (SF) media thrice (DMEM with NEAA), incubated in SF media for 2 hours and again washed with SF media thrice. M114^{hy} or batimastat dissolved in 10% DMSO + 90% Milli-Q water were added (10 μM final conc.) and incubated for 48 hours at 37°C, 5% CO₂. 10 ml of cell culture condition media was collected, filtered through 0.2 μm membrane and concentrated to 2 ml using 5 kDa cut off Vivaspin 20 (Sartorius) and centrifugation at 4,000 rpm, for around 240 min at 4°C. Aliquots of 20 μl were separated by SDS-PAGE using on a 10% acrylamide gel (CBS Scientific cat # FK01012-10) using ClearPAGE SDS running buffer (Tris-Tricine). Proteins were transferred to a PVDF membrane and detected with rabbit polyclonal anti-

MMP-2 antibody (Novus Biologicals; 1000-fold dilution), anti-rabbit IgG-HRP (Novus Biologicals; 5000 dilution) and CN/DAB substrate (Thermo Fisher Scientific).

Plasma stability assays (HPLC): To 720 μ l mouse plasma (Innovative research) 80 μ l (1 mM in H₂O) of peptide solution was added to obtain a final peptide concentration in plasma of 100 μ M. Peptide was incubated in mouse plasma at 37°C in a water bath. Samples of 90 μ l were collected at different time points (0, 0.5, 1, 2, 4, 8, 16 and 32 h) and mixed with 60 μ l of 6 M guanidinium hydrochloride. The samples were then stored at -20°C. After collection of all time points, the samples were centrifuged (11000 g, 5 min) prior to analysis. The stability and degradation of the peptides was analysed by analytical RP-HPLC (Agilent 1260 HPLC system) using an analytical C8 column (Waters, Xbridge C8, 4.6 mm \times 250 mm, 5 μ m, 130 Å) and a linear gradient of 15-65% solvent B (MeCN, 0.1% (v/v) TFA) in solvent A (H₂O, 5% (v/v) MeCN, 0.1% (v/v) TFA) in 30 min at a flow of 1 ml/min. Absorbance was detected at 220 and 280 nm. Peaks corresponding to intact peptide or degradation products were identified by mass spectrometry analysis of the collected fractions using the LCMS-2020 system described above. For the quantification of the intact peptide, area under the curve was calculated for peaks corresponding to intact peptide or with only the N-terminal alanine cleaved. Average values of 220 and 280 nm chromatograms were used.

Plasma stability assays (Functional): Peptide (100 μ l of 1 mM in H₂O) was added to 900 μ l mouse plasma (Innovative Research) to obtain a final peptide concentration of 100 μ M. The mixture was incubated in a water bath at 37°C. At different time points (0, 0.5, 1, 2, 4, 8, 16, and 32 h), samples of 30 μ l were removed, diluted to 200 μ l with aqueous buffer (50 mM Tris-HCl, pH 7.4, 150 mM NaCl, 10 mM CaCl₂) and incubated for 20 min at 65°C to inactivate plasma proteases. The peptide/plasma samples were stored at -20°C until the residual inhibitory activity of the peptides was measured in a MMP-2 inhibition assay. For the activity assay, the peptide/plasma samples were centrifuged for 5 min at 16,000 g, serial 2-fold dilutions of the supernatant prepared (peptide concentration ranges from 0.78 nM to 0.8 μ M) and the residual activity of 0.5 nM MMP-2 measured using 10 μ M Mca-Lys-Pro-Leu-Gly-Leu-Dap(DnP)-Ala-Arg-NH₂ substrate. IC_{50} values were derived from the fitted curve using the equation indicated above. Residual inhibition in % was calculated using the equation $IC_{50,0h}/IC_{50,xh} \times 100$ wherein $IC_{50,0h}$ is the functional strength of the inhibitor at time point 0 and $IC_{50,xh}$ the functional strength of inhibitor after one of the different plasma incubation periods mentioned above.

5.3 Supporting information

Table S5.1. Sequence identity and similarity of catalytic domains of all human MMP

Figure S5.1. Affinity maturation of M21

Figure S5.2. Degradation products of M205 and M208

Figure S5.3. Plasma stability and degradation of M114

Figure S5.4. Plasma stability and degradation of M114hy

Figure S5.5. Plasma stability and degradation of M208hy

Figure S5.6. Stability analysis of end removal and Arg3→Ala modified peptides

Figure S5.7. M114 alanine scan and Tyr4 modifications

Table S5.1. Sequence identity, similarity and BLOSUM62 score of catalytic domains of all human MMPs.

Enzyme	% Identity	% Similarity	BLOSUM62 Score
MMP-13	65	76	592
MMP-9	64	77	557
MMP-3	58	70	521
MMP-20	58	67	517
MMP-12	59	71	506
MMP-10	56	68	493
MMP-1	56	72	486
MMP-8	55	68	482
MMP-7	53	64	469
MMP-24	54	64	441
MMP-11	52	65	430
MMP-27	54	64	427
MMP-26	48	67	425
MMP-14	49	63	425
MMP-16	54	64	424
MMP-15	48	62	405
MMP-25	44	56	348
MMP-17	40	43	331
MMP-19	46	58	327
MMP-28	44	57	320
MMP-23	39	50	278
MMP-21	38	49	230

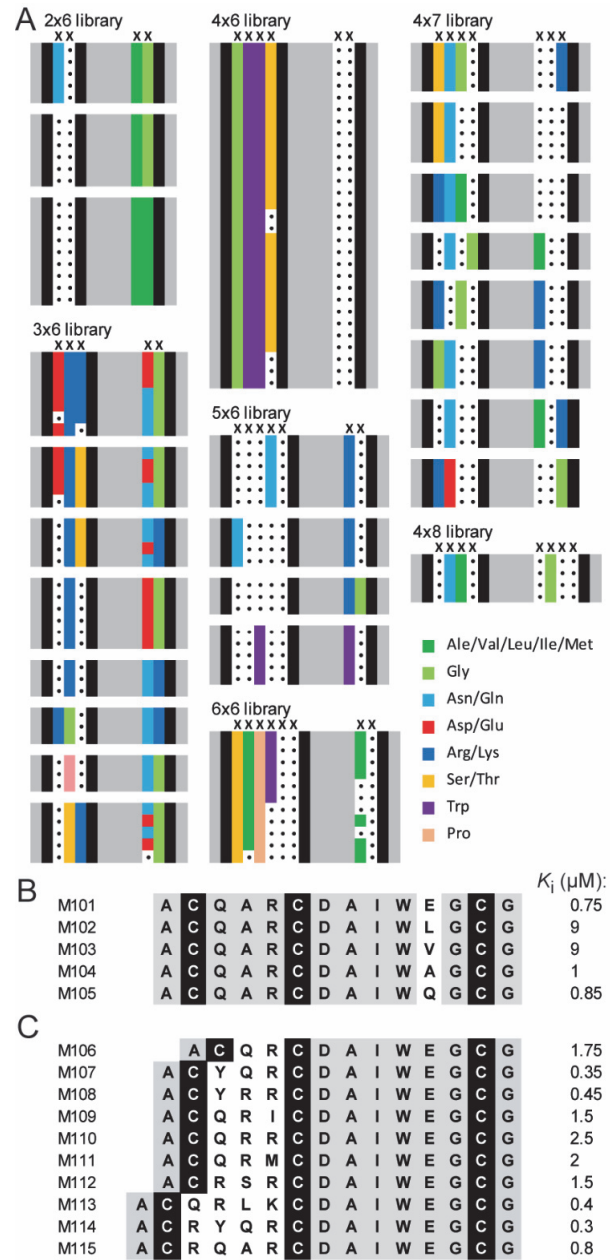


Figure S5.1. (A) Consensus sequences of affinity maturation libraries. (B) Synthesized peptides with QAR motif in first loop. (C) Synthesized peptide for first loop optimization with constant second loop.

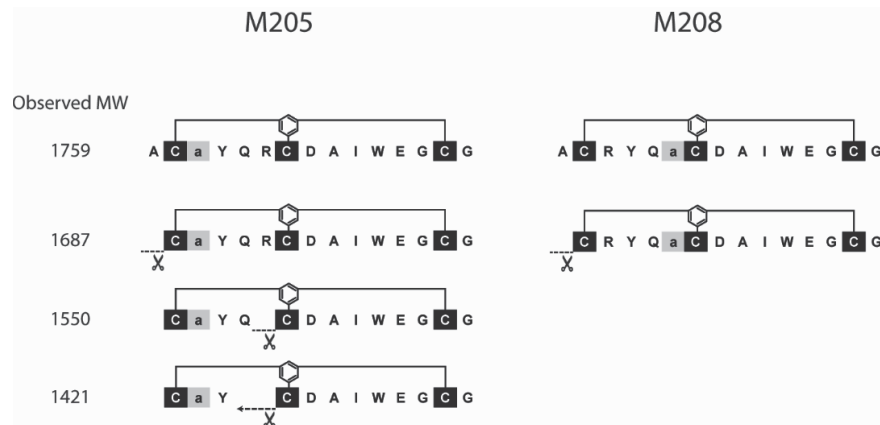


Figure S5.2. Observed degradation products after incubation in mouse plasma.

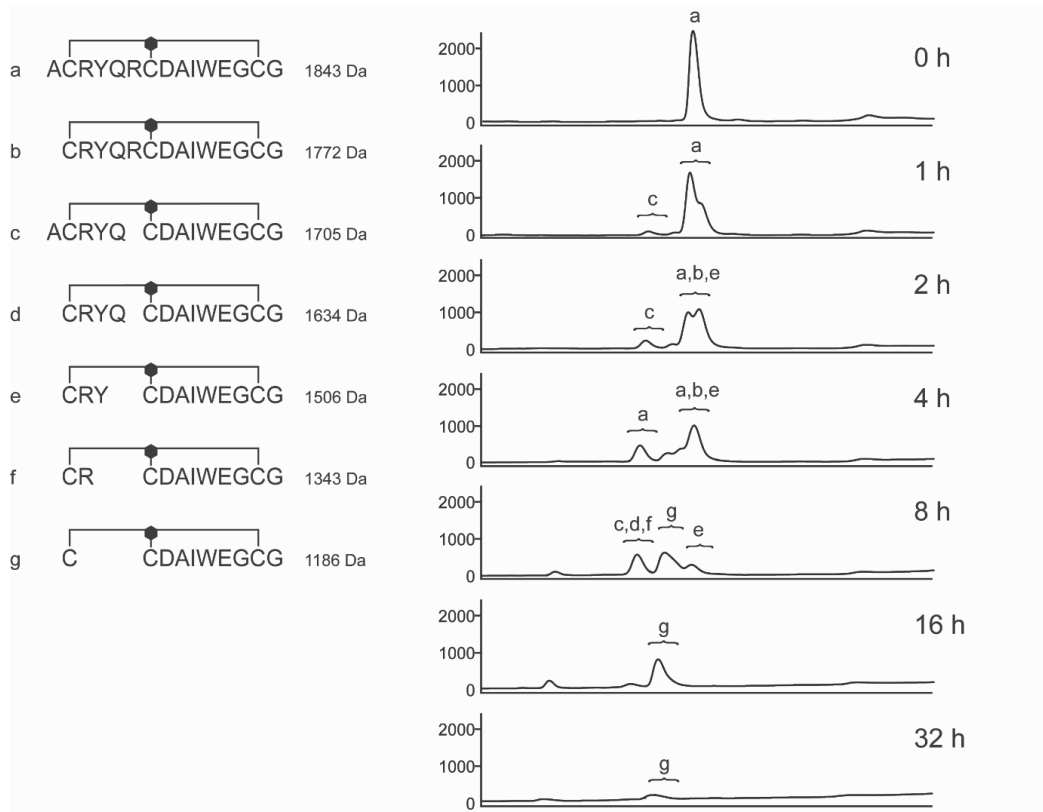


Figure S5.3. Plasma stability analysis of M114

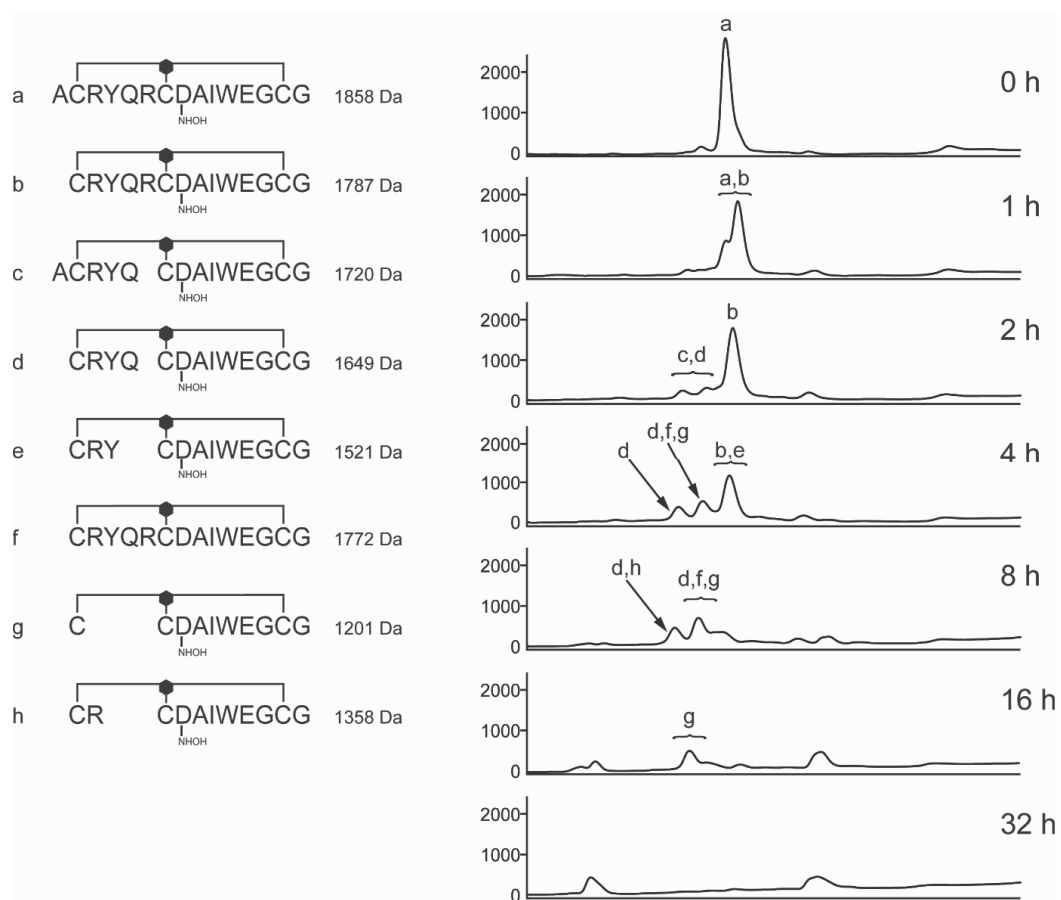


Figure S5.4. Plasma stability analysis of M114^{hy}

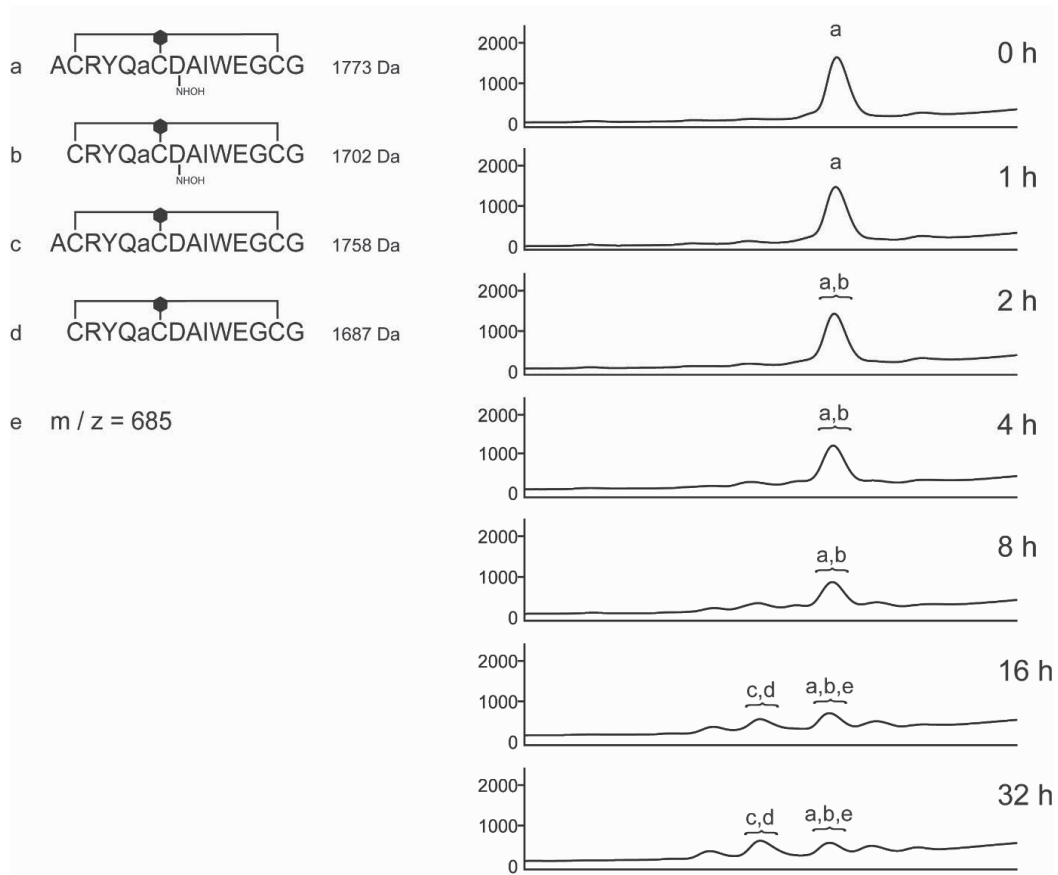


Figure S5.5. Plasma stability analysis of M208^{hy}

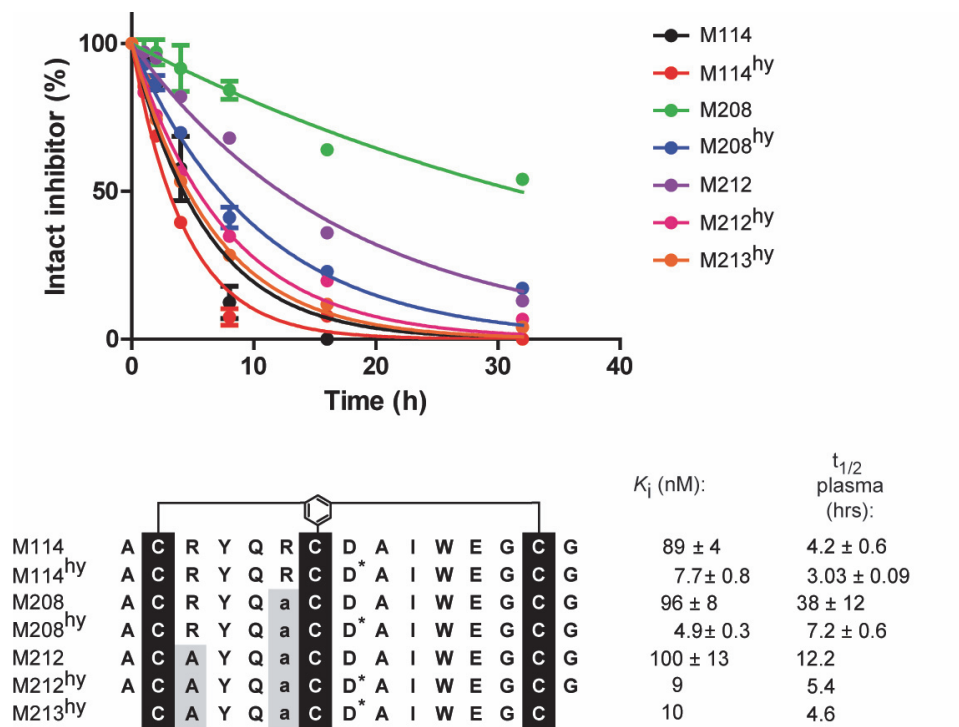


Figure S5.6. Stability analysis of end removal and Arg3→Ala modified peptides

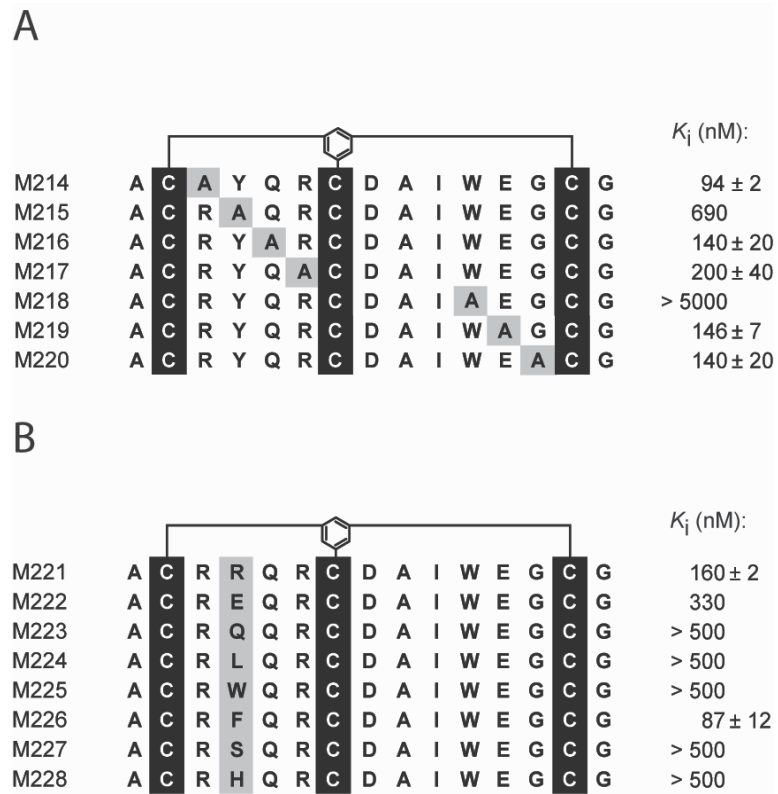


Figure S5.7. Alanine scan and replacement of Tyr4

6. General conclusions and outlook

Peptides are a promising class of therapeutic molecules, which combine properties of small molecules with those of the larger biologicals. However, due to intrinsic limitations of the molecular format, peptide lead compounds often have to undergo extensive medicinal chemistry in order to be optimized into more drug-like compounds. With this PhD thesis, my general objective has been to develop bicyclic peptide hit compounds into molecules that are more likely to be used as therapeutics or research tools. This work has aimed at improving properties such as target affinity, specificity and stability. With a successfully improved FXII inhibitor in hand, my next goal was to characterize the inhibitor in various animal models, in order to evaluate its properties in a therapeutic setting.

In this thesis, I have shown that even though bicyclic peptides isolated directly from phage display are often not optimal compounds for use as therapeutics or research tools, they can be optimized using various approaches. Strategies including D-amino acids incorporation, unnatural amino acid incorporation and macrocycle backbone extension yielded peptides having high affinity and stability. These strategies are now routinely used in our laboratory for the improvement of phage-selected peptides. My PhD work has been divided into three parts, and in this last chapter I will summarize the general conclusions for each of them.

6.1 Backbone extension of a bicyclic peptide

In a first project, I investigated if insertion of one or two carbon atoms in the macrocyclic backbone of a bicyclic peptide FXII inhibitor can improve the binding affinity. The strategy of inserting atoms into naturally derived peptides has been applied previously, but has not been used systematically to improve properties of in-vitro-evolved cyclic peptides. When using libraries composed of canonical amino acids, the atoms in the peptide backbone can only be varied in blocks of three. I therefore used other strategies to insert one or two atoms carbon in the macrocyclic backbone. The first approach was to use β -amino acids, which contribute one extra atom as compared to normal α -amino acids. The second approach was to replace the cysteine residues used for cyclization by single or double homologated analogues, hence adding one or two extra carbon atoms in the backbone. We hypothesized that extending the backbone by single or double atom insertion could lead to small conformational changes, and that this in turn could strengthen existing molecular interactions or allow the formation of new noncovalent contacts with the target.

To identify positions that could benefit from atom insertion we applied a scanning strategy in which we synthesized two series of peptides, one where each amino acid was replaced by glycine and a second where each amino acid was replaced by β -alanine. In this scan, we were able to identify two positions, occupied by Pro6 and Arg11, in which

the affinity loss was similar in both series and hence would potentially allow for atom insertion. We then synthesized peptides with β -analogues in these positions and identified a peptide with 4.7-fold improved affinity upon changing an α arginine residue into one of the β arginine residues. The homologation of cysteine also resulted in affinity improvement in certain positions.

This work shows that by introducing small changes in the backbone of cyclic peptides, the binding affinity can be increased substantially. Since this chemical space is not sampled in libraries using only canonical amino acids, this strategy offers a source for improvement of hit compounds from such libraries. The scanning approach with replacement of amino acids first with glycine and β -alanine provides a method for the identification of positions likely to benefit from atom insertion. Using this approach can save time and money since every residue does not have to be immediately replaced with a set of β -amino acids (there are four β -amino acids for each alpha amino acid). In a second step, we inserted then β -amino acids containing side chains into the promising positions. It has to be noted, that we did not test all the possible four β -amino acids for each of the two positions, due to the lack of commercial availability. It is therefore possible that other β -analogues than the here applied (S)- β 3-homoarginine could affect the properties of the peptide differently, with potentially even further increased affinity and/or stability.

From our results it is not entirely clear how the atom insertion in position Arg11 contributes to the affinity improvement. Since the glycine and β -alanine replaced peptides have similar affinity, we hypothesize that the target interactions of the arginine side chain in this position are more favored for the β -analogue. However, the backbone extension could possibly also introduce more flexibility to the macrocycle and thus affect the interactions of other side-chains. Finally, we later discovered that the substitution of Arg11 to a β -amino acid largely contributed to the increased stability of the bicyclic peptide. The approach of macrocycle backbone extension facilitated by a β -alanine scan can likely be generally applied to in-vitro-evolved peptides with the purpose of improving affinity and proteolytic stability.

6.2 Engineering and preclinical testing of a bicyclic peptide FXII inhibitor

FXII represents a novel target for the development of safe, bleeding free anticoagulants. The development of such anticoagulants has been challenging. FXII has been found to be involved in experimental thrombosis but not in hemostasis and can thus be targeted for this purpose. Several protein-based inhibitors have recently been developed and evaluated, but no high-affinity small molecule has been reported. In the second project of my PhD thesis, I have continued the work of the first project with the objective to optimize a phage display-selected peptide macrocycle FXII inhibitor for in vivo evaluation of selective FXII inhibition by a synthetic molecule. Subsequently I have demonstrated in vivo the peptide's potential of providing safe anticoagulation.

In the phage display selections that were performed to identify the FXII inhibitor FXII618, only the side chains of the 20 canonical amino acids were sampled. In this part of my work, I have used unnatural amino acids containing different side chains to improve the FXII inhibitor lead. I combined i) a substitution to an unnatural amino acid that was identified by a colleague, ii) a substitution to the β -arginine amino acid that I identified in the first project, and iii) two substitutions that I found additionally. An approach in which peptides were synthesized with a coumarin tag allowed me to screen chemically cyclized peptides in unpurified reaction mixtures. This method offers a way to facilitate the screening of larger libraries of chemically modified peptides containing unnatural building blocks, or other synthetic combinatorial libraries, without precedent purification. The peptide combining a total of four amino acid substitutions inhibited the intrinsic coagulation much more efficiently than the lead compound FXII618 in plasma from several species, highlighting the need for strong affinities for inhibitors of FXII.

The pharmacokinetic study in mice, rabbits and pigs showed that FXII900 can be applied intravenously or sub-cutaneously and that it inhibits coagulation in vivo in a concentration dependent manner, without any observed side effects such as general toxicity or prolonged bleeding. The half-life of the peptide is around three times longer in pigs as compared to rabbits, which lies within the expected range when taking into consideration allometric scaling of pharmacokinetic parameters. This indicates that an even longer half-life can be expected in humans. From the study in pigs, a tendency was observed that FXII900 affected aPTT stronger than heparin. The FXII inhibitor could thus potentially be more efficient than the currently used heparin in inhibiting undesired blood coagulation initiated by artificial surfaces present in various medical devices. At the same time, the side effects of bleeding could be reduced.

Thrombus formation was efficiently inhibited in a FeCl_3 model in mice, which clearly demonstrates the potent anticoagulation properties of FXII900. The peptide could likely be administered subcutaneously in order to provide immediate anticoagulation. The reduced device resistance in artificial lungs when applying FXII900 shows that intrinsic coagulation contributes to the clogging of the apparatus. The peptide did not affect bleeding in rabbits which further emphasizes its selectivity towards the intrinsic coagulation pathway. Somewhat surprising, the bleeding times are instead increased in the group receiving no anticoagulants. We speculate that this may be due to the consumption of coagulation factors related to the clot formation in the device. These results show that FXII inhibition by a peptide macrocycle provides safe anticoagulation when used in an artificial lung system and is likely to prolong the functionality of the device in a clinical situation.

The field of anticoagulation drugs has traditionally been relatively conservative, with drugs such as heparin or warfarin being used for decades. However, there has been an unmet medical need for anticoagulants with reduced bleeding risk. During the last decade this has been targeted, for example, by the development of the novel oral anticoagulants (NOAC). These drugs were introduced with the purpose of providing safer alternatives to the widely used vitamin K antagonists, mainly by having reduced intra- and interpatient variability, requiring less frequent monitoring and having insignificant food-drug interactions (320, 321). The NOACs differ from vitamin K antagonists mechanistically by directly inhibiting coagulation factors (FX or thrombin) instead of their biosynthesis. While providing some benefits, the new anticoagulants still induce an increased bleeding risk, which can have severe consequences for patients (322–324).

Several recent studies have been evaluating new strategies for safer anticoagulation in various clinical situations, suggesting a new, open-minded way of thinking in the field. One such study analyzed whether bivalirudin, a direct thrombin inhibitor approved in 2000, could reduce major bleeding events undergoing percutaneous coronary intervention (PCI) (325). Despite previous studies indicating reduced bleeding with the use of bivalirudin, no significant difference could be detected among these parameters between the two groups. In another study the direct thrombin inhibitor Dabigatran was found to significantly lower the bleeding risk when replacing warfarin and aspirin in a combination therapy with a P2Y_{12} inhibitor (326). The NOAC rivaroxaban was evaluated either alone or as dual therapy with aspirin vs aspirin alone. It was found that rivaroxaban was more effective than aspirin for the prevention of recurrent venous thromboembolism with a similar bleeding risk (327). Rivaroxaban was also more effective in combination with aspirin, than aspirin alone in preventing major adverse cardiovascular events, however with a significantly increased bleeding risk (328). Several efforts have also been done to combat the bleeding side-effects of the NOACs, such as development of FX decoy proteins or drug targeting antibodies (322, 329). Given the willingness of testing new

anticoagulant strategies and the concerns about bleeding, we believe that a selective FXII inhibitor such as FXII900 is a strong candidate for clinical evaluation with the potential of providing great benefits, especially in situations where rapid and relatively short anticoagulation is required such as in PCI or CPB.

Another indication where the benefits of anticoagulation is somewhat more unclear is acute ischemic stroke (AIS). The gold standard treatment involves thrombolysis via the administration of recombinant tissue plasminogen activator (330). In a systematic review a correlation was found between early anticoagulant administration and a reduced recurrence of ischemic stroke (331). However, anticoagulation is in general contraindicated due to the very high risk of fatal hemorrhage. Taken together this indicates that bleeding free anticoagulants, such as FXII inhibitors could provide advantages in the treatment of AIS.

Our study has however several limitations. Even though we have found that FXII900 inhibits thrombosis in two different animal models, these situations are to various extent artificial. Although the FeCl₃ model is widely applied to investigate the effect of anticoagulation and/or coagulation factors, its mechanism of action is not well understood. Therefore, it is difficult to determine how well this model represents pathological thrombus formation. As a consequence, it is hard to estimate the thrombus preventing properties of a compound solely evaluated with this model. The artificial lung study represents well the clinical setting of this device. However, in order to better predict the potential of FXII900 a longer study would have been desired, since the devices will be used for longer time periods. In addition, it is not clear how well the rabbits and small size artificial lungs resemble the larger device when actually used in humans.

The work in this project has further demonstrated the extent of improvements that are possible to achieve when unnatural amino acids are applied to bicyclic peptide isolated by phage display. Several of the strategies applied here are now used in our laboratory for the improvement of peptides. Many of the characterization assays and models have been established by me in our laboratory and are now used also for other projects. Finally, FXII900 was patented and an option to a license was recently negotiated with a pharmaceutical company who aims to develop the inhibitor into a drug.

6.3 Development of a bicyclic peptide MMP-2 inhibitor

In the third project of my PhD thesis, my objective was to improve the affinity and stability of a phage-selected bicyclic peptide MMP-2 inhibitor. With the main objective being stability improvement, I had performed a D-alanine scan in order to identify sites for possible stability enhancing modifications. A proteolytic cleavage site could be identified and replaced by a D-amino acid, resulting in an improved stability. At the same time, a glycine residue could also be replaced by a D-amino acid for affinity improvement. Replacing glycine with a D-amino acid was found to before in our lab to be a promising strategy to improve binding affinity (191). In the case of the MMP-2 inhibitor, no crystal structure was obtained, but it is tempting to assume that also the glycine in this peptide has a positive ϕ dihedral angle and therefore benefits from the introduction of a D-amino acid.

Given the challenge of achieving high selectivity for MMP inhibitors, I performed an extensive analysis and specificity screening of the bicyclic peptide MMP-2 inhibitor. The experiments showed that in addition to MMP-2, also MMP-3 was inhibited by the peptide. This is somewhat surprising, since previous MMP-2 inhibitors have been specific for MMP-2 over MMP-3 but have also been inhibiting MMP-9. The specificity could however be increased by a limited number of amino acid substitutions. It is therefore likely that a fully specific inhibitor can be developed by further utilizing this strategy. Another approach in order to yield a more specific inhibitor could be to change the ring sizes of the bicyclic peptide or by adding exocyclic residues at either terminus of the peptide.

The use of MMP inhibitors as anti-cancer therapeutics remains controversial. Inhibitors of MMPs were extensively developed and evaluated in clinical studies in the 1990s and 2000s, but all compounds failed in clinical trials. The failures are often explained by a lack of specificity of the inhibitors, but in addition the role of MMPs in various diseases is not fully understood. It has been postulated that some MMPs are in fact targets in some diseases but anti-targets in others. The multifaceted roles of MMPs together with their high similarity and substrate overlaps make them very challenging therapeutic targets. A high affinity, stable and specific MMP inhibitor, such as the peptide developed in this study, could help to shine light on the functions of the different MMPs in various diseases. A better understanding of the role of individual MMPs may trigger new MMP inhibitor programs in the future.

7. References

1. N. Tsomaia, Peptide therapeutics: Targeting the undruggable space, *Eur. J. Med. Chem.* **94**, 459–470 (2015).
2. M. Góngora-Benítez, J. Tulla-Puche, F. Albericio, Multifaceted roles of disulfide bonds. peptides as therapeutics, *Chem. Rev.* **114**, 901–926 (2014).
3. C. A. Lipinski, F. Lombardo, B. W. Dominy, P. J. Feeney, Experimental and computational approaches to estimate solubility and permeability in drug discovery and development settings, *Adv. Drug Deliv. Rev.* **23**, 3–25 (1997).
4. K. Fosgerau, T. Hoffmann, Peptide therapeutics: Current status and future directions, *Drug Discov. Today* **20**, 122–128 (2015).
5. P. Vlieghe, V. Lisowski, J. Martinez, M. Khrestchatisky, Synthetic therapeutic peptides: science and market, *Drug Discov. Today* **15**, 40–56 (2010).
6. A. Henninot, J. C. Collins, J. M. Nuss, The Current State of Peptide Drug Discovery: Back to the Future?, *J. Med. Chem.* (2017), doi:10.1021/acs.jmedchem.7b00318.
7. J. A. Hutchinson, S. Burholt, I. W. Hamley, Peptide hormones and lipopeptides: from self-assembly to therapeutic applications, *J. Pept. Sci.* **23**, 82–94 (2017).
8. G. Gimpl, F. Fahrenholz, The oxytocin receptor system: structure, function, and regulation., *Physiol. Rev.* **81**, 629–83 (2001).
9. T. A. Treschan, J. Peters, The vasopressin system: physiology and clinical strategies., *Anesthesiology* **105**, 599–612 (2006).
10. M. Theodoropoulou, G. K. Stalla, Somatostatin receptors: From signaling to clinical practice, *Front. Neuroendocrinol.* **34**, 228–252 (2013).
11. World Health Organization, Global Report on Diabetes, (2016), doi:ISBN 978 92 4 156525 7.
12. A. N. Zaykov, J. P. Mayer, R. D. Dimarchi, Pursuit of a perfect insulin, *Nat. Rev. Drug Discov.* **15**, 425–439 (2016).
13. Sanofi, Annual Report 2016, (2016).
14. N. A. Bakh, A. B. Cortinas, M. A. Weiss, R. S. Langer, D. G. Anderson, Z. Gu, S. Dutta, M. S. Strano, Glucose-responsive insulin by molecular and physical design, *Nat. Chem.* **9**, 937–943 (2017).
15. D. Donnelly, The structure and function of the glucagon-like peptide-1 receptor and its ligands, *Br. J. Pharmacol.* **166**, 27–41 (2012).
16. B. Manandhar, J.-M. Ahn, Glucagon-like Peptide-1 (GLP-1) Analogs: Recent Advances, New Possibilities, and Therapeutic Implications, *J. Med. Chem.* **58**, 1020–1037 (2015).
17. L. Prasad-Reddy, D. Isaacs, A clinical review of GLP-1 receptor agonists: Efficacy and

safety in diabetes and beyond, *Drugs Context* **4**, 1–19 (2015).

18. Novo Nordisk, *Company announcement: Ozempic® (semaglutide) approved in the US* (2017).

19. J. Lau, P. Bloch, L. Schäffer, I. Pettersson, J. Spetzler, J. Kofoed, K. Madsen, L. B. Knudsen, J. McGuire, D. B. Steensgaard, H. M. Strauss, D. X. Gram, S. M. Knudsen, F. S. Nielsen, P. Thygesen, S. Reedtz-Runge, T. Kruse, Discovery of the Once-Weekly Glucagon-Like Peptide-1 (GLP-1) Analogue Semaglutide, *J. Med. Chem.* **58**, 7370–7380 (2015).

20. Novartis AG, Novartis Annual Report 2016, (2016).

21. B. Weinstock-Guttman, K. V. Nair, J. L. Glajch, T. C. Ganguly, D. Kantor, Two decades of glatiramer acetate: From initial discovery to the current development of generics, *J. Neurol. Sci.* **376**, 255–259 (2017).

22. Teva Pharmaceutical Industries Ltd, Teva Reports Full Year and Fourth Quarter 2016 Financial Results (2017) (available at http://www.tevapharm.com/news/teva_reports_full_year_and_fourth_quarter_2016_financial_results_02_17.aspx).

23. A. A. Kaspar, J. M. Reichert, Future directions for peptide therapeutics development, *Drug Discov. Today* **18**, 807–817 (2013).

24. J. L. Lau, M. K. Dunn, Therapeutic peptides: Historical perspectives, current development trends, and future directions, *Bioorg. Med. Chem.* (2017), doi:10.1016/j.bmc.2017.06.052.

25. T. Uhlig, T. Kyprianou, F. G. Martinelli, C. A. Oppici, D. Heiligers, D. Hills, X. R. Calvo, P. Verhaert, The emergence of peptides in the pharmaceutical business: From exploration to exploitation, *EuPA Open Proteomics* **4**, 58–69 (2014).

26. M. R. Naylor, A. T. Bockus, M. J. Blanco, R. S. Lokey, Cyclic peptide natural products chart the frontier of oral bioavailability in the pursuit of undruggable targets, *Curr. Opin. Chem. Biol.* **38**, 141–147 (2017).

27. V. J. Hruby, Design of cyclic peptides with biological activities from biologically active peptides: the case of peptide modulators of melanocortin receptors, *Biopolymers* **106**, 884–888 (2016).

28. A. Bhat, L. R. Roberts, J. J. Dwyer, Lead discovery and optimization strategies for peptide macrocycles, *Eur. J. Med. Chem.* **94**, 471–479 (2015).

29. C. J. White, A. K. Yudin, Contemporary strategies for peptide macrocyclization, *Nat. Chem.* **3**, 509–524 (2011).

30. P. Thapa, M. J. Espiritu, C. Cabalteja, J. P. Bingham, The emergence of cyclic peptides: The potential of bioengineered peptide drugs, *Int. J. Pept. Res. Ther.* **20**, 545–551 (2014).

31. C. M. B. K. Kourra, N. Cramer, Converting disulfide bridges in native peptides to stable methylene thioacetals, *Chem. Sci.* **7**, 7007–7012 (2016).
32. V. DU VIGNEAUD, C. RESSLER, S. TRIPPETT, The sequence of amino acids in oxytocin, with a proposal for the structure of oxytocin., *J. Biol. Chem.* **205**, 949–57 (1953).
33. V. du Vigneaud, C. Ressler, J. M. Swan, C. W. Roberts, P. G. Katsoyannis, The Synthesis of Oxytocin 1, *J. Am. Chem. Soc.* **76**, 3115–3121 (1954).
34. The Nobel Foundation, The Nobel Prize in Chemistry 1955 (available at https://www.nobelprize.org/nobel_prizes/chemistry/laureates/1955/index.html).
35. J. D. Dahlke, H. Mendez-Figueroa, L. Maggio, A. K. Hauspurg, J. D. Sperling, S. P. Chauhan, D. J. Rouse, Prevention and management of postpartum hemorrhage: a comparison of 4 national guidelines, *Am. J. Obstet. Gynecol.* **213**, 76.e1-76.e10 (2015).
36. A. Meyer-Lindenberg, G. Domes, P. Kirsch, M. Heinrichs, Oxytocin and vasopressin in the human brain: social neuropeptides for translational medicine, *Nat. Rev. Neurosci.* **12**, 524–538 (2011).
37. G. Miller, The Promise and Perils of Oxytocin, *Science (80-.)*. **339**, 267–269 (2013).
38. E. Rubinstein, Y. Keynan, Vancomycin Revisited - 60 Years Later, *Front. Public Heal.* **2**, 1–7 (2014).
39. R. E. W. Hancock, H. G. Sahl, Antimicrobial and host-defense peptides as new anti-infective therapeutic strategies, *Nat. Biotechnol.* **24**, 1551–1557 (2006).
40. M. Mahlapuu, J. Håkansson, L. Ringstad, C. Björn, Antimicrobial Peptides: An Emerging Category of Therapeutic Agents, *Front. Cell. Infect. Microbiol.* **6**, 1–12 (2016).
41. B. Mojsoska, H. Jenssen, Peptides and peptidomimetics for antimicrobial drug design, *Pharmaceuticals* **8**, 366–415 (2015).
42. N. B. da Cunha, N. B. Cobacho, J. F. C. Viana, L. A. Lima, K. B. O. Sampaio, S. S. M. Dohms, A. C. R. Ferreira, C. de la Fuente-Núñez, F. F. Costa, O. L. Franco, S. C. Dias, The next generation of antimicrobial peptides (AMPs) as molecular therapeutic tools for the treatment of diseases with social and economic impacts, *Drug Discov. Today* **22**, 234–248 (2017).
43. S. A. Survase, L. D. Kagliwal, U. S. Annapure, R. S. Singhal, Cyclosporin A - A review on fermentative production, downstream processing and pharmacological applications, *Biotechnol. Adv.* **29**, 418–435 (2011).
44. A. Zorzi, K. Deyle, C. Heinis, Cyclic peptide therapeutics: past, present and future, *Curr. Opin. Chem. Biol.* **38**, 24–29 (2017).
45. H. A. Schmid, Pasireotide (SOM230): Development, mechanism of action and potential applications, *Mol. Cell. Endocrinol.* **286**, 69–74 (2008).
46. A. P. Bryant, R. W. Busby, W. P. Bartolini, E. A. Cordero, G. Hannig, M. M. Kessler,

- C. M. Pierce, R. M. Solinga, J. V. Tobin, S. Mahajan-Miklos, M. B. Cohen, C. B. Kurtz, M. G. Currie, Linaclotide is a potent and selective guanylate cyclase C agonist that elicits pharmacological effects locally in the gastrointestinal tract, *Life Sci.* **86**, 760–765 (2010).
47. M. Corsetti, J. Tack, Linaclotide: A new drug for the treatment of chronic constipation and irritable bowel syndrome with constipation, *United Eur. Gastroenterol. J.* **1**, 7–20 (2013).
48. J. Castro, A. M. Harrington, P. a Hughes, C. M. Martin, P. Ge, C. M. Shea, H. Jin, S. Jacobson, G. Hannig, E. Mann, M. B. Cohen, J. E. MacDougall, B. J. Lavins, C. B. Kurtz, I. Silos-Santiago, J. M. Johnston, M. G. Currie, L. A. Blackshaw, S. M. Brierley, Linaclotide inhibits colonic nociceptors and relieves abdominal pain via guanylate cyclase-C and extracellular cyclic guanosine 3',5'-monophosphate., *Gastroenterology* **145**, 1334–46–11 (2013).
49. M. Camilleri, Guanylate Cyclase C Agonists: Emerging Gastrointestinal Therapies and Actions, *Gastroenterology* **148**, 483–487 (2015).
50. P. B. Miner Jr, W. D. Koltun, G. J. Wiener, M. De La Portilla, B. Prieto, K. Shailubhai, M. B. Layton, L. Barrow, L. Magnus, P. H. Griffin, A Randomized Phase III Clinical Trial of Plecanatide, a Uroguanylin Analog, in Patients With Chronic Idiopathic Constipation, *Am. J. Gastroenterol.* **112**, 613–621 (2017).
51. R. T. Layer, J. M. McIntosh, Conotoxins: Therapeutic Potential and Application, *Mar. Drugs* **4**, 119–142 (2006).
52. R. Halai, D. J. Craik, Conotoxins: natural product drug leads, *Nat. Prod. Rep.* **26**, 526 (2009).
53. R. J. Clark, J. Jensen, S. T. Nevin, B. P. Callaghan, D. J. Adams, D. J. Craik, The engineering of an orally active conotoxin for the treatment of neuropathic pain, *Angew. Chemie - Int. Ed.* **49**, 6545–6548 (2010).
54. X. Wu, Y. H. Huang, Q. Kaas, D. J. Craik, Cyclisation of Disulfide-Rich Conotoxins in Drug Design Applications, *European J. Org. Chem.* **2016**, 3462–3472 (2016).
55. L. Dardevet, D. Rani, T. A. El Aziz, I. Bazin, J. M. Sabatier, M. Fadl, E. Brambilla, M. De Waard, Chlorotoxin: A helpful natural scorpion peptide to diagnose glioma and fight tumor invasion, *Toxins (Basel)*. **7**, 1079–1101 (2015).
56. P. G. Ojeda, C. K. Wang, D. J. Craik, Chlorotoxin: Structure, activity, and potential uses in cancer therapy, *Biopolymers* **106**, 25–36 (2016).
57. J. M. Maraganore, P. Bourdon, J. Jablonski, K. L. Ramachandran, J. W. Fenton, Design and Characterization of Hirulogs: A Novel Class of Bivalent Peptide Inhibitors of Thrombin, *Biochemistry* **29**, 7095–7101 (1990).
58. T. E. Warkentin, Bivalent direct thrombin inhibitors: hirudin and bivalirudin, *Best Pract. Res. Clin. Haematol.* **17**, 105–125 (2004).

59. S. J. De Veer, J. Weidmann, D. J. Craik, Cyclotides as Tools in Chemical Biology, *Acc. Chem. Res.* **50**, 1557–1565 (2017).
60. J. A. Camarero, Cyclotides, a versatile ultrastable micro-protein scaffold for biotechnological applications, *Bioorganic Med. Chem. Lett.* **27**, 5089–5099 (2017).
61. A. Gould, J. A. Camarero, Cyclotides: Overview and Biotechnological Applications, *ChemBioChem* **18**, 1350–1363 (2017).
62. D. J. Craik, J. Du, Cyclotides as drug design scaffolds, *Curr. Opin. Chem. Biol.* **38**, 8–16 (2017).
63. J. Weidmann, D. J. Craik, Discovery, structure, function, and applications of cyclotides: Circular proteins from plants, *J. Exp. Bot.* **67**, 4801–4812 (2016).
64. J. E. Swedberg, T. Mahatmanto, H. Abdul Ghani, S. J. De Veer, C. I. Schroeder, J. M. Harris, D. J. Craik, Substrate-Guided Design of Selective FXIIa Inhibitors Based on the Plant-Derived *Momordica cochinchinensis* Trypsin Inhibitor-II (MCoTI-II) Scaffold, *J. Med. Chem.* **59**, 7287–7292 (2016).
65. C. T. T. Wong, D. K. Rowlands, C. H. Wong, T. W. C. Lo, G. K. T. Nguyen, H. Y. Li, J. P. Tam, Orally active peptidic bradykinin B 1 receptor antagonists engineered from a cyclotide scaffold for inflammatory pain treatment, *Angew. Chemie - Int. Ed.* **51**, 5620–5624 (2012).
66. Y. Ji, S. Majumder, M. Millard, R. Borra, T. Bi, A. Y. Elnagar, N. Neamati, A. Shekhtman, J. A. Camarero, In vivo activation of the p53 tumor suppressor pathway by an engineered cyclotide, *J. Am. Chem. Soc.* **135**, 11623–11633 (2013).
67. A. D. Cunningham, N. Qvit, D. Mochly-Rosen, Peptides and peptidomimetics as regulators of protein–protein interactions, *Curr. Opin. Struct. Biol.* **44**, 59–66 (2017).
68. M. Pelay-Gimeno, A. Glas, O. Koch, T. N. Grossmann, Structure-Based Design of Inhibitors of Protein-Protein Interactions: Mimicking Peptide Binding Epitopes, *Angew. Chemie Int. Ed.* **54**, 8896–8927 (2015).
69. M. Guharoy, P. Chakrabarti, Secondary structure based analysis and classification of biological interfaces: identification of binding motifs in protein–protein interactions, *Bioinformatics* **23**, 1909–1918 (2007).
70. R. Rezaei Araghi, A. E. Keating, Designing helical peptide inhibitors of protein–protein interactions, *Curr. Opin. Struct. Biol.* **39**, 27–38 (2016).
71. M. J. I. Andrews, A. B. Tabor, Forming stable helical peptides using natural and artificial amino acids, *Tetrahedron* **55**, 11711–11743 (1999).
72. C. E. Schafmeister, J. Po, G. L. Verdine, An All-Hydrocarbon Cross-Linking System for Enhancing the Helicity and Metabolic Stability of Peptides, *J. Am. Chem. Soc.* **122**, 5891–5892 (2000).

73. Y. S. Tan, D. P. Lane, C. S. Verma, Stapled peptide design: principles and roles of computation, *Drug Discov. Today* **21**, 1642–1653 (2016).
74. L. D. Walensky, G. H. Bird, Hydrocarbon-Stapled Peptides: Principles, Practice, and Progress, *J. Med. Chem.* **57**, 6275–6288 (2014).
75. P. M. Cromm, J. Spiegel, T. N. Grossmann, Hydrocarbon Stapled Peptides as Modulators of Biological Function, *ACS Chem. Biol.* **10**, 1362–1375 (2015).
76. Y. H. Lau, P. de Andrade, Y. Wu, D. R. Spring, Peptide stapling techniques based on different macrocyclisation chemistries, *Chem. Soc. Rev.* **44**, 91–102 (2015).
77. A. Patgiri, A. L. Jochim, P. S. Arora, A Hydrogen Bond Surrogate Approach for Stabilization of Short Peptide Sequences in α -Helical Conformation, *Acc. Chem. Res.* **41**, 1289–1300 (2008).
78. D. P. Fairlie, A. Dantas de Araujo, Review stapling peptides using cysteine crosslinking, *Biopolymers* **106**, 843–852 (2016).
79. P. Diderich, D. Bertoldo, P. Dessen, M. M. Khan, I. Pizzitola, W. Held, J. Huelsken, C. Heinis, Phage Selection of Chemically Stabilized α -Helical Peptide Ligands, *ACS Chem. Biol.* **11**, 1422–1427 (2016).
80. R. Rezaei Araghi, J. A. Ryan, A. Letai, A. E. Keating, Rapid Optimization of Mcl-1 Inhibitors using Stapled Peptide Libraries Including Non-Natural Side Chains, *ACS Chem. Biol.* **11**, 1238–1244 (2016).
81. A. J. Huhn, R. M. Guerra, E. P. Harvey, G. H. Bird, L. D. Walensky, Selective Covalent Targeting of Anti-Apoptotic BCL-1 by Cysteine-Reactive Stapled Peptide Inhibitors, *Cell Chem. Biol.* **23**, 1123–1134 (2016).
82. F. Plisson, T. A. Hill, J. M. Mitchell, H. N. Hoang, A. D. de Araujo, W. Xu, A. Cotterell, D. J. Edmonds, R. V. Stanton, D. R. Derksen, P. M. Loria, D. A. Griffith, D. A. Price, S. Liras, D. P. Fairlie, Helixconstraints and amino acid substitution in GLP-1 increase cAMP and insulin secretion but not beta-arrestin 2 signaling, *Eur. J. Med. Chem.* **127**, 703–714 (2017).
83. A. D. de Araujo, J. Lim, A. C. Good, R. T. Skerlj, D. P. Fairlie, Electrophilic Helical Peptides That Bond Covalently, Irreversibly, and Selectively in a Protein–Protein Interaction Site, *ACS Med. Chem. Lett.* **8**, 22–26 (2017).
84. S. H. Gellman, Foldamers: A Manifesto, *Acc. Chem. Res.* **31**, 173–180 (1998).
85. J. W. Checco, S. H. Gellman, Targeting recognition surfaces on natural proteins with peptidic foldamers, *Curr. Opin. Struct. Biol.* **39**, 96–105 (2016).
86. T. A. Martinek, F. Fülöp, Peptidic foldamers: ramping up diversity, *Chem. Soc. Rev.* **41**, 687–702 (2012).
87. R. Gopalakrishnan, A. I. Frolov, L. Knerr, W. J. Drury, E. Valeur, Therapeutic

- potential of foldamers: From chemical biology tools to drug candidates?, *J. Med. Chem.* **59**, 9599–9621 (2016).
88. Z. E. Reinert, W. S. Horne, Protein backbone engineering as a strategy to advance foldamers toward the frontier of protein-like tertiary structure, *Org. Biomol. Chem.* **12**, 8796–8802 (2014).
89. C. M. Grison, J. A. Miles, S. Robin, A. J. Wilson, D. J. Aitken, An α -Helix-Mimicking 12,13-Helix: Designed $\alpha/\beta/\gamma$ -Foldamers as Selective Inhibitors of Protein–Protein Interactions, *Angew. Chemie - Int. Ed.* **55**, 11096–11100 (2016).
90. L. Mathieu, B. Legrand, C. Deng, L. Vezenkov, E. Wenger, C. Didierjean, M. Amblard, M. C. Averlant-Petit, N. Masurier, V. Lisowski, J. Martinez, L. T. Maillard, Helical oligomers of thiazole-based γ -amino acids: Synthesis and structural studies, *Angew. Chemie - Int. Ed.* **52**, 6006–6010 (2013).
91. H. M. Werner, C. C. Cabalteja, W. S. Horne, Peptide Backbone Composition and Protease Susceptibility: Impact of Modification Type, Position, and Tandem Substitution, *ChemBioChem* **17**, 712–718 (2016).
92. X. Chen, E. G. Mietlicki-Baase, T. M. Barrett, L. E. McGrath, K. Koch-Laskowski, J. J. Ferrie, M. R. Hayes, E. J. Petersson, Thioamide Substitution Selectively Modulates Proteolysis and Receptor Activity of Therapeutic Peptide Hormones, *J. Am. Chem. Soc.*, jacs.7b08417 (2017).
93. Y. Shi, P. Teng, P. Sang, F. She, L. Wei, J. Cai, γ -AApeptides: Design, Structure, and Applications, *Acc. Chem. Res.* **49**, 428–441 (2016).
94. P. Teng, Y. Shi, P. Sang, J. Cai, γ -AApeptides as a New Class of Peptidomimetics, *Chem. - A Eur. J.* **22**, 5458–5466 (2016).
95. Y. Shi, S. Challa, P. Sang, F. She, C. Li, G. M. Gray, A. Nimmagadda, P. Teng, T. Odom, Y. Wang, A. van der Vaart, Q. Li, J. Cai, One-Bead–Two-Compound Thioether Bridged Macrocyclic γ -AApeptide Screening Library against EphA2, *J. Med. Chem.* **60**, 9290–9298 (2017).
96. I. Avan, C. D. Hall, A. R. Katritzky, Peptidomimetics via modifications of amino acids and peptide bonds, *Chem. Soc. Rev.* **43**, 3575 (2014).
97. J. Vagner, H. Qu, V. J. Hruby, Peptidomimetics, a synthetic tool of drug discovery, *Curr. Opin. Chem. Biol.* **12**, 292–296 (2008).
98. A. Galán, L. Comor, A. Horvatić, J. Kuleš, N. Guillemin, V. Mrljak, M. Bhide, Library-based display technologies: where do we stand?, *Mol. BioSyst.* **12**, 2342–2358 (2016).
99. A. E. Nixon, D. J. Sexton, R. C. Ladner, Drugs derived from phage display, *MAbs* **6**, 73–85 (2014).
100. Abbvie, Annual report 2016, (2017).

101. K. Brown, Peptidic Tumor Targeting Agents: The Road from Phage Display Peptide Selections to Clinical Applications, *Curr. Pharm. Des.* **16**, 1040–1054 (2010).
102. C. Heinis, G. Winter, Encoded libraries of chemically modified peptides, *Curr. Opin. Chem. Biol.* **26**, 89–98 (2015).
103. S. Ng, E. Lin, P. I. Kitov, K. F. Tjhung, O. O. Gerlits, L. Deng, B. Kasper, A. Sood, B. M. Paschal, P. Zhang, C. C. Ling, J. S. Klassen, C. J. Noren, L. K. Mahal, R. J. Woods, L. Coates, R. Derda, Genetically encoded fragment-based discovery of glycopeptide ligands for carbohydrate-binding proteins, *J. Am. Chem. Soc.* **137**, 5248–5251 (2015).
104. K. F. Tjhung, P. I. Kitov, S. Ng, E. N. Kitova, L. Deng, J. S. Klassen, R. Derda, Silent Encoding of Chemical Post-Translational Modifications in Phage-Displayed Libraries, *J. Am. Chem. Soc.* **138**, 32–35 (2016).
105. D. M. Eckert, V. N. Malashkevich, L. H. Hong, P. A. Carr, P. S. Kim, Inhibiting HIV-1 entry: Discovery of D-peptide inhibitors that target the gp41 coiled-coil pocket, *Cell* **99**, 103–115 (1999).
106. M. Uppalapati, D. J. Lee, K. Mandal, H. Li, L. P. Miranda, J. Lowitz, J. Kenney, J. J. Adams, D. Ault-Riché, S. B. H. Kent, S. S. Sidhu, A Potent d-Protein Antagonist of VEGF-A is Nonimmunogenic, Metabolically Stable, and Longer-Circulating in Vivo, *ACS Chem. Biol.* **11**, 1058–1065 (2016).
107. C. J. Hipolito, H. Suga, Ribosomal production and in vitro selection of natural product-like peptidomimetics: The FIT and RaPID systems, *Curr. Opin. Chem. Biol.* **16**, 196–203 (2012).
108. T. Passioura, H. Suga, A RaPID way to discover nonstandard macrocyclic peptide modulators of drug targets, *Chem. Commun.* **53**, 1931–1940 (2017).
109. L. J. Walport, R. Obexer, H. Suga, Strategies for transitioning macrocyclic peptides to cell-permeable drug leads, *Curr. Opin. Biotechnol.* **48**, 242–250 (2017).
110. S. A. K. Jongkees, S. Caner, C. Tysoe, G. D. Brayer, S. G. Withers, H. Suga, Rapid Discovery of Potent and Selective Glycosidase-Inhibiting De Novo Peptides, *Cell Chem. Biol.* **24**, 381–390 (2017).
111. N. K. Bashiruddin, H. Suga, Construction and screening of vast libraries of natural product-like macrocyclic peptides using in vitro display technologies, *Curr. Opin. Chem. Biol.* **24**, 131–138 (2015).
112. A. Tavassoli, SICLOPPS cyclic peptide libraries in drug discovery, *Curr. Opin. Chem. Biol.* **38**, 30–35 (2017).
113. K. S. Lam, M. Lebl, V. Krchňák, The “one-bead-one-compound” combinatorial library method, *Chem. Rev.* **97**, 411–448 (1997).
114. R. Liu, X. Li, K. S. Lam, Combinatorial chemistry in drug discovery, *Curr. Opin. Chem. Biol.* **38**, 117–126 (2017).

115. A. B. MacConnell, P. J. McEnaney, V. J. Cavett, B. M. Paegel, DNA-Encoded Solid-Phase Synthesis: Encoding Language Design and Complex Oligomer Library Synthesis, *ACS Comb. Sci.* **17**, 518–534 (2015).
116. R. Liu, X. Li, W. Xiao, K. S. Lam, Tumor-targeting peptides from combinatorial libraries, *Adv. Drug Deliv. Rev.* **110–111**, 13–37 (2017).
117. A. Luther, K. Moehle, E. Chevalier, G. Dale, D. Obrecht, Protein epitope mimetic macrocycles as biopharmaceuticals, *Curr. Opin. Chem. Biol.* **38**, 45–51 (2017).
118. N. Srinivas, P. Jetter, B. J. Ueberbacher, M. Werneburg, K. Zerbe, J. Steinmann, B. Van der Meijden, F. Bernardini, A. Lederer, R. L. A. Dias, P. E. Misson, H. Henze, J. Zumbunn, F. O. Gombert, D. Obrecht, P. Hunziker, S. Schauer, U. Ziegler, A. Kach, L. Eberl, K. Riedel, S. J. DeMarco, J. A. Robinson, Peptidomimetic Antibiotics Target Outer-Membrane Biogenesis in *Pseudomonas aeruginosa*, *Science (80-.)*. **327**, 1010–1013 (2010).
119. J. Chatterjee, F. Rechenmacher, H. Kessler, N-methylation of peptides and proteins: an important element for modulating biological functions., *Angew. Chem. Int. Ed. Engl.* **52**, 254–69 (2013).
120. A. F. B. Räder, F. Reichart, M. Weinmüller, H. Kessler, Improving oral bioavailability of cyclic peptides by N -methylation, *Bioorg. Med. Chem.* (2017), doi:10.1016/j.bmc.2017.08.031.
121. S. Sagan, P. Karoyan, O. Lequin, G. Chassaing, S. Lavielle, N- and Calpha-methylation in biologically active peptides: synthesis, structural and functional aspects., *Curr. Med. Chem.* **11**, 2799–822 (2004).
122. A. I. Fernández-Llamazares, J. Spengler, F. Albericio, Review backbone N -modified peptides: How to meet the challenge of secondary amine acylation, *Biopolymers* **104**, 435–452 (2015).
123. Y.-U. Kwon, T. Kodadek, Quantitative Evaluation of the Relative Cell Permeability of Peptoids and Peptides, *J. Am. Chem. Soc.* **129**, 1508–1509 (2007).
124. N. C. Tan, P. Yu, Y. U. Kwon, T. Kodadek, High-throughput evaluation of relative cell permeability between peptoids and peptides, *Bioorganic Med. Chem.* **16**, 5853–5861 (2008).
125. A. G. Jamieson, N. Boutard, D. Sabatino, W. D. Lubell, Peptide Scanning for Studying Structure-Activity Relationships in Drug Discovery, *Chem. Biol. Drug Des.* **81**, 148–165 (2013).
126. A. Rembratt, C. Graugaard-Jensen, T. Senderovitz, J. Norgaard, J. Djurhuus, Pharmacokinetics and pharmacodynamics of desmopressin administered orally versus intravenously at daytime versus night-time in healthy men aged 55-70 years, *Eur. J. Clin. Pharmacol.* **60**, 397–402 (2004).
127. C. W. Gruber, J. Koehbach, M. Muttenthaler, Exploring bioactive peptides from natural sources for oxytocin and vasopressin drug discovery, *Future Med. Chem.* **4**, 1791–

1798 (2012).

128. M. Saito, A. Tahara, T. Sugimoto, 1-desamino-8-D-arginine vasopressin (DDAVP) as an agonist on V1b vasopressin receptor., *Biochem. Pharmacol.* **53**, 1711–7 (1997).

129. M. Singer, Arginine vasopressin vs. terlipressin in the treatment of shock states, *Best Pract. Res. Clin. Anaesthesiol.* **22**, 359–368 (2008).

130. M. Manning, A. Misicka, A. Olma, K. Bankowski, S. Stoev, B. Chini, T. Durroux, B. Mouillac, M. Corbani, G. Guillon, Oxytocin and Vasopressin Agonists and Antagonists as Research Tools and Potential Therapeutics, *J. Neuroendocrinol.* **24**, 609–628 (2012).

131. W. Bauer, U. Briner, W. Doepfner, R. Haller, R. Huguenin, P. Marbach, T. J. Petcher, J. Pless, SMS 201–995: A very potent and selective octapeptide analogue of somatostatin with prolonged action, *Life Sci.* **31**, 1133–1140 (1982).

132. D. S. Nielsen, N. E. Shepherd, W. Xu, A. J. Lucke, M. J. Stoermer, D. P. Fairlie, Orally Absorbed Cyclic Peptides, *Chem. Rev.* **117**, 8094–8128 (2017).

133. L. Anthony, P. U. Freda, From somatostatin to octreotide LAR: evolution of a somatostatin analogue, *Curr. Med. Res. Opin.* **25**, 2989–2999 (2009).

134. C. Bruns, I. Lewis, U. Briner, G. Meno-Tetang, G. Weckbecker, SOM230: a novel somatostatin peptidomimetic with broad somatotropin release inhibiting factor (SRIF) receptor binding and a unique antisecretory profile., *Eur. J. Endocrinol.* **146**, 707–16 (2002).

135. G. Golor, Hu, Ruffin, Buchelt, Bouillaud, Wang, Maldonado, A first-in-man study to evaluate the safety, tolerability, and pharmacokinetics of pasireotide (SOM230), a multireceptor-targeted somatostatin analog, in healthy volunteers, *Drug Des. Devel. Ther.* **6**, 71 (2012).

136. P. Martín-Gago, M. Gomez-Caminals, R. Ramón, X. Verdaguer, P. Martin-Malpartida, E. Aragón, J. Fernández-Carneado, B. Ponsati, P. López-Ruiz, M. A. Cortes, B. Colás, M. J. Macias, A. Riera, Fine-tuning the π - π Aromatic Interactions in Peptides: Somatostatin Analogues Containing Mesityl Alanine, *Angew. Chemie Int. Ed.* **51**, 1820–1825 (2012).

137. P. Martín-Gago, Á. Rol, T. Todorovski, E. Aragón, P. Martin-Malpartida, X. Verdaguer, M. Vallès Miret, J. Fernández-Carneado, B. Ponsati, M. J. Macias, A. Riera, Peptide aromatic interactions modulated by fluorinated residues: Synthesis, structure and biological activity of Somatostatin analogs containing 3-(3',5'-difluorophenyl)-alanine, *Sci. Rep.* **6**, 27285 (2016).

138. J. Erchegyi, R. Cescato, B. Waser, J. E. Rivier, J. C. Reubi, N -Imidazolebenzyl-histidine Substitution in Somatostatin and in Its Octapeptide Analogue Modulates Receptor Selectivity and Function, *J. Med. Chem.* **54**, 5981–5987 (2011).

139. S. T. Staykova, D. W. Wesselinova, L. T. Vezenkova, E. D. Naydenova, Synthesis and in vitro antitumor activity of new octapeptide analogs of somatostatin containing unnatural amino acids, *Amino Acids* **47**, 1007–1013 (2015).

140. T. Barth, I. Krejčí, J. Vaněčková, K. Jost, I. Rychlík, Prolonged action of deamino-carba analogues of oxytocin on the rat uterus in vivo., *Eur. J. Pharmacol.* **25**, 67–70 (1974).
141. L. S. Meshykhi, M. R. Nel, D. N. Lucas, The role of carbetocin in the prevention and management of postpartum haemorrhage, *Int. J. Obstet. Anesth.* **28**, 61–69 (2016).
142. I. Passoni, M. Leonzino, V. Gigliucci, B. Chini, M. Busnelli, Carbetocin is a Functional Selective Gq Agonist That Does Not Promote Oxytocin Receptor Recycling After Inducing β -Arrestin-Independent Internalisation, *J. Neuroendocrinol.* **28** (2016), doi:10.1111/jne.12363.
143. F. Marceau, D. Regoli, Bradykinin receptor ligands: therapeutic perspectives, *Nat. Rev. Drug Discov.* **3**, 845–852 (2004).
144. European Medicines Agency, Annual report of the European Medicines Agency 2008, (2009).
145. F. J. Hock, K. Wirth, U. Albus, W. Linz, H. J. Gerhards, G. Wiemer, S. Henke, G. Breipohl, W. König, J. Knolle, B. A. Schölkens, Hoe 140 a new potent and long acting bradykinin-antagonist: in vitro studies, *Br. J. Pharmacol.* **102**, 769–773 (1991).
146. B. L. Zuraw, HAE therapies: past present and future., *Allergy Asthma. Clin. Immunol.* **6**, 23 (2010).
147. A. Stevenazzi, M. Marchini, G. Sandrone, B. Vergani, M. Lattanzio, Amino acidic scaffolds bearing unnatural side chains: An old idea generates new and versatile tools for the life sciences, *Bioorg. Med. Chem. Lett.* **24**, 5349–5356 (2014).
148. J. Quancard, A. Labonne, Y. Jacquot, G. Chassaing, S. Lavielle, P. Karoyan, Asymmetric Synthesis of 3-Substituted Proline Chimeras Bearing Polar Side Chains of Proteinogenic Amino Acids, *J. Org. Chem.* **69**, 7940–7948 (2004).
149. A. Clemenceau, Q. Wang, J. Zhu, Enantioselective Synthesis of Quaternary α -Amino Acids Enabled by the Versatility of the Phenylselenonyl Group, *Chem. - A Eur. J.* **22**, 18368–18372 (2016).
150. L. P. Miranda, J. R. Holder, L. Shi, B. Bennett, J. Aral, C. V. Gegg, M. Wright, K. Walker, G. Doellgast, R. Rogers, H. Li, V. Valladares, K. Salyers, E. Johnson, K. Wild, Identification of potent, selective, and metabolically stable peptide antagonists to the calcitonin gene-related peptide (CGRP) receptor, *J. Med. Chem.* **51**, 7889–7897 (2008).
151. V. Frey, J. Viaud, G. Subra, N. Cauquil, J. F. Guichou, P. Casara, G. Grassy, A. Chavanieu, Structure-activity relationships of Bak derived peptides: Affinity and specificity modulations by amino acid replacement, *Eur. J. Med. Chem.* **43**, 966–972 (2008).
152. J. K. Murray, Y.-X. Qian, B. Liu, R. Elliott, J. Aral, C. Park, X. Zhang, M. Stenkilsson, K. Salyers, M. Rose, H. Li, S. Yu, K. L. Andrews, A. Colombero, J. Werner, K. Gaida, E. A. Sickmier, P. Miu, A. Itano, J. McGivern, C. V. Gegg, J. K. Sullivan, L. P. Miranda, Pharmaceutical Optimization of Peptide Toxins for Ion Channel Targets: Potent, Selective, and Long-Lived Antagonists of Kv1.3, *J. Med. Chem.* **58**, 6784–6802 (2015).

153. E. Biron, J. Chatterjee, O. Ovadia, D. Langenegger, J. Brueggen, D. Hoyer, H. A. Schmid, R. Jelinek, C. Gilon, A. Hoffman, H. Kessler, Improving oral bioavailability of peptides by multiple N-methylation: Somatostatin analogues, *Angew. Chemie - Int. Ed.* **47**, 2595–2599 (2008).
154. J. Chatterjee, C. Gilon, A. Hoffman, H. Kessler, N-methylation of peptides: A new perspective in medicinal chemistry, *Acc. Chem. Res.* **41**, 1331–1342 (2008).
155. W. M. Hewitt, S. S. F. Leung, C. R. Pye, A. R. Ponkey, M. Bednarek, M. P. Jacobson, R. S. Lokey, Cell-permeable cyclic peptides from synthetic libraries inspired by natural products, *J. Am. Chem. Soc.* **137**, 715–721 (2015).
156. A. T. Bockus, J. A. Schwochert, C. R. Pye, C. E. Townsend, V. Sok, M. A. Bednarek, R. S. Lokey, Going Out on a Limb: Delineating the Effects of β -Branching, N-Methylation, and Side Chain Size on the Passive Permeability, Solubility, and Flexibility of Sanguinamide A Analogues, *J. Med. Chem.* **58**, 7409–7418 (2015).
157. C. L. Ahlback, K. W. Lexa, A. T. Bockus, V. Chen, P. Crews, M. P. Jacobson, R. S. Lokey, Beyond cyclosporine A: conformation-dependent passive membrane permeabilities of cyclic peptide natural products, *Future Med. Chem.* **7**, 2121–2130 (2015).
158. P. Matsson, B. C. Doak, B. Over, J. Kihlberg, Cell permeability beyond the rule of 5, *Adv. Drug Deliv. Rev.* **101**, 42–61 (2016).
159. D. Scanlon, K. S. Harris, A. M. Coley, J. a. Karas, J. L. Casey, A. B. Hughes, M. Foley, Comprehensive N-Methyl Scanning of a Potent Peptide Inhibitor of Malaria Invasion into Erythrocytes Leads to Pharmacokinetic Optimization of the Molecule, *Int. J. Pept. Res. Ther.* **14**, 381–386 (2008).
160. K. S. Harris, J. L. Casey, A. M. Coley, J. A. Karas, J. K. Sabo, Y. Y. Tan, O. Dolezal, R. S. Norton, A. B. Hughes, D. Scanlon, M. Foley, Rapid Optimization of a Peptide Inhibitor of Malaria Parasite Invasion by Comprehensive N -Methyl Scanning, *J. Biol. Chem.* **284**, 9361–9371 (2009).
161. W. G. Rajeswaran, S. J. Hocart, W. A. Murphy, J. E. Taylor, D. H. Coy, Highly potent and subtype selective ligands derived by N-methyl scan of a somatostatin antagonist, *J. Med. Chem.* **44**, 1305–1311 (2001).
162. A. Skogh, A. Lesniak, F. Z. Gaugaz, R. Svensson, G. Lindeberg, R. Fransson, F. Nyberg, M. Hallberg, A. Sandström, Impact of N-methylation of the substance P 1–7 amide on anti-allodynic effect in mice after peripheral administration, *Eur. J. Pharm. Sci.* **109**, 533–540 (2017).
163. S. Sagan, O. Lequin, F. Frank, O. Convert, M. Ayoub, S. Lavielle, G. Chassaing, Calpha methylation in molecular recognition. Application to substance P and the two neurokinin-1 receptor binding sites., *Eur. J. Biochem.* **268**, 2997–3005 (2001).
164. M. Crisma, C. Toniolo, Helical screw-sense preferences of peptides based on chiral, α -tetrasubstituted α -amino acids, *Biopolym. - Pept. Sci. Sect.* **104**, 46–64 (2015).

165. Y. Demizu, M. Doi, H. Yamashita, T. Misawa, M. Oba, M. Kurihara, H. Suemune, M. Tanaka, The side-chain hydroxy groups of a cyclic α,α -disubstituted α -amino acid promote oligopeptide 310-helix packing in the crystalline state, *Biopolymers* **106**, 757–768 (2016).
166. T. Misawa, M. Imamura, Y. Ozawa, K. Haishima, M. Kurihara, Y. Kikuchi, Y. Demizu, Development of helix-stabilized antimicrobial peptides composed of lysine and hydrophobic α,α -disubstituted α -amino acid residues, *Bioorganic Med. Chem. Lett.* **27**, 3950–3953 (2017).
167. M. Oba, M. Kunitake, T. Kato, A. Ueda, M. Tanaka, Enhanced and Prolonged Cell-Penetrating Abilities of Arginine-Rich Peptides by Introducing Cyclic α,α -Disubstituted α -Amino Acids with Stapling, *Bioconjug. Chem.* **28**, 1801–1806 (2017).
168. J. Schwochert, R. Turner, M. Thang, R. F. Berkeley, A. R. Ponkey, K. M. Rodriguez, S. S. F. Leung, B. Khunte, G. Goetz, C. Limberakis, A. S. Kalgutkar, H. Eng, M. J. Shapiro, A. M. Mathiowetz, D. A. Price, S. Liras, M. P. Jacobson, R. S. Lokey, Peptide to Peptoid Substitutions Increase Cell Permeability in Cyclic Hexapeptides, *Org. Lett.* **17**, 2928–2931 (2015).
169. S. A. Fowler, H. E. Blackwell, Structure–function relationships in peptoids: Recent advances toward deciphering the structural requirements for biological function, *Org. Biomol. Chem.* **7**, 1508 (2009).
170. N. P. Chongsiriwatana, J. A. Patch, A. M. Czyzewski, M. T. Dohm, A. Ivankin, D. Gidalevitz, R. N. Zuckermann, A. E. Barron, Peptoids that mimic the structure, function, and mechanism of helical antimicrobial peptides, *Proc. Natl. Acad. Sci.* **105**, 2794–2799 (2008).
171. M. Park, M. Wetzler, T. S. Jardetzky, A. E. Barron, A readily applicable strategy to convert peptides to peptoid-based therapeutics., *PLoS One* **8**, e58874 (2013).
172. M. Boehm, K. Beaumont, R. Jones, A. S. Kalgutkar, L. Zhang, K. Atkinson, G. Bai, J. A. Brown, H. Eng, G. H. Goetz, B. R. Holder, B. Khunte, S. Lazzaro, C. Limberakis, S. Ryu, M. J. Shapiro, L. Tylaska, J. Yan, R. Turner, S. S. F. Leung, M. Ramaseshan, D. A. Price, S. Liras, M. P. Jacobson, D. J. Earp, R. S. Lokey, A. M. Mathiowetz, E. Menhaji-Klotz, Discovery of Potent and Orally Bioavailable Macrocyclic Peptide–Peptoid Hybrid CXCR7 Modulators, *J. Med. Chem.* **60**, 9653–9663 (2017).
173. Y. Gao, S. Amar, S. Pahwa, G. Fields, T. Kodadek, Rapid lead discovery through iterative screening of one bead one compound libraries, *ACS Comb. Sci.* **17**, 49–59 (2015).
174. K. R. Mendes, M. L. Malone, J. M. Ndungu, I. Saponitsky-Kroyter, V. J. Cavett, P. J. McEnaney, A. B. MacConnell, T. D. M. Doran, K. Ronacher, K. Stanley, O. Utset, G. Walzl, B. M. Paegel, T. Kodadek, High-throughput identification of DNA-encoded IgG ligands that distinguish active and latent mycobacterium tuberculosis infections, *ACS Chem. Biol.* **12**, 234–243 (2017).
175. C. A. Rhodes, D. Pei, Bicyclic Peptides as Next-Generation Therapeutics, *Chem. - A*

Eur. J. **23**, 12690–12703 (2017).

176. P. Timmerman, J. Beld, W. C. Puijk, R. H. Meloen, Rapid and quantitative cyclization of multiple peptide loops onto synthetic scaffolds for structural mimicry of protein surfaces, *ChemBioChem* **6**, 821–824 (2005).

177. C. Heinis, T. Rutherford, S. Freund, G. Winter, Phage-encoded combinatorial chemical libraries based on bicyclic peptides., *Nat. Chem. Biol.* **5**, 502–7 (2009).

178. M. Mutter, P. Dumy, P. Garrouste, C. Lehmane, M. Mathieu, C. Peggion, S. Peluso, A. Razaname, G. Tuchscherer, Template assembled synthetic proteins (TASP) as functional mimetics of proteins, *Angew.Chem., Int.Ed.Engl.* **35**, 1481–1485 (1996).

179. R. U. Kadam, J. Juraszek, B. Brandenburg, C. Buyck, W. B. G. Schepens, B. Kesteleyn, B. Stoops, R. J. Vreeken, J. Vermond, W. Goutier, C. Tang, R. Vogels, R. H. E. Friesen, J. Goudsmit, M. J. P. Van Dongen, I. A. Wilson, Potent peptidic fusion inhibitors of influenza virus, *Science (80-.)*. **358**, 496–502 (2017).

180. A. Angelini, L. Cendron, S. Chen, J. Touati, G. Winter, G. Zanotti, C. Heinis, Bicyclic peptide inhibitor reveals large contact interface with a protease target, *ACS Chem. Biol.* **7**, 817–821 (2012).

181. A. Angelini, J. Morales-Sanfrutos, P. Diderich, S. Chen, C. Heinis, Bicyclization and tethering to albumin yields long-acting peptide antagonists., *J. Med. Chem.* **55**, 10187–97 (2012).

182. S. Chen, J. Morales-Sanfrutos, A. Angelini, B. Cutting, C. Heinis, Structurally Diverse Cyclisation Linkers Impose Different Backbone Conformations in Bicyclic Peptides, *ChemBioChem* **13**, 1032–1038 (2012).

183. S. Chen, D. Bertoldo, A. Angelini, F. Pojer, C. Heinis, Peptide ligands stabilized by small molecules., *Angew. Chem. Int. Ed. Engl.* **53**, 1602–6 (2014).

184. S. Chen, I. Rentero Rebollo, S. a Buth, J. Morales-Sanfrutos, J. Touati, P. G. Leiman, C. Heinis, Bicyclic peptide ligands pulled out of cysteine-rich peptide libraries., *J. Am. Chem. Soc.* **135**, 6562–9 (2013).

185. I. R. Rebollo, A. Angelini, C. Heinis, Phage display libraries of differently sized bicyclic peptides, *Med. Chem. Commun.* **4**, 145–150 (2013).

186. I. Rentero Rebollo, M. Sabisz, V. Baeriswyl, C. Heinis, Identification of target-binding peptide motifs by high-throughput sequencing of phage-selected peptides, *Nucleic Acids Res.* **42**, e169 (2014).

187. A. T. Long, E. Kenne, R. Jung, T. A. Fuchs, T. Renné, Contact system revisited: an interface between inflammation, coagulation, and innate immunity, *J. Thromb. Haemost.* **14**, 427–437 (2016).

188. V. Baeriswyl, H. Rapley, L. Pollaro, C. Stace, D. Teufel, E. Walker, S. Chen, G. Winter, J. Tite, C. Heinis, Bicyclic peptides with optimized ring size inhibit human

- plasma kallikrein and its orthologues while sparing paralogous proteases., *ChemMedChem* **7**, 1173–6 (2012).
189. N. Sidenius, F. Blasi, The urokinase plasminogen activator system in cancer: Recent advances and implication for prognosis and therapy, *Cancer Metastasis Rev.* **22**, 205–222 (2003).
190. A. Angelini, P. Diderich, J. Morales-Sanfrutos, S. Thurnheer, D. Hacker, L. Menin, C. Heinis, Chemical macrocyclization of peptides fused to antibody Fc fragments, *Bioconjug. Chem.* **23**, 1856–1863 (2012).
191. S. Chen, D. Gfeller, S. a Buth, O. Michielin, P. G. Leiman, C. Heinis, Improving binding affinity and stability of peptide ligands by substituting glycines with D-amino acids., *Chembiochem* **14**, 1316–22 (2013).
192. L. Pollaro, S. Raghunathan, J. Morales-Sanfrutos, A. Angelini, S. Kontos, C. Heinis, Bicyclic peptides conjugated to an albumin-binding tag diffuse efficiently into solid tumors., *Mol. Cancer Ther.* , 1–12 (2014).
193. A. Zorzi, S. J. Middendorp, J. Wilbs, K. Deyle, C. Heinis, Acylated heptapeptide binds albumin with high affinity and application as tag furnishes long-acting peptides, *Nat. Commun.* **8**, 1–9 (2017).
194. S. Chen, R. Gopalakrishnan, T. Schaer, F. Marger, R. Hovius, D. Bertrand, F. Pojer, C. Heinis, Dithiol amino acids can structurally shape and enhance the ligand-binding properties of polypeptides, *Nat. Chem.* **6**, 1009–1016 (2014).
195. D. Bertoldo, M. M. G. Khan, P. Dessen, W. Held, J. Huelsken, C. Heinis, Phage Selection of Peptide Macrocycles against β -Catenin to Interfere with Wnt Signaling, *ChemMedChem* **11**, 834–839 (2016).
196. R. Nusse, H. Clevers, Wnt/ β -Catenin Signaling, Disease, and Emerging Therapeutic Modalities, *Cell* **169**, 985–999 (2017).
197. P. Diderich, C. Heinis, Phage selection of bicyclic peptides binding Her2, *Tetrahedron* **70**, 7733–7739 (2014).
198. C. Urech-Varenne, F. Radtke, C. Heinis, Phage Selection of Bicyclic Peptide Ligands of the Notch1 Receptor, *ChemMedChem* **10**, 1754–1761 (2015).
199. I. Rentero Rebollo, S. McCallin, D. Bertoldo, J. M. Entenza, P. Moreillon, C. Heinis, Development of Potent and Selective *S. aureus* Sortase A Inhibitors Based on Peptide Macrocycles, *ACS Med. Chem. Lett.* **7**, 606–611 (2016).
200. W. H. Connors, S. P. Hale, N. K. Terrett, DNA-encoded chemical libraries of macrocycles, *Curr. Opin. Chem. Biol.* **26**, 42–47 (2015).
201. A. D. Foster, J. D. Ingram, E. K. Leitch, K. R. Lennard, E. L. Osher, A. Tavassoli, Methods for the Creation of Cyclic Peptide Libraries for Use in Lead Discovery, *J. Biomol. Screen.* **20**, 563–576 (2015).

202. W. J. Fairbrother, H. W. Christinger, A. G. Cochran, G. Fuh, C. J. Keenan, C. Quan, S. K. Shriver, J. Y. K. Tom, J. A. Wells, B. C. Cunningham, Novel Peptides Selected to Bind Vascular Endothelial Growth Factor Target the Receptor-Binding Site, *Biochemistry* **37**, 17754–17764 (1998).
203. V. Baeriswyl, S. Calzavarini, S. Chen, A. Zorzi, L. Bologna, A. Angelillo-Scherrer, C. Heinis, A Synthetic Factor XIIa Inhibitor Blocks Selectively Intrinsic Coagulation Initiation., *ACS Chem. Biol.* **10**, 1861–70 (2015).
204. S. J. Middendorp, J. Wilbs, C. Quarroz, S. Calzavarini, A. Angelillo-Scherrer, C. Heinis, Peptide Macrocyclic Inhibitor of Coagulation Factor XII with Subnanomolar Affinity and High Target Selectivity, *J. Med. Chem.* **60**, 1151–1158 (2017).
205. A. Montero, J. M. Beierle, C. A. Olsen, M. R. Ghadiri, Design, Synthesis, Biological Evaluation, and Structural Characterization of Potent Histone Deacetylase Inhibitors Based on Cyclic α/β -Tetrapeptide Architectures, *J. Am. Chem. Soc.* **131**, 3033–3041 (2009).
206. J. G. Johnson, B. Wang, G. T. Debelouchina, R. P. Novick, T. W. Muir, Increasing AIP Macrocyclic Size Reveals Key Features of agr Activation in *Staphylococcus aureus*, *ChemBioChem* **16**, 1093–1100 (2015).
207. A. Oddo, N. T. Nyberg, N. Frimodt-Møller, P. W. Thulstrup, P. R. Hansen, The effect of glycine replacement with flexible ω -amino acids on the antimicrobial and haemolytic activity of an amphipathic cyclic heptapeptide, *Eur. J. Med. Chem.* **102**, 574–581 (2015).
208. D. Seebach, J. L. Matthews, β -Peptides: a surprise at every turn, *Chem. Commun.* **1**, 2015–2022 (1997).
209. W. S. Horne, L. M. Johnson, T. J. Ketas, P. J. Klasse, M. Lu, J. P. Moore, S. H. Gellman, Structural and biological mimicry of protein surface recognition by α/β -peptide foldamers, *Proc. Natl. Acad. Sci.* **106**, 14751–14756 (2009).
210. L. M. Johnson, S. H. Gellman, in *Methods in Enzymology*, (Elsevier Inc., 2013), vol. 523, pp. 407–429.
211. L. M. Johnson, S. Barrick, M. V. Hager, A. McFedries, E. A. Homan, M. E. Rabaglia, M. P. Keller, A. D. Attie, A. Saghatelian, A. Bisello, S. H. Gellman, A Potent α/β -Peptide Analogue of GLP-1 with Prolonged Action in Vivo, *J. Am. Chem. Soc.* **136**, 12848–12851 (2014).
212. R. W. Cheloha, A. Maeda, T. Dean, T. J. Gardella, S. H. Gellman, Backbone modification of a polypeptide drug alters duration of action in vivo, *Nat. Biotechnol.* **32**, 653–655 (2014).
213. J. W. Checco, D. F. Kreidler, N. C. Thomas, D. G. Belair, N. J. Rettko, W. L. Murphy, K. T. Forest, S. H. Gellman, Targeting diverse protein–protein interaction interfaces with α/β -peptides derived from the Z-domain scaffold, *Proc. Natl. Acad. Sci.* **112**, 4552–4557 (2015).
214. D. W. Jacobsen, O. Catanescu, P. M. DiBello, J. C. Barbato, Molecular targeting by

- homocysteine: a mechanism for vascular pathogenesis, *Clin. Chem. Lab. Med.* **43**, 1076–1083 (2005).
215. G. E. Raskob, P. Angchaisuksiri, A. N. Blanco, H. Buller, A. Gallus, B. J. Hunt, E. M. Hylek, A. Kakkar, S. V. Konstantinides, M. McCumber, Y. Ozaki, A. Wendelboe, J. I. Weitz, Thrombosis: A major contributor to global disease burden, *Thromb. Res.* **134**, 931–938 (2014).
216. J. W. Eikelboom, J. I. Weitz, New Anticoagulants, *Circulation* **121**, 1523–1532 (2010).
217. S. Schulman, M. Crowther, How I treat with anticoagulants in 2012: new and old anticoagulants, and when and how to switch, *Blood* **119**, 3016–3023 (2012).
218. A. Liew, J. W. Eikelboom, M. O'Donnell, R. G. Hart, Assessment of Anticoagulation Intensity and Management of Bleeding With Old and New Oral Anticoagulants, *Can. J. Cardiol.* **29**, S34–S44 (2013).
219. E. Kenne, K. F. Nickel, A. T. Long, T. A. Fuchs, E. X. Stavrou, F. R. Stahl, T. Renné, Factor XII: A novel target for safe prevention of thrombosis and inflammation, *J. Intern. Med.* **278**, 571–585 (2015).
220. H. Weidmann, L. Heikaus, A. T. Long, C. Naudin, H. Schlüter, T. Renné, The plasma contact system, a protease cascade at the nexus of inflammation, coagulation and immunity, *Biochim. Biophys. Acta - Mol. Cell Res.*, 0–1 (2017).
221. T. Renné, M. Pozgajová, S. Grüner, K. Schuh, H.-U. Pauer, P. Burfeind, D. Gailani, B. Nieswandt, Defective thrombus formation in mice lacking coagulation factor XII., *J. Exp. Med.* **202**, 271–81 (2005).
222. Y. Kokoye, I. Ivanov, Q. Cheng, A. Matafonov, S. K. Dickeson, S. Mason, D. J. Sexton, T. Renné, K. McCrae, E. P. Feener, D. Gailani, A comparison of the effects of factor XII deficiency and prekallikrein deficiency on thrombus formation, *Thromb. Res.* **140**, 118–124 (2016).
223. C. Kleinschnitz, G. Stoll, M. Bendszus, K. Schuh, H.-U. Pauer, P. Burfeind, C. Renné, D. Gailani, B. Nieswandt, T. Renné, Targeting coagulation factor XII provides protection from pathological thrombosis in cerebral ischemia without interfering with hemostasis, *J. Exp. Med.* **203**, 513–518 (2006).
224. H.-U. Pauer, T. Renné, B. Hemmerlein, T. Legler, S. Fritzlar, I. Adham, W. Müller-Esterl, G. Emons, U. Sancken, W. Engel, P. Burfeind, Targeted deletion of murine coagulation factor XII gene-a model for contact phase activation in vivo, *Thromb. Haemost.* **92**, 503–508 (2004).
225. A. S. Revenko, D. Gao, J. R. Crosby, G. Bhattacharjee, C. Zhao, C. May, D. Gailani, B. P. Monia, A. R. MacLeod, Selective depletion of plasma prekallikrein or coagulation factor XII inhibits thrombosis in mice without increased risk of bleeding, *Blood* **118**, 5302–5311 (2011).
226. J. W. Yau, P. Liao, J. C. Fredenburgh, A. R. Stafford, A. S. Revenko, B. P. Monia, J. I.

Weitz, Selective depletion of factor XI or factor XII with antisense oligonucleotides attenuates catheter thrombosis in rabbits, *Blood* **123**, 2102–2107 (2014).

227. M. Larsson, V. Rayzman, M. W. Nolte, K. F. Nickel, J. Bjorkqvist, A. Jamsa, M. P. Hardy, M. Fries, S. Schmidbauer, P. Hedenqvist, M. Broome, I. Pragst, G. Dickneite, M. J. Wilson, A. D. Nash, C. Panousis, T. Renné, A Factor XIIa Inhibitory Antibody Provides Thromboprotection in Extracorporeal Circulation Without Increasing Bleeding Risk, *Sci. Transl. Med.* **6**, 222ra17–222ra17 (2014).

228. A. Matafonov, P. Y. Leung, A. E. Gailani, S. L. Grach, C. Puy, Q. Cheng, M. -f. Sun, O. J. T. McCarty, E. I. Tucker, H. Kataoka, T. Renne, J. H. Morrissey, A. Gruber, D. Gailani, Factor XII inhibition reduces thrombus formation in a primate thrombosis model, *Blood* **123**, 1739–1746 (2014).

229. J. W. Yau, A. R. Stafford, P. Liao, J. C. Fredenburgh, R. Roberts, J. L. Brash, J. I. Weitz, Corn trypsin inhibitor coating attenuates the prothrombotic properties of catheters in vitro and in vivo, *Acta Biomater.* **8**, 4092–4100 (2012).

230. Y. Xu, T.-Q. Cai, G. Castriota, Y. Zhou, L. Hoos, N. Jochnowitz, C. Loewrigkeit, J. A. Cook, A. Wickham, J. M. Metzger, M. L. Ogletree, D. A. Seiffert, Z. Chen, Factor XIIa inhibition by Infestin-4: in vitro mode of action and in vivo antithrombotic benefit, *Thromb. Haemost.* **111**, 694–704 (2013).

231. C. M. Barbieri, X. Wang, W. Wu, X. Zhou, A. M. Ogawa, K. O'Neill, D. Chu, G. Castriota, D. A. Seiffert, D. E. Gutstein, Z. Chen, Factor XIIa as a novel target for thrombosis: Target engagement requirement and efficacy in a rabbit model of microembolic signals, *J. Pharmacol. Exp. Ther.* **360** (2017), doi:10.1124/jpet.116.238493.

232. R. M. Sniecinski, W. L. Chandler, Activation of the Hemostatic System During Cardiopulmonary Bypass, *Anesth. Analg.* **113**, 1319–1333 (2011).

233. S. A. Esper, J. H. Levy, J. H. Waters, I. J. Welsby, Extracorporeal membrane oxygenation in the adult: A review of anticoagulation monitoring and transfusion, *Anesth. Analg.* **118**, 731–743 (2014).

234. G. M. Annich, O. Zaulan, M. Neufeld, D. Wagner, M. M. Reynolds, Thromboprophylaxis in Extracorporeal Circuits: Current Pharmacological Strategies and Future Directions, *Am. J. Cardiovasc. Drugs* **17**, 425–439 (2017).

235. K. F. Nickel, A. T. Long, T. A. Fuchs, L. M. Butler, T. Renné, Factor XII as a Therapeutic Target in Thromboembolic and Inflammatory Diseases Highlights, *Arterioscler. Thromb. Vasc. Biol.* **37**, 13–20 (2017).

236. A. Reshef, M. Kidon, I. Leibovich, The Story of Angioedema: from Quincke to Bradykinin, *Clin. Rev. Allergy Immunol.* **51**, 121–139 (2016).

237. J. Krupka, F. May, T. Weimer, I. Pragst, C. Kleinschnitz, G. Stoll, C. Panousis, G. Dickneite, M. W. Nolte, S. G. Meuth, Ed. The Coagulation Factor XIIa Inhibitor rHA-Infestin-4 Improves Outcome after Cerebral Ischemia/Reperfusion Injury in Rats, *PLoS*

One **11**, e0146783 (2016).

238. D. Zamolodchikov, Z.-L. Chen, B. A. Conti, T. Renné, S. Strickland, Activation of the factor XII-driven contact system in Alzheimer's disease patient and mouse model plasma, *Proc. Natl. Acad. Sci.* **112**, 201423764 (2015).

239. Z.-L. Chen, A. S. Revenko, P. Singh, A. R. MacLeod, E. H. Norris, S. Strickland, Depletion of coagulation factor XII ameliorates brain pathology and cognitive impairment in Alzheimer's disease mice, *Blood* **129**, blood-2016-11-753202 (2017).

240. K. Göbel, S. Pankratz, C.-M. Asaridou, A. M. Herrmann, S. Bittner, M. Merker, T. Ruck, S. Glumm, F. Langhauser, P. Kraft, T. F. Krug, J. Breuer, M. Herold, C. C. Gross, D. Beckmann, A. Korb-Pap, M. K. Schuhmann, S. Kuerten, I. Mitroulis, C. Ruppert, M. W. Nolte, C. Panousis, L. Klotz, B. Kehrel, T. Korn, H. F. Langer, T. Pap, B. Nieswandt, H. Wiendl, T. Chavakis, C. Kleinschnitz, S. G. Meuth, Blood coagulation factor XII drives adaptive immunity during neuroinflammation via CD87-mediated modulation of dendritic cells, *Nat. Commun.* **7**, 11626 (2016).

241. A. E. Germenis, M. Speletas, Genetics of Hereditary Angioedema Revisited, *Clin. Rev. Allergy Immunol.* **51**, 170–182 (2016).

242. Australian New Zealand Clinical Trials Registry, Australian New Zealand Clinical Trials Registry (2016) (available at <https://www.anzctr.org.au/Trial/Registration/TrialReview.aspx?id=371625>)).

243. E. Kenne, T. Renné, Factor XII: a drug target for safe interference with thrombosis and inflammation, *Drug Discov. Today* **19**, 1459–1464 (2014).

244. C. Bouckaert, S. Serra, G. Rondelet, E. Dolušić, J. Wouters, J. M. Dogné, R. Frédérick, L. Pochet, Synthesis, evaluation and structure-activity relationship of new 3-carboxamide coumarins as FXIIa inhibitors, *Eur. J. Med. Chem.* **110**, 181–194 (2016).

245. S. J. Middendorp, J. Wilbs, C. Quarroz, S. Calzavarini, A. Angelillo-scherrer, C. Heinis, Peptide macrocycle inhibitor of coagulation factor XII with subnanomolar affinity and high target selectivity Peptide macrocycle inhibitor of coagulation factor XII with subnanomolar affinity and high target selectivity, *J. Med. Chem.* (2017), doi:10.1021/acs.jmedchem.6b01548.

246. J. Wilbs, S. J. Middendorp, C. Heinis, Improving the Binding Affinity of in-Vitro-Evolved Cyclic Peptides by Inserting Atoms into the Macrocycle Backbone, *Chembiochem* **17**, 2299–2303 (2016).

247. C. Duehrkop, R. Rieben, Ischemia/reperfusion injury: Effect of simultaneous inhibition of plasma cascade systems versus specific complement inhibition, *Biochem. Pharmacol.* **88**, 12–22 (2014).

248. J. D. Barr, A. K. Chauhan, G. V Schaeffer, J. K. Hansen, D. G. Motto, Red blood cells mediate the onset of thrombosis in the ferric chloride murine model, *Blood* **121**, 3733–3741 (2013).

249. J. C. Ciciliano, Y. Sakurai, D. R. Myers, M. E. Fay, B. Hechler, S. Meeks, R. Li, J. B. Dixon, L. A. Lyon, C. Gachet, W. A. Lam, Resolving the multifaceted mechanisms of the ferric chloride thrombosis model using an interdisciplinary microfluidic approach, *Blood* **126**, 817–824 (2015).
250. A. Ghosh, W. Li, M. Febbraio, R. G. Espinola, K. R. McCrae, E. Cockrell, R. L. Silverstein, Platelet CD36 mediates interactions with endothelial cell-derived microparticles and contributes to thrombosis in mice, *J. Clin. Invest.* **118**, 1934–1943 (2008).
251. K. A. Amoako, P. J. Montoya, T. C. Major, A. B. Suhaib, H. Handa, D. O. Brant, M. E. Meyerhoff, R. H. Bartlett, K. E. Cook, Fabrication and in vivo thrombogenicity testing of nitric oxide generating artificial lungs, *J. Biomed. Mater. Res. A* **101**, 3511–3519 (2013).
252. R. R. Thiagarajan, R. P. Barbaro, P. T. Rycus, D. M. McMullan, S. A. Conrad, J. D. Fortenberry, M. L. Paden, Extracorporeal Life Support Organization Registry International Report 2016, *ASAIO J.* **63**, 60–67 (2017).
253. Y. Banz, O. M. Hess, S. C. Robson, D. Mettler, P. Meier, A. Haerberli, E. Csizmadia, E. Y. Korchagina, N. V. Bovin, R. Rieben, Locally targeted cytoprotection with dextran sulfate attenuates experimental porcine myocardial ischaemia/reperfusion injury, *Eur. Heart J.* **26**, 2334–2343 (2005).
254. K. E. Cook, J. Maxhimer, D. J. Leonard, C. Mavroudis, C. L. Backer, L. F. Mockros, Platelet and Leukocyte Activation and Design Consequences for Thoracic Artificial Lungs, *ASAIO J.* **48**, 620–630 (2002).
255. A. Page-McCaw, A. J. Ewald, Z. Werb, Matrix metalloproteinases and the regulation of tissue remodelling, *Nat. Rev. Mol. Cell Biol.* **8**, 221–233 (2007).
256. S. Loffek, O. Schilling, C.-W. Franzke, Biological role of matrix metalloproteinases: a critical balance, *Eur. Respir. J.* **38**, 191–208 (2011).
257. S. Amar, L. Smith, G. B. Fields, Matrix metalloproteinase collagenolysis in health and disease, *Biochim. Biophys. Acta - Mol. Cell Res.* **1864**, 1940–1951 (2017).
258. L. Nissinen, V. M. Kähäri, Matrix metalloproteinases in inflammation, *Biochim. Biophys. Acta - Gen. Subj.* **1840**, 2571–2580 (2014).
259. J. M. Wells, A. Gaggari, J. E. Blalock, MMP generated matrikines, *Matrix Biol.* **44–46**, 122–129 (2015).
260. M. Fanjul-Fernández, A. R. Folgueras, S. Cabrera, C. López-Otín, Matrix metalloproteinases: evolution, gene regulation and functional analysis in mouse models, *Biochim. Biophys. Acta* **1803**, 3–19 (2010).
261. D. Bourboulia, W. G. Stetler-Stevenson, Matrix metalloproteinases (MMPs) and tissue inhibitors of metalloproteinases (TIMPs): Positive and negative regulators in tumor cell adhesion, *Semin. Cancer Biol.* **20**, 161–168 (2010).

262. J. Gaffney, I. Solomonov, E. Zehorai, I. Sagi, Multilevel regulation of matrix metalloproteinases in tissue homeostasis indicates their molecular specificity in vivo, *Matrix Biol.* **44–46**, 191–199 (2015).
263. K. Kessenbrock, V. Plaks, Z. Werb, Matrix metalloproteinases: regulators of the tumor microenvironment., *Cell* **141**, 52–67 (2010).
264. L. A. Shuman Moss, S. Jensen-Taubman, W. G. Stetler-Stevenson, Matrix metalloproteinases: changing roles in tumor progression and metastasis., *Am. J. Pathol.* **181**, 1895–9 (2012).
265. E. I. Deryugina, J. P. Quigley, Tumor angiogenesis: MMP-mediated induction of intravasation- and metastasis-sustaining neovasculature, *Matrix Biol.* **44–46**, 94–112 (2015).
266. K. Kessenbrock, C.-Y. Wang, Z. Werb, Matrix metalloproteinases in stem cell regulation and cancer, *Matrix Biol.* **44–46**, 184–190 (2015).
267. L. Nissinen, M. Farshchian, P. Riihilä, V.-M. Kähäri, New perspectives on role of tumor microenvironment in progression of cutaneous squamous cell carcinoma, *Cell Tissue Res.* **365**, 691–702 (2016).
268. F. Ren, R. Tang, X. Zhang, W. M. Madushi, D. Luo, Y. Dang, Z. Li, K. Wei, G. Chen, A. Ahmad, Overexpression of MMP family members functions as prognostic biomarker for breast cancer patients: A systematic review and meta-analysis, *PLoS One* **10**, 1–18 (2015).
269. J. Cathcart, A. Pulkoski-Gross, J. Cao, Targeting matrix metalloproteinases in cancer: Bringing new life to old ideas, *Genes Dis.* **2**, 26–34 (2015).
270. J. A. Sparano, P. Bernardo, P. Stephenson, W. J. Gradishar, J. N. Ingle, S. Zucker, N. E. Davidson, Randomized phase III trial of marimastat versus placebo in patients with metastatic breast cancer who have responding or stable disease after first-line chemotherapy: Eastern Cooperative Oncology Group Trial E2196, *J. Clin. Oncol.* **22**, 4631–4638 (2004).
271. L. J. MacPherson, E. K. Bayburt, M. P. Capparelli, B. J. Carroll, R. Goldstein, M. R. Justice, L. Zhu, S. I. Hu, R. A. Melton, L. Fryer, R. L. Goldberg, J. R. Doughty, S. Spirito, V. Blancuzzi, D. Wilson, E. M. O’Byrne, V. Ganu, D. T. Parker, Discovery of CGS 27023A, a non, peptidic, potent, and orally active stromelysin inhibitor that blocks cartilage degradation in rabbits, *J. Med. Chem.* **40**, 2525–2532 (1997).
272. N. C. Levitt, F. A. Eskens, K. J. O’Byrne, D. J. Propper, L. J. Denis, S. J. Owen, L. Choi, J. A. Foekens, S. Wilner, J. M. Wood, M. Nakajima, D. C. Talbot, W. P. Steward, A. L. Harris, J. Verweij, Phase I and pharmacological study of the oral matrix metalloproteinase inhibitor, MMI270 (CGS27023A), in patients with advanced solid cancer., *Clin. Cancer Res.* **7**, 1912–22 (2001).
273. D. Bissett, K. J. O’Byrne, J. Von Pawel, U. Gatzemeier, A. Price, M. Nicolson, R.

- Mercier, E. Mazabel, C. Penning, M. H. Zhang, M. A. Collier, F. A. Shepherd, Phase III study of matrix metalloproteinase inhibitor prinomastat in non-small-cell lung cancer, *J. Clin. Oncol.* **23**, 842–849 (2005).
274. H. Hirte, I. B. Vergote, J. R. Jeffrey, R. N. Grimshaw, S. Coppieters, B. Schwartz, D. Tu, a Sadura, M. Brundage, L. Seymour, A phase III randomized trial of BAY 12-9566 (tanomastat) as maintenance therapy in patients with advanced ovarian cancer responsive to primary surgery and paclitaxel/platinum containing chemotherapy: a National Cancer Institute of Canada Clinical Trials G, *Gynecol. Oncol.* **102**, 300–8 (2006).
275. R. E. Vandenbroucke, C. Libert, Is there new hope for therapeutic matrix metalloproteinase inhibition?, *Nat. Rev. Drug Discov.* **13**, 904–927 (2014).
276. A. Dufour, C. M. Overall, Missing the target: matrix metalloproteinase antitargets in inflammation and cancer., *Trends Pharmacol. Sci.* **34**, 233–42 (2013).
277. J. M. Cathcart, J. Cao, MMP Inhibitors: Past, present and future., *Front. Biosci. (Landmark Ed.)* **20**, 1164–78 (2015).
278. G. B. Fields, New strategies for targeting matrix metalloproteinases, *Matrix Biol.* **44–46**, 239–246 (2015).
279. I. Sagi, D. Talmi-Frank, V. Arkadash, N. Papo, V. Mohan, Matrix metalloproteinase protein inhibitors: highlighting a new beginning for metalloproteinases in medicine, *Met. Med.* **Volume 3**, 31–47 (2016).
280. M. Levin, Y. Udi, I. Solomonov, I. Sagi, Next generation matrix metalloproteinase inhibitors — Novel strategies bring new prospects, *Biochim. Biophys. Acta - Mol. Cell Res.* **1864**, 1927–1939 (2017).
281. S. Amar, D. Minond, G. B. Fields, Clinical Implications of Compounds Designed to Inhibit ECM-Modifying Metalloproteinases, *Proteomics* **17**, 1600389 (2017).
282. M. Tauro, J. McGuire, C. C. Lynch, New approaches to selectively target cancer-associated matrix metalloproteinase activity., *Cancer Metastasis Rev.* **33**, 1043–57 (2014).
283. N. Sela-Passwell, G. Rosenblum, T. Shoham, I. Sagi, Structural and functional bases for allosteric control of MMP activities: can it pave the path for selective inhibition?, *Biochim. Biophys. Acta* **1803**, 29–38 (2010).
284. a Talvensaaari-Mattila, P. Pääkkö, T. Turpeenniemi-Hujanen, Matrix metalloproteinase-2 (MMP-2) is associated with survival in breast carcinoma., *Br. J. Cancer* **89**, 1270–5 (2003).
285. S.-C. Liu, S.-F. Yang, K.-T. Yeh, C.-M. Yeh, H.-L. Chiou, C.-Y. Lee, M.-C. Chou, Y.-S. Hsieh, Relationships between the level of matrix metalloproteinase-2 and tumor size of breast cancer., *Clin. Chim. Acta.* **371**, 92–6 (2006).
286. T. Itoh, M. Tanioka, H. Yoshida, T. Yoshioka, H. Nishimoto, S. Itohara, Reduced angiogenesis and tumor progression in gelatinase A-deficient mice., *Cancer Res.* **58**, 1048–

51 (1998).

287. G. Bergers, R. Brekken, G. McMahon, T. H. Vu, T. Itoh, K. Tamaki, K. Tanzawa, P. Thorpe, S. Itohara, Z. Werb, D. Hanahan, Matrix metalloproteinase-9 triggers the angiogenic switch during carcinogenesis., *Nat. Cell Biol.* **2**, 737–44 (2000).

288. V. Masson, L. R. de la Ballina, C. Munaut, B. Wielockx, M. Jost, C. Maillard, S. Blacher, K. Bajou, T. Itoh, S. Itohara, Z. Werb, C. Libert, J.-M. Foidart, A. Noël, Contribution of host MMP-2 and MMP-9 to promote tumor vascularization and invasion of malignant keratinocytes., *FASEB J.* **19**, 234–6 (2005).

289. S. Thiolloy, J. R. Edwards, B. Fingleton, D. B. Rifkin, L. M. Matrisian, C. C. Lynch, M. Bogoy, Ed. An Osteoblast-Derived Proteinase Controls Tumor Cell Survival via TGF-beta Activation in the Bone Microenvironment, *PLoS One* **7**, e29862 (2012).

290. A. Tester, M. Waltham, S. Oh, S. Bae, Pro-matrix metalloproteinase-2 transfection increases orthotopic primary growth and experimental metastasis of MDA-MB-231 human breast cancer cells in nude mice, *Cancer Res.* , 652–658 (2004).

291. A. Rossello, E. Nuti, E. Orlandini, P. Carelli, S. Rapposelli, M. Macchia, F. Minutolo, L. Carbonaro, A. Albini, R. Benelli, G. Cercignani, G. Murphy, A. Balsamo, New N-arylsulfonyl-N-alkoxyaminoacetohydroxamic acids as selective inhibitors of gelatinase a (MMP-2), *Bioorganic Med. Chem.* **12**, 2441–2450 (2004).

292. A. Rossello, E. Nuti, P. Carelli, E. Orlandini, M. Macchia, S. Nencetti, M. Zandomenighi, F. Balzano, G. U. Barretta, A. Albini, R. Benelli, G. Cercignani, G. Murphy, A. Balsamo, N-i-Propoxy-N-biphenylsulfonylaminobutylhydroxamic acids as potent and selective inhibitors of MMP-2 and MT1-MMP, *Bioorganic Med. Chem. Lett.* **15**, 1321–1326 (2005).

293. M. Gooyit, W. Song, K. V. Mahasenan, K. Lichtenwalter, M. A. Suckow, V. A. Schroeder, W. R. Wolter, S. Mobashery, M. Chang, O -phenyl carbamate and phenyl urea thiiranes as selective matrix metalloproteinase-2 inhibitors that cross the blood-brain barrier, *J. Med. Chem.* **56**, 8139–8150 (2013).

294. J. E. Meisel, M. Chang, Selective small-molecule inhibitors as chemical tools to define the roles of matrix metalloproteinases in disease, *Biochim. Biophys. Acta - Mol. Cell Res.* **1864**, 2001–2014 (2017).

295. M. Gao, H. Zhang, A. Trivedi, K. V. Mahasenan, V. A. Schroeder, W. R. Wolter, M. A. Suckow, S. Mobashery, L. J. Noble-Haeusslein, M. Chang, Selective Inhibition of MMP-2 Does Not Alter Neurological Recovery after Spinal Cord Injury, *ACS Chem. Neurosci.* **7**, 1482–1487 (2016).

296. N. Adhikari, A. K. Halder, S. Mallick, A. Saha, K. D. Saha, T. Jha, Robust design of some selective matrix metalloproteinase-2 inhibitors over matrix metalloproteinase-9 through in silico/fragment-based lead identification and de novo lead modification: Syntheses and biological assays, *Bioorganic Med. Chem.* **24**, 4291–4309 (2016).

297. J. Song, P. Peng, J. Chang, M. M. Liu, J. M. Yu, L. Zhou, X. Sun, Selective non-zinc binding MMP-2 inhibitors: Novel benzamide Ilomastat analogs with anti-tumor metastasis, *Bioorganic Med. Chem. Lett.* **26**, 2174–2178 (2016).
298. J. Lauer-Fields, K. Brew, J. K. Whitehead, S. Li, R. P. Hammer, G. B. Fields, Triple-helical transition state analogues: A new class of selective matrix metalloproteinase inhibitors, *J. Am. Chem. Soc.* **129**, 10408–10417 (2007).
299. M. W. Ndinguri, M. Bhowmick, D. Tokmina-Roszyk, T. K. Robichaud, G. B. Fields, Peptide-based selective inhibitors of matrix metalloproteinase-mediated activities, *Molecules* **17**, 14230–14248 (2012).
300. J. Deshane, C. C. Garner, H. Sontheimer, Chlorotoxin inhibits glioma cell invasion via matrix metalloproteinase-2, *J. Biol. Chem.* **278**, 4135–4144 (2003).
301. O. Cohen-Inbar, M. Zaaroor, Glioblastoma multiforme targeted therapy: The Chlorotoxin story, *J. Clin. Neurosci.* **33**, 52–58 (2016).
302. N. Sela-Passwell, R. Kikkeri, O. Dym, H. Rozenberg, R. Margalit, R. Arad-Yellin, M. Eisenstein, O. Brenner, T. Shoham, T. Danon, A. Shanzler, I. Sagi, Antibodies targeting the catalytic zinc complex of activated matrix metalloproteinases show therapeutic potential, *Nat. Med.* **18**, 143–147 (2011).
303. S. Pfaffen, T. Hemmerle, M. Weber, D. Neri, Isolation and characterization of human monoclonal antibodies specific to MMP-1A, MMP-2 and MMP-3, *Exp. Cell Res.* **316**, 836–847 (2010).
304. S. Higashi, K. Miyazaki, Identification of a region of β -amyloid precursor protein essential for its gelatinase A inhibitory activity, *J. Biol. Chem.* **278**, 14020–14028 (2003).
305. S. Higashi, K. Miyazaki, Identification of amino acid residues of the matrix metalloproteinase-2 essential for its selective inhibition by β -amyloid precursor protein-derived inhibitor, *J. Biol. Chem.* **283**, 10068–10078 (2008).
306. H. Hashimoto, T. Takeuchi, K. Komatsu, K. Miyazaki, M. Sato, S. Higashi, Structural Basis for Matrix Metalloproteinase-2 (MMP-2)-selective Inhibitory Action of β -Amyloid Precursor Protein-derived Inhibitor, *J. Biol. Chem.* **286**, 33236–33243 (2011).
307. S. Higashi, T. Hirose, T. Takeuchi, K. Miyazaki, Molecular design of a highly selective and strong protein inhibitor against matrix metalloproteinase-2 (MMP-2), *J. Biol. Chem.* **288**, 9066–9076 (2013).
308. K. Kawai, N. Nagata, Metal-ligand interactions: An analysis of zinc binding groups using the Protein Data Bank, *Eur. J. Med. Chem.* **51**, 271–276 (2012).
309. F. Grams, M. Crimmin, L. Hinnes, P. Huxley, M. Pieper, H. Tschesche, W. Bode, Structure Determination and Analysis of Human Neutrophil Collagenase Complexed with a Hydroxamate Inhibitor, *Biochemistry* **34**, 14012–14020 (1995).
310. C. Campestre, M. Agamennone, P. Tortorella, S. Preziuso, A. Biasone, E. Gavuzzo,

- G. Pochetti, F. Mazza, O. Hiller, H. Tschesche, V. Consalvi, C. Gallina, N-Hydroxyurea as zinc binding group in matrix metalloproteinase inhibition: Mode of binding in a complex with MMP-8, *Bioorganic Med. Chem. Lett.* **16**, 20–24 (2006).
311. E. W. Howard, E. C. Bullen, M. J. Banda, Regulation of the autoactivation of human 72-kDa progelatinase by tissue inhibitor of metalloproteinases-2, *J. Biol. Chem.* **266**, 13064–13069 (1991).
312. U. Bergmann, A. Tuuttila, W. G. Stetlerstevenson, K. Tryggvason, Autolytic Activation of Recombinant Human 72-Kilodalton Type-IV Collagenase, *Biochemistry* **Vol 34**, 2819–2825 (1995).
313. B. Lovejoy, A. R. Welch, S. Carr, C. Luong, C. Broka, R. T. Hendricks, J. A. Campbell, K. A. Walker, R. Martin, H. Van Wart, M. F. Browner, Crystal structures of MMP-1 and -13 reveal the structural basis for selectivity of collagenase inhibitors., *Nat. Struct. Biol.* **6**, 217–21 (1999).
314. T. Kohno, H. Hochigai, E. Yamashita, T. Tsukihara, M. Kanaoka, Crystal structures of the catalytic domain of human stromelysin-1 (MMP-3) and collagenase-3 (MMP-13) with a hydroxamic acid inhibitor SM-25453, *Biochem. Biophys. Res. Commun.* **344**, 315–322 (2006).
315. U. Eckhard, P. F. Huesgen, O. Schilling, C. L. Bellac, G. S. Butler, J. H. Cox, A. Dufour, V. Goebeler, R. Kappelhoff, U. auf dem Keller, T. Klein, P. F. Lange, G. Marino, C. J. Morrison, A. Prudova, D. Rodriguez, A. E. Starr, Y. Wang, C. M. Overall, Active site specificity profiling of the matrix metalloproteinase family: Proteomic identification of 4300 cleavage sites by nine MMPs explored with structural and synthetic peptide cleavage analyses, *Matrix Biol.* **49**, 37–60 (2016).
316. K. Edman, M. Furber, P. Hemsley, C. Johansson, G. Pairaudeau, J. Petersen, M. Stocks, A. Tervo, A. Ward, E. Wells, L. Wissler, The discovery of MMP7 inhibitors exploiting a novel selectivity trigger, *ChemMedChem* **6**, 769–773 (2011).
317. L. Geng, J. Gao, W. Cui, Y. Tang, M. Ji, B. Chen, Computational insights into the selectivity mechanism of APP-IP over matrix metalloproteinases, *J. Comput. Aided. Mol. Des.* **26**, 1327–1342 (2012).
318. C. Antoni, L. Vera, L. Devel, M. P. Catalani, B. Czarny, E. Cassar-Lajeunesse, E. Nuti, A. Rossello, V. Dive, E. A. Stura, Crystallization of bi-functional ligand protein complexes, *J. Struct. Biol.* **182**, 246–254 (2013).
319. U. Neumann, H. Kubota, K. Frei, V. Ganu, D. Leppert, Characterization of Mca-Lys-Pro-Leu-Gly-Leu-Dpa-Ala-Arg-NH₂, a fluorogenic substrate with increased specificity constants for collagenases and tumor necrosis factor converting enzyme, *Anal. Biochem.* **328**, 166–173 (2004).
320. C. H. Yeh, P. L. Gross, J. I. Weitz, Evolving use of new oral anticoagulants for treatment of venous thromboembolism, *Blood* **124**, 1020–1028 (2014).

321. Y. H. Mekaj, A. Y. Mekaj, S. B. Duci, E. I. Miftari, New oral anticoagulants: Their advantages and disadvantages compared with vitamin K antagonists in the prevention and treatment of patients with thromboembolic events, *Ther. Clin. Risk Manag.* **11**, 967–977 (2015).
322. S. J. Connolly, M. D. Ezekowitz, S. Yusuf, J. Eikelboom, J. Oldgren, A. Parekh, J. Pogue, P. A. Reilly, E. Themeles, J. Varrone, S. Wang, M. Alings, D. Xavier, J. Zhu, R. Diaz, B. S. Lewis, H. Darius, H.-C. Diener, C. D. Joyner, L. Wallentin, Dabigatran versus Warfarin in Patients with Atrial Fibrillation, *N. Engl. J. Med.* **361**, 1139–1151 (2009).
323. J. H. Levy, A. C. Spyropoulos, C. M. Samama, J. Douketis, Direct oral anticoagulants: New drugs and new concepts, *JACC Cardiovasc. Interv.* **7**, 1333–1351 (2014).
324. T. C. Villines, W. F. Peacock, Safety of direct oral anticoagulants: insights from postmarketing studies, *Am. J. Emerg. Med.* **34**, 9–13 (2016).
325. D. Erlinge, E. Omerovic, O. Fröbert, R. Linder, M. Danielewicz, M. Hamid, E. Swahn, L. Henareh, H. Wagner, P. Hårdhammar, I. Sjögren, J. Stewart, P. Grimfjärd, J. Jensen, M. Aasa, L. Robertsson, P. Lindroos, J. Haupt, H. Wikström, A. Ulvenstam, P. Bhiladvala, B. Lindvall, A. Lundin, T. Tödt, D. Ioanes, T. Råmunddal, T. Kellerth, L. Zagozdzon, M. Götberg, J. Andersson, O. Angerås, O. Östlund, B. Lagerqvist, C. Held, L. Wallentin, F. Scherstén, P. Eriksson, S. Koul, S. James, Bivalirudin versus Heparin Monotherapy in Myocardial Infarction, *N. Engl. J. Med.* **377**, 1132–1142 (2017).
326. C. P. Cannon, D. L. Bhatt, J. Oldgren, G. Y. H. Lip, S. G. Ellis, T. Kimura, M. Maeng, B. Merkely, U. Zeymer, S. Gropper, M. Nordaby, E. Kleine, R. Harper, J. Manassie, J. L. Januzzi, J. M. ten Berg, P. G. Steg, S. H. Hohnloser, Dual Antithrombotic Therapy with Dabigatran after PCI in Atrial Fibrillation, *N. Engl. J. Med.* **377**, 1513–1524 (2017).
327. J. I. Weitz, A. W. A. Lensing, M. H. Prins, R. Bauersachs, J. Beyer-Westendorf, H. Bounameaux, T. A. Brighton, A. T. Cohen, B. L. Davidson, H. Decousus, M. C. S. Freitas, G. Holberg, A. K. Kakkar, L. Haskell, B. van Bellen, A. F. Pap, S. D. Berkowitz, P. Verhamme, P. S. Wells, P. Prandoni, Rivaroxaban or Aspirin for Extended Treatment of Venous Thromboembolism, *N. Engl. J. Med.* **376**, 1211–1222 (2017).
328. J. W. Eikelboom, S. J. Connolly, J. Bosch, G. R. Dagenais, R. G. Hart, O. Shestakovska, R. Diaz, M. Alings, E. M. Lonn, S. S. Anand, P. Widimsky, M. Hori, A. Avezum, L. S. Piegas, K. R. H. Branch, J. Probstfield, D. L. Bhatt, J. Zhu, Y. Liang, A. P. Maggioni, P. Lopez-Jaramillo, M. O'Donnell, A. K. Kakkar, K. A. A. Fox, A. N. Parkhomenko, G. Ertl, S. Störk, M. Keltai, L. Ryden, N. Pogosova, A. L. Dans, F. Lanas, P. J. Commerford, C. Torp-Pedersen, T. J. Guzik, P. B. Verhamme, D. Vinereanu, J.-H. Kim, A. M. Tonkin, B. S. Lewis, C. Felix, K. Yusoff, P. G. Steg, K. P. Metsarinne, N. Cook Bruns, F. Misselwitz, E. Chen, D. Leong, S. Yusuf, Rivaroxaban with or without Aspirin in Stable Cardiovascular Disease, *N. Engl. J. Med.* **377**, 1319–1330 (2017).
329. C. V. Pollack, P. A. Reilly, J. van Ryn, J. W. Eikelboom, S. Glund, R. A. Bernstein, R. Dubiel, M. V. Huisman, E. M. Hylek, C.-W. Kam, P. W. Kamphuisen, J. Kreuzer, J. H. Levy, G. Royle, F. W. Sellke, J. Stangier, T. Steiner, P. Verhamme, B. Wang, L. Young, J.

- I. Weitz, Idarucizumab for Dabigatran Reversal — Full Cohort Analysis, *N. Engl. J. Med.* **377**, 431–441 (2017).
330. E. C. Jauch, J. L. Saver, H. P. Adams, A. Bruno, J. J. B. Connors, B. M. Demaerschalk, P. Khatri, P. W. McMullan, A. I. Qureshi, K. Rosenfield, P. A. Scott, D. R. Summers, D. Z. Wang, M. Wintermark, H. Yonas, Guidelines for the early management of patients with acute ischemic stroke: A guideline for healthcare professionals from the American Heart Association/American Stroke Association, *Stroke* **44**, 870–947 (2013).
331. P. A. Sandercock, C. Counsell, A. K. Kamal, Anticoagulants for acute ischaemic stroke., *Cochrane Database Syst. Rev.* , CD000024 (2008).

Jonas Wilbs

Enthusiastic biochemist with 5 years of experience in academia and industry. Passionate about science focused on therapeutic molecule development. Excellent communication skills obtained through scientific collaborations. Fast learner who can adapt quickly to new environments.



Swedish
14.07.1987
jonaswilbs@gmail.com
+41 788 256 565
Av de Montoie 37
1007 Lausanne (CH)

Key strengths

Target focused
Molecular design
Team work
Analytical mind

Experience

PhD Studies

2014 -

EPFL Lausanne (Prof C. Heinis)

- Developed sub-nanomolar inhibitors in disease areas anticoagulation (FXIIa) and oncology (MMP-2)
- Optimized lead peptides by SAR for affinity, selectivity and stability
- Lead multidisciplinary international collaborations for preclinical characterization of drug candidates
- Communication with CROs
- Established and validated several in vivo and in vitro assays

MSc Thesis

2013

Internship

2012

Summer job

2011

Summer job

2007-2011

AstraZeneca RD Mölndal

- Analyzing particle surface properties of inhalation formulations

Bio21 Research center Melbourne

- Organic synthesis of Rhenium complexes in the group of Paul Donnelly

AkzoNobel Borås

- Analytical chemistry and process operation in paper&pulp chemical factory

Manpower Alingsås

- Different types of manufacturing and service industries. Worked at 10+ different workplaces

Internship

2013

AstraZeneca RD Mölndal

- Correlating surface properties to in vitro performance of inhalation formulations

Education

MSc Chemical Engineering

2007 - 2013

Uppsala University

- Focus on pharmaceutical development, organic and analytical chemistry

Exchange studies

2012

University of Melbourne

- Courses within chemical engineering, organic chemistry and management

Extracurricular activities

Logistics manager

2011

Uppsala University

Career fair UTNARM

- Coordinating fair logistics of 100 visiting companies
- Supervised a team of 20 persons

Volunteer

2008, 2009

Uppsala University

New student reception

- Organizing welcome activities

Skills

Technical

Peptide synthesis

- Peptide conjugation, cyclization and functionalization techniques
- Establishment of new liquid handling scripts on automated peptide synthesizer

In vitro assays

- Experimental design and establishment of new assays
- Enzymatic assays
- Blood coagulation assays
- Isothermal titration calorimetry
- Fluorescence polarization

In vivo experimentation

- Establishment of animal models (Thrombosis, Xenograft)
- Licensed animal experimenter (Swiss Module 1)
- Pharmacokinetics
- Statistical power calculations

Analytical chemistry

- Mass spectrometry
- Analytical HPLC
- SDS-PAGE
- NMR

Others

- Protein purification
- Phage display
- Cell culture
- Scientific writing
- Data analysis

Soft

Project management

Team work

Critical thinking

Teaching

Communication

Scientific contributions

Patents

- Novel inhibitors of the enzyme activated factor xii (fxiia) PCT/EP2016/059435

Awards and grants

- Roche/Swiss Society of Hematology (SSH) best poster award 2017
- American Peptide Symposium 2017 travel grant
- Doctoral school EPFL travel grant

Presentations

- Oral presentation LS2 meeting, Bern, Feb 2017
- Oral presentation SSH annual meeting, Lausanne May 2017
- Oral presentation American Peptide Symposium main event, Whistler June 2017
- Poster presentation Benzon Symposium 63, Aug 2017 Copenhagen

Languages

Swedish

- Native

French

- Limited proficiency

English

- Full professional proficiency

German

- Working proficiency (C1)

Publications

1) Wilbs, J., Middendorp, S.J., Heinis, C. **Improving the Binding Affinity of in Vitro-Evolved Cyclic Peptides by Inserting Atoms into the Macrocycle Backbone**, *ChemBioChem*, 2016

2) Middendorp, S.J., Wilbs, J., Quarroz, C., Calzavarini, S., Angelillo-Scherrer, A., Heinis, C. **Peptide macrocycle inhibitor of coagulation factor XII with subnanomolar affinity and high target selectivity**, *Journal of Medicinal Chemistry*, 2017

3) Zorzi, A., Middendorp, S.J., Wilbs, J., Deyle, K., Heinis, C. **Acyated heptapeptide binds albumin with high affinity and application as tag furnishes long-acting peptides**, *Nature Communications*, 2017

4) Wilbs et al., **A peptide macrocycle FXII inhibitor provides safe anticoagulation in a preclinical thrombosis model and in artificial lungs**, *Manuscript in preparation*

5) Wilbs et al., **Identification and lead optimization of a potent and selective bicyclic peptide MMP-2/3 inhibitor**, *Manuscript in preparation*

Interests

Biking

Sports

Traveling